Understanding the Determinants of Environmental Resistomes in Urban and Natural Ecosystems

Zhen-Zhen Yan

ORCID: 0000-0002-9410-4753

Submitted in total fulfilment for the degree of

Doctor of Philosophy

October 2021

School of Agriculture and Food

Faculty of Veterinary and Agricultural Sciences

The University of Melbourne

Abstract

The spread of antibiotic resistance genes (ARGs) is a great public health threat faced by humanity in the 21st century. However, our understanding of the abiotic and biotic factors determining the distribution of ARGs in the environment is lacking. This knowledge gap hampers our ability to design efficient management strategies to mitigate the dissemination of environmental ARGs.

Soil and plant phyllosphere are the two largest environmental habitats of microorganisms and the most important reservoirs of environmental ARGs. In urban ecosystems, soil and plants in green spaces are major interfaces between environmental microbiome and human microbiome, which are closely related to the welling being of urban residents. In this study, we investigated resistome profiles and bacterial community assemblies in soil and plant phyllosphere samples collected from 40 urban parks across Melbourne, Australia. A total of 218 and 217 unique ARGs, which confer resistance to all major classes of antibiotics commonly used in humans and animals, were identified in soil and plant phyllosphere samples, respectively suggesting that urban green spaces were important reservoirs of ARGs. The results of correlation analyses indicated that the abundance of ARGs was significantly ($P < 0.001$) positively correlated with industrial factors (represented by the numbers of industries in a region). Structural equation model revealed that industrial distribution was one of the most important factors that contributed to the variations in resistome profiles in urban green spaces after accounting for multiple drivers. We further explored the main factors influencing the assemblies of bacterial communities in urban green spaces. Industrial development was also identified as a key factor in shaping bacterial communities as variation partitioning analysis results revealed that industrial factors could explain 20% and 28% of the variations in soil and grass phyllosphere bacterial communities, respectively.

In natural ecosystems, ARGs are considered as an important proxy of ecosystem multifunctionality. To explore the biogeographic patterns of ARGs in natural ecosystems, we constructed ARG abundance atlas for plant phyllosphere and soil from an over 4,000 km transect across eastern and northern Australia. The results revealed that plant phyllosphere and soil resistomes exhibited opposite biogeographic patterns. The results of Spearman's correlation analysis and structural equation model revealed that ARG abundance in plant phyllosphere was mainly related to the community assemblies of co-occurring bacterial, fungal, and protistan communities. However, ARG abundance in soil was mainly correlated with mean annual temperature, mean annual precipitation and soil nutrition content. These results indicated the distinct roles of biotic and abiotic factors in shaping resistomes in plant phyllosphere and soil and could potentially explain the observed contrasting biogeographic patterns of ARG abundance in these two different environmental habitats.

Given the profound roles of soil fauna on the evolution and spreading of ARGs, we also profiled the resistomes in termite mounds, which is a unique habitat for diverse microorganisms. By collecting termite mound and soil samples from an over 1,500 km transect in northern Australia, we found that both the abundance and diversity of ARGs in termite mounds were significantly ($P < 0.001$) lower than that in surrounding bulk soils. Further analyses revealed that the differences between termite mound and bulk soil resistomes might result from the substantial increases in pH and nutrient availability due to termite mound formation. These results provided valuable implications for utilizing soil faunal activity for the regulating of the dissemination of environmental ARGs.

Taken together, this thesis provided important evidence that both urban and natural environments are critical reservoirs of ARGs. In urban environments, changes in ARGs were more impacted by anthropogenic factors, particularly industrial development. In natural environments, climatic and edaphic factors were the main predictors of resistome profile. We also found that the resistome profiles in soil and plant phyllosphere were distinct from each other suggesting the important roles of habitat properties in influencing resistome profiles. These findings advance our understanding of the biogeographical distribution patterns of ARGs in the environmental settings and provide important scientific data for refining the management strategies to combat the spreading of environmental ARGs, a potential major threat to the public health.

Keywords: antibiotic resistance genes, urban microbiome, soil, plant phyllosphere, microbial community assembly, environmental filtering.

Declaration

This is to certify that:

(i) the thesis comprises only my original work towards the PhD except where indicated in the Preface,

(ii) due acknowledgement has been made in the text to all other material used,

(iii) the thesis is fewer than 100 000 words in length, exclusive of tables, maps, bibliographies, and appendices.

Zhen-Zhen Yan

October 2021

Preface

This thesis is the original work of the candidate, Zhen-Zhen Yan. This thesis is comprised of six chapters including an introduction chapter, followed by four research chapters, and a conclusions chapter. The research chapters have been published in peer-reviewed journals and are written in manuscript format according to the specific format of individual journals. The candidate is the first author of all the research chapters who is responsible for planning, execution, and preparation of work for publication. Co-authors, including Bao Anh Thi Nguyen, Chaoyu Li, Hang-Wei Hu, Jizheng He, Qinglin Chen, Yongguan Zhu, and Yujing Zhang, assisted the candidate with sample collection, experimental design, and polishing the manuscripts.

The manuscripts included in this thesis are presented in the following order:

Chapter 2

Yan, Z.Z., Chen, Q.L., Zhang, Y.J., He, J.Z., and Hu, H.W. (2019) Antibiotic resistance in urban green spaces mirrors the pattern of industrial distribution. *Environmental International*, 132:105016.

https://doi.org/10.1016/j.envint.2019.105106

Chapter 3

Yan, Z.Z., Chen, Q.L., Zhang, Y.J., He, J.Z., and Hu, H.W. (2020) Industrial development as a key factor explaining variances in soil and grass phyllosphere microbiomes in urban green spaces. *Environmental Pollution*, 261:114201.

https://doi.org/10.1016/j.envpol.2020.114201

Chapter 4

Yan, Z.Z., Chen, Q.L., Li, C.Y., Nguyen, B.A.T., Zhu, Y.G., He, J.Z., and Hu, H.W. (2021) Biotic and abiotic factors distinctly drive contrasting biogeographic patterns between phyllosphere and soil resistomes in natural ecosystems. *ISME Communications*, 1:13.

http://doi.org/10.1038/s43705-021-00012-4

Chapter 5

Yan, Z.Z., Chen, Q.L., Li. C.Y., Nguyen, B.A.T., Zhu, Y.G., He, J.Z. and Hu, H.W. (2021) Termite mound formation reduces the abundance and diversity of soil resistomes. *Environmental Microbiology*, 23: 7661-7670.

https://doi.org/10.1111/1462-2920.15631

Acknowledgements

First and foremost, I would like to express my thanks to my supervisors, Dr. Hang-Wei Hu, Prof. Jizheng (Jim) He, and Dr. Qinglin Chen for their continuous encouragement and support. I am very grateful for the opportunity to meet Jim four years ago which lead to the start of my PhD. I would like to thank Hang-Wei for his unfailing support and step-by-step guidance during my whole candidature. I would like to thank Qinglin for always being generous with his time and being so patient in mentoring me through the data analysis and the writing of manuscripts.

Thanks should also be given to A/Prof. Helen Suter. I have been fortunate to have Helen as my advisor not only because of the valuable academic advice she gave me but also for her being so emotionally supportive during the difficult times of the pandemic. I would like to thank Dr. Yujing Zhang for generously sharing her experience and knowledge with me. My PhD project was based on field surveys. Therefore, I would like to express my gratitude to those who helped me with the sample collection. I would like to thank Chunhe Gu, Zhibo Luo, Hang Gao, Chaoyu Li, and Bing Han for their kind help with the sampling across Melbourne. I would like to thank Hang-Wei, Qinglin, and Chaoyu who I worked with for the large-scale sampling across the eastern and northern part of Australia. I consider myself very lucky for having such an unforgettable experience. I would like to thank everyone in the soils group: my committee chair Prof. Deli Chen; Michael Hall and Qing Xie for their help with lab works, my colleagues and friends, Baobao Pan, Wei Zhang, Xiuming Zhang, Chaoyu Li, Bao Anh (Selena) Nguyen, and Dr. Xia Liang for their accompany and the fun we had together.

I would also like to express my special thank to my Master's supervisor Dr. Ken Ng and Prof. Mohan Singh who inspired me to start the PhD. They were the reasons that I decided to pursue a career in research.

I would like to thank all my family members and friends for their encouragement and understanding. Finally, deepest thanks go to my parents for their unconditional love and support. It was the security my mom and dad gave me makes me brave enough to face any challenges in my PhD and life. Thanks for being there every step of the way when I am pursuing my dreams.

This PhD project was financially supported by the Australian Research Council (ARC). The candidate was supported by Melbourne International Research Scholarship and Melbourne International Fee Remission Scholarship.

Table of Contents

Abstract i

Declaration iv

Preface v

Acknowledgements vii

Table of Contents ix

List of Tables xi

List of Figures xiii

Chapter 1: Introduction 1

1.1 Background 1

1.2 Knowledge gaps 9

1.3 Objectives of the study and organization of the thesis 10

1.4 Significance of the study 11

References 12

Chapter 2 Characterization of the key factors in influencing antibiotic resistomes in urban ecosystems 18

Chapter 3: Characterization of the key factors in influencing bacterial community assemblies in urban ecosystems 44

Chapter 4: Characterization of the biogeographic patterns of antibiotic resistomes in natural ecosystems 76

Chapter 5: Characterizations of the impacts of changes in habitat properties on antibiotic resistome profile 104

Chapter 6: General discussion and conclusions.....141

6.1 Key findings and general discussion.....141

6.2 Conclusions.....144

6.3 Implications of the study.....145

6.4 Limitations of the study 146

6.5 Suggestions for future study 146

References.....150

List of Tables

Chapter 2

Table 1. Spearman's ranked correlation coefficients between industrial factors and the abundance of ARGs and MGEs.

Table S1. Detailed information about all the 40 urban parks investigated in this study.

Table S2. Anthropogenic parameters about all the 120 sampling sites at Statistical Area Level 4.

Table S3. List of soil properties of the 120 soil samples analyzed.

Chapter 3

Table 1. Spearman's ranked correlation coefficient between soil properties and anthropogenic parameters and microbial community compositions (the first axis values of PCoA analysis) in the soil and grass phyllosphere samples from urban green spaces.

Table S1. Detailed information of sampling sites.

Table S2. Anthropogenic parameters of Statistical Area Level 2 (SA2) regions where the urban green spaces are located in.

Table S3. List of analysed soil properties of the 120 soil samples from urban green spaces.

Chapter 4

Table 1. Spearman's correlation between ARG abundance and selected biotic and abiotic factors.

Table S1. Moran's I for each axis of the Moran's eigenvector maps.

Table S2. Spearman's correlation between the abundances and selected biotic and abiotic factors. Significant correlations ($P < 0.05$) are indicated as bold fonts.

Chapter 5

Table S1. List of primers for the targeted antibiotic resistance genes in this study and their classification by target drug and mechanism of resistance.

Table S2. Climatic factors used in this study.

Table S3. Physiochemical properties of termite mounds and bulk soil samples

List of Figures

Chapter 2

Figure 1. Resistome profiles based on the relative abundance of ARGs in grass phyllosphere and soil samples. (A) Boxplot of the relative abundance of ARGs detected in samples. * Indicates $P < 0.05$ determined by paired t-test. (B) Principal coordinate analysis (PCoA) based on the Bray-Curtis distance showing the distribution patterns of ARGs in samples.

Figure 2. (A) Classification of ARGs detected in grass phyllosphere and soil based on the mechanisms of resistance. (B) The antibiotic to which the ARGs confer resistance.

Figure 3. Ordinary least square (OLS) regression showing the relationships between the relative abundance of ARGs and that of the total MGEs and clinical class 1 integron-integrase gene (*intl1*) in grass phyllosphere and soil samples.

Figure 4. (A) Bacterial alpha diversity in phyllosphere and soil samples. *** indicates $P < 0.001$ determined by paired t-test. (B) Principal coordinate analysis (PCoA) based on the Bray-Curtis distance showing the distribution pattern of bacterial communities (beta diversity) in phyllosphere and soil samples.

Figure 5. Frequency distribution of ARGs in grass phyllosphere and soil.

Figure 6. Structural equation models (SEMs) showing the direct and indirect effects of multiple factors on the abundance of ARGs in grass phyllosphere (A) and soil (B). Numbers adjacent to arrows are standardized path coefficients. The width of the arrows is proportional to the strength of path coefficients. R^2 indicates the proportion of variance in ARG abundance explained by the model. Significant levels are indicated as ** $P < 0.01$ and *** $P < 0.001$. Standardized effects are derived from the structural equation models.

Figure S1. Distribution of the 40 urban parks investigated in this study.

Figure S2. *A prior* SEM for grass phyllosphere samples and soil samples, based on the hypothesized causal relationships between multiple factors and the abundance of ARGs.

Figure S3. The community compositions of bacterial community at the phylum level in grass phyllosphere and soil samples.

Chapter 3

Figure 1. Venn diagram showing the numbers of unique and shared genera in soil and grass phyllosphere samples (A). Boxplot showing the Shannon index (alpha diversity) in soil and grass phyllosphere samples. *** Indicated $P < 0.001$ determined by Mann-Whitney-Wilcoxon test. The white squares indicate the mean values (B). Principal coordinate analysis (PCoA) based on the Bray-Curtis distance showing the distribution patterns of microbiome in soil and grass phyllosphere (beta diversity (C).

Figure 2. Cladograms of the LEfSe analysis results indicating differences of taxa between soil and grass phyllosphere in urban green spaces and national parks. For each taxon, the red and blue denote the significantly higher abundance ($\alpha > 0.01$, LDA score > 2.0) in urban green spaces and national parks, respectively. Yellow denotes that taxon is not significantly different between urban green spaces and national parks.

Figure 3. Ordinary least square (OLS) regression model showing the relationships between soil properties and microbial community compositions (the first axis values of PCoA analysis) in soil and grass phyllosphere in urban green spaces.

Figure 4. Ordinary least square (OLS) regression model showing the relationships between anthropogenic parameters and microbial community compositions (the first axis values of PCoA analysis) in soil and grass phyllosphere in urban green spaces.

Figure 5. Variation partitioning analysis (VPA) showing the effect in soil properties, soil bacterial communities, social-economic factors, and industrial factors on the alternation of soil (A) and grass phyllosphere (B) communities.

Figure S1. Bacterial community compositions in soil and grass phyllosphere samples across sampling sites at phylum level.

Figure S2. Distribution bar-plot of bacterial community composition in soil (A) and grass phyllosphere (B) samples across different urban green spaces and national parks at the phylum level.

Figure S3. Heatmap of bacterial community compositions in soil (A) and grass phyllosphere (B) samples across the investigated urban green spaces and national parks at genera level.

Figure S4. Boxplot showing the Shannon index (alpha diversity) in soil and grass phyllosphere samples in the 40 urban green spaces and three national parks. *** Indicates $P < 0.001$ determined by Mann-Whitney-Wilcoxon test. The white squares indicate the mean values (A). Principal coordinate analysis (PCoA) based on Bray-Curtis distance showing the distribution patterns of microbiome in soil and grass phyllosphere samples (beta diversity).

Chapter 4

Figure 1. Locations and photos of the sampling sites. The blue spots represent the 100 sites where both plant and soil samples were collected. The red spots represent the 19 sites where only soil samples were collected.

Figure 2. Characteristics of the ARGs detected in the phyllosphere and soil samples. Violin plots and box plots showing the numbers of detected ARGs (A) and the absolute abundance of all detected ARGs (B). Symbol (***) indicates Wilcoxon rank-sum test $P < 0.001$. White squares inside the box plots indicate the mean values. Large-scale atlas of the spatial distributions of ARG abundance in phyllosphere (C) and soil (D) across eastern and northern Australia. The compositions of ARGs detected in the samples are displayed in the bottom area charts. Samples showing in the area charts were ordered by ascending in the latitude of the sampling locations.

Figure 3. Characteristics of bacterial, fungal, and protistan communities in phyllosphere and soils. (A) Violin plots and boxplots showing the Shannon index of bacterial, fungal, and protistan communities in phyllosphere and soils. Symbol (***) indicates Wilcoxon rank-sum test $P < 0.001$. White squares inside the box plots indicate the mean values. (B) Nonmetric multidimensional ordinations of the microbial community structures at the OTU level among the phyllosphere and soil samples based on the Bray–Curtis distance. Symbol (***) indicates ANOSIM $P < 0.001$.

Figure 4. Distance-decay relationships for ARGs, bacterial, fungal, and protistan communities at the OTU level in the phyllosphere and soil samples. Symbol (***) indicates ordinary least regression $P < 0.001$. Significant correlations ($P < 0.05$) and no significant correlation ($P > 0.05$) are shown in solid lines and dashed line, respectively.

Figure 5. Drivers of ARG abundances in phyllosphere and soils. Structure equation models (SEMs) illustrating the direct and indirect effects of multiple factors on the variations in ARG abundance in phyllosphere (A) and soils (B). The width of the arrows is proportional to the strength of path coefficients shown by the numbers

adjacent to the arrows. R2 indicates the proportion of variations in ARG abundance explained by the models. Symbol (*) indicates $P < 0.05$; symbol (**) indicates $P < 0.01$; symbol (***) indicates $P < 0.001$. Standardised effects were derived from the SEMs.

Figure S1. Heatmap showing the abundance of the ARGs detected in the phyllosphere samples.

Figure S2. Heatmap showing the abundance of the ARGs detected in the soil samples.

Figure S3. Nonmetric multidimensional scaling ordinations showing the ARG profiles in phyllosphere and soils based on the Bray-Curtis distance and ARG abundances (copies per gram sample).

Figure S4. Large-scale atlas of the abundances of the dominant ARG classes in phyllosphere across eastern and northern Australia.

Figure S5. Large-scale atlas of the abundance of the dominant ARG class in soils across eastern and northern Australia.

Figure S6. Violin plots and boxplots showing the alpha-diversity index of bacterial, fungal, and protistan communities in the phyllosphere and soils as revealed by the numbers of observed species. *** indicates Wilcoxon rank0sum test $P < 0.001$. White squares inside the box plots indicate the mean values.

Figure S7. Area charts showing taxonomic compositions of the bacterial (A), fungal (B), and protistan (C) communities at the phylum level. Samples were ordered by ascending in the latitude of the sampling locations.

Figure S8. Violin plots and boxplots showing bacterial abundances in the phyllosphere and soils as revealed by copy numbers of 16S rRNA gene. *** indicates Wilcoxon rank0sum test $P < 0.001$. White squares inside the box plots indicate the mean values.

Chapter 5

Figure 1. Comparison of the microbial and physicochemical properties between termite mounds and soil samples. *** Indicates Wilcoxon rank-sum test P < 0.001.

Figure 2. Profiles of the resistomes in termite mounds and soil samples. (A) Relative abundance and Shannon index of antibiotic resistance genes (ARGs) in termite mounds and bulk soils. Error bars represented as mean ± standard deviation. *** Indicates Wilcoxon rank-sum test $P < 0.001$. (B) Principal coordinate analysis (PCoA) based on the Bray-Curtis distance showing the overall distribution patterns in the termite mounds and soils. (C) Classification of the ARGs detected on the mechanisms of the resistance genes. (D) Bipartite network analysis revealing the shared and unique ARGs in termite mounds and soil.

Figure 3. Main determinants of the relative abundance of ARGs in termite mounds and soil. (A) Spearman's correlation matrix. (B) Significant ($P < 0.05$) and the best fit (determined based on the corrected Akaike Information Criterion) polynomial fits of ARG relative abundance of selected determinants. Red and black lines represent first- and second-order polynomial fits, respectively.

Figure 4. Schematic summary of the impact of termite mound formation on soil ARGs. Termite nesting activity led to increases in soil pH and nutrient availability, which could alter the inter-kingdom interaction between bacteria and fungi and shift the soil resistome.

Figure S1. Locations of the sampling sites and photos of termite mounds.

Figure S2. Bacterial abundances in each termite mound and bulk soil samples.

Figure S3. Fungal abundances in each termite mound and bulk soil samples.

Figure S4. Absolute abundances of ARGs in each termite mound and bulk soil samples.

Figure S5. Relative abundances of ARGs in each termite mound and bulk soil samples.

Chapter 1: Introduction

1.1 Background

Antibiotic resistance - a global challenge

The discovery and synthetic of antibiotics are arguably one of the most important achievements of the 20th century or even the entire human history (Nesme and Simonet, 2015). The use of antibiotics in treating bacterial infections has greatly contributed to better public health and led to significant reductions in both morbidity and mortality of hospitalized patients and thus contributed to the doubling of human life span in the 20th century (Demain, 2009). The use of antibiotics not only has revolutionized medicine but also has significantly increased agricultural and livestock productivity when used as veterinary medicine or growth promoter (Andersson and Hughes, 2010). However, the development of antibiotic resistance and the spread of antibiotic resistance genes (ARGs) has put the advances of antibiotics at risk (Vikesland et al., 2017). In the face of the drying of antibiotic development pipeline together with the emergence of new antibiotic resistance mechanisms, antibiotic resistance has put health systems at a great threat (WHO, 2019). According to the World Health Organization, the spread of ARGs has become one of the most serious challenges faced by humanity in the 21st century (WHO, 2019).

After almost a half-century of clinical use of antibiotics, bacterial infections have once again become a leading cause of mortality around the world in recent years (Vikesland et al., 2017). Although the exact death toll related to antibiotic resistance is hard to estimate, this issue can be addressed by several reports. According to the Centers for Disease Control and Prevention (CDC) of the United States, each year more than 2.8 million antibiotic resistance infections happen in the U.S. and more than 35,00 people die due to antibiotic-resistant infections. If counting other infections that are not typically resistant to antibiotics but are

associated with antibiotic use, for example, *Clostridioides difficile*, the infection toll would exceed 3 million and the death toll will reach 48,000 (CDC, 2019). Worldwide, currently, more than 700,000 people die every year related to antibiotic resistance infections including 230,000 people who lose their lives due to multidrug-resistant tuberculosis (WHO, 2019). In addition, more and more infections such as urinary tract infections, respiratory tract infections and sexually transmitted infections are becoming dangerous due to the loss of antibiotic effectiveness (WHO, 2019). The world is already suffering from the consequences of antibiotic resistance now. Without effective strategies to avert this potentially disastrous crisis, the impacts of antibiotic resistance faced by future generations will be more uncontrollable. According to United Nations, if no action is taken the death toll related to antibiotic-resistant infections will exceed 10 million by 2050, and up to 24 million people will live in extreme poverty related to problems caused by antibiotic resistance (WHO, 2019).

Environmental antibiotic resistance

At the beginning of the problem of antibiotic resistance, research focus was largely within the clinical sector. However, during the last years, a growing body of evidence has indicated that the environment is the origin and a vast reservoir of ARGs acquired by human microbiome. Environmental ARGs have been recognised as a type of environmental containment and a critical factor contributing to the development of antibiotic resistance that poses risks to public health (Pruden et al., 2006). It has been demonstrated that a large proportion of environmental ARGs shares the same genetic sequences as those detected in human gut and faecal microorganisms suggested transmissions potential of environmental ARGs to human pathogens and commensals (Nesme et al., 2014, Forsberg et al., 2014). The link between environmental and human resistomes was better demonstrated by some later studies. By conducting a complimentary analysis of antibiotic resistance in pristine

environments, Obermeier et al. (2020) provided evidence that most clinically relevant resistomes are associated with natural resistomes. In addition, the comparative analysis of human gut and environmental resistome conducted by Sun et al. (2020a) provided direct evidence that living environment can persistently shape human gut microbiota and antibiotic resistome. With the recognition of the important roles of the environment in the dissemination of ARGs, it has been recommended that to decipher the complex antibiotic resistance ecology, it would be necessary to shift the spotlight to resistomes in the environment (Nesme and Simonet, 2015). Different from the strict clinical definition of antibiotic resistance, the environmental resistome includes all ARGs and their precursors in both pathogenic and non-pathogenic bacteria (Wright, 2007).

In the environment, ARGs in soil and plant microbiomes are attracting growing attention. Soil is recognized as the largest environmental reservoir of ARGs which account for around one-third of known ARGs in public repositories (Nesme et al., 2014). One important reason for the prevalence of ARGs in soil ecosystems is that the majority of antibiotics used today as human and veterinary medicine including penicillin, cephalosporin, tetracycline, lincomycin, and cycloserine, are all isolated from soil microorganisms (Nwosu, 2001). In addition, soil is an environment with extremely high genetic diversity and thus favouring horizontal gene transfer (HGT) which has been recognized as a critical contributing factor to the dissemination of ARGs among bacterial cells (Nesme and Simonet, 2015). Plant microbiome represents an important bridge for the exchange of microorganisms in human microbiome and those in the environmental microbiome and thus could act as a major pathway for the transmission of environmental ARGs to human pathogens (Chen et al., 2019). Food consumption is one of the most important pathways for human exposure to ARGs in the environmental microbiome. Daily consumption of fruits and vegetables, which are commonly eaten raw, has been identified as a major route for the acquisition of ARGs by human

microbiome (Verraes et al., 2013). Plants can uptake antibiotic residuals from animal manure, an organic fertilizer commonly used for increasing crop productivity, which can apply selection pressure on the plant microbiome for ARGs and contribute to the spread of antibiotic resistance in human food chain (Chen et al., 2019). Another important pathway for the transmission of ARGs from the environment to human microbiome is through skin-surface contact via plant phyllosphere (Chen et al., 2019). Owing to rapid urbanization, a growing proportion of human population are residing in urban environments. Visiting urban green spaces, for example, parks, community gardens, and urban forests are therefore becoming the major way for urban residents to contact nature for health benefits. However, urban green spaces are also identified as hot spots of ARGs as they are commonly irrigated with reclaimed wastewater (Laforest-Lapointe et al., 2016).

Resistomes in urban ecosystems

Currently, the whole world is undergoing rapid urbanization. According to the United Nations report, in 2018 more than half (around 55%) of the global population are residing in urban environments (Nations, 2018). In addition, the expansion of urban areas has been projected to continue at a faster rate in the near future (Nations, 2018). Under such a situation, it is of increasing significance to have a better understanding of the microbiomes and resistomes in urban ecosystems and evaluate the potential human health risks associated with 'microbial exposure' in urban environments.

Urban ecosystems are greatly impacted by human activities. Therefore, urban ecosystems are featured with unique physical, chemical, and thus biological and microbiological properties different from any natural ecosystem which is shaped by anthropogenic activities (Li et al., 2018). Anthropogenic activities have been identified to greatly contribute to the dissemination and accumulation of ARGs in urban ecosystems.

Human population density and building density are found to be positively correlated with soil ARG abundance and the occurrences of mobile genetic elements (MGEs) that can facilitate the HGT of ARGs (Nesme and Simonet, 2015). In urban ecosystems, the misuse and overuse of antibiotics in human and animal healthcare is one of the most important contributing factors to the selection for ARGs (Varela et al., 2014). The undigested antibiotics in human and animal faeces would unavoidably discharge with hospital effluent (Varela et al., 2014). Since current wastewater treatment systems cannot effectively remove all antibiotics in wastewater, urban wastewater treatment plants are identified as a hotspot of antibiotics and thus ARGs (Huang et al., 2019). Several other anthropogenic activities that are not associated with direct selection pressure for ARGs have also been reported can indirectly contribute to the dissemination of ARGs in urban ecosystems. For example, the consumption of non-antibiotic pharmaceuticals, such as anti-inflammatories, ibuprofen, naproxen, diclofenac, and lipid-lowering drugs, at clinically and environmentally relevant concentrations was reported to significantly increase the spread of ARGs by stimulating bacterial uptake of exogenous ARGs (Wang et al., 2020). In addition, anthropogenic air pollution was identified as an important driver in accelerating global dissemination of ARGs (Zhu et al., 2020). Accordingly, there are growing interests in the research of ARGs in urban ecosystems. However, currently, information regarding the occurrences of ARGs and the factors that influence the dissemination of ARGs in urban environments that are not associated with direct or indirect selection pressure for ARGs are still very limited.

Resistomes in natural ecosystems

As a natural phenomenon, antibiotic resistance has a long history of being ubiquitous in natural ecosystems (D'Costa et al., 2011, Allen et al., 2010). It has been suggested that the first occurrence of ARGs in natural ecosystems can be traced back to around 2Gyr ago

(Allen et al., 2010). This suggestion is supported by compelling evidence provided by many studies which consistently detected the occurrence of ARGs in various environments that have been isolated from human settlement for a long time including 30,000 years old Beringia permafrost, ancient Lechuguilla caves, Arctic and Antarctica glacier, and water from deep-sea (D'Costa et al., 2011, Bhullar et al., 2012). Therefore, the better mitigation of the expanding crisis of antibiotic resistance calls for a more in-depth understanding of the ARGs in natural ecosystems which may provide valuable information regarding the evolutionary mechanisms of ARGs (Lee et al., 2020).

In natural ecosystems, ARGs are associated with a variety of ecosystem functions other than as a weapon against antibiotics. Ecosystem functions of ARGs include mediating the signal transfer among microbial cells, acting as detoxification agents, and improving bacterial pathogenicity (Martínez, 2008). Therefore, ARGs have been proposed as an important proxy of ecosystem multifunctionality (Delgado-Baquerizo et al., 2020). To explore the evolutionary mechanisms of ARGs in natural ecosystems and to gain a better understanding of their ecosystem functions, efforts have been made in the last few years to explore the factors influencing resistome profiles. Various environmental factors have been identified to play important roles in influencing resistome profiles in natural ecosystems. For example, Sun et al. (2020b) found that ARG abundance in soil increases with soil inorganic nitrogen concentrations. Li et al. (2020) reported that in pristine ecosystems, temperature and soil organic carbon concentration were the major environmental factors in influencing ARG abundance and diversity. Zhang et al. (2019) identified that salinity was the predominant factor in shaping the resistome profiles and influencing ARG abundance in ocean and river beach soils. Yang et al. (2019) found that stratification and geography was the most important factor in influencing the composition of aquatic resistomes. In addition, some studies noticed that biotic stresses also could exert from the antagonism between bacterial and fungal communities

were another important factor in influencing the abundance and class of ARGs in natural ecosystems (Bahram et al., 2018, Boer et al., 2005). Furthermore, some other stress such as heavy metal contamination, soil salinization, were also identified to be associated with variations in soil resistome proliferation (Guo et al., 2018, Kang et al., 2018, Zhang et al., 2019). A potential explanation for these observations could be that the genotypic responses of bacteria to multiple biotic and abiotic environmental stresses are similar to their responses to the pressure from the presence of antibiotics (McMahon et al., 2007). That is because according to evolutionary theories, it could be inefficient for a microbial community to evolve resistance to only a single stress factor since the development of resistance is commonly associated with a considerable 'fitness cost' (Andersson and Hughes, 2010). Although several studies are aiming to explore the factors shaping environmental resistome profiles in natural ecosystems, currently a systematic understanding of how environmental resistomes in natural ecosystems are shaped is still lacking. A clear understanding of the relationships between different environmental stresses and the development of antibiotic resistance and the most important determinant factor of resistome profile of different ecosystems is still vacant. To gain a better understanding of how resistomes in natural ecosystems are shaped a systematic investigation of a variety of natural ecosystem types is still needed.

Techniques used for the study of environmental antibiotic resistance

Conventionally, culture-based methods are used for the study of environmental ARGs. A standard process of culture-based analysis of ARGs in environmental samples includes bacterial isolation, purification and exerting antimicrobial stress to determine the resistance patterns in the samples (Li et al., 2019). A significant advantage of culture-based method is low cost as it does not require elaborated facilities and expensive consumables. Another important advantage of culture-based methods over other methods is that they are the only

method that would enable the testing of antimicrobial susceptibility of bacteria which can be used for the identification of novel ARGs or resistance mechanisms (Walsh, 2013). However, culture-based methods are associated with high risks of underestimation of ARGs as they cannot detect ARGs in non-culturable bacteria or non-expressed or silent ARGs (Zhu et al., 2013, Li et al., 2019). However, common environmental pathogens, including *Listeria monocytogenes*, *Salmonella*, *E.coli* and *Campylobacter jejuni*, can enter a non-cultural state (Li et al., 2019)

To overcome the disadvantages of culture-based methods, molecular detection methods started to be widely used in environmental antibiotic resistance studies in the last decades. Commonly used molecular detection methods include polymerase chain reaction (PCR), quantitative PCR (qPCR), and high-throughput quantitative real-time PCR. Since molecular detection methods enable *in situ* analysis and the identification of ARGs in non-culturable bacteria, they can provide a much better reflection of the total ARG pool in an environment than culture-based methods (Li et al., 2019). However, molecular detection methods are associated with the disadvantage of being unable to reflect the real transmission risks of ARGs and primer bias (Li et al., 2019).

Another popular technique for the study of environmental antibiotic resistance is metagenomic analysis. A significant advantage of metagenomic analysis is that it can simultaneously carry out bacterial taxonomy and gene annotation analyses directly from environmental samples. Therefore, compare with molecular detection methods, metagenomics can provide a better reflection of the relationships between microbes and their environmental habitats (Liu et al., 2019, Su et al., 2017). In addition, metagenomics can also avoid problems of molecular detection methods including primer bias and unsuitable primer design (Li et al., 2019). However, metagenomics is also associated with its own short comes. Firstly, metagenomic sequencing is still PCR depended, therefore its sensitivity and accuracy can still

be affected by PCR biases. In addition, lacking sequencing depth is a common problem associated with metagenomic analysis, especially for environmental samples that have a complex microbial composition, for example, soil (Li et al., 2019). In summary, each technique is associated with its advantages and disadvantages. To have a complete characterization of antibiotic resistance in an environment, simultaneously adopting several techniques may be necessary.

1.2 Knowledge gaps

To date, most of the scientific investigations of environmental resistomes have focused on selective pressures related to direct antibiotic usage, including the use of antibiotics in human medication and livestock production, and indirect antibiotic use, for example, application of manure and sewage as fertilizers and wastewater irrigation (Chen et al., 2017, Han et al., 2018). However, the selective pressures are not able to explain the widespread of ARGs in environments that are isolated from the hotspots of antibiotic use, particularly in natural environments.

Another crucial knowledge gap in environmental antibiotic resistance research is that resistomes in plant microbiome, especially the plant phyllosphere (the aerial part of plants) has long been overlooked. Till now, systematic investigations of the relationships between plant phyllosphere and soil resistomes are still lacking. Due to the close relationships between plant and soil, soil is commonly considered as the most important source of plant phyllosphere microorganisms and thus ARGs (Bai et al., 2015). Recently, however, a phyllosphere intrinsic resistome that could not be identified in soil has been reported, suggesting that the mechanisms of ARG evolution in plant phyllosphere and oil in different ecosystems would be necessary for a better understanding of the dissemination of environmental antibiotic resistance and would

contribute to the development of efficient strategies for mitigating problems associated with the spread and of environmental ARGs.

1.3 Objectives of the study and organization of the thesis

Chapter 1 of the thesis is an introductory chapter that covers the background of the study, a literature review on current knowledge about environmental antibiotic resistance, knowledge gaps, objectives of the study, and significance of the study. Chapters 2 to 5 are four research chapters. The specific objectives of each research chapter are as follows:

i. Chapter 2 was an investigation of the occurrence and distribution of ARGs in plant phyllosphere and soil in urban ecosystems aiming to identify the most important factors in influencing the abundance of ARGs in urban environments that are not under direct or indirect selection pressure from antibiotics.

ii. Chapter 3 was an investigation of the most important factors in shaping the assemblies of bacterial communities (the potential hosts of ARGs) in urban ecosystems based on the same set of samples as in Chapter 2. The main objective of this study was to test the hypothesis that in urban ecosystems without antibiotic selection pressure, antibiotic resistome profiles and bacterial community assemblies are shaped by same forces.

iii. Chapter 4 aimed to investigate the biogeographic patterns of resistomes in plant phyllosphere and soil across a large spatial scale and to identify the roles of environmental factors including spatial distance, the interaction among co-occurring microbial communities, climatic and edaphic factors in shaping the resistome profiles in natural ecosystems (Chapter 4).

iv. To gain a more comprehensive understanding of environmental resistomes in natural ecosystems. In Chapter 5 we explored the impacts of soil faunal activities (i.e. termite mound formation) in influencing soil resistome. The main objective of this study was

to investigate whether the changes in soil properties due to soil faunal activities would alter the responses of soil resistome to environmental influences.

1.4 Significance of the study

This study provided new evidence that industrial development related to urbanization is one of the most important factors in influencing both the resistome profiles and bacterial community assemblies in urban ecosystems. In addition, we found that the impacts of industrial development were more significant for the communities in soil than those in plant phyllosphere. These findings provided new insights into the management of potential public health risks associated with 'microbial exposure' in urban ecosystems and would provide valuable information for urban planning in the face of the current rapid rate of urbanization. Moreover, the study provided a systematic investigation of the biogeographic patterns of plant phyllosphere and soil resistomes in natural ecosystems. The findings that the resistome profiles in plant phyllosphere and soil were differently impacted by biotic and abiotic stresses provided novel ecological insights into the evolution of environmental ARGs and their roles in ecosystem multifunctionality.

References

Allen, H.K., Donato, J., Wang, H.H., Cloud-Hansen, K.A., Davies, J., and Handelsman, J. (2010) Call of the wild: antibiotic resistance genes in natural environments. Nat. Rev. Microbiol., 8:251-259.

Andersson, D.I., and Hughes, D. (2010) Antibiotic resistance and its cost: is it possible to reverse resistance? Nat. Rev. Microbiol., 8:260.

Bahram, M., Hildebrand, F., ForslunD, S.K., Anderson, J.L., Soudzilovskaia, N.A., Bodegom, P.M., Bengtsson-Palme, J., Anslan, S., Coelho, L.P., Harend, H., Huerta-Cepas, J., Medema, M.H., Maltz, M.R., Mundra, S., Olsson, P.A., Pent, M., Polme, S., Sunagawa, S., Ryberg, M., Tedersoo, L., and Bork, P. (2018) Structure and function of the global topsoil microbiome. *Nature*, 560:233-237.

Bai, Y., Muller, D.B., Srinivas, G., Garrido-Oter, R., Potthoff, E., Rott, M., Dombrowski, N., Munch, P.C., spaepen, S., Remus-Emsermann, M., Huttel, B., Mchardy, A.C., Vorholt, J.A., and Schulze-Lefert, P. (2015) Functional overlap of the Arabidopsis leaf and root microbiota. *Nature*, 528:364-369.

Bhullar, K., Waglechner, N., Pawlowski, A., Koteva, K., Banks, E.D., Johnston, M.D., Barton, H.A., and Wright, G.D. (2012) Antibiotic resistance is prevalent in an isolated cave microbiome. *PLoS One*, 7:e34953.

Boer, W., Folman, L.B., Summerbell, R.C., and Boddy, L. (2005) Living in a fungal world: impact of fungi on soil bacterial niche development. *FEMS Microbiol. Rev.*, 29:795-811.

Centers for Disease Control and Prevention (2019) Antibiotic Resistance Threats in the United States. https://www.cdc.gov/drugresistance/pdf/threats-report/2019-ar-threats-report-508.pdf

Chen, Q.L., Cui, H.L., Su, J.Q., Penuelas, J., and Zhu, Y.G. (2019) Antibiotic Resistomes in Plant Microbiomes. *Trends Plant Sci*., 24:530-541.

Chen, Q.L., An, X.L., Zhu, Y.G., Su, J.Q., Gillings, M.R., Ye, Z.L., and Cui, L. (2017) Application of Struvite Alters the Antibiotic Resistome in Soil, Rhizosphere, and Phyllosphere. *Environ. Sci. Technol.*, 51:8149-8157.

D'Costa, V.M., King, C.E., Kalan, L., Morar, M., Sung, W.W., Schwarz, C., Froese, D., Zazula, G., Calmels, F., Debruyne, R., Golding, G.B., Poinar, H.N., and Wright, G.D. (2011) Antibiotic resistance is ancient. *Nature*, 477:457-461.

Delgado-Baquerizo, M., Reich, P.B., Trivedi, C., Eldridge, D.J., Abades, S., Alfaro, F.D., Bastida, F., Berhe, A.A., Cutler, N.A., Gallardo, A., Garcia-Velazquez, L., Hart, S.C., Hayes, P.E., He, J.Z., Hseu, Z.Y., Hu, H.W., Kirchmair, M., Neuhauser, S., Perez, C.A., Reed, S.C., Santos, F., Sullivan, B.W., Trivedi, P., Wang, J.T., Weber-Grullon, L., Williams, M.A., and Singh, B.K. (2020) Multiple elements of soil biodiversity drive ecosystem functions across biomes. *Nat. Ecol. Evol.*, 4:210-220.

Demain, A.L. (2009) Antibiotics: natural products essential to human health. *Med. Res. Rev.*, 29:821-842.

Forsberg, K.J., Patel, S., Gibson, M.K., Lauber, C.L., Knight, R., Fierer, N., and Dantas, G. (2014) Bacterial phylogeny structures soil resistomes across habitats. *Nature*, 509:612-616.

Guo, T., Lou, C., Zhai, W., Tang, X., Hashmi, M.Z., Murtaza, R., Li, Y., Liu, X. and Xu, J. (2018) Increased occurrence of heavy metals, antibiotics and resistance genes in surface soil after long-term application of manure. *Sci Total Environ,* 635: 995-1003.

Han, X.M., Hu, H.W., Chen, Q.L., Yang, L.Y., Li, H.L., Zhu, Y.G., Li, X.Z., and Ma, Y.B. (2018) Antibiotic resistance genes and associated bacterial communities in

agricultural soils amended with different sources of animal manures. *Soil Biol. Biochem.*, 126:91-102.

Huang, H., Zeng, S., Dong, X., Li, D., Zhang, Y., He, M., and Du, P. (2019) Diverse and abundant antibiotics and antibiotic resistance genes in an urban water system. *J. Environ. Manage.*, 231:494-503.

Kang, W., Zhang, Y.J., Shi, X., He, J.Z. and Hu, H.W. (2018) Short-term copper exposure as a selection pressure for antibiotic resistance and metal resistance in agricultural soil. *Environ Sci Pollut Res Int,* 25:29314-29324.

Laforest-Lapointe, I., Messier, C. and Kembel, S.W. (2016) Host species identity, site and time drive temperate tree phyllosphere bacterial community structure. *Microbiome,* 4: 27.

Lee, K., Kim, D.W., Lee, D.H., Kim, Y.S., Bu, J.H., Cha, J.H., Thawng, C.N., Hwang, E.M., Seong, H.J., Sul, W.J., Wellington, E.M.H., Quince, C. and Cha, C.J. (2020) Mobile resistome of human gut and pathogen drives anthropogenic bloom of antibiotic resistance. *Microbiome,* 8:2.

Li, B., Chen, Z., Zhang, F., Liu, Y., and Yan, T. (2020) Abundance, diversity and mobility potential of antibiotic resistance genes in pristine Tibetan Plateau soil as revealed by soil metagenomics. *FEMS Microbiol. Ecol.*, 96:fiaa172.

Li, G., Sun, G.X., Ren, Y., Luo, X.S., and Zhu, Y.G. (2018) Urban soil and human health: a review. *Eur. J. Soil Sci.*, 69:196-215.

Li, N., Liu, C., Zhang, Z., Li, H., Song, T., Liang, T., Li, B., Li, L., Feng, S., Su, Q., Ye, J. and Zhu, C. (2019) Research and Technological Advances Regarding the Study of the Spread of Antimicrobial Resistance Genes and Antimicrobial-Resistant Bacteria Related to Animal Husbandry. *Int J Environ Res Public Health,* 24:4896.

Liu, X., Xiao, P., Guo, Y., Liu, L. and Yang, J. (2019) The impacts of different high-throughput profiling approaches on the understanding of bacterial antibiotic resistance genes in a freshwater reservoir. *Sci Total Environ,* 693:133585.

Martínez, J. L. (2008) Antibiotics and antibiotic resistance genes in natural environments. *Science*, 321:365-367.

Mcmahon, M.A., Xu, J., Moore, J.E., Blair, I.S., and Mcdowell, D.A. (2007) Environmental stress and antibiotic resistance in food-related pathogens. *Appl. Environ. Microbiol.*, 73:211-7.

Nesme, J., Cécillon, S., Delmont, T.O., Monier, J.M., Vogel, T.M., and Simonet, P. (2014) Large-scale metagenomic-based study of antibiotic resistance in the environment. *Curr. Biol.*, 24:1096-1100.

Nesme, J., and Simonet, P. (2015) The soil resistome: a critical review on antibiotic resistance origins, ecology and dissemination potential in telluric bacteria. *Environ. Microbiol.*, 17:913-930.

Nwosu, V.C. (2001) Antibiotic resistance with particular reference to soil microorganisms. *Res. Microbiol.* 152:421-430.

Obermeier, M.M., Wicaksono, W.A., Taffner, J., Bergna, A., Poehlein, A., Cernava, T., Lindstaedt, S., Lovric, M., Müller Bogotá, C.A. and Berg, G. (2020) Plant resistome profiling in evolutionary old bog vegetation provides new clues to understand emergence of multi-resistance. *ISME J.* 15:921-937.

Pruden, A., Pei, R., Storteboom, H., and Carlson, K.H. (2006) Antibiotic resistance genes as emerging contaminants: studies in northern Colorado. *Environ. Sci. Technol.*, 40:7445-7450.

Su, J.Q., An, X.L., Li, B., Chen, Q.L., Gillings, M.R., Chen, H., Zhang, T. and Zhu, Y.G. (2017.) Metagenomics of urban sewage identifies an extensively shared antibiotic resistome in China. *Microbiome,* 5:84.

Sun, J., Liao, X.P., D'Souza, A.W., Boolchandani, M., Li, S.H., Cheng, K., Luis Martinez, J., Li, L., Feng, Y.J., Fang, L.X., Huang, T., Xia, J., Yu, Y., Zhou, Y.F., Sun, Y.X., Deng, X.B., Zeng, Z.L., Jiang, H.X., Fang, B.H., Tang, Y.Z., Lian, X.L., Zhang, R.M., Fang, Z.W., Yan, Q.L., Dantas, G. and Liu, Y.H. (2020)a Environmental remodeling of human gut microbiota and antibiotic resistome in livestock farms. *Nat Commun,* 11:1427.

Sun, S., Lu, C., Liu, J., Williams, M.A., Yang, Z., Gao, Y., and Hu, X. (2020) Antibiotic resistance gene abundance and bacterial community structure in soils altered by Ammonium and Nitrate Concentrations. *Soil Biol. Biochem.*, 149:107965.

United Nations (2018) Revision of world urbanization prospects. UN Department of Economic and Social Affairs. https://www.un.org/development/desa/publications/2018-revision-of-world-urbanization-prospects.html

Varela, A.R., Andre, S., Nunes, O.C. and Manaia, C.M. (2014) Insights into the relationship between antimicrobial residues and bacterial populations in a hospital-urban wastewater treatment plant system. *Water Res.,* 54:327-36.

Verraes, C., Van boxstael, S., Van Meervenne, E., Van Coillie, E., Butaye, P., Catry, B., De Schaetzen, M.A., Van Huffel, X., Imberechts, H., Dierick, K., Daube, G., Saegerman, C., De Block, J., Dewulf, J. and Herman, L. (2013) Antimicrobial resistance in the food chain: a review. *Int. J. Environ. Res. Public Health,* 10:2643-69.

Vikesland, P.J., Pruden, A., Alvarez, P.J.J., Aga, D., Burgmann, H., Li, X.D., Manaia, C.M., Nambi, I., Wigginton, K., Zhang, T. and Zhu, Y.G. (2017) Toward a Comprehensive

Strategy to Mitigate Dissemination of Environmental Sources of Antibiotic Resistance. *Environ. Sci. Technol.,* 51:13061-13069.

Walsh, F. (2013) Investigating antibiotic resistance in non-clinical environments. *Front. Microbiol.,* 4:19.

Wang, Y., Lu, J., Engelstädter, J., Zhang, S., Ding, P., Mao, L., Yuan, Z., Bond, P.L. and Guo, J. (2020) Non-antibiotic pharmaceuticals enhance the transmission of exogenous antibiotic resistance genes through bacterial transformation. *ISME J.* 14:2179-2196.

World Health Organization. (2019) New report calls for urgent action to avert antimicrobial resistance crisis. https://www.who.int/news/item/29-04-2019-new-report-calls-for-urgent-action-to-avert-antimicrobial-resistance-crisis

Wright, G.D. (2007) The antibiotic resistome: the nexus of chemical and genetic diversity. *Nat. Rev. Microbiol.*, 5:175-86.

Yang, Y., Li, Z., Song, W., Du, L., Ye, C., Zhao, B., Liu, W., Deng, D., Pan, Y., Lin, H. and Cao, X. (2019) Metagenomic insights into the abundance and composition of resistance genes in aquatic environments: Influence of stratification and geography. *Environ. Int.,* 127:371-380.

Zhang, Y.J., Hu, H.W., Yan, H., Wang, J.T., Lam, S.K., Chen, Q.L., Chen, D., and He, J.Z. (2019) Salinity as a predominant factor modulating the distribution patterns of antibiotic resistance genes in ocean and river beach soils. *Sci. Total. Environ.*, 668:193-203.

Zhu, G., Wang, X., Yang, T., Su, J., Qin, Y., Wang, S., Gillings, M., Wang, C., Ju, F., Lan, B., Liu, C., Li, H., Long, X.E., Wamg, X., Jetten, M.S.M., Wang, Z. and Zhu, Y.G. (2020) Air pollution could drive global dissemination of antibiotic resistance genes. *ISME J.* 15:270-281.

Chapter 2 Characterization of the key factors in influencing antibiotic resistomes in urban ecosystems

This chapter is based on a published article entitled:

Antibiotic resistance in urban green spaces mirrors the pattern of industrial distribution.

Environmental International, 132:105016. https://doi.org/10.1016/j.envint.2019.105106

Environment International 132 (2019) 105106

Contents lists available at ScienceDirect

Environment International

journal homepage: www.elsevier.com/locate/envint

Antibiotic resistance in urban green spaces mirrors the pattern of industrial distribution

Zhen-Zhen Yan, Qing-Lin Chen*, Yu-Jing Zhang, Ji-Zheng He, Hang-Wei Hu*

Faculty of Veterinary and Agricultural Sciences, The University of Melbourne, VIC 3010, Australia

ARTICLE INFO

Handling Editor: Yong-Guan Zhu

Keywords:
Resistome
Urban green spaces
Phyllosphere
Anthropogenic activities
Public health

ABSTRACT

Urban green spaces are closely related to the activities and health of urban residents. Turf grass and soil are two major interfaces between the environmental and human microbiome, which represent potential pathways for the spread of antibiotic resistance genes (ARGs) from environmental to human microbiome through skin-surface contact. However, the information regarding the prevalence of ARGs in urban green spaces and drivers in shaping their distribution patterns remain unclear. Here, we profiled a wide spectrum of ARGs in grass phyllosphere and soils from 40 urban parks across Greater Melbourne, Australia, using high throughput quantitative PCR. A total of 217 and 218 unique ARGs and MGEs were detected in grass phyllosphere and soils, respectively, conferring resistance to almost all major classes of antibiotics commonly used in human and animals. The plant microbiome contained a core resistome, which occupied > 84% of the total abundance of ARGs. In contrast, no core resistome was identified in the soil microbiome. The difference between plant and soil resistome composition was attributed to the difference in bacterial community structure and intensity of environmental and anthropogenic influence. Most importantly, the abundance of ARGs in urban green spaces was significantly positively related to industrial factors including total number of business, number of manufacturing, and number of electricity, gas, water and waste services in the region. Structural equation models further revealed that industrial distribution was a major factor shaping the ARG profiles in urban green spaces after accounting for multiple drivers. These findings have important implications for mitigation of the potential risks posed by ARGs to urban residents.

1. Introduction

Antibiotic resistance genes (ARGs) as a new environmental contaminant of global concern (Pruden et al., 2006) have posed serious threat to human health and resulted in great societal and economic cost worldwide (Andersson and Hughes, 2010; Vikesland et al., 2017). ARGs are ancient in the environment (Berendonk et al., 2015). The environment serves as both the source (Forsberg et al., 2012; Berendonk et al., 2015; Hu et al., 2018) and potential dissemination route of ARGs (Martinez, 2009; Bengtsson-Palme et al., 2018). To mitigate the risk of ARGs, emerging attentions have been devoted to environmental resistome (the collection of ARGs in pathogenic and non-pathogenic bacteria (Wright, 2007)) and factors shaping their distribution patterns (Zhu et al., 2017b; Hu et al., 2018). Urban environment is a unique ecosystem with particular biological, chemical and physical properties different from any natural environment, and is characterized by the close relationships with public health and daily life (Su et al., 2017; Li et al., 2018). According to the United Nations (2018) report, the proportion of world population residing in urban areas was 55% in 2018 and is projected to grow up to 68% by 2050. Given the global trend of urbanization, it is of increasing significance to shed lights into the diversity and composition of resistome in urban microbiomes and their potential risks to public health.

In recent years, numerous studies have investigated the occurrence and abundance of ARGs in various urban environments including urban agricultural system (Mafiz et al., 2018), residential areas with potential metal pollution (Knapp et al., 2017), urban parks irrigated with reclaimed water (Wang et al., 2014; Han et al., 2016), municipal waste landfill areas (Chen et al., 2017b), and urban water system (Huang et al., 2019). These studies consistently reported a high diversity and abundance of ARGs, but majority of them focused on the hotspots of ARGs such as agricultural (Mafiz et al., 2018) and waste (Chen et al., 2017b) related systems in the urban environment. Limited information, however, is available regarding the urban environment with minimal agricultural, waste, or any other point source pollution. The lack of knowledge in the distribution of ARGs and factors shaping the

* Corresponding authors.
E-mail addresses: qinglin.chen@unimelb.edu.au (Q.-L. Chen), hang-wei.hu@unimelb.edu.au (H.-W. Hu).

https://doi.org/10.1016/j.envint.2019.105106
Received 20 June 2019; Received in revised form 5 August 2019; Accepted 16 August 2019
Available online 29 August 2019
0160-4120/ © 2019 The Authors. Published by Elsevier Ltd. This is an open access article under the CC BY-NC-ND license (http://creativecommons.org/licenses/BY-NC-ND/4.0/).

resistome in general urban environment has hampered our ability to effectively tackle antibiotic resistance as a public health problem.

For people living in urban regions, visiting to urban green spaces is one of the most common outdoor activities (Moore et al., 2003). Urban green spaces are mostly used for recreational activities such as jogging and picnicking. In such activities, direct skin contact with turf grass and soil, which are both rich reservoirs of microorganisms, is unavoidable. In this context, urban green spaces provide a potential route for the transmission of environmental microbiome including antibiotic resistant bacteria to human microbiome through skin-surface contact. It is therefore necessary to explore the resistome in urban green spaces in order to understand and monitor the potential human health risk through exposure to ARGs in both grass phyllosphere (Chen et al., 2019) and soil.

In the present study, we collected grass and soil samples from 40 urban parks in Greater Melbourne, Australia. Considering the potential heterogeneity in microbial composition in the urban environment (Mafiz et al., 2018), three samples (by mixing nine soil cores for each sample) were collected from each park to avoid the overlook of variation in samples from the same site. By employing high-throughput qPCR to profile a large spectrum of ARGs, we sought to obtain a comprehensive view of the resistome in urban green spaces with minimal point source pollution. The main aims of this study were to (1) investigate the occurrence and distribution of ARGs in plant (phyllosphere) and soil microbiome in urban green spaces; and (2) identify the most important factors in influencing the abundance and composition of ARGs in urban green spaces.

2. Materials and methods

2.1. Sampling sites and sample collection

Grass and soil samples were collected during May 2018 from 40 urban parks across Greater Melbourne (Fig. S1) as representative of the urban environment with intense anthropogenic impact. During the period of sample collection, weathers were mostly sunny without any rainfall, and temperature ranged from 12.6 to 19.5 °C. None of the sampling parks was under any potential point source pollution such as reclaimed water irrigation (Yi et al., 2019; Han et al., 2016). At each park, three soil samples were collected at a distance of at least 100 m away from each other, and nine soil cores taken from the surface 5 cm soil were mixed for each sample. Grass samples were collected from the above ground part of the plants using sterilized scissors. In total, 120 samples were collected for each sample type (i.e. plant and soil). Detailed sampling site information is shown in Table S1. All samples were transferred into sterilized plastic bags and transported on ice to the laboratory immediately after collection. A portion of the soil samples were gently crumbed to pass through a 2-mm sieve for soil properties analysis and the rest were stored at −80 °C before DNA extraction.

2.2. Soil properties characterization

All soil property analyses were conducted according to the Soil Chemical Methods – Australia (Rayment and Lyons, 2011). Briefly, soil electronic conductivity (EC) and pH were measured in 1:5 soil: water suspension. Soil total carbon (TC) and total nitrogen (TN) were measured via Dumas combustion method using LECO FP628 analyser (LECO Australia Pty Ltd., Baulkham Hills, NSW). Concentrations of heavy metals Cu and Fe were measured by Mehlich 3 multi element test using an Optima 8300 ICP-OSE spectrometer (PerkinElmer, Waltham, Massachusetts, US). Soil cation exchange capacity (CEC) was determined by measuring the concentration of exchangeable bases (Ca^{2+}, Mg^{2+}, Na^{+} and K^{+}) using an Optima 8300 ICO-OES Spectrometer (PerkinElmer, Waltham, Massachusetts, US).

2.3. Collection of anthropogenic parameter data

Anthropogenic parameter data were collected at the Statistical Area Level 4 (SA4) region level. SA4 regions are geographical areas defined in the Australian Statistical Geography Standards using criteria reflecting a balance between respective considerations including population and labour markets. SA4 regions were used for the output of a variety of data including data from 2016 Census of Population and Housing, and Australia Bureau of Statistic (ABS) Labour Force Survey data (ABS, 2016). In the current study, the samplings sites encompassed six SA4 regions i.e. Melbourne – North West, Melbourne – North East, Melbourne – Inner South, Melbourne – Inner, Melbourne – Inner East, and Melbourne – West. Anthropogenic parameters for the SA4 regions were collected from the ABS website (ABS, 2018). Specifically, population densities (people per km^2) were calculated by dividing the population by land area of the SA4 regions; data of median equivalised total household income (AU $ per week) were collected as representative of income of the SA4 regions; data of total number of business, the number of manufacturing and number of electricity, gas, water and waste services were collected as representative of industrial development of the SA4 regions. These parameters were divided into two categories: residential factors including population density (people per km^2) and median equivalised total household income (AU$ per week); and industrial factors including total number of business, number of manufacturing, number of electricity, gas, water and waste services (Table S2).

2.4. DNA extraction

Soil DNA was extracted from 0.25 g soil with the DNeasy PowerSoil Kit (QIAGEN Pty Ltd., Chadstone Centre, VIC, Australia) according to the manufacturer's instructions. Grass phyllosphere DNA was extracted according to previous methods (Chen et al., 2017a; Zhu et al., 2017a; Zhang et al., 2019a) with slight modifications. For each sample, around 10 g grass sample was weighted into 4 sterilized 50 ml centrifuge tubes (around 2.5 *g* grass per tube) with 30 ml autoclaved 0.01 M phosphate buffered saline supplemented with 0.02% Tween 20 in each tube. The tubes were shaken at 250 rpm for 2 h. The obtained solutions were filtered with 40 μm nylon cell strainers into new sterilized 50 ml centrifuge tubes and centrifuged at 4500 rpm for 15 min. After centrifugation, the pellets in all four tubes were transferred into one tube and centrifuged at 4500 rpm for 15 min. The obtained pellets were used for DNA extraction using the DNeasy PowerSoil Kit. The concentrations and quality of all extracted DNA were checked by spectrophotometric analysis using a NanoDrop ND2000c spectrophotometer and agarose gel electrophoresis. The extracted DNA was stored at −20 °C till use.

2.5. High-throughput quantitative PCR

High-throughput qPCR (HT-qPCR) was performed to determine the diversity (i.e. numbers of detected target genes) and abundance of ARGs using the Wafergen SmartChip Real-Time PCR system (Fremont, CA, USA). The HT-qPCR array contained 296 primers, including 285 targeting at ARGs conferring resistance to antibiotics intensively used in human and animals, eight transposon-transposase genes, class 1 integron-integrase gene (*intI1*), clinical class 1 integron-integrase gene (*cintI1*) and the16S rRNA gene (Hu et al., 2016). Amplification was conducted in a 100 nl reaction system. The thermal cycle included an initial enzyme activation at 95 °C for 10 min, followed by 40 cycles of denature at 95 °C for 30 s and annealing at 60 °C for 30 s. The melting process were automatically generated by the Wafergen software. Only well data with single melting peak and an amplification efficiency within 1.8–2.2 were retained. A cycle threshold (C_T) value of 27 was used as detection limit (Zhu et al., 2013). The relative abundances of ARGs and MGEs compared to 16S rRNA gene were calculated with the $2^{-\Delta C_T}$ method, where $\Delta C_T = C_{T(ARG/MGE)} - C_{T(16S\ rRNA\ gene)}$

(Schmittgen and Livak, 2008).

2.6. qPCR analysis of the bacterial 16S rRNA gene

Real-time qPCR analysis of the bacterial 16S rRNA gene in the samples was performed on a Bio-Rad CFX384 Real-Time PCR Detection system (Bio-Rad, Hercules, USA) using the same primer pair with HT-qPCR. Each 20 μl amplification system contained 10 μl SensiMix SYBR No-ROX reagent (Bioline, London, UK), 0.8 μl each primer (10 μM), and 2 μl DNA template. The following amplification condition was used: an initial enzyme activation at 95 °C for 10 min, followed by 35 cycles of denaturation at 95 °C for 10 s, simultaneous annealing and extension at 55 °C for 30 s. To verify the specificity of the PCR amplicons, a melting profile from 65 °C to 95 °C was included in the PCR program immediately following the thermal cycles. To generate the standard curves, PCR amplicons of the bacterial 16S rRNA gene using the same primer pair were purified and ligated into the pGEM-T easy vector (Promega, Madison, WI, USA), and then transformed into JM109 competent cells. The colonies containing the correct inserts of the bacterial 16S rRNA gene sequence were selected for plasmid DNA extraction. Ten-fold serial dilutions of the extracted plasmid DNA were used for standard curve generation.

2.7. Illumine sequencing and data processing

The hypervariable V3 – V4 region of the bacterial 16S rRNA gene was amplified for the bacterial community composition characterization using the barcode primer pair 341F: CCTACGGGRBGCASCAG and 806R: GGACTACYVGGGTATCTAAT (Yu et al., 2005) on the Illumina Miseq platform at Australian Genome Research Facility. The thermal condition was 94 °C for 10 min, followed by 25 cycles of 94 °C for 10 s, then 60 °C for 30 s. After filtering adaptor sequences and barcodes, removing ambiguous nucleotides and low-quality reads, the cleaned raw pair-ended reads were merged using FLASH (Magoč and Salzberg, 2011). Further data processing including operational taxonomic unit (OTU) picking, de-multiplexing sequences and assignment of merged sequences to samples was conducted using Quantitative Insights into Microbial Ecology (QIIME) (Caporaso et al., 2010). OTUs were defined based on the similarity threshold of 97% using UCLUST (Edgar, 2010). Chimeric sequences, chloroplast and mitochondrial OTUs and singleton OTUs were discarded from the final OTU data set. Taxonomic classification and quantification of OTUs were performed against the Greengenes 16S rRNA database version 13.5 (McDonald et al., 2012). Raw sequences have been deposited in the National Center for Biotechnology Information (NCBI) Sequence Read Archive (SRA) under the accession number PRJNA549108 (SRP201640).

2.8. Statistical analysis

Mathematical operations on raw data such as average, sum etc. were conducted in Microsoft Excel 2016 (Microsoft, USA). All statistical analysis was considered significant at $P < 0.05$ level. Principal coordinate analysis (PCoA) based on the Bray-Curtis distance and Adonis test were conducted to evaluate the profiles of resistome and microbiome using the 'vegan' package (Oksanen et al., 2007) in R 3.5.2 (R Core Team, 2015). Ordinary least square (OLS) regression models were constructed to determine the relationships between the abundance of MGEs, *cint1* gene and ARGs and visualized using the 'ggplot 2' package (Wickham, 2016) in R. Correlations between anthropogenic factors and resistomes were investigated by Spearman's ranked correlation using SPSS 25.

2.9. Random forest modelling and structural equation models construction

Random forest modelling (Breiman, 2001) was used to identify the main predictors of antibiotic resistome in urban green spaces with the package of 'randomForest' (Liaw and Wiener, 2002) and 'rfPermute' (Archer, 2016) in R. In our random forest models, MGEs, soil properties (Table S3), anthropogenic factors, bacterial abundance, and the relative abundance of the ten most abundant phyla in the samples were included as predictors of ARG abundance. Increase in the mean square error (MSE) was used to determine the importance of drivers of ARG abundance. The MSE was computed for each tree and averaged across 5000 trees (Delgado-Baquerizo et al., 2016; Trivedi et al., 2016).

We generated structural equation models (SEMs) (Pugesek et al., 2003) to test the casual relationships between soil properties, industrial factors, bacterial abundance and diversity, and abundance of MGEs and ARGs. *A prior* model was established based on known effects and relationships among the drivers of resistome (Fig. S2). Pairwise correlations among standardized data using *Z*-scores were determined using SPSS 25. The covariance matrixes were imported into AMOS 25 for SEM construction. The overall goodness of fit for SEMs was determined by multiple goodness-of-fit criteria: $\chi 2$ test $P > 0.05$, goodness-of-fit index (GFI) > 0.90, root mean square error of approximation (RMSEA) < 0.10 (Schermelleh-Engel et al., 2003). Standardized total effects of each drivers on ARG abundance were calculated by summing both direct and indirect effects.

3. Results

3.1. Characterization of resistome in urban green spaces

By using HT-qPCR, a total of 217 and 218 unique ARGs and MGEs were detected in all grass phyllosphere and soil samples, respectively.

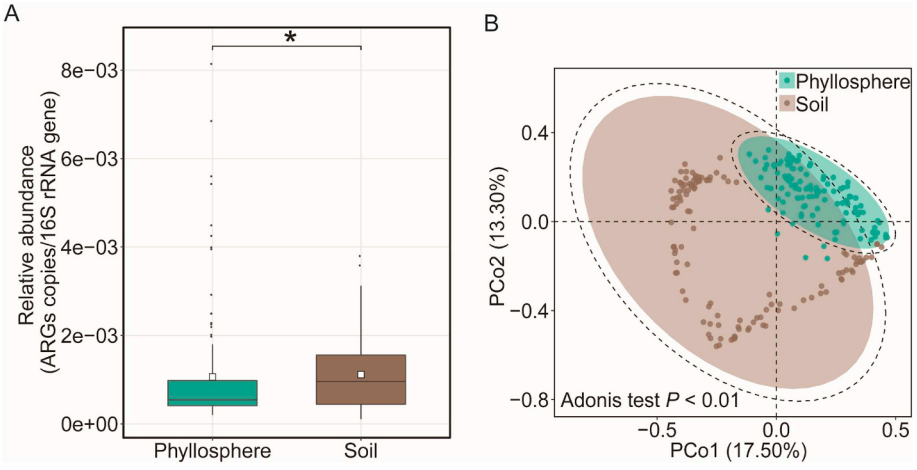

Fig. 1. Resistome profiles based on the relative abundance of ARGs in grass phyllosphere and soil samples. (A) Boxplot of the relative abundance of ARGs detected in samples * indicates $P < 0.05$ determined by paired *t*-test. (B) Principal coordinate analysis (PCoA) based on the Bray-Curtis distance showing the distribution patterns of ARGs in samples.

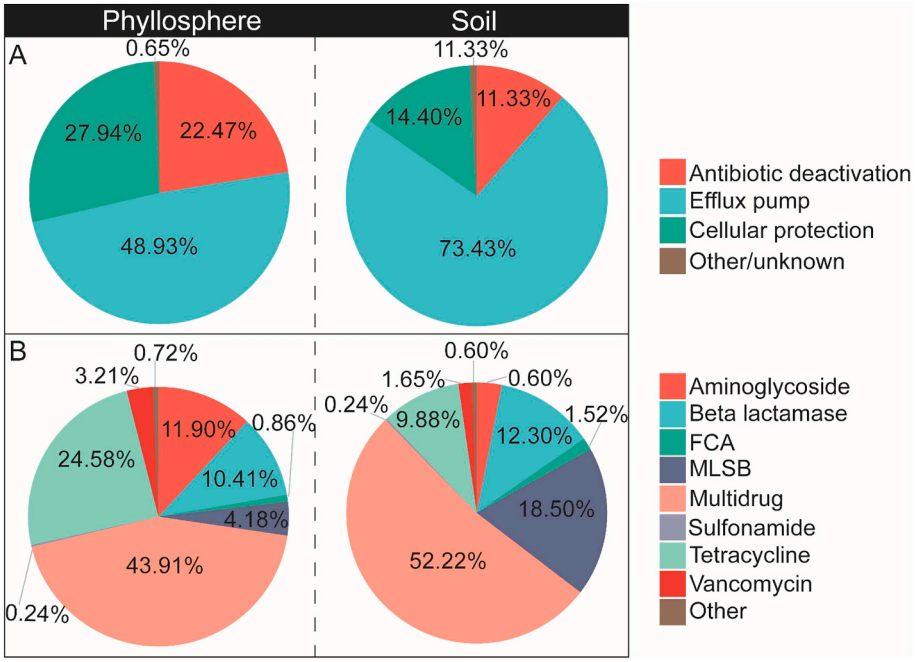

Fig. 2. (A) Classification of ARGs detected in grass phyllosphere and soil based on the mechanism of resistance. (B) The antibiotic to which the ARGs confer resistance.

The normalized relative abundance of ARGs in soil was significantly higher than that in grass phyllosphere (paired *t*-test, $P < 0.05$) (Fig. 1A). The Bray-Curtis distance based PCoA (Fig. 1B) showed that ARGs in grass phyllosphere clustered together and were separated from those in soil along both PCo1 and PCo2 axes, which explained 13.30% and 17.50% of the variance of ARGs, respectively. This result indicated that the overall pattern of ARGs in soil was distinct from that in grass phyllosphere, which was supported by the Adonis test result ($P < 0.01$).

The detected ARGs encompassed all three major antibiotic resistance mechanisms, with efflux pump being the dominant resistance mechanism (Fig. 2A). Based on the class of antibiotics the genes confer resistance to, we classified ARGs into eight types i.e. aminoglycoside, beta-lactams, sulfonamide, chloramphenicol and amphenicol (FCA), macrolide-lincosamide-streptogramin B (MLSB), multidrug, tetracycline, and vancomycin resistance genes. Multidrug resistance genes were the most abundant type of ARGs, which accounted for 43.91% and 52.22% of the total abundance in grass phyllosphere and soil, respectively (Fig. 2B). The second and third most abundant types of ARGs were tetracycline (24.58%) and aminoglycoside (11.90%) in grass phyllosphere, compared to MLSB (18.50%) and beta lactamase (12.30%) in soil (Fig. 2B).

In addition to ARGs, diverse mobile genetic elements (MGEs) were also detected. Eight MGEs including six transposon-transposase genes, class 1 integron-integrase gene (*intI1*) and clinical class 1 integron-integrase gene (*cintI1*) were detected in either soil or grass phyllopshere. Due to the important role of MGEs in spreading ARGs via horizontal gene transfer (HGT), the relationships between the abundance of ARGs and MGEs were determined using the ordinary least-square (OLS) regression model. Positive linear relationships were observed between the abundance of ARGs and MGEs in both grass phyllosphere ($R^2 = 0.568$, $P < 0.01$) and soil ($R^2 = 0.673$, $P < 0.01$) (Fig. 3). Besides the abundance of total MGEs, the relationships between the abundance of ARGs and clinical class 1 integron-integrase gene (*intI1*) were also maintained in both grass phyllosphere samples ($R^2 = 0.345$, $P < 0.01$) and soil samples ($R^2 = 0.664$, $P < 0.01$) (Fig. 3).

3.2. Characterization of microbial community in urban green spaces

In total, 8,763,444 and 7,679,982 high-quality sequences were obtained by Miseq sequencing for grass phyllosphere and soil, respectively. These sequences were clustered into OTUs at 97% similarity level. Overall, 1,414,528 and 2,987,180 OTUs were used for downstream analysis for grass phyllosphere and soil, respectively. In grass phyllosphere, the OTUs were assembled into 35 phyla and 115 classes. Proteobacteria were the most abundant phylum, accounting for 77.14% of the total bacterial sequences (Fig. S3). The second and third most abundant phyla were Bacteroides (18.04%) and Actinobacteria (2.96%) (Fig. S3). For soil, the OTUs were assembled into 45 phyla and 141 classes. Actinobacteria (41.58%) and Proteobacteria (30.64%) were top two dominant phyla followed by Acidobacteria (10.94%) (Fig. S3). Bacterial alpha-diversity in soil was significantly higher than that in grass phyllosphere (paired *t*-test, $P < 0.001$), which was confirmed by both Chao1 estimator and Shannon diversity index (Fig. 4A). The Bray-Curtis distance based PCoA revealed a significant (Adonis test $P < 0.01$) difference in bacterial profiles between the grass phyllosphere and soil (Fig. 4B). Soil samples well clustered together and were separated from grass phyllosphere samples along the PCo1 axis, which explained 11.03% of the total variance.

3.3. Core resistome and core microbiome in urban green spaces

In grass phyllosphere, 33 genes were shared among > 80% of the samples, which accounted for up to 84.25% of the total abundance of the resistome (Fig. 5). These frequently occurred genes were defined as the grass phyllosphere core resistome. The grass phyllosphere core resistome was dominated by genes associated with multidrug and tetracycline resistance genes and MGEs (Fig. S4). As for the soil samples, no core resistome was identified, as only three genes (*cintI1*, *oprJ* and *oleC*) were shared by > 80% of the samples (accounting for < 25% of the total abundance of ARGs).

The core microbiomes in urban green spaces were also identified. For grass phyllosphere, 13.59% of genera were shared among > 80% of the samples, which accounted for 97.78% of the total sequences (Fig. S5). For soil, 24.90% of genera were shared among > 80% of the

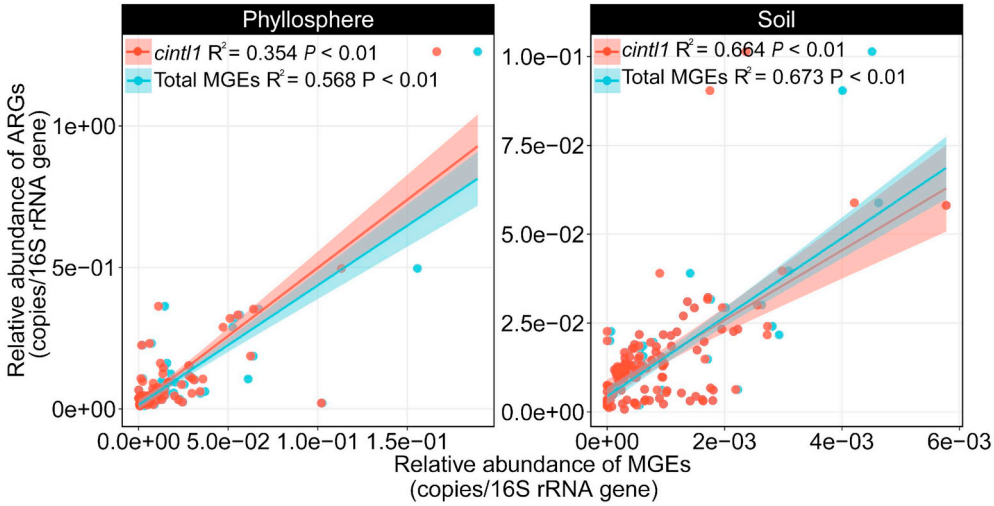

Fig. 3. Ordinary least square (OLS) regression showing the relationships between the relative abundance of ARGs and that of total MGEs and clinical class 1 integron-integrase gene (*cintl1*) in grass phyllosphere and soil samples.

samples, which accounted for 96.22% of the total sequences (Fig. S5).

3.4. Correlations between anthropogenic factors and resistome in urban green spaces

In general, industrial factors exhibited more intensive correlations with soil resistome than with grass phyllosphere resistome (Table 1). No significant positive correlations were observed between residential factors and resistome in either grass phyllosphere or soil. On the contrary, significant positive correlations between industrial factors and resistome were identified. For instance, in grass phyllosphere, the number of electricity, gas, water and waste services and number of manufacturing were significantly ($P < 0.05$) and positively correlated with the abundance of total ARGs and FCA resistance genes, respectively (Table 1). For soil, all industrial factors were significantly and positively correlated with the abundance of total ARGs ($P < 0.01$) and aminoglycoside resistance genes ($P < 0.05$) and (Table 1). In addition, the number of manufacturing and number of electricity, gas, water and waste services were significantly ($P < 0.05$) and positively correlated with the abundance of various classes of ARGs including aminoglycoside, beta-lactams, multidrug, and vancomycin resistance genes (Table 1).

3.5. Multi-drivers accounting for resistome in urban green spaces

Heteroscedastic nature of the results indicated that multiple factors could potentially impact the resistome profiles in urban green spaces. Therefore, we used random forest modelling to identify the main predictors of the abundance of ARGs in both sample types. The results showed that MGEs and bacterial abundance were the two most important drivers of the ARG abundance in grass phyllosphere (Fig. S6A). The abundance of MGEs was the most important driver of the ARG abundance in soil, while anthropogenic factors had unneglectable contributions to ARG abundance (Fig. S6B).

Structural equation models (SEMs) were used to further explore the casual relationships between multiple factors and the ARG abundance. Our SEMs explained 28% and 63% of the variances of ARG abundances in grass phyllosphere and soil, respectively (Fig. 6). In both grass phyllosphere and soil, the abundance of MGEs was the most dominant positive factor shaping the ARG profile (Fig. 6), which was consistent with the random forest analysis (Fig. S6). The most important finding of our SEMs was that industrial factors had direct positive effects on the abundance of ARGs in both grass phyllosphere ($\lambda = 0.14$, $P < 0.01$) and soil ($\lambda = 0.15$, $P < 0.01$) even when accounting for multiple factors, which was in consistence with Spearman's ranked correlation

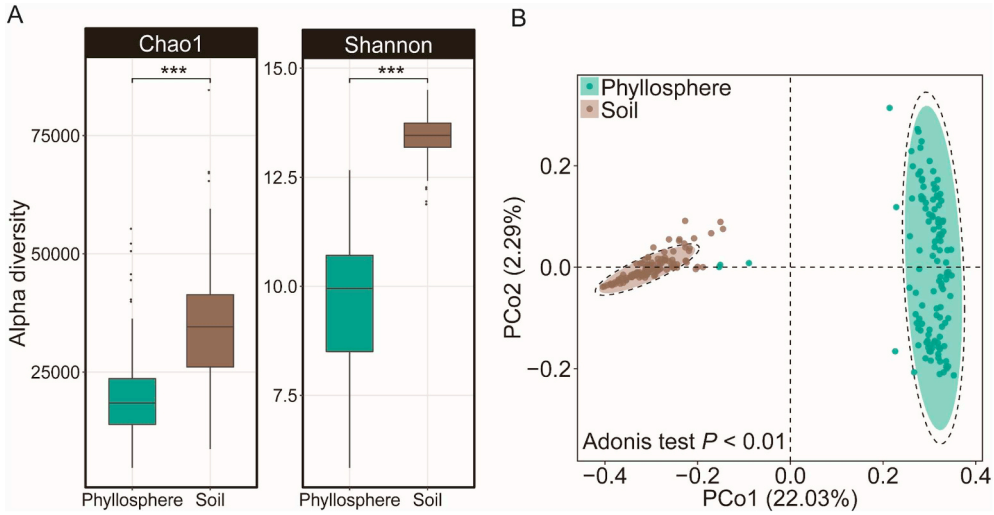

Fig. 4. (A) Bacterial alpha diversity in phyllosphere and soil samples, *** indicates $P < 0.001$ determined by paired *t*-test. (B) Principal coordinate analysis (PCoA) based on the Bray-Curtis distance showing the distribution pattern of bacterial communities (beta diversity) in phyllosphere and soil samples.

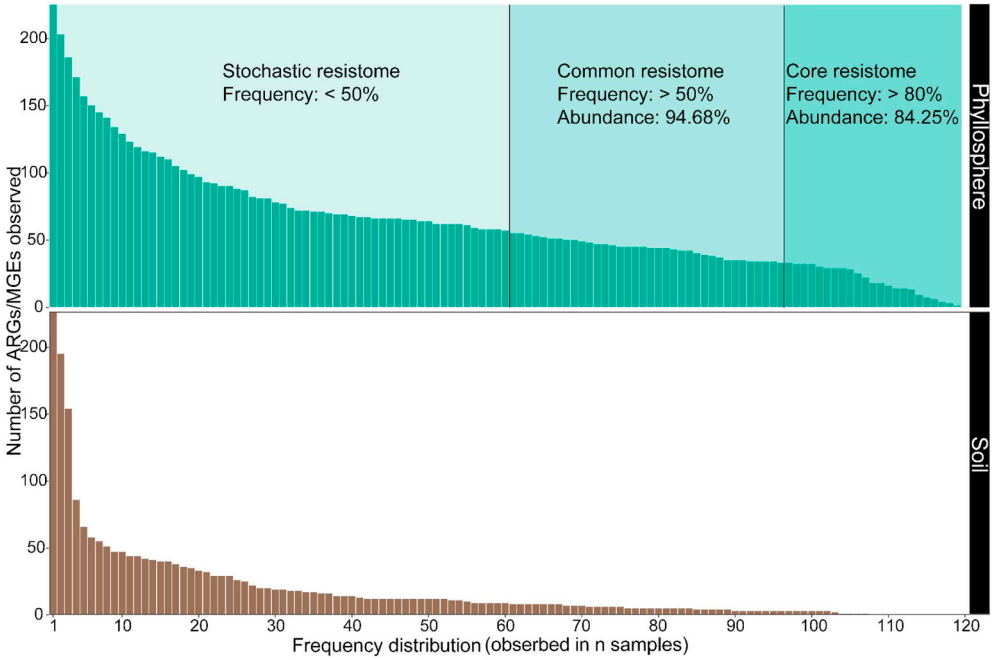

Fig. 5. Frequency distribution of ARGs in grass phyllosphere and soil.

Table 1
Spearman's ranked correlation coefficients between industrial factors and the abundance of ARGs and MGEs.

Items		Industrial factors		
		Total number of business	Number of manufacturing	Number of electricity, gas, water and waste services
Phyllosphere	Total ARGs	0.089	0.166	**0.201***
	Aminoglycoside	−0.016	0.020	0.032
	Beta Lactamase	−0.015	0.066	0.086
	FCA	0.071	**0.181***	0.174
	Multidrug	−0.011	−0.005	−0.005
	Vancomycin	−0.062	0.0250	0.0550
Soil	Total ARGs	**0.180***	**0.290****	**0.387****
	Aminoglycoside	**0.182***	**0.247****	**0.290****
	Beta Lactamase	0.013	**0.185***	**0.223***
	FCA	−0.0020	−0.0180	−0.019
	Multidrug	0.139	**0.231***	**0.342****
	Vancomycin	0.115	**0.193***	**0.235****

Note:
* $P < 0.05$.
** $P < 0.01$. Significant correlations ($P < 0.05$) are indicated in bold.

results (Table 1).

4. Discussion

4.1. Antibiotic resistance in urban green spaces

In the present study, diverse ARGs were detected in both grass phyllosphere and soil in urban parks, which indicated that urban green spaces, which are closely related to public daily life, are hotspots of antibiotic resistance. A core resistome was identified in grass phyllosphere but not in soil (Fig. 5), indicating that there were dominant and stable ARGs shared by grass phyllopshere across the 40 urban parks but not by soils. There are two potential reasons that may explain the difference between grass phyllosphere and soil resistomes. (1) It has been reported that bacterial phylogeny is a primary determinant of resistome content in diverse environments including soil (Forsberg et al., 2014), drinking water (Jia et al., 2015) and vegetables (Zhu et al., 2017a). Our SEMs also confirmed that for both sample types, bacterial diversity indirectly impacted ARG profiles through its direct impact on the MGE abundance (Fig. 6). The less diverse bacterial community in grass phyllosphere, compared with soil, could be the major contributor to the variations of ARGs between soil and phyllosphere (Fig. 4A). (2) Compared with soil microbiome, the plant microbiome is more easily affected by the fluctuation in surrounding abiotic conditions such as moisture, temperature and radiation (Cordovez et al., 2019), which may act as stress factors contributing to the development of the bacterial resistance (Storz and Hengge, 2010; Zhang et al., 2019b).

Horizontal gene transfer (HGT) mediated by MGEs may facilitate the dissemination of ARGs across different phylogeny (Gaze et al., 2011; Gillings, 2014). MGEs are efficient vehicles in carrying ARGs (Marti et al., 2014), for example, class 1 integron can be used by bacteria to stockpile and express exogenous resistance genes (An et al., 2018a). In this study, a high diversity of MGEs was consistently detected in both grass phyllosphere and soil in urban parks. Our SEMs together with random forest modelling (Fig. S6) indicated that MGEs were the most important factor shaping the abundance of ARGs in both phyllosphere and soil, consistent with the OLS regression model that the abundance of ARGs was significantly correlated with that of MGEs (Fig. 3). Our findings are in line with previous observations that the phyllosphere and rhizosphere are key areas for HGT (Chen et al., 2017b; An et al., 2018b), because of the high possibility of cell clustering and biofilm forming due to the high bacterial metabolic rates and mobility in such areas (Van Elsas et al., 2003; Danhorn and Fuqua, 2007). Together these results indicated that the potential of HGT in spreading ARGs in urban green spaces should not be overlooked.

4.2. Industrial distribution shaping the distribution of ARGs

The present study was conducted in urban parks with no point source pollution, and there was minimal difference in environmental factors, such as temperature and rainfall, among the sampling sites. Thus, the diverse ARGs detected are likely influenced or contributed by anthropogenic influence. Notably, strong correlations between the abundance of ARGs and *cintI1* gene, which was recognized as a marker of anthropogenic impact (Gillings et al., 2015), were detected in both

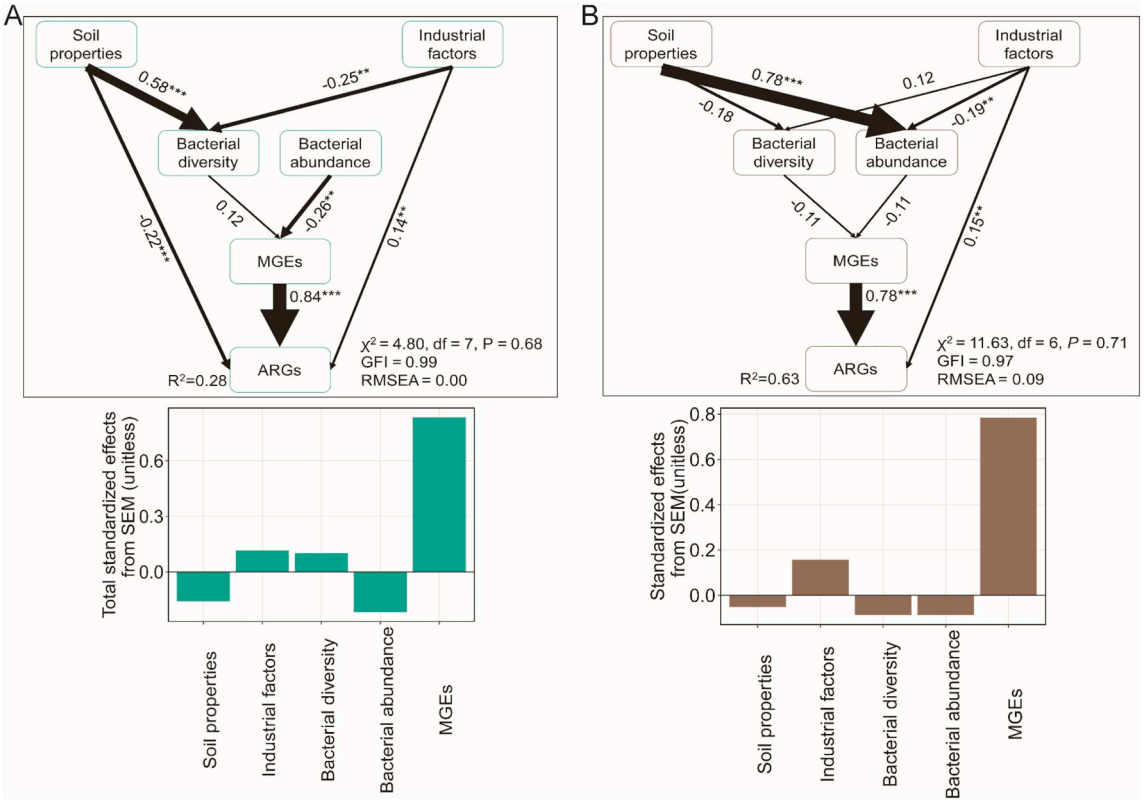

Fig. 6. Structural equation models (SEMs) showing the direct and indirect effects of multiple factors on the abundance of ARGs in grass phyllosphere (A) and soil (B). Numbers adjacent to arrows are standardized path coefficients. Width of the arrows is proportional to the strength of path coefficients. R^2 indicates the proportion of variance in ARG abundance explained by the model. Significant levels are indicated as $^{**}P < 0.01$ and $^{***}P < 0.001$. Standardized effects are derived from the structural equation models.

grass phyllosphere and soil (Fig. 3). No positive correlation was observed between residential factors (population density and median equivalised total household income) and the abundance of ARGs in either grass phyllosphere or soil. These findings are in agreement with a recent study by Zhu et al. (2017b), which suggested that population or gross domestic product was not a sensitive indicator for the distribution of antibiotic resistance. However, we observed that industrial factors substantially contributed to the occurrence of ARGs in urban green spaces (Table 1). The SEM results showed that industrial factors had direct and positive impacts on the ARG abundance in both grass and soil. The significant correlations between industrial factors, particularly the number of manufacturing and electricity, gas, water and waste services, with the abundance of aminoglycoside, beta lactamase, multidrug, and vancomycin resistance genes (Table 1), demonstrated that industrial pollution might be an important source of these types of ARGs in urban green spaces.

One of the potential explanations for the observed differences between residential and industrial factors in impacting resistome in urban green spaces might be the differences in the chemical compositions between municipal and industrial wastes in the waste treatment processes (Fiorentino et al., 2019; Pärnänen et al., 2019). It has been demonstrated that compared to municipal waste, industrial waste is characterized by a high concentration of metals (Fiorentino et al., 2019; Dolar et al., 2016). Metal contamination is often associated with antibiotic resistance due to the potential co-selection process of ARGs and certain metal resistance genes (Baker-Austin et al., 2006; Hu et al., 2016; Hu et al., 2017). In this study, the urban parks studied are all under no direct sewage pollution. Therefore, atmospheric deposition of industrial pollutants, rather than industrial wastewater contamination, was more likely to be one of the key reasons for the dominant contribution of industrial distribution to the resistome in urban green spaces. This finding is supported by several former studies that reported the threats of airborne transmission of ARGs in urban environments (Li et al., 2016; Echeverria-Palencia et al., 2017).

5. Conclusions

In summary, the present study provided a comprehensive profile of resistome in urban green spaces. Our results showed that urban green spaces with no point source pollution are potential reservoir of diverse ARGs. A core resistome was observed in grass phyllosphere but not in soil microbiome. We found that industrial factors are the major drivers shaping the resistome profile in urban green spaces and contributing to elevated level of ARGs. These findings extend our knowledge regarding the distribution patterns of ARGs in general urban environments closely related to the daily life of urban residents and have implications for the management of the potential public health risk related to the transmission of environmental ARGs to human pathogens.

Declaration of competing interest

We declare no conflict of interest.

Acknowledgements

This work was financially supported by the Australian Research Council (DP170103628).

Appendix A. Supplementary data

Supplementary data to this article can be found online at https://doi.org/10.1016/j.envint.2019.105106.

References

An, X.L., Chen, Q.L., Zhu, D., Zhu, Y.G., Gillings, M.R., Su, J.Q., 2018a. Impact of wastewater treatment on the prevalence of integrons and the genetic diversity of integron gene cassettes. Appl. Environ. Microbiol. 84, e02766–17.

An, X.L., Chen, Q.L., Zhu, D., Su, J.Q., 2018b. Distinct effects of struvite and biochar amendment on the class 1 integron antibiotic resistance gene cassettes in phyllosphere and rhizosphere. Sci. Total Environ. 631–632, 668–676.

Andersson, D.I., Hughes, D., 2010. Antibiotic resistance and its cost: is it possible to reverse resistance? Nat. Rev. Microbiol. 8, 260.

Archer, E., 2016. rfPermute: Estimate Permutation P-Values for Random Forest Importance Metrics. R Package (Zenodo), Version, 2.

Australian Bureau of Statistics (ABS), 2016. Australian Statistical Geography Standard (ASGS): Volume 1 - Main Structure and Greater Capital City Statistical Areas. https://www.abs.gov.au/.

Australian Bureau of Statistics (ABS), 2018. Data by Region. https://itt.abs.gov.au/itt/r.jsp?databyregion&ref=CTA2#/.

Baker-austin, C., Wright, M.S., Stepanauskas, R., Mcarthur, J., 2006. Co-selection of antibiotic and metal resistance. Trends Microbiol. 14, 176–182.

Bengtsson-palme, J., Kristiansson, E., Larsson, D.G.J., 2018. Environmental factors influencing the development and spread of antibiotic resistance. FEMS Microbiol. Rev. 42.

Berendonk, T.U., Manaia, C.M., Merlin, C., Fatta-kassinos, D., Cytryn, E., Walsh, F., Bürgmann, H., Sørum, H., Norström, M., Pons, M.N., 2015. Tackling antibiotic resistance: the environmental framework. Nat. Rev. Microbiol. 13, 310.

Breiman, L., 2001. Random forests. Mach. Learn. 45, 5–32.

Caporaso, J.G., Kuczynski, J., Stombaugh, J., Bittinger, K., Bushman, F.D., Costello, E.K., Fierer, N., Pena, A.G., Goodrich, J.K., Gordon, J.I., 2010. QIIME allows analysis of high-throughput community sequencing data. Nat. Methods 7, 335.

Chen, Q.L., An, X.L., Zhu, Y.G., Su, J.Q., Gillings, M.R., Ye, Z.L., Cui, L., 2017a. Application of struvite alters the antibiotic resistome in soil, rhizosphere, and phyllosphere. Environ. Sci. Technol. 51, 8149–8157.

Chen, Q.L., Li, H., Zhou, X.Y., Zhao, Y., Su, J.Q., Zhang, X., Huang, F.Y., 2017b. An underappreciated hotspot of antibiotic resistance: the groundwater near the municipal solid waste landfill. Sci. Total Environ. 609, 966–973.

Chen, Q.L., Cui, H.L., Su, J.Q., Penuelas, J., Zhu, Y.G., 2019. Antibiotic resistomes in plant microbiomes. Trends Plant Sci. 24, 530–541.

Cordovez, V., Dini-andreote, F., Carrion, V.J., Raaijmakers, J.M., 2019. Ecology and evolution of plant microbiomes. Annu. Rev. Microbiol. 73. https://doi.org/10.1146/annurev-micro-090817-062524.

Danhorn, T., Fuqua, C., 2007. Biofilm formation by plant-associated bacteria. Annu. Rev. Microbiol. 61, 401–422.

Delgado-baquerizo, M., Maestre, F.T., Reich, P.B., Jeffries, T.C., Gaitan, J.J., Encinar, D., Berdugo, M., Campbell, C.D., Singh, B.K., 2016. Microbial diversity drives multifunctionality in terrestrial ecosystems. Nat. Commun. 7, 10541.

Dolar, D., Košutić, K., Strmecky, T., 2016. Hybrid processes for treatment of landfill leachate: coagulation/UF/NF-RO and adsorption/UF/NF-RO. Sep. Purif. Technol. 168, 39–46.

Echeverria-Palencia, C.M., Thulsiraj, V., Tran, N., Ericksen, C.A., Melendez, I., Sanchez, M.G., Walpert, D., Yuan, T., Ficara, E., Senthilkumar, N., Sun, F., Li, R., Hernandez-Cira, M., Gamboa, D., Haro, H., Paulson, S.E., Zhu, Y., Jay, J.A., 2017. Disparate antibiotic resistance gene quantities revealed across 4 major cities in California: a survey in drinking water, air, and soil at 24 public parks. ACS Omega 2, 2255–2263.

Edgar, R.C., 2010. Search and clustering orders of magnitude faster than BLAST. Bioinformatics 26, 2460–2461.

Fiorentino, A., Di Cesare, A., Eckert, E.M., Rizzo, L., Fontaneto, D., Yang, Y., Corno, G., 2019. Impact of industrial wastewater on the dynamics of antibiotic resistance genes in a full-scale urban wastewater treatment plant. Sci. Total Environ. 646, 1204–1210.

Forsberg, K.J., Reyes, A., Wang, B., Selleck, E.M., Sommer, M.O., Dantas, G., 2012. The shared antibiotic resistome of soil bacteria and human pathogens. Science 337, 1107–1111.

Forsberg, K.J., Patel, S., Gibson, M.K., Lauber, C.L., Knight, R., Fierer, N., Dantas, G., 2014. Bacterial phylogeny structures soil resistomes across habitats. Nature 509, 612.

Gaze, W.H., Zhang, L., Abdouslam, N.A., Hawkey, P.M., Calvo-bado, L., Royle, J., Brown, H., Davis, S., Kay, P., Boxall, A.B., 2011. Impacts of anthropogenic activity on the ecology of class 1 integrons and integron-associated genes in the environment. ISME J 5, 1253.

Gillings, M.R., 2014. Integrons: past, present, and future. Microbiol. Mol. Biol. Rev. 78, 257–277.

Gillings, M.R., Gaze, W.H., Pruden, A., Smalla, K., Tiedje, J.M., ZHU, Y.G., 2015. Using the class 1 integron-integrase gene as a proxy for anthropogenic pollution. ISME J 9, 1269–1279.

Han, X.M., Hu, H.W., Shi, X.Z., Wang, J.T., Han, L.L., Chen, D., He, J.Z., 2016. Impacts of reclaimed water irrigation on soil antibiotic resistome in urban parks of Victoria, Australia. Environ. Pollut. 211, 48–57.

Hu, H.W., Wang, J.T., Li, J., Li, J.J., Ma, Y.B., Chen, D., He, J.Z., 2016. Field-based evidence for copper contamination induced changes of antibiotic resistance in agricultural soils. Environ. Microbiol. 18, 3896–3909.

Hu, H.W., Wang, J.T., Li, J., Shi, X.Z., Ma, Y., Chen, D., He, J.Z., 2017. Long-term nickel contamination increases the occurrence of antibiotic resistance genes in agricultural soils. Environ. Sci. Technol. 51, 790–800.

Hu, H.W., Wang, J.T., Singh, B.K., Liu, Y.R., Chen, Y.L., Zhang, Y.J., He, J.Z., 2018. Diversity of herbaceous plants and bacterial communities regulates soil resistome across forest biomes. Environ. Microbiol. 20, 3186–3200.

Huang, H., Zeng, S., Dong, X., Li, D., Zhang, Y., He, M., Du, P., 2019. Diverse and abundant antibiotics and antibiotic resistance genes in an urban water system. J. Environ. Manag. 231, 494–503.

Jia, S., Shi, P., Hu, Q., Li, B., Zhang, T., Zhang, X.X., 2015. Bacterial community shift drives antibiotic resistance promotion during drinking water chlorination. Environ. Sci. Technol. 49, 12271–12279.

Knapp, C.W., Callan, A.C., Aitken, B., Shearn, R., Koenders, A., Hinwood, A., 2017. Relationship between antibiotic resistance genes and metals in residential soil samples from Western Australia. Environ. Sci. Pollut. Res. Int. 24, 2484–2494.

Li, J., Zhou, L., Zhang, X., Xu, C., Dong, L., Yao, M., 2016. Bioaerosol emissions and detection of airborne antibiotic resistance genes from a wastewater treatment plant. Atmos. Environ. 124, 404–412.

Li, G., Sun, G.X., Ren, Y., Luo, X.S., Zhu, Y.G., 2018. Urban soil and human health: a review. Eur. J. Soil Sci. 69, 196–215.

Liaw, A., Wiener, M., 2002. Classification and regression by randomForest. R, News. 2, 18–22.

Mafiz, A., Perera, L.N., He, Y., Zhang, W., Xiao, S., Hao, W., Sun, S., Zhou, K., Zhang, Y., 2018. Case study on the soil antibiotic resistome in an urban community garden. Int. J. Antimicrob. Agents 52, 241–250.

Magoč, T., Salzberg, S.L., 2011. FLASH: fast length adjustment of short reads to improve genome assemblies. Bioinformatics 27, 2957–2963.

Marti, E., Variatza, E., Balcazar, J.L., 2014. The role of aquatic ecosystems as reservoirs of antibiotic resistance. Trends Microbiol. 22, 36–41.

Martinez, J.L., 2009. Environmental pollution by antibiotics and by antibiotic resistance determinants. Environ. Pollut. 157, 2893–2902.

Mcdonald, D., Price, M.N., Goodrich, J., Nawrocki, E.P., Desantis, T.Z., Probst, A., Andersen, G.L., Knight, R., Hugenholtz, P., 2012. An improved Greengenes taxonomy with explicit ranks for ecological and evolutionary analyses of bacteria and archaea. ISME J 6, 610.

Moore, M., Gould, P., Keary, B.S., 2003. Global urbanization and impact on health. Int. J. Hyg. Environ. Health 206, 269–278.

Oksanen, J., Kindt, R., Legendre, P., O'Hara, B., Stevens, M.H.H., Oksanen, M.J., Suggests, M.A.S.S., 2007. The Vegan Package. Community Ecology Package. 10. pp. 631–637.

Pärnänen, K.M.M., Narciso-da-rocha, C., Kneis, D., Berendonk, T.U., Cacace, D., Do, T.T., Elpers, C., Fatta-kassinos, D., Henriques, I., Jaeger, T., Karkman, A., Martinez, J.L., Michael, S.G., Michael-kordatou, I., O'sullivan, K., Rodriguez-mozaz, S., Schwartz, T., Sheng, H., Sørum, H., Stedtfeld, R.D., Tiedje, J.M., Giustina, S.V.D., Walsh, F., Vazmoreira, I., Virta, M., Manaia, C.M., 2019. Antibiotic resistance in European wastewater treatment plants mirrors the pattern of clinical antibiotic resistance prevalence. Sci. Adv. 5, eaau9124.

Pruden, A., Pei, R., Storteboom, H., Carlson, K.H., 2006. Antibiotic resistance genes as emerging contaminants: studies in northern Colorado. Environ. Sci. Technol. 40, 7445–7450.

Pugesek, B.H., Tomer, A., Von eye, A., 2003. Structural Equation Modeling: Applications in Ecological and Evolutionary Biology. Cambridge University Press.

R core team 2015. R Core Team. A Language and Environment for Statistical Computing. R Foundation for Statistical Computing, Vienna, Austria 2015. ISBN 3–900051–07–0, http://www. R–project. org/.

Rayment, G.E., Lyons, D.J., 2011. Soil Chemical Methods: Australasia. CSIRO publishing.

Schermelleh-engel, K., Moosbrugger, H., Müller, H., 2003. Evaluating the fit of structural equation models: tests of significance and descriptive goodness-of-fit measures. MPR online 8, 23–74.

Schmittgen, T.D., Livak, K.J., 2008. Analyzing real-time PCR data by the comparative C T method. Nat. Protoc. 3, 1101.

Storz, G., Hengge, R., 2010. Bacterial Stress Responses. American Society for Microbiology Press.

Su, J.Q., An, X.L., Li, B., Chen, Q.L., Gillings, M.R., Chen, H., Zhang, T., Zhu, Y.G., 2017. Metagenomics of urban sewage identifies an extensively shared antibiotic resistome in China. Microbiome 5, 84.

Trivedi, P., Delgado-baquerizo, M., Trivedi, C., Hu, H., Anderson, I.C., Jeffries, T.C., Zhou, J., Singh, B.K., 2016. Microbial regulation of the soil carbon cycle: evidence from gene-enzyme relationships. ISME J 10, 2593–2604.

United Nations, 2018. Revision of World Urbanization Prospects. UN Department of Economic and Social Affairs.

Van elsas, J.D., Turner, S., Bailey, M.J., 2003. Horizontal gene transfer in the phytosphere. New Phytol. 157, 525–537.

Vikesland, P.J., Pruden, A., Alvarez, P.J.J., Aga, D., Burgmann, H., Li, X.D., Manaia, C.M., Nambi, I., Wigginton, K., Zhang, T., Zhu, Y.G., 2017. Toward a comprehensive strategy to mitigate dissemination of environmental sources of antibiotic resistance. Environ. Sci. Techno. 51, 13061–13069.

Wang, F.H., Qiao, M., Su, J.Q., Chen, Z., Zhou, X., Zhu, Y.G., 2014. High throughput profiling of antibiotic resistance genes in urban park soils with reclaimed water irrigation. Environ. Sci. Technol. 48, 9079–9085.

Wickham, H., 2016. ggplot2: Elegant Graphics for Data Analysis. Springer.

Wright, G.D., 2007. The antibiotic resistome: the nexus of chemical and genetic diversity. Nat. Rev. Microbiol. 5, 175–186.

Yi, X., Wang, M., ZHOU, Z., 2019. The potential impact of naturally produced antibiotics, environmental factors, and anthropogenic pressure on the occurrence of erm genes in urban soils. Environ. Pollut. 245, 282–289.

Yu, Y., Lee, C., Kim, J., Hwang, S., 2005. Group-specific primer and probe sets to detect methanogenic communities using quantitative real-time polymerase chain reaction. Biotechnol. Bioeng. 89, 670–679.

Zhang, Y.J., Hu, H.W., Chen, Q.L., Singh, B.K., Yan, H., Chen, D., He, J.Z., 2019a. Transfer of antibiotic resistance from manure amended soils to vegetable microbiomes.

Environ. Int. 130, 104912.
Zhang, Y.J., Hu, H.W., Yan, H., Wang, J.T., Lam, S.K., Chen, Q.L., CHEN, D., He, J.Z., 2019b. Salinity as a predominant factor modulating the distribution patterns of antibiotic resistance genes in ocean and river beach soils. Sci. Total Environ. 668, 193–203.
Zhu, Y.G., Johnson, T.A., Su, J.Q., Qiao, M., Guo, G.X., Stedtfeld, R.D., Hashsham, S.A., Tiedje, J.M., 2013. Diverse and abundant antibiotic resistance genes in Chinese swine farms. Proc. Natl. Acad. Sci. U. S. A. 110, 3435–3440.
Zhu, B., Chen, Q., Chen, S., Zhu, Y.G., 2017a. Does organically produced lettuce harbor higher abundance of antibiotic resistance genes than conventionally produced? Environ. Int. 98, 152–159.
Zhu, Y.G., Zhao, Y., Li, B., Huang, C.L., Zhang, S.Y., Yu, S., Chen, Y.S., Zhang, T., Gillings, M.R., SU, J.Q., 2017b. Continental-scale pollution of estuaries with antibiotic resistance genes. Nat. Microbiol. 2, 16270.

Supplementary data for Antibiotic resistance in urban green spaces mirrors the pattern of industrial distribution

Zhen-Zhen Yan [a], Qing-Lin Chen [a,*], Yu-Jing Zhang [a], Ji-Zheng He [a], Hang-Wei Hu [a,*]

[a] *Faculty of Veterinary and Agricultural Sciences, The University of Melbourne, VIC 3010, Australia*

*Author for correspondence: Qing-Lin Chen, E-mail: qinglin.chen@unimelb.edu.au or Hang-Wei Hu, E-mail: hang-wei.hu@unimelb.edu.au

Table S1. Detailed information about all the 40 urban parks investigated in this study.

Sample site ID	Green space Name	Statistic Area Level 4 (SA4) name	Suburb	Post code
1	Parker Reserve	North West	Coburg North	3058
2	Parker Reserve	North West	Coburg North	3058
3	Parker Reserve	North West	Coburg North	3058
4	Charles Mutton Reserve	North West	Fawkner	3060
5	Charles Mutton Reserve	North West	Fawkner	3060
6	Charles Mutton Reserve	North West	Fawkner	3060
7	Greensborough Park	North East	Greensborough	3088
8	Greensborough Park	North East	Greensborough	3088
9	Greensborough Park	North East	Greensborough	3088
10	Hibiscus Park	North East	Bundoora	3083
11	Hibiscus Park	North East	Bundoora	3083
12	Hibiscus Park	North East	Bundoora	3083
13	Bricker Reserve	Inner South	Moorabbin	3189
14	Bricker Reserve	Inner South	Moorabbin	3189
15	Bricker Reserve	Inner South	Moorabbin	3189
16	Banksia Reserve Playground	Inner South	Beaumaris	3193
17	Banksia Reserve Playground	Inner South	Beaumaris	3193
18	Banksia Reserve Playground	Inner South	Beaumaris	3193
19	Dendy Park	Inner South	Brighton East	3187
20	Dendy Park	Inner South	Brighton East	3187
21	Dendy Park	Inner South	Brighton East	3187
22	Carrum Pirate Ship Park	Inner South	Carrum	3197
23	Carrum Pirate Ship Park	Inner South	Carrum	3197
24	Carrum Pirate Ship Park	Inner South	Carrum	3197
25	Princess Park	Inner South	Caulfied South	3162
26	Princess Park	Inner South	Caulfied South	3162
27	Princess Park	Inner South	Caulfied South	3162
28	Harleston Park	Inner South	Elsternwick	3185
29	Harleston Park	Inner South	Elsternwick	3185
30	Harleston Park	Inner South	Elsternwick	3185
31	Lord Reserve	Inner South	Carnegie	3163
32	Lord Reserve	Inner South	Carnegie	3163
33	Lord Reserve	Inner South	Carnegie	3163
34	Victoria Gardens	Inner	Prahran	3181
35	Victoria Gardens	Inner	Prahran	3181
36	Victoria Gardens	Inner	Prahran	3181
37	Brookville Gardens	Inner	Toorak	3142
38	Brookville Gardens	Inner	Toorak	3142
39	Brookville Gardens	Inner	Toorak	3142
40	Citizens Park	Inner	Richmond	3121
41	Citizens Park	Inner	Richmond	3121

42	Citizens Park	Inner	Richmond	3121
43	Garden City Reserve	Inner	Port Melbourne	3207
44	Garden City Reserve	Inner	Port Melbourne	3207
45	Garden City Reserve	Inner	Port Melbourne	3207
46	Templestowe Reserve	Inner East	Templestowe	3106
47	Templestowe Reserve	Inner East	Templestowe	3106
48	Templestowe Reserve	Inner East	Templestowe	3106
49	Macleay Park	Inner East	Balwyn North	3104
50	Macleay Park	Inner East	Balwyn North	3104
51	Macleay Park	Inner East	Balwyn North	3104
52	Schramms Reserve	Inner East	Doncaster	3108
53	Schramms Reserve	Inner East	Doncaster	3108
54	Schramms Reserve	Inner East	Doncaster	3108
55	Bennettswood Reserve	Inner East	Burwood	3125
56	Bennettswood Reserve	Inner East	Burwood	3125
57	Bennettswood Reserve	Inner East	Burwood	3125
58	Lynden Park	Inner East	Camberwell	3124
59	Lynden Park	Inner East	Camberwell	3124
60	Lynden Park	Inner East	Camberwell	3124
61	Eley Park	Inner East	Blackburn South	3130
62	Eley Park	Inner East	Blackburn South	3130
63	Eley Park	Inner East	Blackburn South	3130
64	Central Gardens	Inner East	Hawthorn	3122
65	Central Gardens	Inner East	Hawthorn	3122
66	Central Gardens	Inner East	Hawthorn	3122
67	Malvern Public Gardens	Inner South	Malvern	3144
68	Malvern Public Gardens	Inner South	Malvern	3144
69	Malvern Public Gardens	Inner South	Malvern	3144
70	Fitzroy Gardens	Inner	East Melbourne	3002
71	Fitzroy Gardens	Inner	East Melbourne	3002
72	Fitzroy Gardens	Inner	East Melbourne	3002
73	Queens Park	Inner	Moonee Ponds	3039
74	Queens Park	Inner	Moonee Ponds	3039
75	Queens Park	Inner	Moonee Ponds	3039
76	Batman Park	Inner	Northcote	3070
77	Batman Park	Inner	Northcote	3070
78	Batman Park	Inner	Northcote	3070
79	Flagstaff Gardens	Inner	West Melbourne	3003
80	Flagstaff Gardens	Inner	West Melbourne	3003
81	Flagstaff Gardens	Inner	West Melbourne	3003
82	Atherton Reserve	Inner	Fitzroy	3065
83	Atherton Reserve	Inner	Fitzroy	3065
84	Atherton Reserve	Inner	Fitzroy	3065
85	Carlton Gardens	Inner	Carlton	3053

86	Carlton Gardens	Inner	Carlton	3053
87	Carlton Gardens	Inner	Carlton	3053
88	H.P. Zwar Park	North East	Preston	3072
89	H.P. Zwar Park	North East	Preston	3072
90	H.P. Zwar Park	North East	Preston	3072
91	Brimbank Park	North West	Keilor East	3033
92	Brimbank Park	North West	Keilor East	3033
93	Brimbank Park	North West	Keilor East	3033
94	A J Davis Reserve	North West	Airport West	3042
95	A J Davis Reserve	North West	Airport West	3042
96	A J Davis Reserve	North West	Airport West	3042
97	Napier Park	North West	Strathmore	3041
98	Napier Park	North West	Strathmore	3041
99	Napier Park	North West	Strathmore	3041
100	Selwyn Park	West	Albion	3020
101	Selwyn Park	West	Albion	3020
102	Selwyn Park	West	Albion	3020
103	Cairnlea Park	West	Cairnlea	3023
104	Cairnlea Park	West	Cairnlea	3023
105	Cairnlea Park	West	Cairnlea	3023
106	Braybrook Park	West	Braybrook	3019
107	Braybrook Park	West	Braybrook	3019
108	Braybrook Park	West	Braybrook	3019
109	Pioneer Park	West	Sydenham	3037
110	Pioneer Park	West	Sydenham	3037
111	Pioneer Park	West	Sydenham	3037
112	Mappin Reserve	West	Seddon	3011
113	Mappin Reserve	West	Seddon	3011
114	Mappin Reserve	West	Seddon	3011
115	Logan Reserve	West	Altona	3018
116	Logan Reserve	West	Altona	3018
117	Logan Reserve	West	Altona	3018
118	Bruce Comben Reserve	West	Altona Meadows	3028
119	Bruce Comben Reserve	West	Altona Meadows	3028
120	Bruce Comben Reserve	West	Altona Meadows	3028

Table S2. Anthropogenic parameters about all the 120 sampling sites at Statistical Areal level 4 region level collected.

Sampling Site	Population density (people/km2)	Median equivalised total household income (AU$/week)	Total number of business	Number of manufacturing	Number of electracy, gas, water & waste services
1	243	808	30190	1775	112
2	243	808	30190	1775	112
3	243	808	30190	1775	112
4	243	808	30190	1775	112
5	243	808	30190	1775	112
6	243	808	30190	1775	112
7	288	888	39651	1774	126
8	288	888	39651	1774	126
9	288	888	39651	1774	126
10	288	888	39651	1774	126
11	288	888	39651	1774	126
12	288	888	39651	1774	126
13	2681	1116	48512	1867	113
14	2681	1116	48512	1867	113
15	2681	1116	48512	1867	113
16	2681	1116	48512	1867	113
17	2681	1116	48512	1867	113
18	2681	1116	48512	1867	113
19	2681	1116	48512	1867	113
20	2681	1116	48512	1867	113
21	2681	1116	48512	1867	113
22	2681	1116	48512	1867	113
23	2681	1116	48512	1867	113
24	2681	1116	48512	1867	113
25	2681	1116	48512	1867	113
26	2681	1116	48512	1867	113
27	2681	1116	48512	1867	113
28	2681	1116	48512	1867	113
29	2681	1116	48512	1867	113
30	2681	1116	48512	1867	113
31	2681	1116	48512	1867	113
32	2681	1116	48512	1867	113
33	2681	1116	48512	1867	113
34	4626	1190	104076	2609	223
35	4626	1190	104076	2609	223
36	4626	1190	104076	2609	223
37	4626	1190	104076	2609	223
38	4626	1190	104076	2609	223

39	4626	1190	104076	2609	223
40	4626	1190	104076	2609	223
41	4626	1190	104076	2609	223
42	4626	1190	104076	2609	223
43	4626	1190	104076	2609	223
44	4626	1190	104076	2609	223
45	4626	1190	104076	2609	223
46	2630	1064	46270	969	71
47	2630	1064	46270	969	71
48	2630	1064	46270	969	71
49	2630	1064	46270	969	71
50	2630	1064	46270	969	71
51	2630	1064	46270	969	71
52	2630	1064	46270	969	71
53	2630	1064	46270	969	71
54	2630	1064	46270	969	71
55	2630	1064	46270	969	71
56	2630	1064	46270	969	71
57	2630	1064	46270	969	71
58	2630	1064	46270	969	71
59	2630	1064	46270	969	71
60	2630	1064	46270	969	71
61	2630	1064	46270	969	71
62	2630	1064	46270	969	71
63	2630	1064	46270	969	71
64	2630	1064	46270	969	71
65	2630	1064	46270	969	71
66	2630	1064	46270	969	71
67	2681	1116	48512	1867	113
68	2681	1116	48512	1867	113
69	2681	1116	48512	1867	113
70	4626	1190	104076	2609	223
71	4626	1190	104076	2609	223
72	4626	1190	104076	2609	223
73	4626	1190	104076	2609	223
74	4626	1190	104076	2609	223
75	4626	1190	104076	2609	223
76	4626	1190	104076	2609	223
77	4626	1190	104076	2609	223
78	4626	1190	104076	2609	223
79	4626	1190	104076	2609	223
80	4626	1190	104076	2609	223
81	4626	1190	104076	2609	223
82	4626	1190	104076	2609	223

83	4626	1190	104076	2609	223
84	4626	1190	104076	2609	223
85	4626	1190	104076	2609	223
86	4626	1190	104076	2609	223
87	4626	1190	104076	2609	223
88	288	888	39651	1774	126
89	288	888	39651	1774	126
90	288	888	39651	1774	126
91	243	808	30190	1775	112
92	243	808	30190	1775	112
93	243	808	30190	1775	112
94	243	808	30190	1775	112
95	243	808	30190	1775	112
96	243	808	30190	1775	112
97	243	808	30190	1775	112
98	243	808	30190	1775	112
99	243	808	30190	1775	112
100	559	843	49862	1892	205
101	559	843	49862	1892	205
102	559	843	49862	1892	205
103	559	843	49862	1892	205
104	559	843	49862	1892	205
105	559	843	49862	1892	205
106	559	843	49862	1892	205
107	559	843	49862	1892	205
108	559	843	49862	1892	205
109	559	843	49862	1892	205
110	559	843	49862	1892	205
111	559	843	49862	1892	205
112	559	843	49862	1892	205
113	559	843	49862	1892	205
114	559	843	49862	1892	205
115	559	843	49862	1892	205
116	559	843	49862	1892	205
117	559	843	49862	1892	205
118	559	843	49862	1892	205
119	559	843	49862	1892	205
120	559	843	49862	1892	205

Table S3. List of soil properties of the 120 soil samples analysed.

Sampling Site	pH	EC (ds/m)	TC (%)	TN (%)	Cu (mg/kg)	Fe (mg/kg)	CEC (cmol/kg)
1	6.12	0.27	5.4	0.47	3	189	19.95
2	6.12	0.34	5.7	0.55	2	209	21.40
3	6.23	0.29	5.7	0.52	3	198	20.52
4	6.18	0.11	3.1	0.29	2	294	11.16
5	6.21	0.14	3.8	0.36	2	233	15.21
6	6.23	0.15	4.8	0.44	2	207	17.04
7	6.36	0.11	2.7	0.26	8	289	11.35
8	6.44	0.12	2.7	0.27	8	316	11.76
9	6.32	0.11	2.5	0.25	8	273	10.84
10	5.56	0.16	5.6	0.52	2	324	16.67
11	5.77	0.13	4.5	0.39	2	246	17.17
12	5.72	0.14	4.7	0.42	2	268	15.127
13	5.9	0.18	5.6	0.43	8	273	13.65
14	5.91	0.19	6.1	0.47	8	256	14.625
15	5.91	0.20	6.2	0.48	9	268	14.77
16	5.71	0.09	5	0.42	1	318	8.957
17	5.7	0.10	5.4	0.46	1	348	9.29
18	5.65	0.10	5.1	0.45	2	178	9.08
19	5.86	0.11	4.6	0.4	2	173	9.36
20	5.93	0.10	4.4	0.37	2	175	9.90
21	5.89	0.11	4.2	0.37	2	174	9.99
22	6.31	0.12	2.4	0.21	2	287	9.46
23	6.27	0.12	2.9	0.25	1	279	11.12
24	6.26	0.15	3.1	0.27	2	292	10.99
25	6.24	0.20	4.1	0.34	2	156	10.76
26	6.17	0.20	3.9	0.31	3	167	11.21
27	6.3	0.19	3.3	0.25	2	152	9.52
28	6.26	0.08	3.6	0.24	3	212	11.06
29	6.43	0.10	3.3	0.25	3	150	11.93
30	6.49	0.10	3.3	0.25	3	184	11.54
31	6.15	0.12	3.8	0.31	3	298	10.56
32	6.16	0.12	4.2	0.34	3	306	11.25
33	6.12	0.12	3.7	0.3	2	296	10.72
34	5.84	0.13	3.3	0.27	4	285	8.93
35	5.72	0.17	3.6	0.3	4	260	9.57
36	5.84	0.20	3.3	0.28	4	246	10.19
37	6.15	0.12	4.4	0.38	2	267	13.82
38	6.15	0.12	4.1	0.34	2	292	12.76
39	6.12	0.13	4.4	0.38	3	286	14.06
40	6.81	0.13	4.4	0.34	7	216	17.41
41	6.82	0.14	4.2	0.34	7	207	17.19

42	6.84	0.14	4.3	0.35	7	117	17.37
43	6.89	0.11	5.1	0.36	6	214	13.89
44	6.91	0.11	4.6	0.32	8	111	14.57
45	6.88	0.11	4.7	0.34	8	114	6.33
46	7.38	0.13	3.7	0.28	2	209	18.16
47	7.35	0.13	4.4	0.31	2	203	20.02
48	7.43	0.13	4	0.29	2	217	21.07
49	5.63	0.06	3.2	0.26	1	317	6.88
50	5.75	0.06	3.3	0.27	1	315	8.07
51	5.79	0.06	3.5	0.29	1	318	8.11
52	6.17	0.17	4.4	0.39	3	209	15.26
53	6.14	0.16	4.3	0.39	3	182	15.08
54	6.14	0.16	4	0.36	3	194	14.58
55	5.98	0.12	1.8	0.17	1	251	6.27
56	6.04	0.13	1.8	0.17	1	246	15.47
57	6.05	0.12	1.7	0.16	1	240	5.89
58	5.7	0.10	4.6	0.4	2	281	12.23
59	5.75	0.09	4.3	0.36	1	255	11.33
60	5.78	0.09	4.3	0.37	1	273	11.23
61	5.8	0.11	4.9	0.42	2	246	13.48
62	5.82	0.11	4.9	0.43	2	257	13.58
63	5.84	0.10	4.9	0.43	2	240	13.18
64	6.3	0.12	5	0.38	4	298	17.83
65	6.32	0.12	4.9	0.37	3	252	18.44
66	6.27	0.12	4.9	0.37	4	317	17.46
67	6.69	0.11	4.9	0.38	2	197	17.67
68	6.89	0.12	4.4	0.35	2	198	17.98
69	6.8	0.12	4.5	0.36	2	173	16.64
70	6.51	0.17	6.3	0.49	11	246	23.59
71	6.5	0.17	5.8	0.46	11	234	23.35
72	6.53	0.16	5.8	0.46	11	241	24.45
73	5.74	0.18	9.5	0.67	4	237	26.42
74	5.89	0.15	8.6	0.59	4	231	26.10
75	5.84	0.16	9.5	0.66	3	221	26.43
76	7.44	0.27	4.6	0.38	3	192	26.85
77	7.38	0.28	4.7	0.39	3	203	25.38
78	7.4	0.26	4.6	0.38	3	209	28.84
79	7.29	0.16	8.1	0.57	16	249	34.61
80	7.11	0.15	7.6	0.53	15	245	33.90
81	7.08	0.17	7.4	0.51	15	243	33.98
82	5.94	0.13	5.9	0.48	2	151	19.83
83	5.9	0.13	5.6	0.47	2	137	19.87
84	5.9	0.14	5.8	0.49	2	157	19.68
85	6.37	0.18	9.6	0.65	7	274	33.87

86	6.31	0.17	9.7	0.68	8	294	32.91
87	6.33	0.18	9.1	0.65	7	250	30.56
88	6.97	0.16	4.6	0.4	3	179	21.17
89	7.05	0.17	5.1	0.44	3	191	19.41
90	7.09	0.18	5.2	0.45	3	179	21.40
91	7	0.12	6.6	0.42	3	139	27.57
92	6.93	0.12	5.8	0.39	3	150	26.98
93	6.97	0.12	6.3	0.4	3	150	27.55
94	7.65	0.26	4.9	0.43	4	68	42.73
95	7.68	0.24	5.3	0.46	3	58	43.19
96	7.71	0.24	5.2	0.44	4	70	42.17
97	6.59	0.19	7.8	0.62	2	167	27.91
98	6.43	0.17	7.6	0.59	2	182	24.20
99	6.57	0.19	7.8	0.61	2	185	26.59
100	6.75	0.19	4.6	0.38	3	236	18.60
101	6.55	0.18	3.2	0.28	2	255	17.24
102	6.65	0.19	3.9	0.34	2	265	18.23
103	7.56	0.13	2.1	0.16	2	110	14.21
104	7.66	0.15	2.3	0.18	2	125	14.70
105	7.8	0.17	2.5	0.19	2	125	17.91
106	7.83	0.24	3.8	0.31	3	98	33.61
107	7.98	0.26	2.9	0.25	3	100	34.23
108	7.71	0.22	4.1	0.31	3	99	33.24
109	6.81	0.13	4.7	0.37	3	138	28.26
110	6.77	0.13	4.6	0.36	3	137	27.49
111	6.73	0.13	4.3	0.38	3	143	28.71
112	6.18	0.27	4.2	0.36	2	206	17.47
113	6.2	0.23	4	0.35	2	210	17.01
114	6.26	0.23	3.9	0.36	2	217	16.63
115	7.09	0.89	9.2	0.86	3	95	51.23
116	7.1	0.73	9.6	0.91	3	92	50.06
117	7.22	0.91	9.1	0.84	3	88	52.14
118	6.65	0.35	5.2	0.41	2	170	22.49
119	6.41	0.30	6.7	0.56	2	166	23.37
120	6.45	0.29	5	0.4	2	172	21.50

Figure S1. Distribution of the 40 urban parks investigated in this study.

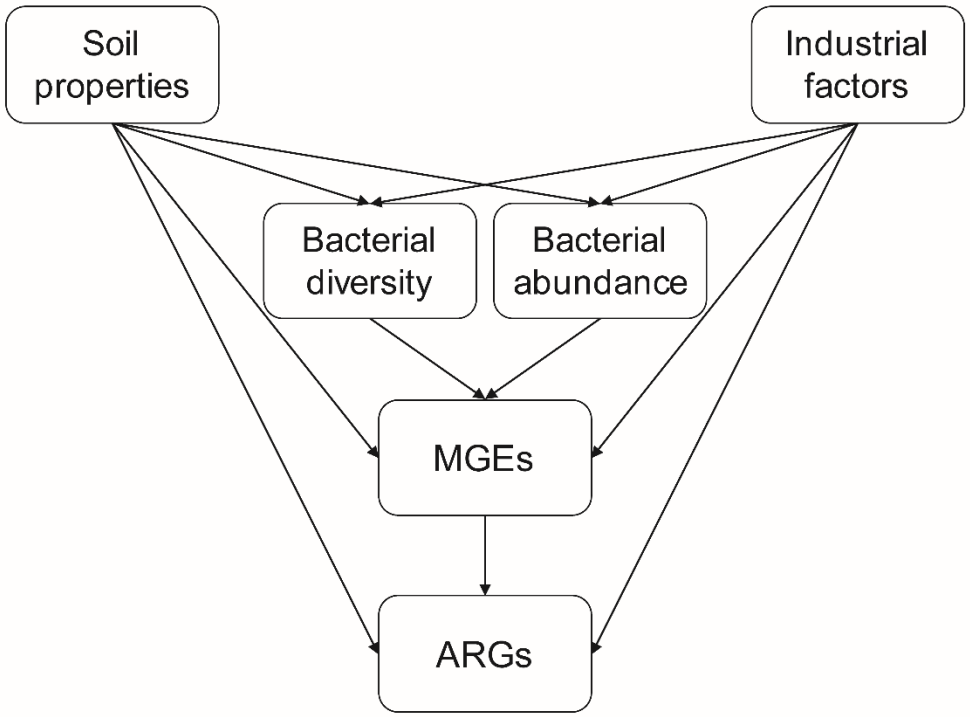

Figure S2. *A prior* SEM for grass phyllosphere samples and soil samples, based on the hypothesized causal relationships between multiple factors and the abundance of ARG.

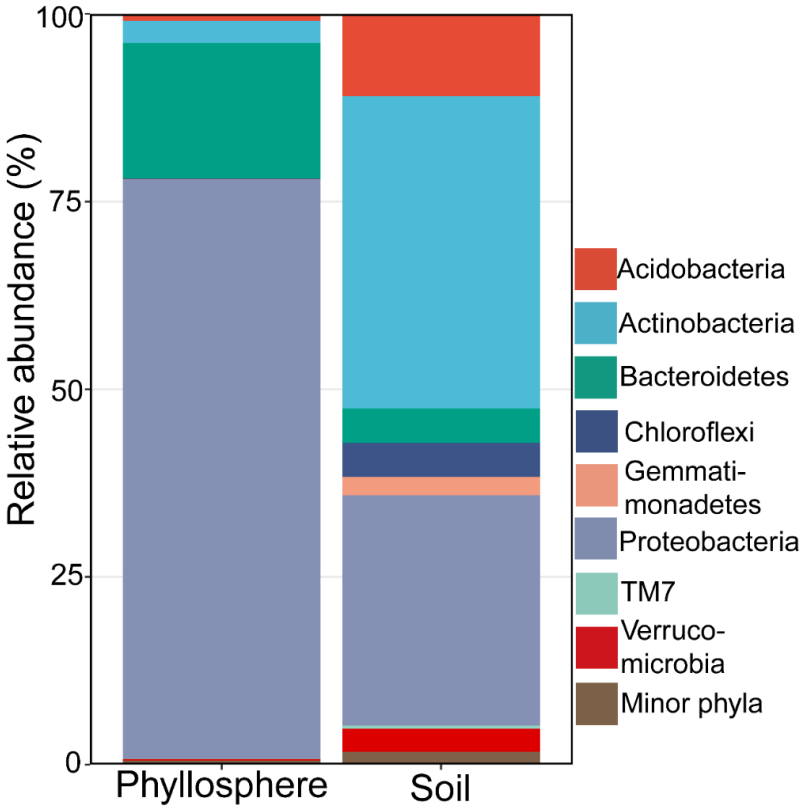

Figure S3. The community compositions of bacterial at the phylum level in grass phyllosphere and soil samples.

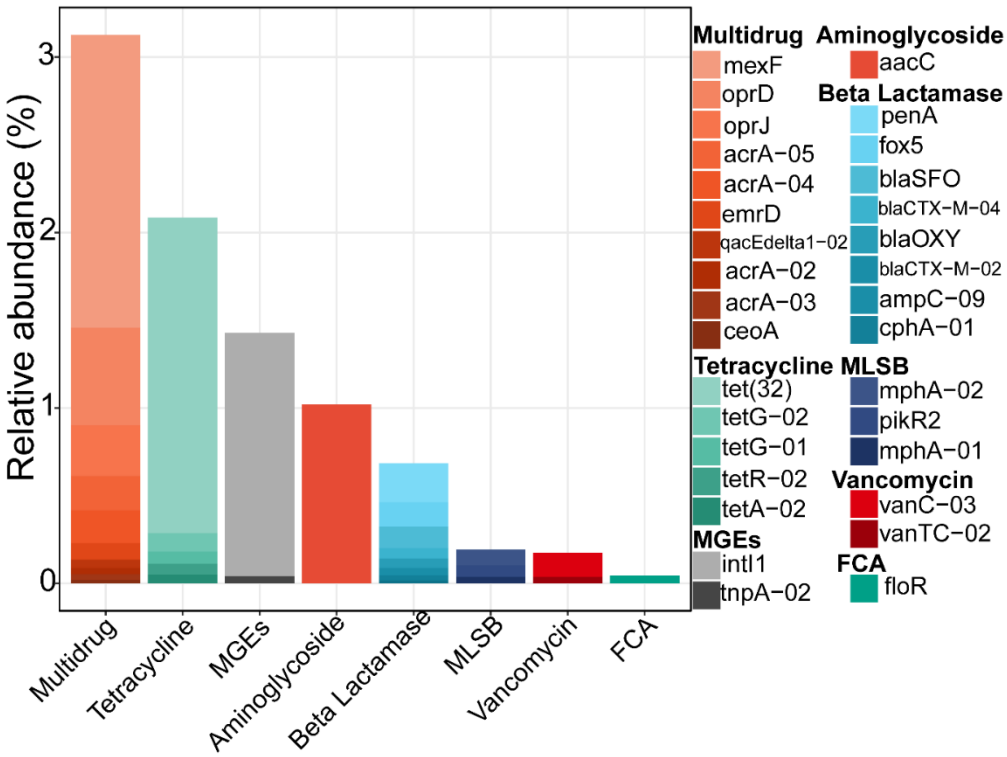

Figure S4. Taxonomic composition of the core resistome in grass phyllosphere samples.

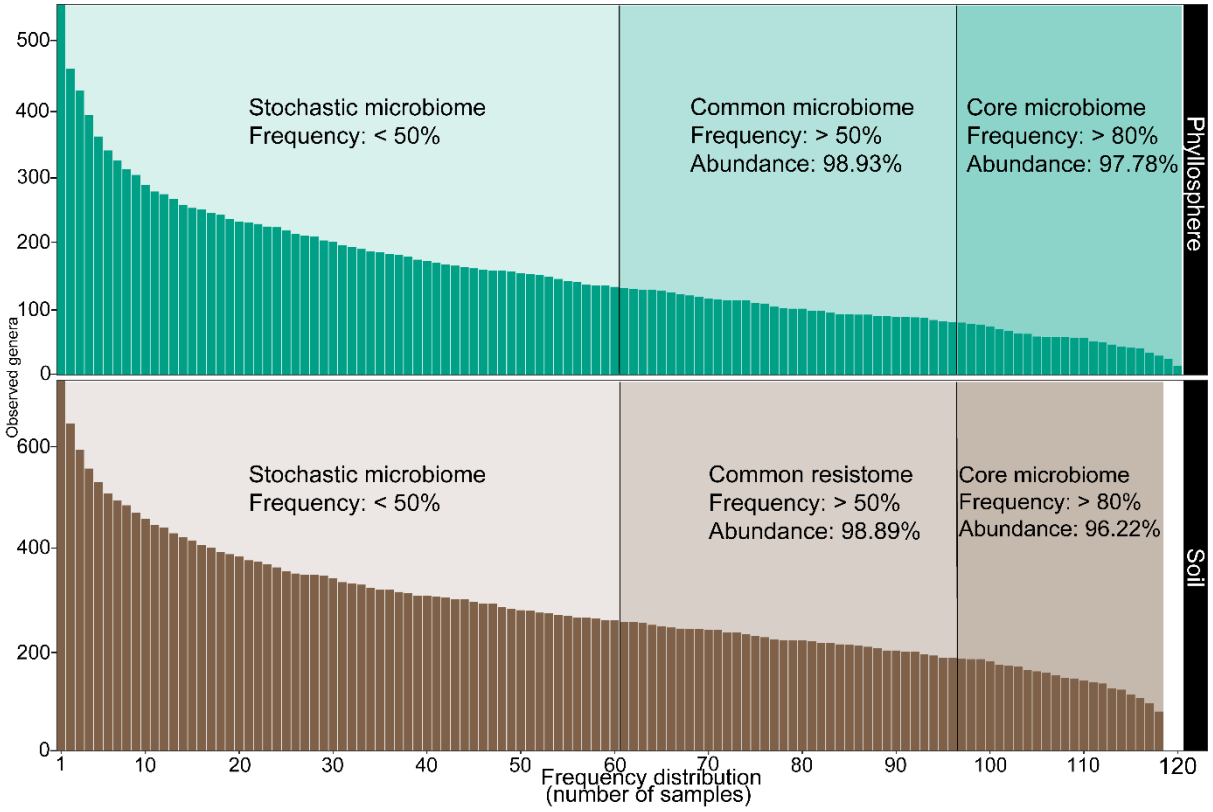

Figure S5. Frequency distribution of microbial taxa (at the genus level) in grass phyllosphere and soil samples.

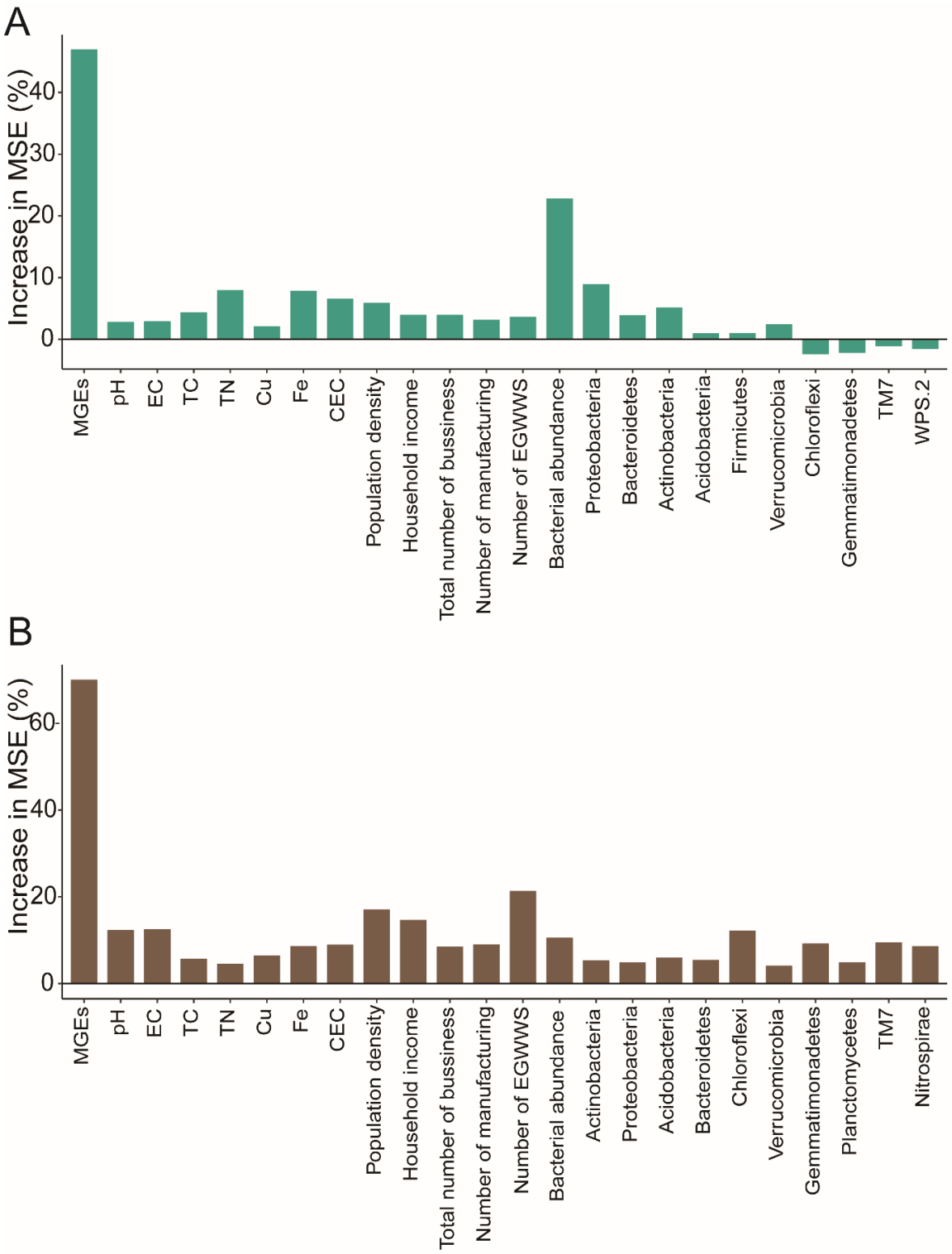

Figure S6. Random forest predictor importance, as measured by percentage of increase in mean square error (MSE) of the relative abundance of ARGs in (A) grass phyllosphere and (B) soil samples in urban green spaces. EGWWS: short for electracy, gas, water & waste services

Chapter 3: Characterization of the key factors in influencing bacterial community assemblies in urban ecosystems

This chapter is based on a published article entitled:

Industrial development as a key factor explaining variances in soil and grass phyllosphere microbiomes in urban green spaces. *Environmental Pollution*, 261:114201. https://doi.org/10.1016/j.envpol.2020.114201

Environmental Pollution 261 (2020) 114201

Contents lists available at ScienceDirect

Environmental Pollution

journal homepage: www.elsevier.com/locate/envpol

Industrial development as a key factor explaining variances in soil and grass phyllosphere microbiomes in urban green spaces☆

Zhen-Zhen Yan , Qing-Lin Chen , Yu-Jing Zhang , Ji-Zheng He , Hang-Wei Hu *

Faculty of Veterinary and Agricultural Sciences, The University of Melbourne, VIC, 3010, Australia

ARTICLE INFO

Article history:
Received 16 December 2019
Received in revised form
10 February 2020
Accepted 15 February 2020
Available online 19 February 2020

Keywords:
Green spaces
Urban microbiome
Human health
Urbanization
Phyllosphere

ABSTRACT

Microbiota in urban green spaces underpin ecosystem services that are essential to environmental health and human wellbeing. However, the factors shaping the microbial communities in urban green spaces, especially those associated with turf grass phyllosphere, remain poorly understood. The lack of this knowledge greatly limits our ability to assess ecological, social and recreational benefits of urban green spaces in the context of global urbanization. In this study, we used amplicon sequencing to characterize soil and grass phyllosphere bacterial communities in 40 urban green spaces and three minimally disturbed national parks in Victoria, Australia. The results indicated that urbanization might have shown different impacts on soil and grass phyllosphere microbial communities. The bacterial diversity in soil but not in grass phyllosphere was significantly higher in urban green spaces than in national parks. Principal coordinate analysis revealed significant differences in the overall patterns of bacterial community composition between urban green spaces and national parks for both soil and grass phyllosphere. Industrial development, as represented by the number of industries in the region, was identified as a key driver shaping the bacterial community profiles in urban green spaces. Variation partitioning analysis suggested that industrial factors together with their interaction with other factors explained 20% and 28% of the variances in soil and grass phyllosphere bacterial communities, respectively. The findings highlight the importance of industrial development in driving the spatial patterns of urban microbiomes, and have important implication for the management of microbiomes in urban green spaces.

© 2020 Elsevier Ltd. All rights reserved.

1. Introduction

Microorganisms, as a vital component of the urban ecosystem, play a critical role in regulating ecosystem services (Eldridge et al., 2019; Hui et al., 2017; Kabisch, 2015), such as pollutant remediation, nutrient cycling and genetic diversity preservation (Escobedo et al., 2011; Groffman et al., 2009; Ramirez et al., 2014, Strohbach and HAASE, 2012). These ecosystem functions are important in reducing the growing global burden of urban-associated chronic diseases and maintaining the wellbeing of urban environment and city dwellers. There has been evidence that exposure of humans to microorganisms associated with soil and plants in urban green spaces could reduce the dysfunction of immune system and supress inflammation (Flies et al., 2017; Flies et al., 2018). During the past several decades, the massive transition of human population from rural to urban living has resulted in dramatic alternations of land use types which may consequently change the environmental habitats for microorganisms (Grimm et al., 2008; Li et al., 2018; Zhu et al., 2011). A better understanding of how anthropogenic disturbance impacts microbial community profiles in the urban environment is essential to prediction and mitigation of the influence of urbanization on ecosystem functioning (Falkowski et al., 2008; Kaye et al., 2005; Reese et al., 2016).

Soil and the aerial part (phyllosphere) of turf grass are the two largest habitats for microorganisms in urban green spaces (Crowther et al., 2019; Lindow and Brandl, 2003; Peñuelas and Terradas, 2014; Vorholt, 2012). Urban ecosystem is subject to intensive management practices, and therefore the microbial communities in urban green spaces are not only influenced by environmental factors (e.g. soil properties and climate factors) (Hui et al., 2017; Wang et al., 2018a) but also by anthropogenic activities. Urban environment is considered as a social economic ecosystem (Cadenasso et al., 2007; Pickett et al., 2011) characterized by high human population density and rapid economic growth (Wang et al.,

☆ This paper has been recommended for acceptance by Klaus Kümmerer.

* Corresponding author.
E-mail address: hang-wei.hu@unimelb.edu.au (H.-W. Hu).

https://doi.org/10.1016/j.envpol.2020.114201
0269-7491/© 2020 Elsevier Ltd. All rights reserved.

2018a; Zhu et al., 2017). The increasing demand for material by a growing population is usually associated with urban expansion, resulting in an increasing number of industries in the region, which is considered as another important measurement of urbanization (Xu et al., 2014). To date, a few studies have reported that urbanization can substantially change the microbiota in urban green spaces (Francini et al., 2018; Hui et al., 2017; Ramirez et al., 2014; Wang et al., 2018a; Xu et al., 2014), but it remains largely unknown which aspects of urbanization account for the major variance in microbial community profiles in urban green spaces. Additionally, previous studies have mostly focused on the impact of urbanization on soil microbiota but overlooked the plant phyllosphere microbiota despite the significance of phyllosphere as an important environmental habitat for microorganisms. As a vast environment with an estimated area of >1 billion km^2 across the globe (Vorholt, 2012; Woodward and Lomas, 2004), phyllosphere is described as a formidable playground for testing fundamental ecological principles in microbiology (Meyer and Leveau, 2012). In addition to promoting plant growth and production (Canto and Herrera, 2012; Grady et al., 2019; Taghavi et al., 2009), phyllosphere microbiomes have other important ecosystem functions, for example participating in Earth's biogeochemical cycles through moderating plant ethanol emission and contributing to nitrogen fixation (Galbally and Kirstine, 2002; Fürnkranz et al., 2008). In addition, phyllosphere microbiomes are closely linked to human health as phyllosphere is the potential bridge between environmental microbiome and human microbiome (Chen et al., 2018).

In this study, we used Illumina Miseq sequencing to analyse microbial communities in soil and grass phyllosphere samples collected from 40 urban green spaces across the Greater Melbourne metropolitan. As the capital of Australian state Victoria and the second most populous city in Oceania (ABS, 2019), Melbourne is a highly urbanized city with a long legacy of public green space development. In addition, samples from three national parks from remote Victoria were studied as representative of environments with minimal anthropogenic disturbance. Multiple factors including soil properties and anthropogenic parameters were collected to interpret their impacts on the microbial community profiles in urban green spaces. The main aims of this study were to (i) determine the potential differences and links between soil and grass phyllosphere bacterial communities; (ii) compare the bacterial community profiles in highly urbanized environment with those in minimally disturbed natural environment; and (iii) determine the most important factors shaping the bacterial community profiles in urban green spaces.

2. Material and methods

2.1. Sampling

Soil and grass samples were collected during May 2018 from 40 urban parks across Greater Melbourne metropolitan and three national parks in remote Victoria, Australia. All samples were collected on sunny or cloudy days with no rainfall event. The daytime temperature during the sample collection period ranged from 12.6 °C to 19.5 °C. At each park, three independent samples for each sample type (i.e. soil and grass) were collected. The surface 5 cm of soil and aerial parts of grass were collected. All samples were immediately transported in sterilized plastic bags on ice to the laboratory after collection. In total, for each sample type, 120 samples were collected from urban green spaces and nine samples were collected from national parks, resulting in a total of 258 soil and grass samples. Detailed information of sampling sites is provided in Table S1. A portion of soil samples were air dried and gently crumbed to pass through a 2 mm sieve for characterization of soil properties. The rest of the samples were stored at −80 °C prior to DNA extraction.

2.2. Soil properties characterization

Soil pH and electronic conductivity (EC) were measured in 1:5 soil water suspension using Orion Star A215 pH/Conductivity Benchtop Multiparameter Meter (Thermo Scientific Inc., Waltham, MA, USA). Soil cation change capacity (CEC) was determined by the concentration of exchangeable bases (Ca^{2+}, Mg^{2+}, Na^{+}, and K^{+}) in 1 M ammonium acetate at pH 7 measured using an Optima 8300 ICO-OES spectrometer (PerkinElmer, Waltham, MA, USA). Soil total carbon (TC) and total nitrogen (TN) were measured by Dumas combustion method using LECO FP628 analyser (LECO Corp, Michigan, USA). Soil mineral nitrogen including extractable ammonium and nitrate were measured in 1 M KCl solution using Skalar San^{++} continuous flow analyser (Skalar Analytical B.V. Tinstraat, Bread, Netherland).

2.3. Anthropogenic parameters collection

Anthropogenic parameters of the Statistical Area Level 2 (SA2), in which the investigated urban green spaces are located, were collected from Australia Bureau of Statistic (ABS) website (https://itt.abs.gov.au/itt/r.jsp?databyregion). SA2s are medium sized statistical area that represent socially and economically interacted communities and significant urban areas in the Australia Statistical Geography Standards. SA2s are primary output regions of ABS non-census and intercensal data (ABS, 2016). In this study, the 40 urban green spaces investigated are in 40 SA2s across Greater Melbourne metropolitan without overlap. Data of five anthropogenic parameters were collected, and these parameters were divided into two categories: social economic factors including population density (people km-2) and median equivalised total household income (weekly AU$); and industrial factors including total number of industries, number of construction and manufacturing industries (Table S2).

2.4. DNA extraction and sequencing

Soil and grass phyllosphere DNA were extracted using the DNeasy PowerSoil Kit (QIAGEN Pty Ltd., Hilden, Germany). Soil DNA was extracted from 0.25 g soil according to the supplier's manual. Grass phyllosphere DNA was extracted using a previous method (Chen et al., 2017; Zhang et al., 2019) with some modifications. Briefly, 5 g grass was weighted into a 50 ml sterilized centrifuge tube containing 45 ml autoclaved 0.01 M phosphate buffered saline with 0.02% Tween 20. The tubes were shaken at 30 °C and 200 rpm for 2 h using a shaking incubator. After shaking, the solution was filtered through a 40 μm nylon cell strainer into a new sterilized 50 ml centrifuge tube, and centrifuged at 4500 rpm for 30 min. After centrifugation, the supernatant was discarded, and the obtained pellets were transferred into the PowerBead tubes provided by the DNA extraction kit. The quality and concentration of the extracted DNA were assessed by agarose gel electrophoresis and spectrophotometric analysis using a NanoDrop ND2000c spectrophotometer (NanoDrop Technologies, Wilmington, DE, USA).

The V3 − V4 hypervariable region of the 16 S rRNA gene was amplified using the primer pair 341 F and 806 R for sequencing (Klindworth et al., 2013). Sequencing was performed on the Illumina Miseq platform at Australian Genome Research Facility. The PCR amplification protocol for the Illumina library generation was as follows: an initial enzyme activation and denaturation at 94 °C for 3 min, followed by 32 cycles of 94 °C for 45 s, 55 °C for 45 s and 72 °C for 90 s with a final extension at 72 °C for 10 min. After

sequencing, the barcode and adaptor sequences were removed, and ambiguous nucleotides and low-quality reads were filtered. The cleaned raw pair-ended sequencing reads were merged using FLASH (Magoč and Salzberg, 2011) and demultiplexed using Quantitative Insight into Microbial Ecology (QIIME) (Caporaso et al., 2010). Operational taxonomic unit (OTU) picking was conducted based on the threshold of 97% similarity level using UCLUST (Edgar, 2010). Chimeric and singleton OTUs, as well as chloroplast and mitochondrial OTUs were removed from the final OTU data set. Taxonomic classification and OTU quantification were performed against Greengenes 16 S rRNA database version 13.8 (Mcdonald et al., 2012).

2.5. Statistical analysis

All statistical tests were considered significant at $P < 0.05$ level. Bacteria community compositions at the phylum level were visualized using the 'ggplot2' (Wickham, 2016) package in R (R Core Team, 2015). Log-transformed relative abundances of dominant genera identified in samples from different parks were present in heatmaps using the 'pheatmap' package (Kolde and Kolde, 2015). Venn diagram was used to illustrate the shared and unique bacterial taxa in soil and grass phyllosphere samples using the 'VennDiagram' package (Chen and Boutros, 2011). Differences in bacterial α-diversity between soil and grass phyllosphere and samples from urban green spaces and national parks were explored using Mann-Whitney-Wilcoxon test and visualized using the 'ggplot2' package (Wickham, 2016). Principal coordinate analysis (PCoA) based on the Bray-Curtis distance was conducted to evaluate the separation of microbial communities using the 'labdsv' package (Roberts and Robers, 2016). Adonis test and variation partitioning analysis (VPA) were conducted using the 'vegan' package (Oksanen et al., 2013). Significant differences in specific bacterial taxa between urban green spaces and national parks were identified by liner discriminant analysis (LDA) effect size (LEfSe) according to the instructions (http://huttenhower.sph.harvard.edu/galaxy/root). The threshold on the LDA logarithmic was set at 2.0 and $\alpha = 0.01$ (Chen et al., 2017). The correlations between microbial community composition at the genus level (first axis values of PCoA analysis) and soil properties and anthropogenic parameters were explored by Spearman's ranked correlation analysis using the 'psych' package (Revelle and Revelle, 2015). P values of the Spearman's correlation analyses were corrected using Benjamini-Hochberg procedure. Ordinary least square (OLS) regression models were used to determine the linear relationships between microbial community composition and anthropogenic parameters and soil properties, and were visualized using the 'ggplot2' package (Wickham, 2016).

2.6. Availability of data and materials

Raw sequencing data of 16 S rRNA gene of the soil and grass phyllosphere samples were deposited in the National Center for Biotechnology Information (NCBI) Sequence Read Archive (SRA) under the accession number of PRJNA549108.

3. Results

3.1. Soil properties

Three independent soil samples were collected from each of the 40 urban green spaces. In total, 120 soil samples were characterized for physiochemical properties. The soil properties, including soil pH, EC (ds m^{-1}), CEC (com kg^{-1}), TC (%), TN (%), ammonium (mg L^{-1}) and nitrate (mg L^{-1}) contents are summarised in Table S3. Soil pH ranged from 5.56 to 7.98, and more than 80% of the soils had pH values below 7. Only 23 soil samples were alkalescent or alkaline. Soil EC ranged from 0.06 (ds m^{-1}) to 0.91 (ds m^{-1}). In general, nutrients in the soil samples were low with total C and N ranging from 1.70 to 9.71% and 0.16–0.91%, respectively.

3.2. Characteristics of bacterial communities in soil and grass phyllosphere

Bacterial community profiles in soil and grass phyllosphere at different taxonomic levels from phylum to genus were characterized. After assembling and quality filtering, 8,732,777 and 9,783,785 high quality sequences were obtained for soil and grass phyllosphere samples, respectively. The sequences were clustered into OTUs at 97% similarity level.

For soil samples, 1,071,713 OTUs were assembled into 50 phyla, 174 classes, 374 orders, 633 families, and 1246 genera. At the phylum level, Actinobacteria (accounting for 40.74% of sequences) were the most abundant phylum detected in soil samples from urban green spaces, followed by Proteobacteria (31.97%) and Acidobacteria (10.48%). (Fig. S1). Soils from national parks were dominated by the phylum Proteobacteria (66.71%) followed by the second and third most abundant phyla of Actinobacteria (13.71%) and Verrucomicrobia (8.44%) (Fig. S1). There was no significant difference between the bacterial community compositions among samples from different urban parks. Soils from all 40 urban parks were dominated by Actinobacteria and Proteobacteria, which accounted for 18.21–56.39% and 22.48–41.68% of the sequences of samples from different parks, respectively (Fig. S2A). Compared with soils from urban parks, the dominance of the phylum Proteobacteria was more apparent for soils from national parks. For soil samples from all three national parks, Proteobacteria accounted for more than half of the sequences (Fig. S2A). At the genus level, 374 genera were detected in all investigated parks. According to the heatmap showing the abundances of the 48 dominant genera (defined as those accounting for > 5% sequences in each sample (Wang et al., 2018b)), the bacterial communities were dominated by a few genera of the phyla Actinobacteria and Proteobacteria in soil samples from most of the investigated parks (Fig. S3A).

For grass phyllosphere samples, 389,809 OTUs were assembled into 40 phyla, 131 classes, 260 orders, 456 families and 946 genera. At the phylum level, Proteobacteria (accounting for 77.17% and 72.54% of sequences for samples from urban parks and national parks, respectively), Bacteroidetes (17.99% and 8.77%), and Actinobacteria (2.95% and 8.49%) were the three most abundant phyla for samples from both urban green spaces and national parks (Fig. S1). Only seven phyla were detected in grass phyllosphere from all investigated parks (Fig. S2B). For samples from both urban and national parks, microbial communities were dominated by the phylum Proteobacteria, which accounted for 42.18–95.31% and 63.35–79.45% of sequences, respectively (Fig. S2B). At the genus level, 81 genera were detected in all investigated parks. The abundances of all these genera are presented by heatmap (Fig. S3B). There was no significant difference in the bacterial communities between urban and national parks and among different urban parks. Bacterial communities of grass phyllosphere samples from all the investigated parks were dominated by a few bacterial genera belonging to the phyla Proteobacteria and Bacteroides (Fig. S3B).

The shared and unique bacterial genera in soil and grass phyllosphere sample were explored using the Venn diagram. A total of 855 bacterial genera were detected in both soil and grass phyllosphere samples, 400 genera were detected only in soil samples, and 91 genera only in grass phyllosphere samples (Fig. 1A). The α diversity as revealed by the Shannon index was significantly higher (Mann-Whitney-Wilcoxon test, $P < 0.001$) in the soil than that in

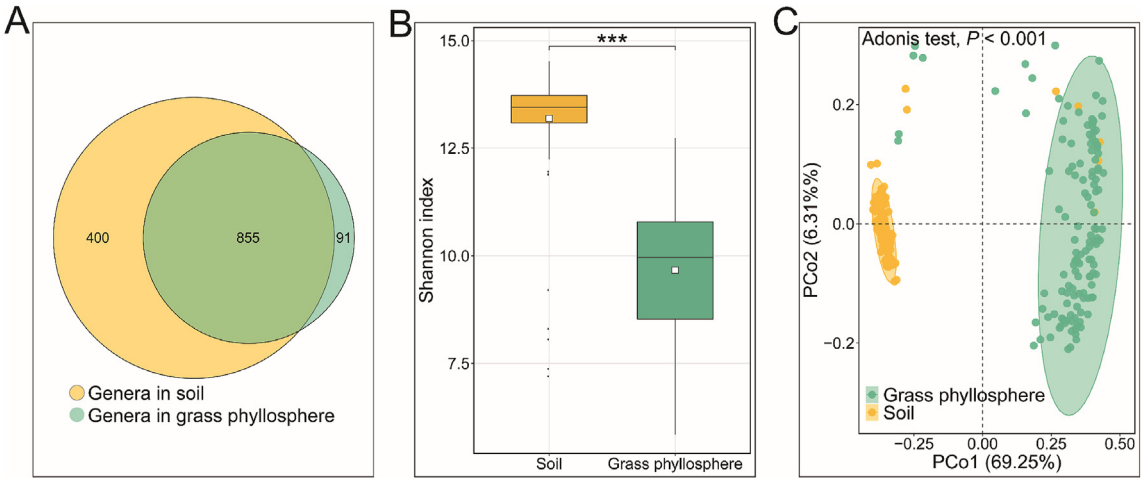

Fig. 1. Venn diagram showing the numbers of unique and shared genera in soil and grass phyllosphere samples (A), boxplots showing the Shannon index (α diversity in soil and grass phyllosphere samples. *** indicates $P < 0.001$ determined by Mann-Whitney-Wilcoxon test. The white squares indicate the mean values (B). and principal coordinate analysis (PCoA) based on the Bray-Curtis distance showing the distribution patterns of microbiome in soil and grass phyllosphere (β diversity) (C).

the grass phyllosphere (Fig. 1B). PCoA analysis based on the Bray-Curtis distance revealed a significant difference in microbial communities at the genus level between soil and phyllosphere (Adonis test, $P < 0.001$), which were well separated along the PCo1 axis (Fig. 1C).

3.3. Soil and grass phyllosphere bacterial communities in urban green spaces and national parks

The soil from urban green spaces had significantly higher α diversity than those from national parks (Mann-Whitney-Wilcoxon test, $P < 0.001$) (Fig. S4A). There was no significant difference between the α diversity of grass phyllosphere from urban green spaces and national parks (Fig. S4A). The β diversity analysis indicated that the overall compositions of bacterial communities in urban green spaces were distinct from those in national parks for both soil and grass phyllosphere at the genus level (Adonis test, $P < 0.001$) (Fig. S4B).

Bacterial taxa that were significantly different between the urban green spaces and national parks were identified by LEfSe analysis and visualized in cladogram (Fig. 2). A total of 29 bacterial taxa were significantly enriched in the soil from urban green spaces ($P < 0.05$), for example, the phyla Actinobacteria, Chloroflexi, Firmicutes, Gemmatimonadetes, and Nitrospira were significantly enriched in soil from urban green spaces (Fig. 2). In contrast, only two bacterial taxa were significantly enriched in soil from national parks (Fig. 2). As for grass phyllosphere, only six bacterial taxa had higher relative abundances in samples from urban green spaces, whereas 19 bacterial taxa belonging to the phyla of Acidobacteria, Chloroflexi, and Verrucomicrobia, as well as Alphaproteobacteria, and Deltaproteobacteria of the phylum Proteobacteria were significantly enriched in samples from national parks (Fig. 2).

3.4. Factors shaping the bacterial community compositions in urban green spaces

Spearman's ranked correlation analysis revealed that bacterial community compositions in soil and grass phyllosphere were significantly correlated with a range of anthropogenic parameters including population density (people km^{-2}), median equivalised total household income (weekly AU$), and total number of industries ($P < 0.01$) (Table 1). However, only one soil property, soil EC (ds m^{-1}), was significantly correlated with soil bacterial community composition ($P < 0.01$) (Table 1). Similarly, grass phyllosphere bacterial community composition was significantly correlated with various anthropogenic parameters but had no significant correlation with any soil property analysed (Table 1). Similar to the results of correlation analysis, OLS regression model revealed that soil EC was the only soil property significantly linearly correlated with the soil bacterial community composition (Fig. 3). Soil properties including soil EC, CEC, TN, and TC were significantly linearly correlated with the bacterial community composition of grass phyllosphere samples (Fig. 3). According to the OLS regression analysis results, all analysed anthropogenic parameters except the number of construction industries were significantly related to soil bacterial community composition (Fig. 4). Similarly, three out of the five analysed anthropogenic parameters including median equivalised total household income, total number of industries, and the number of construction industries were significantly related to the bacterial community composition in grass phyllosphere (weekly AU$), (Fig. 4).

VPA analysis was conducted to decipher the key contributors to the variance in soil and grass phyllosphere bacterial communities in urban green spaces. For soil, the selected variables explained 36% of the variance in bacterial community (Fig. 5A). Soil properties and social economic factors accounted for 13% and 2% of the variance, respectively (Fig. 5A). The interaction between soil properties and social economic factors and industrial factors both explained 1% of the variance (Fig. 5A). Notably, industrial factors individually contributed 19% to the variance, and were the most important factors shaping the soil bacterial community composition (Fig. 5A). For grass phyllosphere, the selected variables explained 89% of the variance in bacterial community (Fig. 5B). Compared to soil, the contribution of anthropogenic parameters to the variance in bacterial community was less apparent for grass phyllosphere. Social economic factors and industrial factors individually explained only 1% and 3% of the variances, respectively (Fig. 5B). Soil related biotic and abiotic factors, including soil microbial community and soil properties, as well as their interactions, explained 50% of the variance in grass phyllosphere bacterial community (Fig. 5B). However, it should be noted that industrial factors still played an unneglectable role in shaping grass phyllosphere bacterial community through interacting with other factors, which explained 25% of the variance (Fig. 5B).

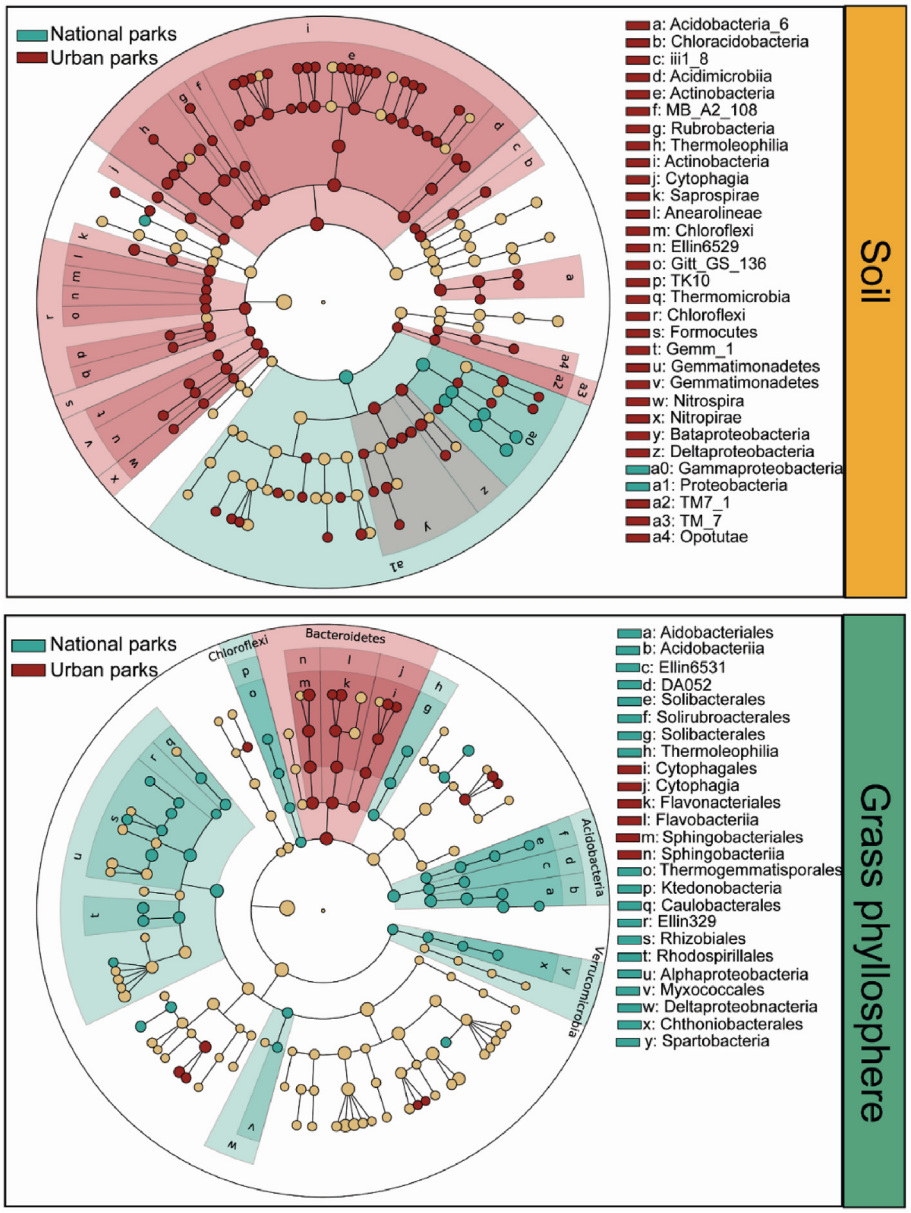

Fig. 2. Cladograms of the LEfSe analysis results indicating differences of taxa between soil and grass phyllosphere in urban green spaces and national parks. For each taxon, the red and blue denote the significantly higher abundance ($\alpha > 0.01$, LDA score > 2.0) in urban green spaces and national parks, respectively. Yellow denotes that taxon not significantly different between urban green spaces and national parks. (For interpretation of the references to colour in this figure legend, the reader is referred to the Web version of this article.)

Table 1
Spearman's ranked correlation coefficient between soil properties and anthropogenic parameters and microbial community compositions (the first axis values of PCoA analysis) in the soil and grass phyllosphere samples from urban green spaces.

	Soil properties							Anthropogenic parameters				
								Socio-economic factors		Industrial distribution		
	pH	EC (ds m^{-1})	CEC (cmol kg^{-1})	Total carbon (%)	Total nitrogen (%)	Ammonium (mg L^{-1})	Nitrate (mg L^{-1})	Population density (people km^{-2})	Median equivalised total household income (weekly AU$)	Total number of industries	Number of construction industries	Number of manufacturing industries
Soil bacterial community	−0.051	**−0.242**[a]	−0.107	0.001	−0.023	0.104	0.155	**0.307**[a]	**0.266**[a]	**0.411***	0.151	0.010
Grass phyllosphere microbial community	0.108	−0.091	0.150	0.105	0.068	−0.011	0.141	0.118	**0.238**[a]	**0.401**[a]	**0.267**[a]	0.172

[a] Indicates significant level of $P < 0.01$. Significant correlations are shown in bold text.

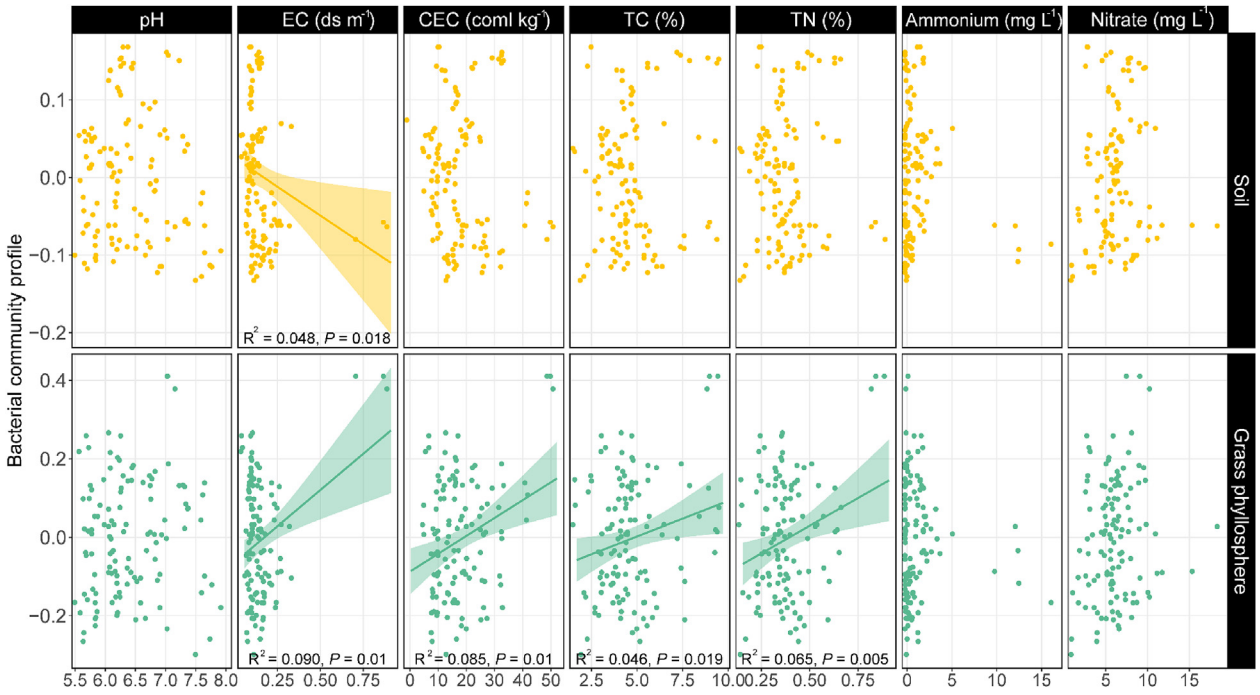

Fig. 3. Ordinary least square (OLS) regression model showing the relationships between soil properties and microbial community compositions (the first axis values of PCoA analysis) in soil and grass phyllosphere in urban green spaces. (For interpretation of the references to colour in this figure legend, the reader is referred to the Web version of this article.)

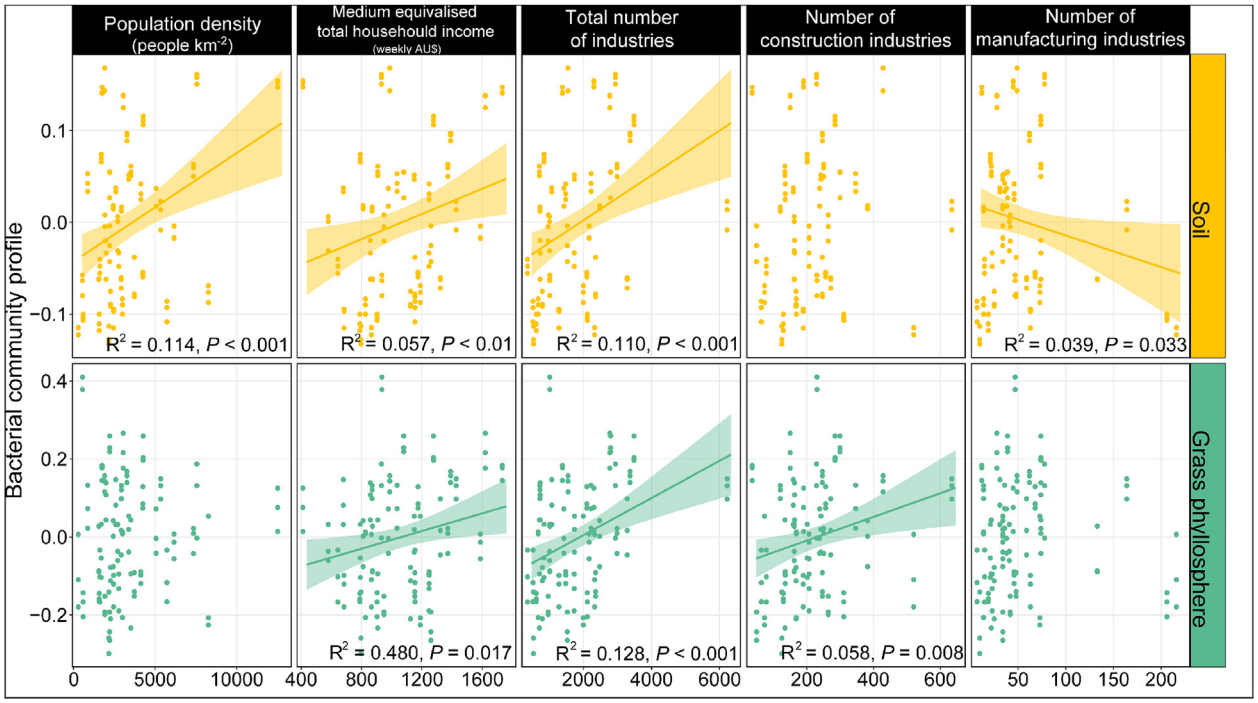

Fig. 4. Ordinary least square (OLS) regression model showing the relationships between anthropogenic parameters and microbial community compositions (the first axis values of PCoA analysis) in soil and grass phyllosphere in urban green spaces. (For interpretation of the references to colour in this figure legend, the reader is referred to the Web version of this article.)

4. Discussion

4.1. Distinct responses of soil and grass phyllosphere bacterial communities to urbanization

The impact of urbanization on microbial diversity has received substantial attention, because loss of microbial diversity could potentially lead to serious environmental and human health problems (Philippot et al., 2013; Rook, 2009; Wang et al., 2018b). The significantly higher soil bacterial α diversity in urban green spaces than in national parks (Fig. S4A) indicated that urbanization might lead to an increase in soil bacterial diversity. Other studies of

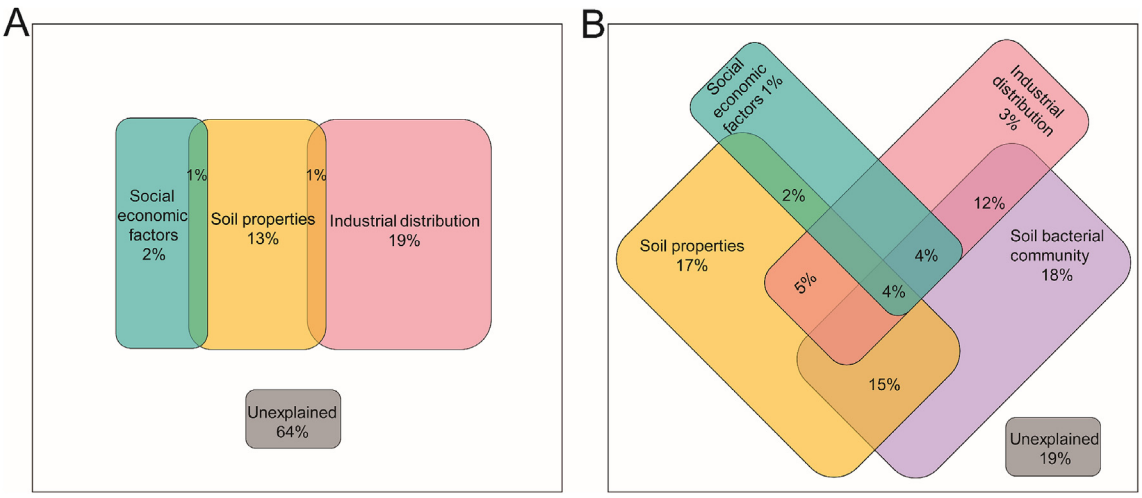

Fig. 5. Variation partitioning analysis (VPA) showing the effects of soil properties, soil bacterial communities, social economic factors and industrial factors on the alternation of soil (A) and grass phyllosphere microbial communities(B).

soil microbial diversity in parks of highly urbanized cities have reported similar results. A prior study reported that as a proxy of urbanization, the increase in human population density is associated with the increase in soil bacterial α diversity in urban green spaces in Chicago, USA (Wang et al., 2018a). Another study reported that urban park soils from Shanghai, China had a high bacterial diversity (Wang et al., 2018b). One potential explanation for the higher soil bacterial diversity in urban green spaces could be that, different from soils in national parks with minimal disturbance, soils in urban green spaces are commonly under intensive management. For example, fertilization and irrigation, which may increase the environmental heterogeneity and provide diverse ecological niches for soil microbes, contribute to a higher soil bacterial α diversity. Another key element that could contribute to the elevated level of bacterial diversity in urban environment is environmental pollution. The increase in population density and excessive use of urban land are associated with increased level of various organic and inorganic pollutants (Liang and Yang, 2019), which may also increase the habitat heterogeneity and diversify the nutrient sources, resulting in the elevated bacterial diversity in urban green spaces. However, Xu et al. (2014) suggested that soil bacterial diversity in urban parks in China was not associated with urbanization factors. Multiple factors could lead to the inconsistency in results across different studies, such as differences in laboratory methods, sampling strategies, and sample handling practices. In this case, the range of study area could be one of the main reasons for the discrepancies among study results. This study, Wang et al. (2018a) and Wang et al. (2018b) investigated urban green spaces in only one metropolitan area. However, Xu et al. (2014) collected samples from 16 cities across China. As the largest developing country, the urbanization rate of China is rapid and has increased greatly during the last decade (Liang and Yang, 2019). Therefore, the disagreement among studies could also derive from the different levels of urbanization. The inconsistency in results also indicated the complexity of factors influencing microbial diversity in the urban environment. Therefore, it is necessary to identify the key factors shaping the soil microbiome in the context of urbanization.

Different from previous studies focusing on soil microbiome only, this study also investigated the impact of urbanization on the grass phyllosphere microbiome. Phyllosphere is an enormous environment for ecosystem functions that is densely populated by diverse microorganisms (Vorholt, 2012; Woodward and Lomas, 2004). Bacteria, the most dominant group of microorganisms in the phyllosphere, can reach a surprisingly dense population of 10^5 bacterial cells per mm^{-2} leaf surface (Remus-Emsermann and Schlechter, 2018). The huge bacterial population in phyllosphere is composed mostly by commensals and beneficial symbionts, but also can include plant pathogens and even human pathogens (Dees et al., 2015; Delmotte et al., 2009; Lindow and Brandl, 2003; Yan et al., 2019). As turf grass is the direct intermedia between human skin microbiome and environmental microbiome, the microbial community in grass phyllosphere in urban green spaces could closely link to the health of urban residents (Chen et al., 2019). Our results suggested that compared to soil microbiome, the impact of urbanization on grass phyllosphere microbiome might be less apparent as there was no significant difference in phyllosphere bacterial α diversity between urban green spaces and remote national parks (Fig. S4A).

The significant differences in the bacterial community compositions (β diversity) between urban green spaces and national parks of both soil and grass phyllosphere revealed by PCoA analysis (Fig. S4B) indicated that urbanization could have altered both soil and grass phyllosphere microbial community profiles. However, the responses of soil and grass phyllosphere microbiomes to urbanization are different. According to the LEfSe analysis (Fig. 2), more bacterial taxa, including those associated with Actinobacteria, Chloroflexi, and Verrucomicrobia, were significantly enriched in soils from urban green spaces but significantly enriched in grass phyllosphere from national parks.

The potential different impacts of urbanization on soil and grass phyllosphere microbiomes could be attributed to the differences between the soil and phyllosphere environments. As the aerial part of plants, phyllosphere is a highly dynamic environment which is subject to frequent fluctuations of various environmental conditions, such as changes in temperature, moisture and UV radiation (Cordovez et al., 2019). All these factors could minimize the impact of urbanization on grass phyllosphere microbiota. Particularly, due to the ephemeral nature of grass, environmental pollutants cannot persist on grass phyllosphere for a long time. These factors could lead to no significant difference in the bacterial diversity between urban green spaces and national parks, and not many bacterial taxa enriched in grass phyllosphere. In contrast, soil is a relatively stable underground environment that is not easily impacted by environmental fluctuations but has a tight dependency on human regulation. Human activities could both directly shift the soil microbial

community, for example bring adventitious microorganisms to the soil ecosystem, and indirectly influence soil microbiota by changing soil properties and thus modifying the habitats of microorganisms (Geisen et al., 2019). More importantly, it has been widely reported that environmental organic pollutants are persistent in soil (Jones and De Voogt, 1999; Klánová et al., 2008; Manz et al., 2001; Reid et al., 2000) and could have profound impact on soil microbial community.

4.2. Industrial development as an important factor shaping the bacterial communities in urban green spaces

We characterized the relationships between soil and grass phyllosphere bacterial community compositions in urban green spaces with a variety of factors including soil properties, social economic factors and industrial factors. Although several soil properties have been identified as key drivers shaping soil microbial community (Wang et al., 2018a; Xu et al., 2014; Yan et al., 2016), in the present study, surprisingly, soil properties were not among the most important factors shaping either soil or grass phyllosphere bacterial community profile. Particularly, soil pH, which has been widely reported to be a primary factor shaping soil microbial community profile (Y. Hu et al., 2013; Xu et al., 2014; Yan et al., 2016), had no significant relationship with bacterial community composition of either sample type as suggested by the correlation (Table 1) and regression (Fig. 3) analyses. In this study, both the soil and phyllosphere bacterial communities in urban green spaces were dominated by Actinobacteria and Proteobacteria. These two bacterial taxa accounted for 72.71% and 80.12% of bacterial sequences for soil and grass phyllosphere, respectively (Fig. S1). It has been reported that the abundances of these two taxa were not sensitive to soil pH (Xu et al., 2014; Yan et al., 2016). The weak correlation between soil pH and the bacterial community compositions could be attributed to the insensitivity of the dominant bacterial taxa to soil pH. In addition, because of the relatively uniform environmental condition of our sampling range, there was no great variance in soil properties from different sampling sites (Table S3). This suggests that compared with the differences in environmental factors among the sampling sites, the variance in the urbanization degrees of the regions might play a more significant role in shaping the bacterial community profiles. Based on the correlation and regression analyses, we found that anthropogenic changes, including changes in social economic factors and industrial factors, were important drivers shaping both soil and grass phyllosphere bacterial community profiles in urban green spaces.

Among the urbanization related anthropogenic changes, industrial development was proposed to be one of the key drivers shaping bacterial community profiles in urban green spaces. For soil, VPA analysis revealed that industrial factors (i.e. the number of industries in the region), which independently explained 19% of the total variance in soil bacterial community (Fig. 5A), was the dominant predictor among all selected variables. For grass phyllosphere, although industrial factors individually explained only 3% of the variance, the interaction between industrial factors and other factors, including social economic factors, soil properties, and soil bacterial community, together explained 25% of the variance in grass phyllosphere bacterial community (Fig. 5B). Such results indicate that industrial development might be a dominant factor in shaping both soil and grass phyllosphere bacterial community profiles. The crucial effect of industrial development on the urban might mainly derive from environmental pollution, which is a major consequence of industrialization (Cherniwchan, 2012; Liang and Yang, 2019). Air pollution due to industrial emission is a crucial problem being faced by regions with an increased number of industries (Chauhan and Pawar, 2010; Han et al., 2014), which could have subtle and overt impact on airborne microbial community (Babich and Lighthart, 1974). The replacement of natural land cover with impervious surface, such as cement roads, parking lots, and other constructions, in industrialized area could further contribute to the alternation of airborne bacterial community (Docherty et al., 2018; Mhuireach et al., 2016). The deposition of air particles is highly likely to result in changes in the bacterial community compositions of both surface soil and grass phyllosphere microbiotas in urban green spaces. In addition, heavy metal pollution in the surface soils resulting from industrial wastewater discharge is another key problem faced by regions undergoing industrialization (Dolar et al., 2016; Fiorentino et al., 2019; H.W. Hu et al., 2013) which could greatly impact soil microbial communities.

5. Conclusions

In this study, we comprehensively characterized the soil and grass phyllosphere bacterial communities in urban green spaces. Our findings indicated that urbanization could have altered bacterial community profiles, and the alternations were different for below ground (soil) and above ground (grass phyllosphere) microbiomes. Most importantly, we found that compared with soil properties, anthropogenic changes, particularly industrial development may play a more significant role in shaping bacterial community profiles in urban settings. These findings expended our knowledge of the microbiota in urban green spaces and could have important implication for achieving better urban planning and urban green space management practices toward maximising the benefits of urban infrastructure.

Declaration of competing interest

The authors declare no conflict of interest.

CRediT authorship contribution statement

Zhen-Zhen Yan: Data curation, Methodology, Formal analysis, Writing - original draft. **Qing-Lin Chen:** Methodology, Writing - review & editing. **Yu-Jing Zhang:** Writing - review & editing. **Ji-Zheng He:** Writing - review & editing, Funding acquisition, Project administration. **Hang-Wei Hu:** Writing - review & editing, Funding acquisition, Project administration.

Acknowledgements

This work was financially supported by Australian Research Council (DP170103628).

Appendix A. Supplementary data

Supplementary data to this article can be found online at https://doi.org/10.1016/j.envpol.2020.114201.

References

ABS, 2016. Australian Statistical Geography Standard (ASGS): volume 1 - main structure and greater capital city statistical areas, July 2016. https://www.abs.gov.au/ausstats.

ABS, 2019. Regional population growth, Australia, 2017-2018. https://www.abs.gov.au/ausstats/abs@.nsf/mf/3218.0.

Babich, H., Lighthart, B., 1974. Air pollution and microbial ecology. Crit. Rev. Environ. Sci. Technol. 4, 353–421.

Cadenasso, M.L., Pickett, S.T., Schwarz, K., 2007. Spatial heterogeneity in urban ecosystems: reconceptualizing land cover and a framework for classification. Front. Ecol. Environ. 5, 80–88.

Canto, A., Herrera, C.M., 2012. Micro-organisms behind the pollination scenes:

microbial imprint on floral nectar sugar variation in a tropical plant community. Ann. Bot. 110, 1173–1183.
Caporaso, J.G., Kuczynski, J., Stombaugh, J., Bittinger, K., Bushman, F.D., Costello, E.K., Fierer, N., Pena, A.G., Goodrich, J.K., Gordon, J.I., 2010. QIIME allows analysis of high-throughput community sequencing data. Nat. Methods 7, 335.
Chauhan, A., Pawar, M., 2010. Assessment of ambient air quality status in urbanization, industrialization and commercial centers of Uttarakhand (India). N.Y. Sci. J. 3, 85–94.
Chen, H., Boutros, P.C., 2011. VennDiagram: a package for the generation of highly-customizable Venn and Euler diagrams in R. BMC Bioinf. 12, 35.
Chen, Q.-L., An, X.-L., Li, H., Zhu, Y.-G., Su, J.-Q., Cui, L., 2017. Do manure-borne or indigenous soil microorganisms influence the spread of antibiotic resistance genes in manured soil? Soil Biol. Biochem. 114, 229–237.
Chen, Q.-L., Cui, H.-L., Su, J.-Q., Penuelas, J., Zhu, Y.-G., 2019. Antibiotic resistomes in plant microbiomes. Trends Plant Sci. 24, 530–541.
Chen, Q.L., An, X.L., Zheng, B.X., Ma, Y.B., Su, J.Q., 2018. Long-term organic fertilization increased antibiotic resistome in phyllosphere of maize. Sci. Total Environ. 645, 1230–1237.
Cherniwchan, J., 2012. Economic growth, industrialization, and the environment. Resour. Energy Econ. 34, 442–467.
Cordovez, V., Dini-Andreote, F., Carrion, V.J., Raaijmakers, J.M., 2019. Ecology and evolution of plant microbiomes. Annu. Rev. Microbiol. 73, 69–88.
Crowther, T.W., van den Hoogen, J., Wan, J., Mayes, M.A., Keiser, A.D., Mo, L., Averill, C., Maynard, D.S., 2019. The global soil community and its influence on biogeochemistry. Science 365.
Dees, M.W., Lysøe, E., Nordskog, B., Brurberg, M.B., 2015. Bacterial communities associated with surfaces of leafy greens: shift in composition and decrease in richness over time. Appl. Environ. Microbiol. 81, 1530–1539.
Delmotte, N., Knief, C., Chaffron, S., Innerebner, G., Roschitzki, B., Schlapbach, R., von Mering, C., Vorholt, J.A., 2009. Community proteogenomics reveals insights into the physiology of phyllosphere bacteria. Proc. Natl. Acad. Sci. U.S.A. 106, 16428–16433.
Docherty, K.M., Pearce, D.S., Lemmer, K.M., Hale, R.L., 2018. Distributing regionally, distinguishing locally: examining the underlying effects of local land use on airborne bacterial biodiversity. Environ. Microbiol. 20, 3529–3542.
Dolar, D., Košutić, K., Strmecky, T., 2016. Hybrid processes for treatment of landfill leachate: coagulation/UF/NF-RO and adsorption/UF/NF-RO. Separ. Purif. Technol. 168, 39–46.
Edgar, R.C., 2010. Search and clustering orders of magnitude faster than BLAST. Bioinformatics 26, 2460–2461.
Eldridge, D.J., Travers, S.K., Val, J., Wang, J.-T., Liu, H., Singh, B.K., Delgado-Baquerizo, M., 2019. Grazing regulates the spatial heterogeneity of soil microbial communities within ecological networks. Ecosystems 1–11.
Escobedo, F.J., Kroeger, T., Wagner, J.E., 2011. Urban forests and pollution mitigation: analyzing ecosystem services and disservices. Environ. Pollut. 159, 2078–2087.
Falkowski, P.G., Fenchel, T., Delong, E.F., 2008. The microbial engines that drive Earth's biogeochemical cycles. Science 320, 1034–1039.
Fiorentino, A., Di Cesare, A., Eckert, E.M., Rizzo, L., Fontaneto, D., Yang, Y., Corno, G., 2019. Impact of industrial wastewater on the dynamics of antibiotic resistance genes in a full-scale urban wastewater treatment plant. Sci. Total Environ. 646, 1204–1210.
Flies, E.J., Skelly, C., Lovell, R., Breed, M.F., Phillips, D., Weinstein, P., 2018. Cities, biodiversity and health: we need healthy urban microbiome initiatives. Cities & Health 2, 143–150.
Flies, E.J., Skelly, C., Negi, S.S., Prabhakaran, P., Liu, Q., Liu, K., Goldizen, F.C., Lease, C., Weinstein, P., 2017. Biodiverse green spaces: a prescription for global urban health. Front. Ecol. Environ. 15, 510–516.
Francini, G., Hui, N., Jumpponen, A., Kotze, D.J., Romantschuk, M., Allen, J.A., Setälä, H., 2018. Soil biota in boreal urban greenspace: responses to plant type and age. Soil Biol. Biochem. 118, 145–155.
Fürnkranz, M., Wanek, W., Richter, A., Abell, G., Rasche, F., Sessitsch, A., 2008. Nitrogen fixation by phyllosphere bacteria associated with higher plants and their colonizing epiphytes of a tropical lowland rainforest of Costa Rica. ISME J. 2, 561.
Galbally, I.E., Kirstine, W., 2002. The production of methanol by flowering plants and the global cycle of methanol. J. Atmos. Chem. 43, 195–229.
Geisen, S., Wall, D.H., Van der Putten, W.H., 2019. Challenges and opportunities for soil biodiversity in the anthropocene. Curr. Biol. 29, R1036–R1044.
Grady, K.L., Sorensen, J.W., Stopnisek, N., Guittar, J., Shade, A., 2019. Assembly and seasonality of core phyllosphere microbiota on perennial biofuel crops. Nat. Commun. 10, 4135.
Grimm, N.B., Faeth, S.H., Golubiewski, N.E., Redman, C.L., Wu, J., Bai, X., Briggs, J.M., 2008. Global change and the ecology of cities. Science 319, 756–760.
Groffman, P.M., Williams, C.O., Pouyat, R.V., Band, L.E., Yesilonis, I.D., 2009. Nitrate leaching and nitrous oxide flux in urban forests and grasslands. J. Environ. Qual. 38, 1848–1860.
Han, L., Zhou, W., Li, W., Li, L., 2014. Impact of urbanization level on urban air quality: a case of fine particles (PM2. 5) in Chinese cities. Environ. Pollut. 194, 163–170.
Hu, Y., Liu, X., Bai, J., Shih, K., Zeng, E.Y., Cheng, H., 2013a. Assessing heavy metal pollution in the surface soils of a region that had undergone three decades of intense industrialization and urbanization. Environ. Sci. Pollut. Res. 20, 6150–6159.
Hu, H.W., Zhang, L.M., Dai, Y., Di, H., He, J.Z., 2013b. pH-dependent distribution of soil ammonia oxidizers across a large geographical scale as revealed by high-throughput pyrosequencing. J. Soils Sediements 13, 1439–1449.
Hui, N., Jumpponen, A., Francini, G., Kotze, D.J., Liu, X., Romantschuk, M., Strommer, R., Setala, H., 2017. Soil microbial communities are shaped by vegetation type and park age in cities under cold climate. Environ. Microbiol. 19, 1281–1295.
Jones, K.C., De Voogt, P., 1999. Persistent organic pollutants (POPs): state of the science. Environ. Pollut. 100, 209–221.
Kabisch, N., 2015. Ecosystem service implementation and governance challenges in urban green space planning—the case of Berlin, Germany. Land Use Pol. 42, 557–567.
Kaye, J.P., Mcculley, R., Burke, I., 2005. Carbon fluxes, nitrogen cycling, and soil microbial communities in adjacent urban, native and agricultural ecosystems. Global Change Biol. 11, 575–587.
Klánová, J., Matykiewiczová, N., Máčka, Z., Prošek, P., Láska, K., Klán, P., 2008. Persistent organic pollutants in soils and sediments from James Ross Island, Antarctica. Environ. Pollut. 152, 416–423.
Klindworth, A., Pruesse, E., Schweer, T., Peplies, J., Quast, C., Horn, M., Glockner, F.O., 2013. Evaluation of general 16S ribosomal RNA gene PCR primers for classical and next-generation sequencing-based diversity studies. Nucleic Acids Res. 41, e1.
Kolde, R., Kolde, M.R., 2015. Package 'pheatmap'. R Package 1 (7).
Li, G., Sun, G.X., Ren, Y., Luo, X.S., Zhu, Y.G., 2018. Urban soil and human health: a review. Eur. J. Soil Sci. 69, 196–215.
Liang, W., Yang, M., 2019. Urbanization, economic growth and environmental pollution: evidence from China. Sustain. Comput-Infor. 21, 1–9.
Lindow, S.E., Brandl, M.T., 2003. Microbiology of the phyllosphere. Appl. Environ. Microbiol. 69, 1875–1883.
Magoč, T., Salzberg, S.L., 2011. FLASH: fast length adjustment of short reads to improve genome assemblies. Bioinformatics 27, 2957–2963.
Manz, M., Wenzel, K.-D., Dietze, U., Schüürmann, G., 2001. Persistent organic pollutants in agricultural soils of central Germany. Sci. Total Environ. 277, 187–198.
Mcdonald, D., Price, M.N., Goodrich, J., Nawrocki, E.P., Desantis, T.Z., Probst, A., Andersen, G.L., Knight, R., Hugenholtz, P., 2012. An improved Greengenes taxonomy with explicit ranks for ecological and evolutionary analyses of bacteria and archaea. ISME J. 6, 610.
Meyer, K.M., Leveau, J.H., 2012. Microbiology of the phyllosphere: a playground for testing ecological concepts. Oecologia 168, 621–629.
Mhuireach, G., Johnson, B.R., Altrichter, A.E., Ladau, J., Meadow, J.F., Pollard, K.S., Green, J.L., 2016. Urban greenness influences airborne bacterial community composition. Sci. Total Environ. 571, 680–687.
Oksanen, J., Blanchet, F.G., Kindt, R., Legendre, P., Minchin, P.R., O'Hara, R., Simpson, G.L., Solymos, P., Stevens, M.H.H., Wagner, H., 2013. Package 'vegan'. Community ecology package version 2, 1–295.
Peñuelas, J., Terradas, J., 2014. The foliar microbiome. Trends Plant Sci. 19, 278–280.
Philippot, L., Spor, A., Hénault, C., Bru, D., Bizouard, F., Jones, C.M., Sarr, A., Maron, P.-A., 2013. Loss in microbial diversity affects nitrogen cycling in soil. ISME J. 7, 1609.
Pickett, S.T., Cadenasso, M.L., Grove, J.M., Boone, C.G., Groffman, P.M., Irwin, E., Kaushal, S.S., Marshall, V., Mcgrath, B.P., Nilon, C.H., 2011. Urban ecological systems: Scientific foundations and a decade of progress. J. EnviroN. Manage. 92, 331–362.
R Core Team, 2015. A Language and Environment for Statistical Computing. R Foundation for Statistical Computing, Vienna, Austria. http://www.R-project.Org.
Ramirez, K.S., Leff, J.W., Barberan, A., Bates, S.T., Betley, J., Crowther, T.W., Kelly, E.F., Oldfield, E.E., Shaw, E.A., Steenbock, C., Bradford, M.A., Wall, D.H., Fierer, N., 2014. Biogeographic patterns in below-ground diversity in New York City's Central Park are similar to those observed globally. Proc. Biol. Sci. 281.
Reese, A.T., Savage, A., Youngsteadt, E., Mcguire, K.L., Koling, A., Watkins, O., Frank, S.D., Dunn, R.R., 2016. Urban stress is associated with variation in microbial species composition-but not richness-in Manhattan. ISME J. 10, 751–760.
Reid, B.J., Jones, K.C., Semple, K.T., 2000. Bioavailability of persistent organic pollutants in soils and sediments—a perspective on mechanisms, consequences and assessment. Environ. Pollut. 108, 103–112.
Remus-Emsermann, M.N.P., Schlechter, R.O., 2018. Phyllosphere microbiology: at the interface between microbial individuals and the plant host. New Phytol. 218, 1327–1333.
Revelle, W., Revelle, M.W., 2015. Package 'psych'. The comprehensive R Archive Network.
Roberts, D.W., Robers, M.D., 2016. Labdsv: ordination and multivariate analysis for ecology. http://ecology.msu.montana.edu/labdsv/R.
Rook, G.A., 2009. Review series on helminths, immune modulation and the hygiene hypothesis: the broader implications of the hygiene hypothesis. Immunology 126, 3–11.
Strohbach, M.W., Haase, D., 2012. Above-ground carbon storage by urban trees in Leipzig, Germany: analysis of patterns in a European city. Landsc. Urban Plann. 104, 95–104.
Taghavi, S., Garafola, C., Monchy, S., Newman, L., Hoffman, A., Weyens, N., Barac, T., Vangronsveld, J., Van der Lelie, D., 2009. Genome survey and characterization of endophytic bacteria exhibiting a beneficial effect on growth and development of poplar trees. Appl. Environ. Microbiol. 75, 748–757.
Vorholt, J.A., 2012. Microbial life in the phyllosphere. Nat. Rev. Microbiol. 10, 828.
Wang, H., Cheng, M., Dsouza, M., Weisenhorn, P., Zheng, T., Gilbert, J.A., 2018a. Soil bacterial diversity is associated with human population density in urban greenspaces. Environ. Sci. Technol. 52, 5115–5124.

Wang, X., Wu, J., Kumari, D., 2018b. Composition and functional genes analysis of bacterial communities from urban parks of Shanghai, China and their role in ecosystem functionality. Landsc. Urban Plann. 177, 83–91.
Wickham, H., 2016. ggplot2: Elegant Graphics for Data Analysis. Springer.
Woodward, F., Lomas, M., 2004. Vegetation dynamics–simulating responses to climatic change. Biol. Rev. 79, 643–670.
Xu, H.J., Li, S., Su, J.Q., Nie, S., Gibson, V., Li, H., Zhu, Y.G., 2014. Does urbanization shape bacterial community composition in urban park soils? A case study in 16 representative Chinese cities based on the pyrosequencing method. FEMS Microbiol. Ecol. 87, 182–192.
Yan, B., Li, J., Xiao, N., Qi, Y., Fu, G., Liu, G., Qiao, M., 2016. Urban-development-induced changes in the diversity and composition of the soil bacterial community in Beijing. Sci. Rep. 6, 38811.
Yan, Z.Z., Chen, Q.L., Zhang, Y.J., He, J.Z., Hu, H.W., 2019. Antibiotic resistance in urban green spaces mirror the pattern of industrial distribution. Environ. Int. 132, 105106.
Zhang, Y.-J., Hu, H.-W., Chen, Q.-L., Singh, B.K., Yan, H., Chen, D., He, J.-Z., 2019. Transfer of antibiotic resistance from manure-amended soils to vegetable microbiomes. Environ. Int. 130.
Zhu, Y.-G., Ioannidis, J.P., Li, H., Jones, K.C., Martin, F.L., 2011. Understanding and Harnessing the Health Effects of Rapid Urbanization in China. ACS Publications.
Zhu, Y.G., Zhao, Y., Li, B., Huang, C.L., Zhang, S.Y., Yu, S., Chen, Y.S., Zhang, T., Gillings, M.R., Su, J.Q., 2017. Continental-scale pollution of estuaries with antibiotic resistance genes. Nat. Microbiol. 2, 16270.

Supplementary data for Industrial development as a key factor explaining variances in soil and grass phyllosphere microbiomes in urban green spaces

Zhen-Zhen Yan [a], Qing-Lin Chen [a, *], Yu-Jing Zhang [a], Ji-Zheng He [a], Hang-Wei Hu [a, *]

[a] Faculty of Veterinary and Agricultural Sciences, The University of Melbourne, VIC 3010, Australia

Corresponding Authors at Faculty of Veterinary and Agricultural Sciences, The University of Melbourne

*E-mail: qinglin.chen@unimelb.edu.au or hang-wei.hu@unimelb.edu.au

Contents

Table S1 Detailed information of sampling sites.

Table S2 Anthropogenic parameters of Statistical Area Level 2 (SA2) regions where the urban green spaces locate in.

Table S3 List of analysed soil properties of the 120 soil samples from urban green spaces

Fig. S1 Bacterial community compositions in soil and grass phyllosphere samples across sampling sites at phylum level.

Fig. S2. Distribution bar-plot of bacterial community compositions in soil (A) and grass phyllosphere (B) samples across different urban green spaces and national parks at phylum level.

Fig. S3. Heatmap of bacterial community compositions in soil (A) and grass phyllosphere (B) samples across the investigated urban green spaces and national parks at genera level.

Fig. S4. Boxplots showing the Shannon index (α diversity) in soil and grass phyllosphere samples in the 40 urban green spaces and three national parks. *** indicates $P < 0.001$ determined by paired t-test(A); and principal coordinate analysis (PCoA) based on the Bray-Curtis distance showing the distribution patterns of microbiome in soil and grass phyllosphere samples (β diversity) (B).

Table S1 Detailed information of sampling sites.

Sample site ID	Green space Name	Statistic Area Level 2 (SA2) name	Suburb/Region name	Post code	Latitude	Longitude
U1	Parker Reserve	Coburg North	Coburg North	3058	37°43'20.30"S	144°58'2.56"E
U2	Parker Reserve	Coburg North	Coburg North	3058	37°43'22.53"S	144°58'3.08"E
U3	Parker Reserve	Coburg North	Coburg North	3058	37°43'17.40"S	144°58'1.07"E
U4	Charles Mutton Reserve	Fawkner	Fawkner	3060	37°42'49.99"S	144°58'12.46"E
U5	Charles Mutton Reserve	Fawkner	Fawkner	3060	37°42'50.12"S	144°58'9.37"E
U6	Charles Mutton Reserve	Fawkner	Fawkner	3060	37°42'49.86"S	144°58'16.41"E
U7	Greensborough Park	Greensborough	Greensborough	3088	37°42'0.76"S	145° 6'23.72"E
U8	Greensborough Park	Greensborough	Greensborough	3088	37°42'2.45"S	145° 6'22.59"E
U9	Greensborough Park	Greensborough	Greensborough	3088	37°41'59.92"S	145° 6'16.54"E
U10	Hibiscus Park	Bundoora-North	Bundoora	3083	37°41'2.01"S	145° 3'43.57"E
U11	Hibiscus Park	Bundoora-North	Bundoora	3083	37°41'3.11"S	145° 3'43.71"E
U12	Hibiscus Park	Bundoora-North	Bundoora	3083	37°41'1.97"S	145° 3'45.35"E
U13	Bricker Reserve	Moorabbin-Heatherton	Moorabbin	3189	37°56'27.67"S	145° 3'6.42"E

U14	Bricker Reserve	Moorabbin-Heatherton	Moorabbin	3189	37°56'29.98"S	145° 3'4.88"E
U15	Bricker Reserve	Moorabbin-Heatherton	Moorabbin	3189	37°56'31.77"S	145° 3'3.48"E
U16	Banksia Reserve Playground	Beaumaris	Beaumaris	3193	37°59'12.17"S	145° 2'31.58"E
U17	Banksia Reserve Playground	Beaumaris	Beaumaris	3193	37°59'9.90"S	145° 2'32.34"E
U18	Banksia Reserve Playground	Beaumaris	Beaumaris	3193	37°59'10.69"S	145° 2'29.98"E
U19	Dendy Park	Brighton East	Brighton East	3187	37°55'31.45"S	145° 1'23.98"E
U20	Dendy Park	Brighton East	Brighton East	3187	37°55'32.89"S	145° 1'20.83"E
U21	Dendy Park	Brighton East	Brighton East	3187	37°55'34.22"S	145° 1'25.40"E
U22	Carrum Pirate Ship Park	Carrum - Patterson Lakes	Carrum	3197	38° 4'35.75"S	145° 8'2.39"E
U23	Carrum Pirate Ship Park	Carrum - Patterson Lakes	Carrum	3197	38° 4'35.50"S	145° 7'59.92"E
U24	Carrum Pirate Ship Park	Carrum - Patterson Lakes	Carrum	3197	38° 4'38.22"S	145° 7'55.86"E
U25	Princess Park	Caulfied - South	Caulfied South	3162	37°53'37.50"S	145° 1'28.37"E
U26	Princess Park	Caulfied - South	Caulfied South	3162	37°53'39.11"S	145° 1'30.42"E
U27	Princess Park	Caulfied - South	Caulfied South	3162	37°53'36.81"S	145° 1'35.46"E

U28	Harleston Park	Elsternwick	Elsternwick	3185	37°52'52.10"S	145° 0'35.06"E
U29	Harleston Park	Elsternwick	Elsternwick	3185	37°52'53.00"S	145° 0'32.84"E
U30	Harleston Park	Elsternwick	Elsternwick	3185	37°52'53.50"S	145° 0'35.63"E
U31	Lord Reserve	Carnegie	Carnegie	3163	37°53'39.68"S	145° 2'56.80"E
U32	Lord Reserve	Carnegie	Carnegie	3163	37°53'38.23"S	37°53'38.23"S
U33	Lord Reserve	Carnegie	Carnegie	3163	37°53'41.83"S	145° 3'1.45"E
U34	Victoria Gardens	Prahran-Windsor	Prahran	3181	37°51'6.75"S	145° 0'3.68"E
U35	Victoria Gardens	Prahran-Windsor	Prahran	3181	37°51'7.04"S	145° 0'3.03"E
U36	Victoria Gardens	Prahran-Windsor	Prahran	3181	37° 51'7.03"E	145° 0'3.01"E
U37	Brookville Gardens	Toorak	Toorak	3142	37°50'43.81"S	37°50'43.81"S
U38	Brookville Gardens	Toorak	Toorak	3142	37°50'43.49"S	145° 0'32.10"E
U39	Brookville Gardens	Toorak	Toorak	3142	37°50'43.07"S	145° 0'35.02"E
U40	Citizens Park	Richmond (Vic.)	Richmond	3121	37°49'0.32"S	145° 0'2.53"E
U41	Citizens Park	Richmond (Vic.)	Richmond	3121	37°48'59.93"S	37°48'59.93"S
U42	Citizens Park	Richmond (Vic.)	Richmond	3121	37°49'1.69"S	145° 0'4.04"E
U43	Garden City Reserve	Port Melbourne	Port Melbourne	3207	37°50'11.08"S	144°55'47.35"E

U44	Garden City Reserve	Port Melbourne	Port Melbourne	3207	37°50'13.37"S	144°55'50.80"E
U45	Garden City Reserve	Port Melbourne	Port Melbourne	3207	37°50'10.95"S	37°50'10.95"S
U46	Templestowe Reserve	Templestowe	Templestowe	3106	37°45'14.52"S	145° 8'14.12"E
U47	Templestowe Reserve	Templestowe	Templestowe	3106	37°45'14.42"S	145° 8'15.63"E
U48	Templestowe Reserve	Templestowe	Templestowe	3106	37°45'16.54"S	145° 8'11.76"E
U49	Macleay Park	Balwyn North	Balwyn North	3104	37°48'4.88"S	145° 4'31.23"E
U50	Macleay Park	Balwyn North	Balwyn North	3104	37°48'3.62"S	145° 4'32.60"E
U51	Macleay Park	Balwyn North	Balwyn North	3104	37°48'5.91"S	145° 4'32.47"E
U52	Schramms Reserve	Doncaster	Doncaster	3108	37°46'58.83"S	145° 8'1.69"E
U53	Schramms Reserve	Doncaster	Doncaster	3108	37°47'1.10"S	145° 7'59.80"E
U54	Schramms Reserve	Doncaster	Doncaster	3108	37°47'0.73"S	145° 8'2.23"E
U55	Bennettswood Reserve	Burwood	Burwood	3125	37°50'54.44"S	145° 6'43.46"E
U56	Bennettswood Reserve	Burwood	Burwood	3125	37°50'51.51"S	145° 6'45.15"E
U57	Bennettswood Reserve	Burwood	Burwood	3125	37°50'57.05"S	145° 6'45.34"E
U58	Lynden Park	Camberwell	Camberwell	3124	37°50'36.34"S	145° 5'11.72"E
U59	Lynden Park	Camberwell	Camberwell	3124	37°50'38.81"S	145° 5'12.65"E

U60	Lynden Park	Camberwell	Camberwell	3124	37°50'38.04"S	145° 5'6.31"E
U61	Eley Park	Blackburn South	Blackburn South	3130	37°50'45.23"S	145° 8'34.33"E
U62	Eley Park	Blackburn South	Blackburn South	3130	37°50'44.83"S	145° 8'36.44"E
U63	Eley Park	Blackburn South	Blackburn South	3130	37°50'43.73"S	145° 8'33.14"E
U64	Central Gardens	Hawthorn	Hawthorn	3122	37°49'16.06"S	145° 2'29.33"E
U65	Central Gardens	Hawthorn	Hawthorn	3122	37°49'18.00"S	145° 2'27.44"E
U66	Central Gardens	Hawthorn	Hawthorn	3122	37°49'14.96"S	145° 2'31.59"E
U67	Malvern Public Gardens	Malvern - Glen Iris	Malvern	3144	37°51'25.03"S	145° 2'7.30"E
U68	Malvern Public Gardens	Malvern - Glen Iris	Malvern	3144	37°51'23.82"S	145° 2'8.77"E
U69	Malvern Public Gardens	Malvern - Glen Iris	Malvern	3144	37°51'20.57"S	145° 2'8.56"E
U70	Fitzroy Gardens	East Melbourne	East Melbourne	3002	37°48'45.94"S	144°58'51.36"E
U71	Fitzroy Gardens	East Melbourne	East Melbourne	3002	37°48'50.47"S	144°58'45.74"E
U72	Fitzroy Gardens	East Melbourne	East Melbourne	3002	37°48'42.46"S	144°58'57.72"E
U73	Queens Park	Moonee Ponds	Moonee Ponds	3039	37°45'43.70"S	37°45'43.70"S
U74	Queens Park	Moonee Ponds	Moonee Ponds	3039	37°45'43.95"S	144°55'27.56"E
U75	Queens Park	Moonee Ponds	Moonee Ponds	3039	37°45'42.11"S	144°55'24.19"E

U76	Batman Park	Northcote	Northcote	3070	37°49'18.34"S	144°57'26.08"E
U77	Batman Park	Northcote	Northcote	3070	37°49'18.80"S	144°57'23.70"E
U78	Batman Park	Northcote	Northcote	3070	37°49'18.94"S	144°57'21.71"E
U79	Flagstaff Gardens	North Melbourne	West Melbourne	3003	37°48'38.46"S	144°57'15.65"E
U80	Flagstaff Gardens	North Melbourne	West Melbourne	3003	37°48'35.44"S	144°57'18.43"E
U81	Flagstaff Gardens	North Melbourne	West Melbourne	3003	37°48'33.59"S	37°48'33.59"S
U82	Atherton Reserve	Fitzroy	Fitzroy	3065	37°48'11.98"S	144°58'45.28"E
U83	Atherton Reserve	Fitzroy	Fitzroy	3065	37°48'12.93"S	144°58'46.01"E
U84	Atherton Reserve	Fitzroy	Fitzroy	3065	37°48'12.81"S	144°58'44.11"E
U85	Carlton Gardens	Carlton	Carlton	3053	37°48'19.51"S	144°58'17.39"E
U86	Carlton Gardens	Carlton	Carlton	3053	37°48'20.30"S	144°58'14.83"E
U87	Carlton Gardens	Carlton	Carlton	3053	37°48'20.15"S	144°58'12.44"E
U88	H.P. Zwar Park	Preston-West	Preston	3072	37°44'27.80"S	144°59'46.74"E
U89	H.P. Zwar Park	Preston-West	Preston	3072	37°44'31.45"S	144°59'47.78"E
U90	H.P. Zwar Park	Preston-West	Preston	3072	37°44'31.10"S	144°59'44.17"E
U91	Brimbank Park	Keilor	Keilor East	3033	37°44'2.40"S	144°50'13.22"E

U92	Brimbank Park	Keilor	Keilor East	3033	37°44'1.94"S	144°49'58.45"E
U93	Brimbank Park	Keilor	Keilor East	3033	37°43'54.11"S	144°50'17.52"E
U94	A J Davis Reserve	Airport West	Airport West	3042	37°43'41.99"S	144°52'26.40"E
U95	A J Davis Reserve	Airport West	Airport West	3042	37°43'42.86"S	144°52'23.65"E
U96	A J Davis Reserve	Airport West	Airport West	3042	37°43'45.54"S	144°52'24.35"E
U97	Napier Park	Strathmore	Strathmore	3041	37°44'28.28"S	144°55'7.90"E
U98	Napier Park	Strathmore	Strathmore	3041	37°44'28.15"S	144°55'10.18"E
U99	Napier Park	Strathmore	Strathmore	3041	37°44'26.36"S	144°55'4.91"E
U100	Selwyn Park	Ardeer - Albion	Albion	3020	37°46'51.27"S	144°48'51.66"E
U101	Selwyn Park	Ardeer - Albion	Albion	3020	37°46'53.14"S	144°48'53.11"E
U102	Selwyn Park	Ardeer - Albion	Albion	3020	37°46'50.00"S	144°48'53.65"E
U103	Cairnlea Park	Cairnlea	Cairnlea	3023	37°45'35.68"S	144°47'44.24"E
U104	Cairnlea Park	Cairnlea	Cairnlea	3023	37°45'35.98"S	144°47'42.99"E
U105	Cairnlea Park	Cairnlea	Cairnlea	3023	37°45'36.77"S	144°47'44.79"E
U106	Braybrook Park	Braybrook	Braybrook	3019	37°47'13.78"S	144°51'17.84"E
U107	Braybrook Park	Braybrook	Braybrook	3019	37°47'12.17"S	144°51'19.15"E

U108	Braybrook Park	Braybrook	Braybrook	3019	37°47'15.04"S	144°51'20.62"E
U109	Pioneer Park	Sydenham	Sydenham	3037	37°41'13.06"S	37°41'13.06"S
U110	Pioneer Park	Sydenham	Sydenham	3037	37°41'15.28"S	144°45'31.88"E
U111	Pioneer Park	Sydenham	Sydenham	3037	37°41'13.56"S	144°45'42.77"E
U112	Mappin Reserve	Seddo - Kingsville	Seddon	3011	37°48'33.67"S	144°53'50.51"E
U113	Mappin Reserve	Seddo - Kingsville	Seddon	3011	37°48'33.04"S	144°53'51.48"E
U114	Mappin Reserve	Seddo - Kingsville	Seddon	3011	37°48'35.68"S	144°53'49.61"E
U115	Logan Reserve	Altona	Altona	3018	37°52'12.15"S	144°49'46.08"E
U116	Logan Reserve	Altona	Altona	3018	37°52'12.13"S	144°49'45.07"E
U117	Logan Reserve	Altona	Altona	3018	37°52'11.30"S	144°49'47.39"E
U118	Bruce Comben Reserve	Altona - Meadows	Altona Meadows	3028	37°52'19.19"S	144°46'1.12"E
U119	Bruce Comben Reserve	Altona - Meadows	Altona Meadows	3028	37°52'20.45"S	144°45'59.82"E
U120	Bruce Comben Reserve	Altona - Meadows	Altona Meadows	3028	37°52'17.88"S	144°46'3.48"E
N1	Yarra ranges national park	NA	Reefton	3799	37˚38'11"S	145˚54'23"E
N2	Yarra ranges national park	NA	Reefton	3799	37˚37'53"S	145˚54'28"E

N3	Yarra ranges national park	NA	Reefton	3799	37˚37'52"S	145˚54'31"E
N4	Lake Eildon national park	NA	Central highlands (Victoria)	3660	37˚14'33"S	145˚57'14"E
N5	Lake Eildon national park	NA	Central highlands (Victoria)	3660	37˚14'2"S	145˚57'7"E
N6	Lake Eildon national park	NA	Central highlands (Victoria)	3660	37˚13'52"S	145˚54'10"E
N7	Kinglake national park	NA	Kinglake	3763	37˚25'28"S	145˚15'48"E
N8	Kinglake national park	NA	Kinglake	3763	37˚27'33"S	145˚14'29"E
N9	Kinglake national park	NA	Kinglake	3763	37˚27'37"S	145˚14'19"E

Table S2 Anthropogenic parameters of Statistical Area Level 2 (SA2) regions where the urban green spaces locate in.

	Socio-economic parameters		**Industrial distribution**		
SA2 name	Population density (people km^{-2})	Median equivalised total household income (weekly AU$)	Total number of industries	Number of construction industries	Number of manufacturing industries
Coburg North	1777	898	1130	174	137
Fawkner	2943	605	1126	174	45
Greensborough	2136	1013	1661	440	53
Bundoora-North	1801	815	735	141	23

Moorabbin-Heatherton	817	929	2231	322	210
Beaumaris	2447	1285	1644	61	38
Brighton East	3010	1273	1846	218	27
Carrum - Patterson Lakes	2155	974	1084	276	46
Caulfied - South	3955	1179	2472	258	52
Elsternwick	4366	1274	1597	147	50
Carnegie	5291	1003	1539	250	42
Prahran-Windsor	7582	1397	3102	262	78
Toorak	3281	1646	2892	162	32
Richmond (Vic.)	5576	1452	6331	646	168
Port Melbourne	6395	1614	2282	218	38
Templestowe	1100	1061	2339	358	40
Balwyn North	2451	1105	2910	311	43
Doncaster	2667	836	2591	394	38
Burwood	2814	705	1186	171	35
Camberwell	3156	1348	3402	283	63
Blackburn South	3168	896	840	132	18
Hawthorn	4498	1303	3599	296	78
Malvern - Glen Iris	3510	1416	3485	258	66

East Melbourne	1979	1759	1502	48	16
Moonee Ponds	3611	1175	1853	254	38
Northcote	4478	1200	2216	268	72
North Melbourne	7797	958	3054	241	82
Fitzroy	8505	1216	2116	85	77
Carlton	12753	437	2421	202	49
Preston-West	3745	933	826	146	26
Keilor	518	891	2443	532	220
Airport West	2226	884	848	175	78
Strathmore	2503	1150	908	179	29
Ardeer - Albion	1843	669	477	90	19
Cairnlea	2399	821	648	137	14
Braybrook	2690	709	1396	201	67
Sydenham	3232	851	786	180	18
Seddo - Kingsville	5959	1180	636	75	11
Altona	775	961	1129	242	51
Altona - Meadows	1936	818	961	213	25

Table S3 List of analysed soil properties of the 120 soil samples from urban green spaces

Sample ID	pH	EC (ds m^{-1})	CEC (coml kg^{-1})	Total carbon (%)	Total nitrogen (%)	Ammonium (mg L^{-1})	Nitrate (mg L^{-1})
SU1	6.12	0.27	19.95	5.41	0.47	1.86	12.20
SU2	6.12	0.34	21.39	5.75	0.55	12.50	18.80
SU3	6.23	0.29	20.52	5.66	0.52	10.20	15.80
SU4	6.18	0.11	11.16	3.10	0.29	3.14	4.90
SU5	6.21	0.14	15.20	3.85	0.36	2.55	6.30
SU6	6.23	0.15	17.04	4.75	0.44	2.64	7.42
SU7	6.36	0.11	11.35	2.68	0.26	1.57	3.31
SU8	6.44	0.12	11.76	2.72	0.27	1.89	3.23
SU9	6.32	0.11	10.84	2.54	0.25	1.23	3.04
SU10	5.56	0.16	16.67	5.63	0.52	0.54	9.18
SU11	5.77	0.13	17.17	4.45	0.39	0.20	7.81
SU12	5.72	0.14	15.12	4.71	0.42	0.20	7.80
SU13	5.90	0.18	13.65	5.57	0.43	0.83	8.73
SU14	5.91	0.19	14.62	6.06	0.47	1.00	8.56
SU15	5.91	0.20	14.77	6.16	0.48	1.03	8.78
SU16	5.71	0.09	8.95	4.97	0.42	1.64	4.43
SU17	5.70	0.10	9.29	5.38	0.46	1.67	4.38
SU18	5.65	0.10	9.08	5.07	0.45	1.67	4.47
SU19	5.86	0.11	9.36	4.60	0.40	0.20	6.18
SU20	5.93	0.10	9.90	4.36	0.37	0.27	6.27
SU21	5.89	0.11	9.99	4.18	0.37	0.71	5.62
SU22	6.31	0.12	9.46	2.40	0.21	0.56	6.78
SU23	6.27	0.12	11.11	2.90	0.25	0.56	6.90
SU24	6.26	0.15	10.98	3.12	0.27	0.68	7.13
SU25	6.24	0.20	10.76	4.15	0.34	1.24	10.70
SU26	6.17	0.20	11.21	3.92	0.31	1.11	11.60
SU27	6.30	0.19	9.52	3.26	0.25	1.09	10.50
SU28	6.26	0.08	11.06	3.56	0.24	0.74	4.53
SU29	6.43	0.10	11.93	3.33	0.25	0.62	6.04
SU30	6.49	0.10	11.54	3.28	0.25	0.55	5.63
SU31	6.15	0.12	10.56	3.82	0.3	4.10	3.37

SU32	6.16	0.12	11.25	4.175	0.34	3.78	3.26
SU33	6.12	0.12	10.71	3.66	0.30	3.63	3.55
SU34	5.84	0.13	8.93	3.25	0.27	2.55	7.16
SU35	5.72	0.17	9.57	3.59	0.30	3.09	9.48
SU36	5.84	0.20	10.19	3.298	0.28	5.50	11.4
SU37	6.15	0.12	13.82	4.38	0.38	0.56	8.19
SU38	6.15	0.12	12.76	4.14	0.34	0.39	7.56
SU39	6.12	0.13	14.06	4.35	0.38	0.32	8.55
SU40	6.81	0.13	17.41	4.38	0.34	0.27	6.54
SU41	6.82	0.14	17.19	4.22	0.34	0.20	6.91
SU42	6.84	0.14	17.37	4.26	0.35	0.20	6.73
SU43	6.89	0.11	13.89	5.11	0.36	0.20	6.03
SU44	6.91	0.11	14.57	4.62	0.32	0.24	6.42
SU45	6.88	0.11	6.33	4.69	0.34	0.20	5.94
SU46	7.38	0.13	18.16	3.72	0.281	0.20	6.69
SU47	7.35	0.13	20.02	4.40	0.31	0.20	7.17
SU48	7.43	0.13	21.07	4.01	0.29	0.20	6.28
SU49	5.63	0.06	6.88	3.24	0.26	1.64	3.59
SU50	5.75	0.06	8.07	3.26	0.27	2.01	3.18
SU51	5.79	0.07	8.11	3.49	0.29	2.18	3.44
SU52	6.17	0.17	15.26	4.37	0.39	1.45	6.84
SU53	6.14	0.16	15.08	4.35	0.39	1.39	7.24
SU54	6.14	0.16	14.58	4.04	0.36	1.08	7.00
SU55	5.98	0.12	6.27	1.83	0.17	1.63	5.44
SU56	6.04	0.13	15.47	1.80	0.17	1.91	6.14
SU57	6.05	0.12	5.89	1.70	0.16	1.43	5.58
SU58	5.70	0.10	12.23	4.56	0.40	0.75	5.74
SU59	5.75	0.09	11.33	4.26	0.36	0.20	5.29
SU60	5.78	0.09	11.23	4.31	0.37	0.29	5.40
SU61	5.80	0.11	13.48	4.89	0.42	1.51	6.48
SU62	5.82	0.11	13.58	4.91	0.43	2.04	6.66
SU63	5.84	0.10	13.18	4.92	0.43	1.88	6.03
SU64	6.30	0.12	17.83	5.00	0.38	0.49	5.77
SU65	6.32	0.12	18.44	4.93	0.37	1.21	6.34
SU66	6.27	0.12	17.46	4.94	0.37	0.84	5.82

SU67	6.69	0.11	17.67	4.93	0.38	0.75	6.94
SU68	6.89	0.12	17.98	4.43	0.35	0.52	6.83
SU69	6.80	0.12	16.64	4.52	0.36	0.83	6.98
SU70	6.51	0.17	23.59	6.29	0.49	0.20	10.00
SU71	6.50	0.17	23.35	5.82	0.46	0.24	10.20
SU72	6.53	0.158	24.45	5.82	0.46	0.40	9.45
SU73	5.74	0.18	26.42	9.48	0.67	2.08	7.38
SU74	5.89	0.15	26.10	8.64	0.59	2.50	6.99
SU75	5.84	0.16	26.43	9.52	0.66	2.25	7.41
SU76	7.44	0.27	26.85	4.60	0.38	0.23	5.15
SU77	7.38	0.28	25.38	4.72	0.39	0.20	5.37
SU78	7.40	0.26	28.84	4.63	0.38	0.21	6.16
SU79	7.29	0.156	34.61	8.10	0.57	0.20	5.03
SU80	7.11	0.15	33.90	7.64	0.53	0.20	5.48
SU81	7.08	0.17	33.98	7.43	0.51	0.20	6.06
SU82	5.94	0.13	19.83	5.89	0.48	2.34	5.40
SU83	5.90	0.13	19.87	5.57	047	0.49	5.50
SU84	5.90	0.14	19.68	5.77	0.49	0.53	6.95
SU85	6.37	0.18	33.87	9.62	0.652	2.26	8.17
U86	6.31	0.17	32.91	9.712	0.682	2.23	8.13
U87	6.33	0.18	30.56	9.14	0.65	2.28	8.42
U88	6.97	0.16	21.17	4.59	0.40	0.20	6.11
U89	7.05	0.17	19.41	5.11	0.44	0.20	6.47
U90	7.09	0.18	21.40	5.20	0.45	0.20	7.06
U91	7.00	0.12	27.57	6.60	0.42	0.20	3.87
U92	6.93	0.12	26.98	5.75	0.39	0.20	4.07
U93	6.97	0.12	27.55	6.29	0.40	0.20	4.06
U94	7.65	0.26	42.73	4.85	0.43	0.20	8.40
U95	7.68	0.24	43.19	5.30	0.46	0.20	7.88
U96	7.71	0.24	42.17	5.16	0.44	0.48	9.41
U97	6.59	0.19	27.91	7.83	0.62	0.78	6.23
U98	6.43	0.17	24.20	7.63	0.59	0.79	6.31
U99	6.57	0.19	26.59	7.83	0.61	0.94	6.37
U100	6.75	0.19	18.60	4.59	0.38	2.29	2.32
U101	6.55	0.18	17.24	3.20	0.28	1.46	2.15

U102	6.65	0.19	18.23	3.90	0.34	2.04	2.18
U103	7.56	0.14	14.21	2.14	0.16	0.35	1.30
U104	7.66	0.15	14.70	2.31	0.18	0.42	1.49
U105	7.80	0.17	17.91	2.49	0.19	0.44	1.35
U106	7.83	0.24	33.61	3.80	0.31	0.24	3.40
U107	7.98	0.26	34.23	2.90	0.25	0.33	3.03
U108	7.71	0.22	33.24	4.15	0.31	0.38	3.06
U109	6.81	0.13	28.26	4.69	0.37	0.25	4.93
U110	6.77	0.13	27.49	4.60	0.36	0.24	5.23
U111	6.73	0.13	28.71	4.32	0.38	0.30	4.94
U112	6.18	0.27	17.47	4.24	0.364	16.50	6.06
U113	6.20	0.23	17.01	3.98	0.35	12.80	6.03
U114	6.26	0.23	16.63	3.90	0.36	12.90	6.33
U115	7.09	0.89	51.23	9.20	0.86	0.54	9.53
U116	7.10	0.73	50.06	9.65	0.91	0.54	7.93
U117	7.22	0.91	52.15	9.06	0.84	0.29	10.70
U118	6.65	0.35	22.49	5.24	0.41	0.35	9.55
U119	6.41	0.30	23.37	6.69	0.56	0.47	10.30
U120	6.45	0.29	21.50	4.98	0.40112	0.77	8.44

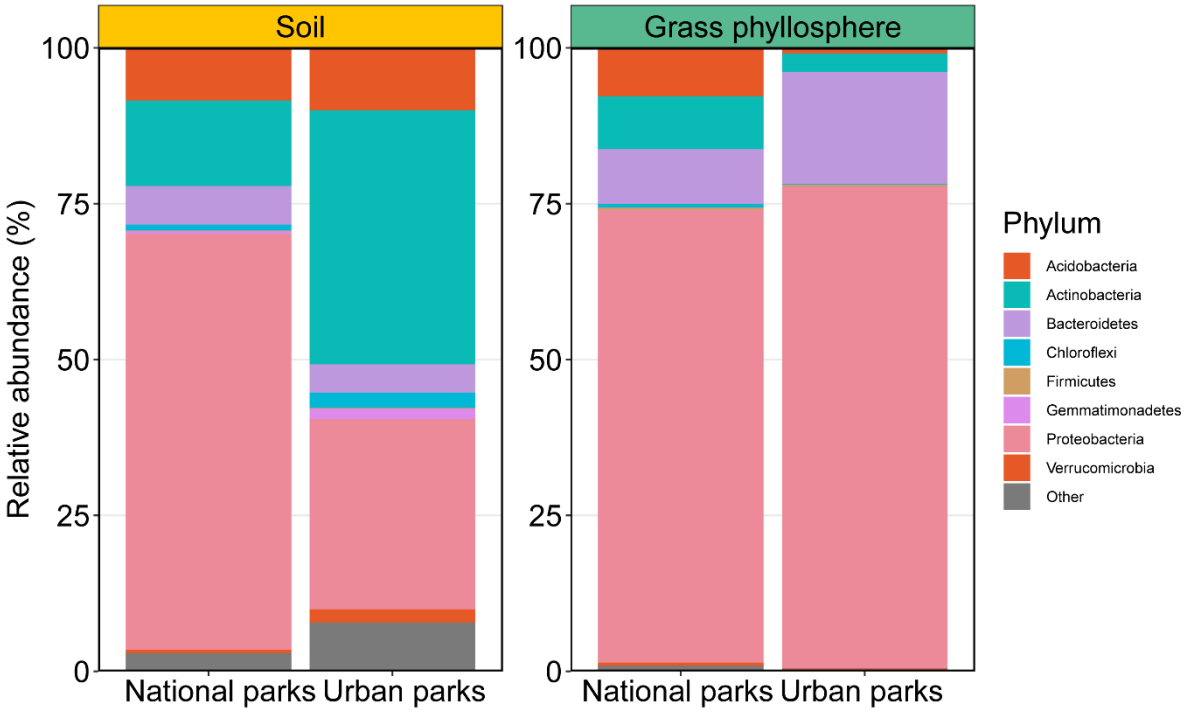

Fig. S1. Bacterial community compositions in soil and grass phyllosphere samples across sampling sites at phylum level.

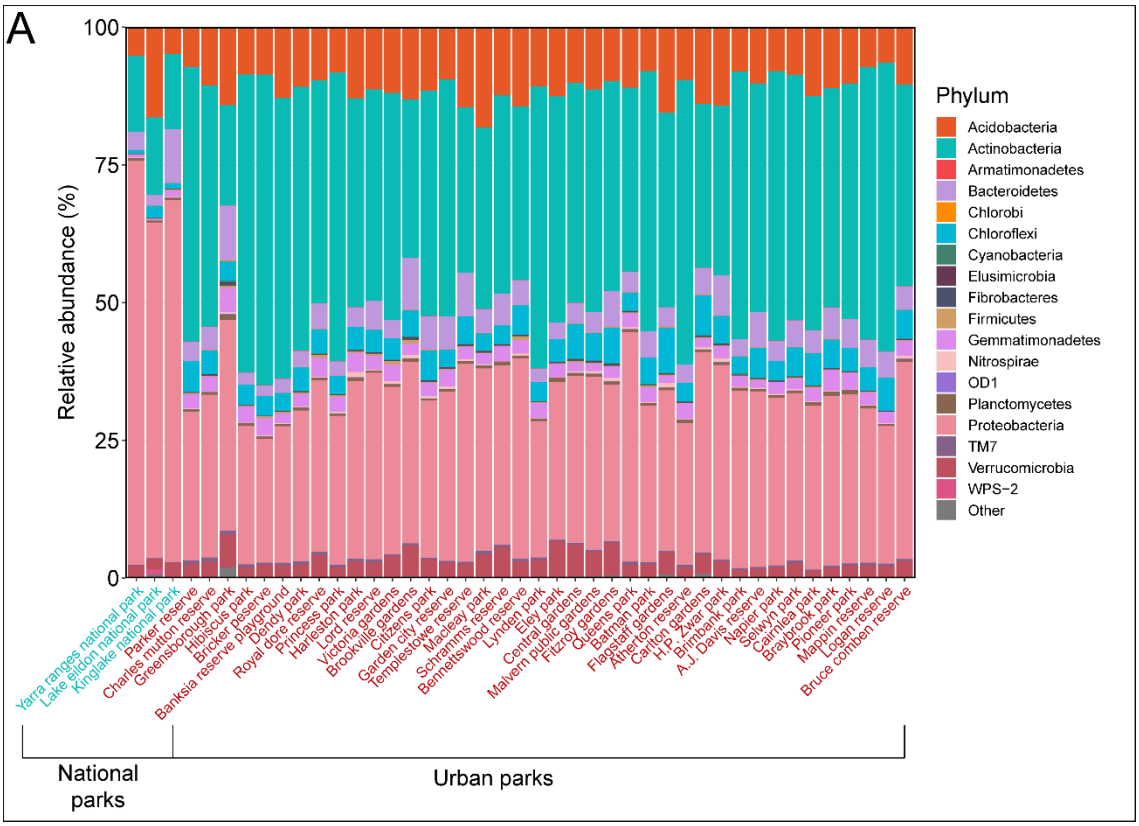

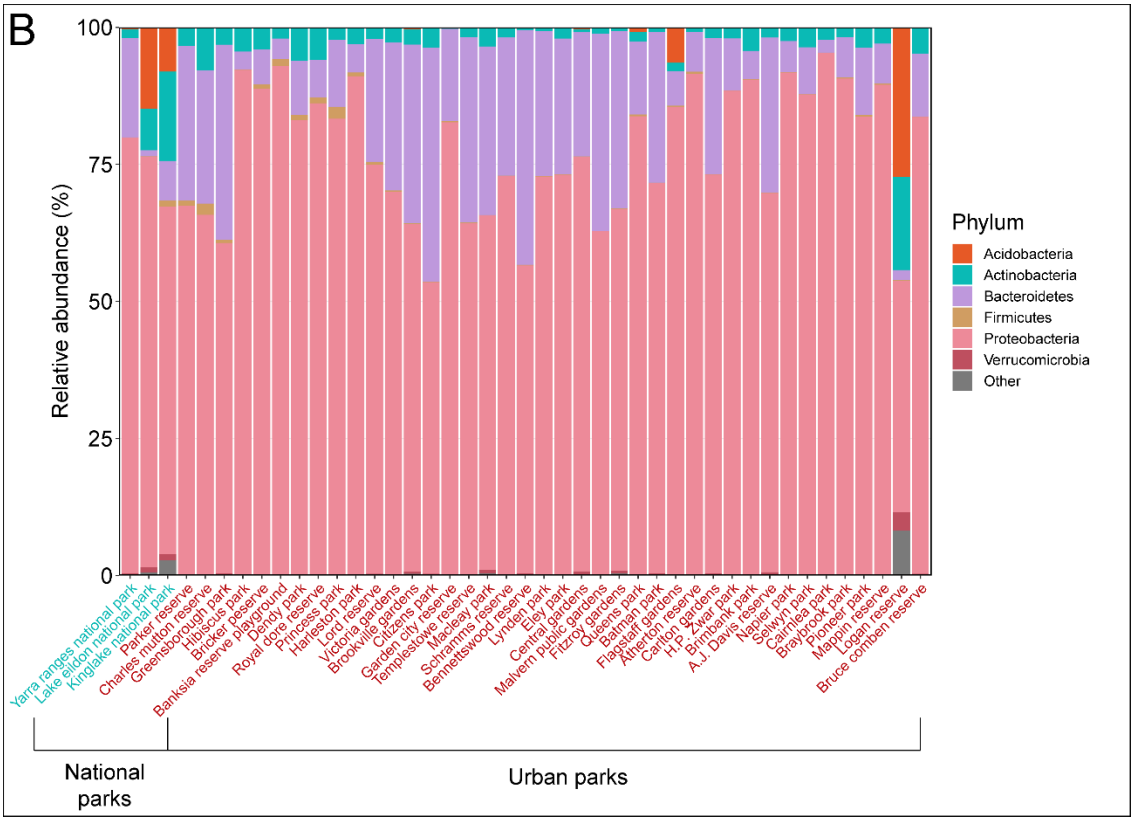

Fig. S2. Distribution bar-plot of bacterial community compositions in soil (A) and grass phyllosphere (B) samples across different urban green spaces and national parks at the phylum level.

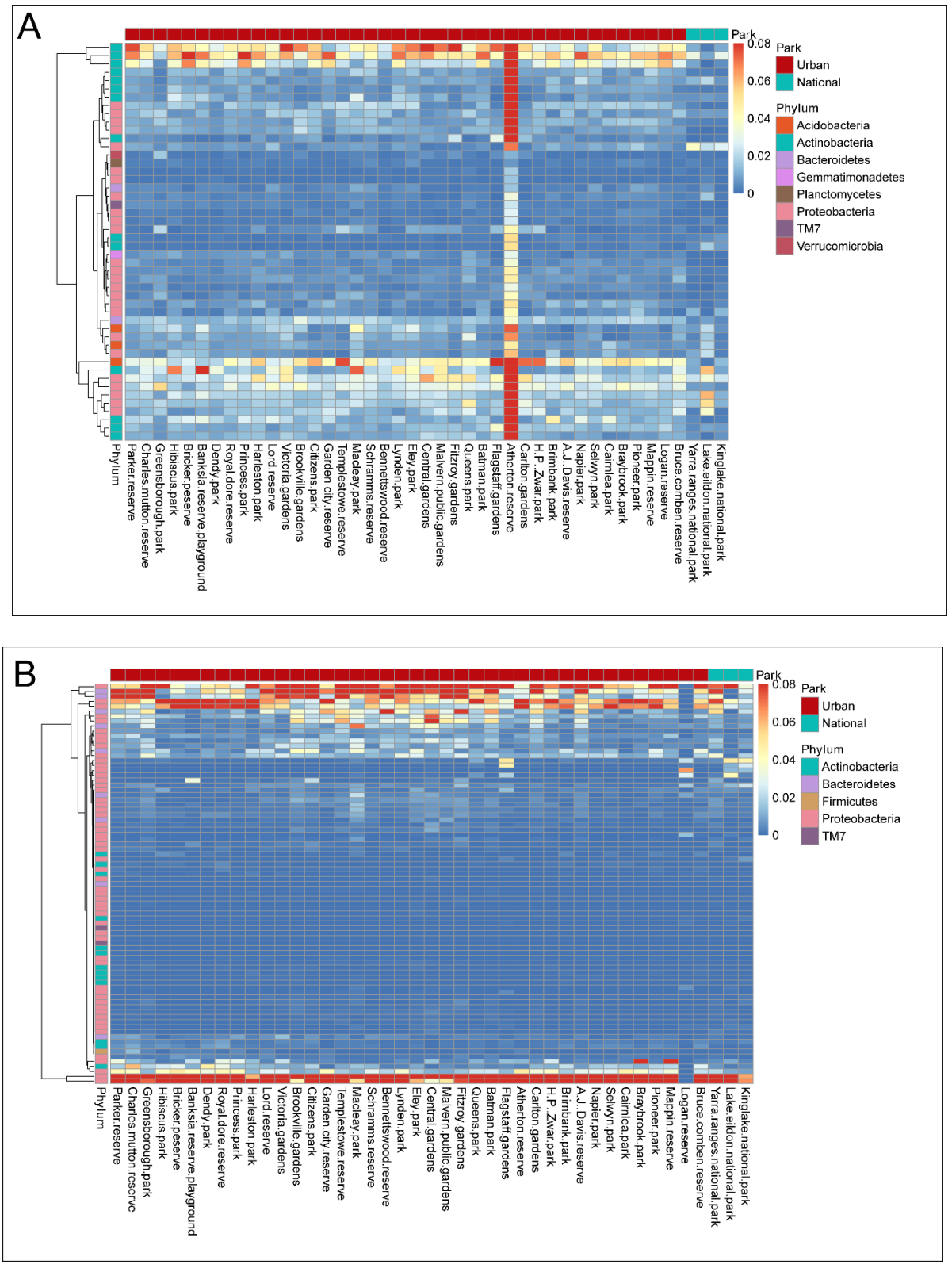

Fig. S3. Heatmap of bacterial community compositions in soil (A) and grass phyllosphere (B) samples across the investigated urban green spaces and national parks at genera level.

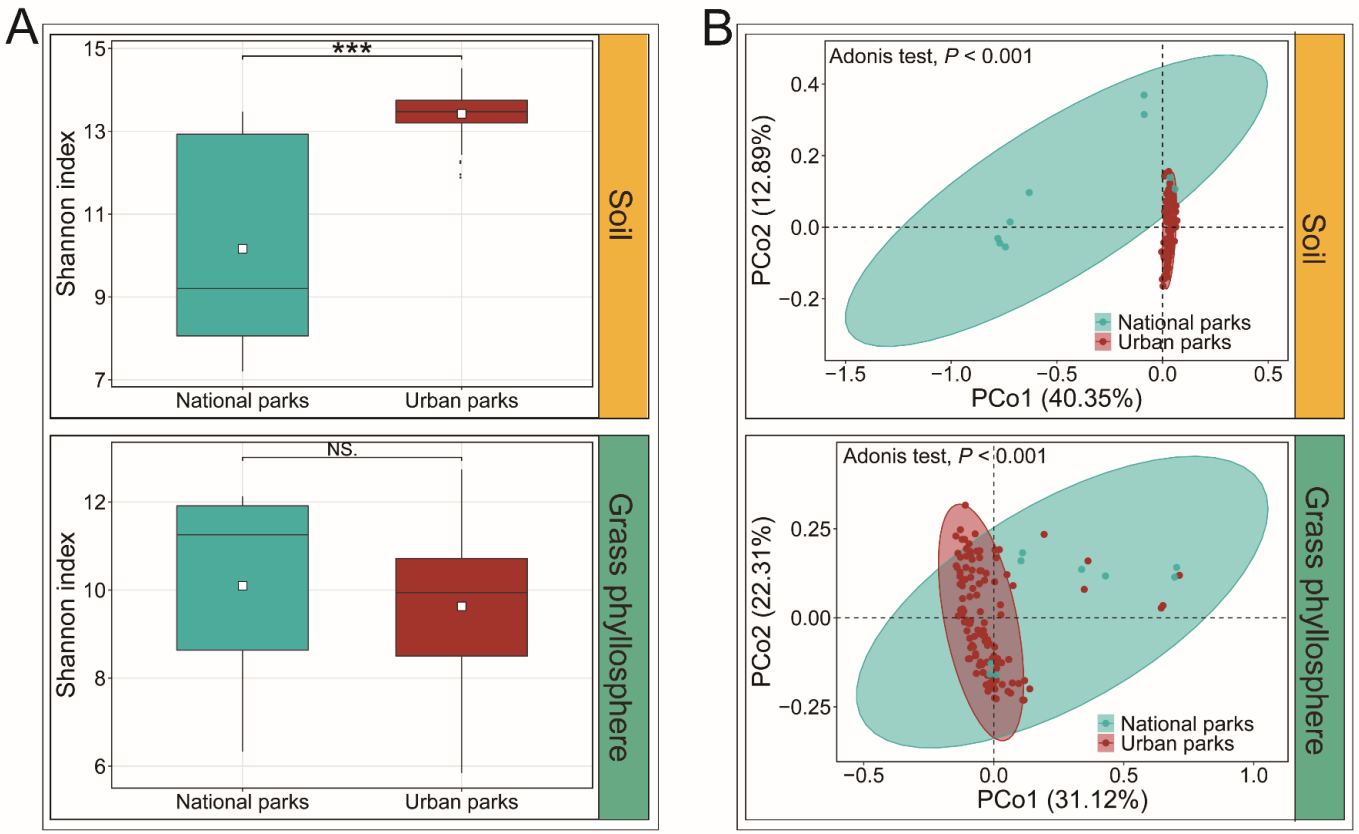

Fig. S4. Boxplots showing the Shannon index (α diversity) in soil and grass phyllosphere samples in the 40 urban green spaces and three national parks. *** indicates $P < 0.001$ determined by Mann-Whitney-Wilcoxon test. The white squares indicate the mean values (A). Principal coordinate analysis (PCoA) based on the Bray-Curtis distance showing the distribution patterns of microbiome in soil and grass phyllosphere samples (β diversity) (B).

Chapter 4: Characterization of the biogeographic patterns of antibiotic resistomes in natural ecosystems

This chapter is based on a published article entitled:

Biotic and abiotic factors distinctly drive contrasting biogeographic patterns between phyllosphere and soil resistomes in natural ecosystems. *ISME Communications*, 1:13. https://doi.org/10.1038/s43705-021-00012-4

ISME

www.nature.com/ismecomms

ARTICLE OPEN

Biotic and abiotic factors distinctly drive contrasting biogeographic patterns between phyllosphere and soil resistomes in natural ecosystems

Zhen-Zhen Yan[1], Qing-Lin Chen[1✉], Chao-Yu Li[1], Bao-Anh Thi Nguyen[1], Yong-Guan Zhu[2], Ji-Zheng He[1] and Hang-Wei Hu[1✉]

© The Author(s) 2021

The phyllosphere and soil are two of the most important reservoirs of antibiotic resistance genes (ARGs) in terrestrial ecosystems. However, comparative studies on the biogeographic patterns of ARGs in these two habitats are lacking. Based on the construction of ARG abundance atlas across a > 4,000 km transect in eastern and northern Australia, we found contrasting biogeographic patterns of the phyllosphere and soil resistomes, which showed their distinct responses to the biotic and abiotic stresses. The similarity of ARG compositions in soil, but not in the phyllosphere, exhibited significant distance-decay patterns. ARG abundance in the phyllosphere was mainly correlated with the compositions of co-occurring bacterial, fungal and protistan communities, indicating that biotic stresses were the main drivers shaping the phyllosphere resistome. Soil ARG abundance was mainly associated with abiotic factors including mean annual temperature and precipitation as well as soil total carbon and nitrogen. Our findings demonstrated the distinct roles of biotic and abiotic factors in shaping resistomes in different environmental habitats. These findings constitute a major advance in our understanding of the current environmental resistomes and contribute to better predictions of the evolution of environmental ARGs by highlighting the importance of habitat difference in shaping environmental resistomes.

ISME Communications (2021)1:13 ; https://doi.org/10.1038/s43705-021-00012-4

INTRODUCTION

The links between microbial distribution patterns and their underlying drivers are a core topic of microbial ecology.[1] Previous studies have revealed that the distribution patterns of soil microbial communities can vary markedly across space.[2–6] Endemic abiotic factors, including climate,[4,6] the availability of growth-limiting nutrients,[2,3] soil salinity,[7] and soil pH,[5] have been demonstrated to be important in determining the biogeographic patterns of soil microbial communities. In addition to abiotic factors, the inter-kingdom interactions among co-occurring microbial communities also play important roles in governing the biogeographic patterns and functional diversity of soil microbial communities.[8–10] For example, the antagonism between bacterial and fungal communities can lead to the production of antibiotics by some bacterial and fungal cells, which exert selection pressure for the evolution of antibiotic resistance genes (ARGs).[8,11] ARGs, which are estimated to have existed in natural ecosystems since 2 Gyr ago, play important roles in ecosystem multifunctionality (i.e. multiple ecosystem functions and services).[12–14] Other than as a defense strategy of bacteria to thwart the onslaught of antibiotics,[15] ARGs are associated with a variety of other ecosystem functions such as trafficking signals, facilitating the detoxification of metabolic intermediates and enhancing bacterial pathogenicity.[14,16] Therefore, an adequate evaluation of the biogeographic patterns of the resistomes (the collection of ARGs in communities of both pathogenic and non-pathogenic bacteria[17]) and their main driving factors is critical to advance our understanding of the spread and evolution of antibiotic resistance in natural settings under the on-going global change.

The phyllosphere (the aerial part of plants)[18] and soil[19,20] have been ranked as two of the most important reservoirs of environmental antibiotic resistance in terrestrial ecosystems. Owing to the inherently close relationship between plants and soil, there is a constant exchange of microbes between the phyllosphere and soil habitat, and thus the phyllosphere and soil could be important sources of ARGs for each other.[21–23] However, because of the different conditions of plant surface and soil, the phyllosphere microbiota can be significantly different from the microbiota in the soils surrounding the plants.[24–26] Due to the covering of hydrophobic cuticles and influences by ultraviolet radiation and plant metabolisms, the phyllosphere is an oligotrophic and stressful environment with a relatively lower microbial diversity compared to soil.[22] Regardless of the plant species, phyllosphere microbiota from different locations is dominated by only a few bacteria phyla including Actinobacteria, Bacteroidetes, Firmicutes and Proteobacteria.[27,28] By contrast, the soil is considered to harbour the most diverse microbial groups on Earth[29] which are highly variable among different locations across the globe.[30] In addition, a previous study found that some ARGs were not shared by the phyllosphere and surrounding soil[23] suggesting that the evolutionary mechanisms of the phyllosphere and soil resistomes might be unique from each other. The

[1]School of Agriculture and Food, Faculty of Veterinary and Agricultural Sciences, The University of Melbourne, Parkville, VIC, Australia. [2]Key Laboratory of Urban Environment and Health, Institute of Urban Environment, Chinese Academy of Sciences, Xiamen, China. ✉email: qinglin.chen@unimelb.edu.au; hang-we.hu@unimelb.edu.au

Received: 6 November 2020 Revised: 2 March 2021 Accepted: 11 March 2021
Published online: 14 April 2021

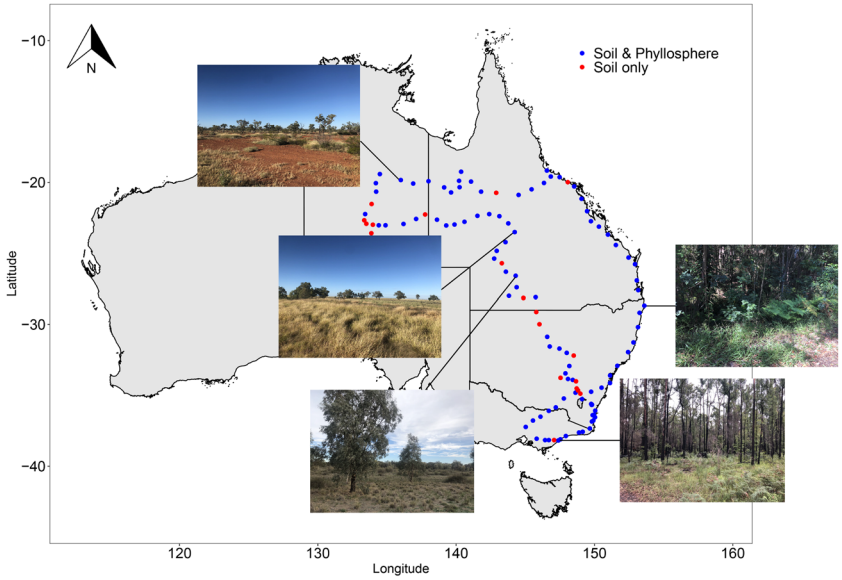

Fig. 1 Locations and photos of the sampling sites. The blue spots represent the 100 sites where both plant and soil samples were collected. The red spots represent the 19 sites where only soil samples were collected.

comparative studies on the biogeographic patterns of the phyllosphere and soil resistomes, however, are lacking. This knowledge gap greatly impedes our ability in predicting the dissemination and evolution of antibiotic resistance in natural terrestrial ecosystems. Here, we conducted a large-scale investigation of the resistomes in the phyllosphere of predominant herbaceous vegetation types and soil from an >4000 km transect, which encompassed the major representative ecosystem types across eastern and northern Australia (i.e., forest, shrubland and grassland; Fig. 1). We aimed to address a set of questions that are critical to the understanding of environmental ARGs in natural terrestrial ecosystems including (i) How do the biogeographic patterns of resistomes in distinct environmental habitats of the phyllosphere and soil differ across a large spatial scale? (ii) What are the roles of spatial distance, co-occurring microbial communities and abiotic climatic and edaphic factors in shaping the biogeographic patterns of resistomes in these two habitats? We hypothesized that the different natures of the phyllosphere and soil environments would lead to unique responses of microbial communities to biotic and abiotic factors which would lead to distinct biogeographic patterns of resistomes for the two habitats.

RESULTS

Large-scale atlas of the phyllosphere and soil resistomes

Using high-throughput quantitative PCR (HT-qPCR), we detected 264 and 268 ARGs in the 103 phyllosphere and 295 soil samples, respectively. More diverse (Fig. 2A) but less abundant (Fig. 2B) ARGs were detected in the phyllosphere than in soil (Wilcoxon rank-sum test, $P < 0.001$). The abundance of ARGs (copies/gram sample) ranged from 1.25×10^6 to 5.98×10^9 (with a median value of 3.43×10^7) for the phyllosphere (Fig. S1) and 1.12×10^7 to 2.26×10^9 (with a median of 7.73×10^7) for soil (Fig. S2). The ubiquitous (detected in all samples) and abundant (accounting for >40% of the total abundance) ARG classes were identified as dominant ARG classes. Multidrug resistance genes (i.e., efflux pumps that resistant to multiple classes of antibiotics), and beta-lactamase resistance genes were dominant in the phyllosphere resistome, which accounted for 85.26% of the total ARG abundance (Fig. 2C, insertion). The soil resistome was dominated by multidrug resistance genes which accounted for 54.25% of the total ARG abundance (Fig. 2D, insertion).

The resistomes in the phyllosphere and soil were well separated from each other as revealed by the nonmetric multidimensional scaling (NMDS) ordinations (ANOSIM $R = 0.555$, $P < 0.001$; Fig. S3). The distribution patterns of the ARG abundances were predicted using the kriging interpolation method. The results revealed that, for the phyllosphere resistome, more abundant ARGs were predicted in the southern and western parts of Australia than in the northern and eastern parts (Fig. 2C). An almost opposite trend of ARG abundance was observed for the soil resistome with the highest ARG abundance to be predicted in the northeast coastal regions of Australia (Fig. 2D). Similar trends in biogeographic patterns were observed for the dominant ARG class(es) in both phyllosphere (Fig. S4) and soil (Fig. S5).

Characteristics of bacterial, fungal and protistan communities

The high-quality sequences obtained from amplicon sequencing of the 16 S rRNA gene, the internal transcribed spacer (ITS) region, and the 18 S rRNA gene were clustered into 40,997 bacterial, 29,525 fungal and 23,545 protistan operational taxonomic units (OTUs) at 97% similarity level, respectively. The alpha-diversity of all the three investigated microbial communities in soil was significantly higher than that in the phyllosphere (Wilcoxon rank-sum test, $P < 0.001$; Figs. 3A and S6). Clear separations between the microbial communities in the phyllosphere and soil were revealed by the NMDS ordinations (bacterial community: ANOSIM $R = 0.948$, $P < 0.001$, fungal community: ANOSIM $R = 0.228$, $P < 0.001$; protistan community: ANOSIM $R = 0.652$, $P < 0.001$; Fig. 3B). Proteobacteria was the most abundant bacterial phylum in the phyllosphere, which accounted for 79.38% of the 16 S rRNA gene sequences, followed by Actinobacteria (9.61%; Fig. S7A). Actinobacteria was the most abundant bacterial phylum in the soil which accounted for 37.73% of the 16 S rRNA gene sequences. The second most abundant bacterial phylum in soil was Proteobacteria which accounted for 24.86% of the 16 S rRNA gene sequences (Fig. S7A). The majority of the ITS region sequences belonged to the fungal phylum Ascomycota, which accounted for 92.32% and 78.59% of total sequences in the phyllosphere and soil, respectively (Fig. S7B). The three most abundant protistan phyla in the phyllosphere were Metazoa (54.73%) of the kingdom Opisthokonta, and Ciliophora (20.78%), and Apicomplexa (13.91%) of the kingdom AlveolataM (Fig. S7C). For soil, Metazoa (44.20%) was the most abundant protistan phylum, followed by Cercozoa

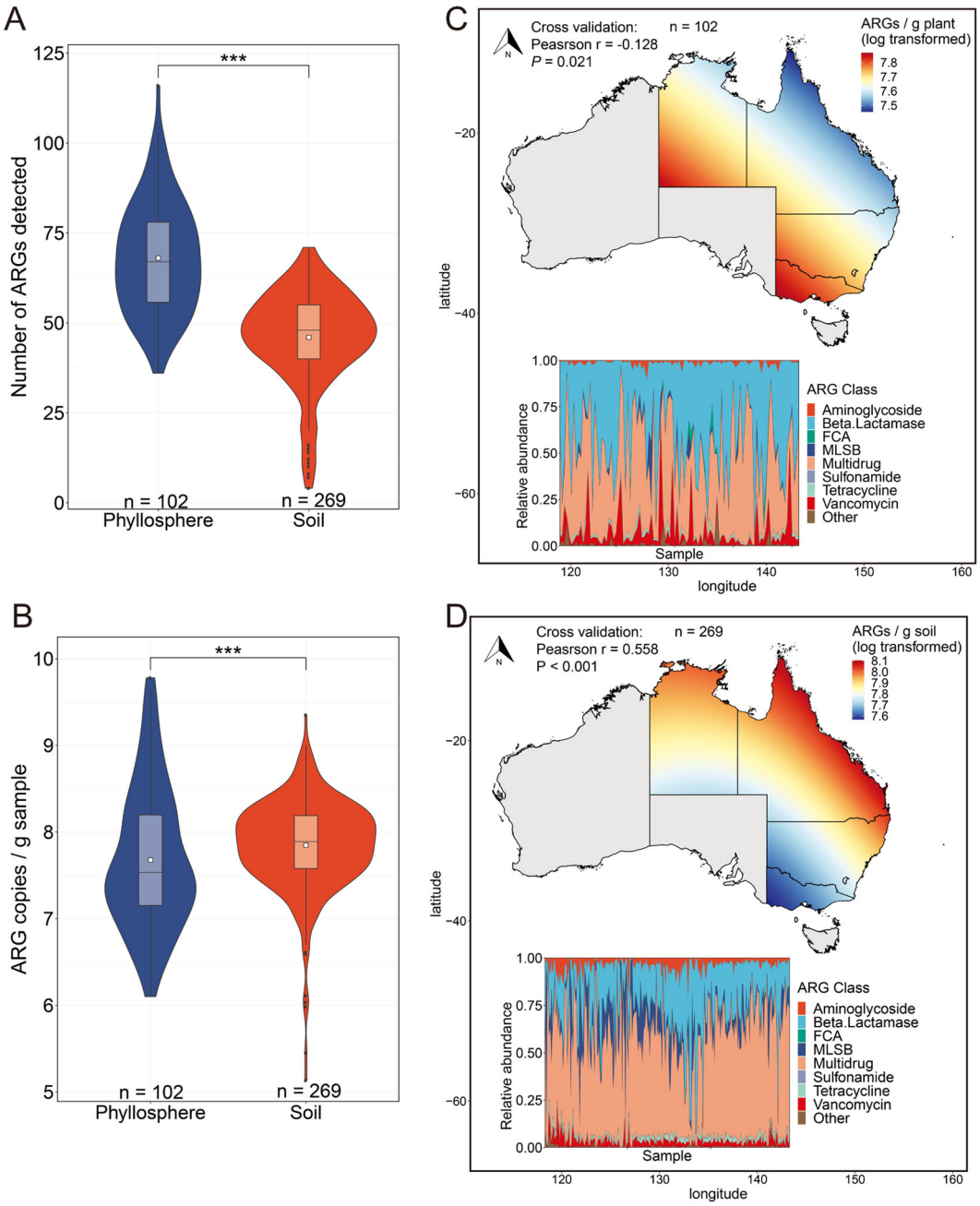

Fig. 2 Characteristics of the ARGs detected in the phyllosphere and soil samples. Violin plots and box plots showing the numbers of detected ARGs (**A**) and the absolute abundance of all detected ARGs (**B**). Symbol (***) indicates Wilcoxon rank-sum test $P < 0.001$. White squares inside the box plots indicate the mean values. Large-scale atlas of the spatial distributions of ARG abundance in phyllosphere (**C**) and soil (**D**) across eastern and northern Australia. The compositions of ARGs detected in the samples are displayed in the bottom area charts. Samples showing in the area charts were ordered by ascending in the latitude of the sampling locations. FCA fluoroquinolone, quinolone, florfenicol, chloramphenicol and amphenicol resistance genes, MLSB Macrolide-Lincosamide-Streptogramin B resistance genes. Multidrug Efflux pump genes that resistant to multiple classes of antibiotics.

(29.56%) of the kingdom Rhizaria and Ciliophora (25.24%; Fig. S7C). Analysis of the difference in the abundances of bacteria in the phyllosphere and soil showed that the bacterial abundance in soil was significantly higher than that in the phyllosphere (Wilcoxon rank-sum test $P < 0.001$; Fig. S8).

Distance-decay relationships for the resistomes and microbial communities and spatial configuration of the sampling sites

The distance-decay relationships (DDRs) for ARGs and microbial communities in the phyllosphere and soil were estimated. For the phyllosphere resistome, no DDR was observed for neither the entire resistome (Fig. 4) nor the dominant ARG classes (Fig. S9). For the soil resistome, although DDR was significant ($P < 0.001$) for both the entire resistome (Fig. 4) and the dominant ARG class (Fig. S9), the effect sizes were remarkably small ($R^2 < 0.1$), indicating weak decay of resistome similarity with geographic distance. Significant ($P < 0.001$) DDRs were observed for all three investigated microbial communities in both the phyllosphere and soil (Fig. 4) with the soil microbial communities having larger effect sizes (bacterial community: $R^2 = 0.205$; fungal community: $R^2 = 0.191$; protistan community: $R^2 = 0.083$) than the corresponding phyllosphere communities (bacterial community: $R^2 = 0.007$;

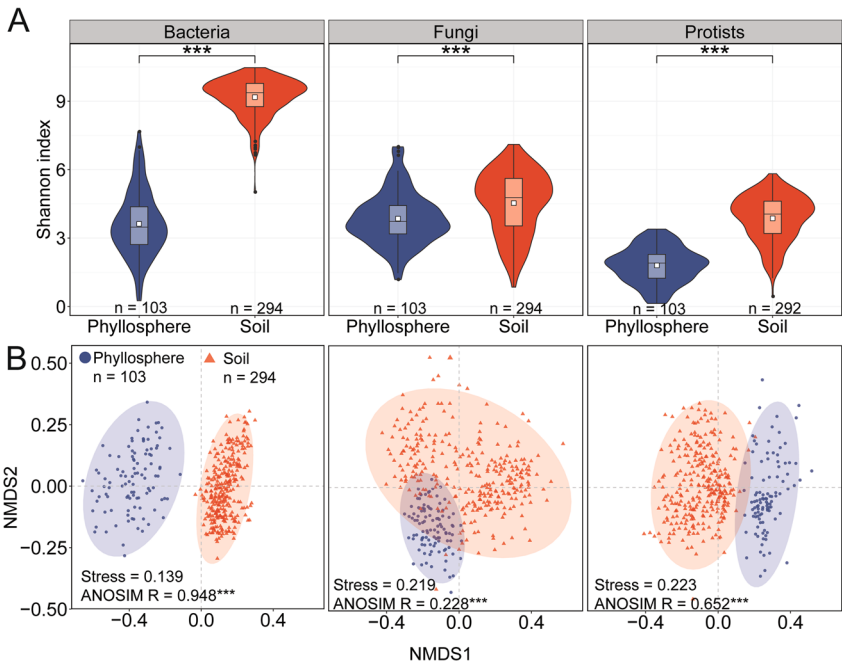

Fig. 3 Characteristics of bacterial, fungal and protistan communities in phyllosphere and soils. A Violin plots and boxplots showing the Shannon index of bacterial, fungal and protistan communities in phyllosphere and soils. Symbol (***) indicates Wilcoxon rank-sum test $P < 0.001$. White squares inside the box plots indicate the mean values. **B** Nonmetric multidimensional ordinations of the microbial community structures at the OTU level among the phyllosphere and soil samples based on the Bray–Curtis distance. Symbol (***) indicates ANOSIM $P < 0.001$.

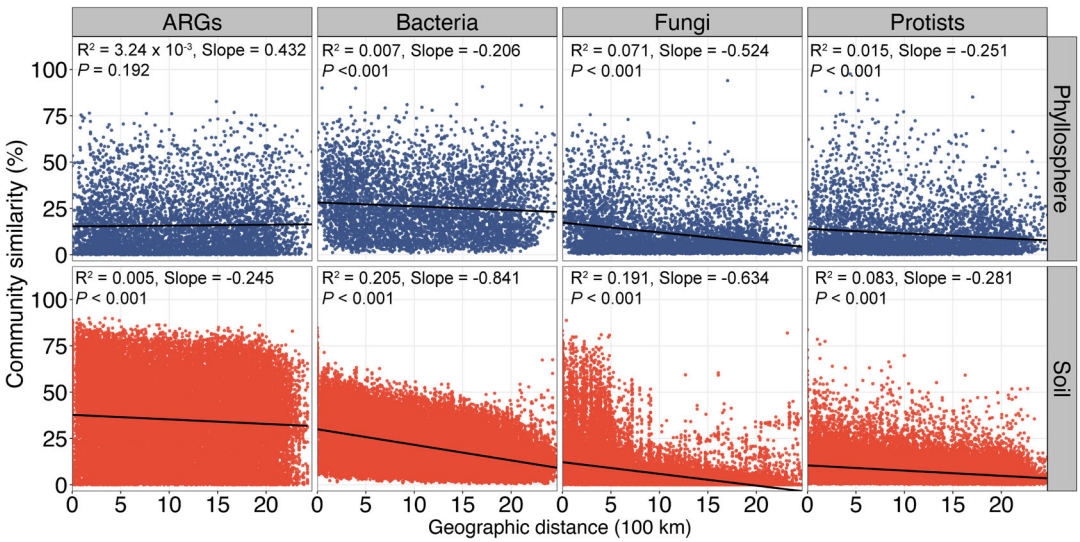

Fig. 4 Distance-decay relationships for ARGs, bacterial, fungal and protistan communities at the OTU level in the phyllosphere and soil samples. Symbol (***) indicates ordinary least regression $P < 0.001$. Significant correlations ($P < 0.05$) and no significant correlation ($P > 0.05$) are shown in solid lines and dashed line, respectively.

fungal community: $R^2 = 0.071$; protistan community: $R^2 = 0.015$). In addition, the slopes of distance-decay curves were steeper for the soil microbial communities (bacterial community: slope = −0.841; fungal community: slope = −0.191; protistan community: slope = −0.083,) than the corresponding phyllosphere communities (bacterial community: slope = −0.206; fungal community: slope = −0.524; protistan community: slope = −0.281).

Variations in the spatial configuration among the sampling sites were explored by the Moran's eigenvector maps (MEMs).[31] The eigenvalues and Moran's *I* of the MEMs for the sampling sites are summarised in Fig. S10A and Table S1, respectively. The MEMs revealed that our sampling sites showed a significant clustering pattern (autocorrelation) at a large-scale. The autocorrelations of the sampling sites get weaker with the decrease in spatial scale. Examples of some significant MEMs (MEMs with positive eigenvalues and significant Moran's *I*) are mapped in geographic space (Fig. S10B).

Drivers of ARG abundance in the phyllosphere and the soil environments

Spearman's correlation analysis revealed that ARG abundance in the phyllosphere was not only significantly ($P < 0.001$) positively

correlated with the bacterial community composition, but also was significantly ($P < 0.05$) correlated with the community compositions of fungal and protistan communities. However, none of the investigated abiotic factors was significantly correlated with the phyllosphere ARG abundance (Table 1). In contrast, soil ARG abundance was significantly ($P < 0.05$) positively correlated with abiotic factors including mean annual temperature (MAT) and mean annual precipitation (MAP), as well as soil total carbon (TC) and total nitrogen (TN), but not with the compositions of any investigated microbial communities (Table 1). Similar relationships between the abundances of ARGs of the dominant class(es) with these biotic and abiotic factors were found for both the phyllosphere and soil samples (Table S2).

To further explore how space differently impacts the observed distinct biogeographic patterns of the soil and phyllosphere resistomes, distance-based redundancy analysis (dbRDA) was conducted with the most influential MEMs (top five largest axes of the MEMs) and edaphic as well climatic factors of each sampling sites as explanatory variables. The dbRDA results reveal that the soil resistome was not only significantly influenced by edaphic factors but also significantly impacted by changes in spatial configurations and corresponding changes in MAT and MAP (Fig. S11A). However, the phyllosphere resistome was only significantly impacted by spatial configuration at large-scale (MEM1) and MAP (Fig. S11B).

The direct and indirect contributions of different factors to the variations in the ARG abundances were further illustrated with structural equation models (SEMs), which explained 21 and 35% of the variations in the ARG abundance for the phyllosphere and the soil resistomes, respectively (Fig. 5). For the phyllosphere

Table 1. Spearman's correlation between ARG abundance and selected biotic and abiotic factors.

Microbial community compositions			Climatic factors		Edaphic factors			
Bacterial NMDS1	**Fungal NMDS1**	**Protistan NMDS1**	**MAT (°C)**	**MAP (mm)**	**TC (%)**	**TN (%)**	**pH**	
0.636	**−0.333**	**0.281**	−0.060	−0.128	−0.088	0.002	0.084	**Phyllosphere**
***P* < 0.001**	***P* = 0.001**	***P* = 0.004**	*P* = 0.546	*P* = 0.201	*P* = 0.379	*P* = 0.981	*P* = 0.403	
0.044	0.021	0.106	**0.177**	**0.203**	**0.217**	**0.232**	0.041	**Soil**
***P* = 0.472**	*P* = 0.731	*P* = 0.086	***P* = 0.004**	***P* = 0.001**	***P* < 0.001**	***P* < 0.001**	*P* = 0.501	

Significant correlations ($P < 0.05$) are indicated as bold fonts.

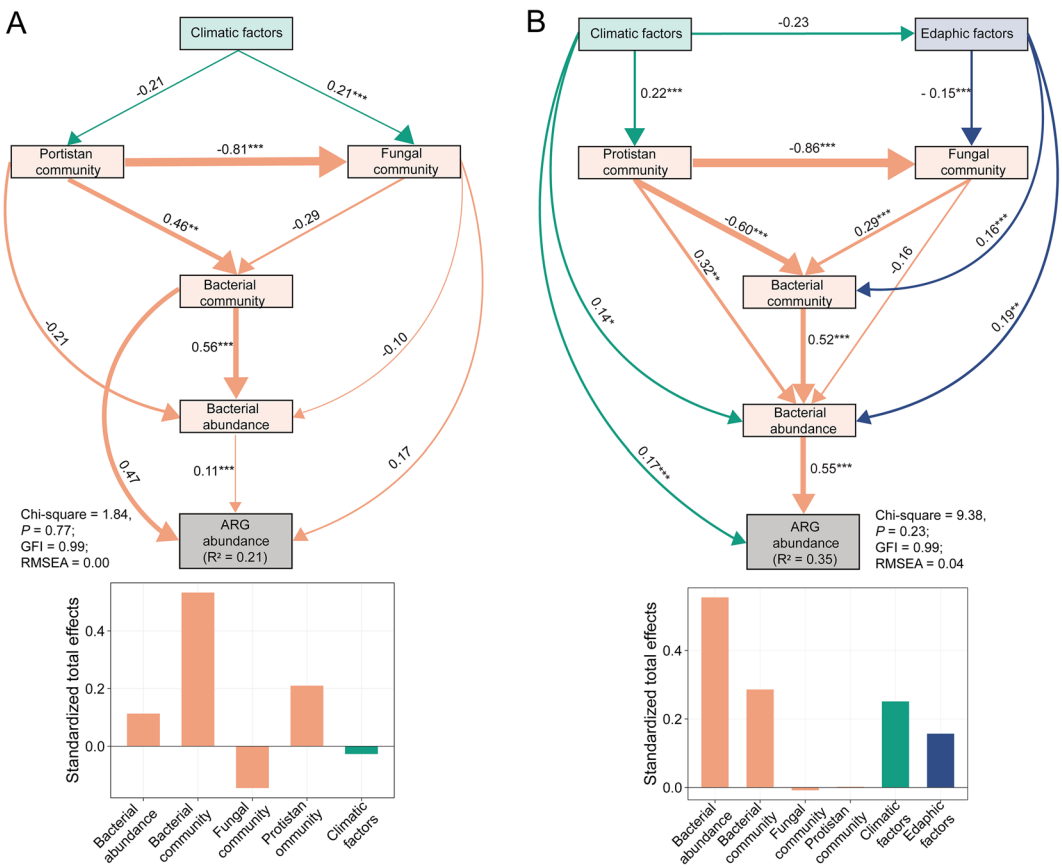

Fig. 5 Drivers of ARG abundances in phyllosphere and soils. Structure equation models (SEMs) illustrating the direct and indirect effects of multiple factors on the variations in ARG abundance in phyllosphere (**A**) and soils (**B**). The width of the arrows is proportional to the strength of path coefficients shown by the numbers adjacent to the arrows. R^2 indicates the proportion of variations in ARG abundance explained by the models. Symbol (*) indicates < 0.05; symbol (**) indicates $P < 0.01$; symbol (***) indicates $P < 0.001$. Standardised effects were derived from the SEMs. GFI goodness of fit index, RMSEA root mean square error of approximation.

resistome, bacterial and fungal community compositions and bacterial abundance had direct impacts on ARG abundance. Fungal and protistan community compositions had indirect impacts on ARG abundance through impacting bacterial community composition and abundance. However, climatic factors only had a weak impact on phyllosphere ARG abundance through influencing fungal and protistan community compositions (Fig. 5A). For the soil resistome, the only biotic factor directly impacting the ARG abundance was the abundance of bacteria. Fungal and protistan community compositions only had indirect impacts on ARG abundance through impacting on bacterial abundance. Compared to fungal and protistan communities, climatic and edaphic factors had relatively strong impacts on the variation in soil ARG abundance. Particularly, climatic factors had both direct and indirect impacts on the variation in soil ARG abundance (Fig. 5B).

DISCUSSION

Contrasting resistome profiles in the phyllosphere and soil

In this study, we presented a large-scale investigation into the phyllosphere and soil resistomes across a variety of natural ecosystems. Our results revealed contrasting resistome profiles in the phyllosphere and soil with the phyllosphere harbouring more diverse but less abundant ARGs than soil (Fig. 2). A possible reason for the higher ARG diversity in the phyllosphere than soil is that, as an open habitat, the phyllosphere is subject to wide sources of microorganisms, and ARGs, including those transmitted by insects and aerosols.[21] A previous study reported that for phyllosphere and soil from the same location, the types of phyllosphere specialist ARGs are more than soil specialist ARGs.[23] The differences in the abundance of ARGs in the phyllosphere and soil may mainly be attributed to the differences in the background bacteria abundances, which are the potential hosts of ARGs. The comparison of 16 S rRNA gene copy numbers revealed that the bacterial abundance in the soil was more than one order of magnitude higher than that in the phyllosphere (Fig. S8). In addition, the accumulation of ARGs in soil may also contribute to the significantly higher ARG abundance in soil than in the phyllosphere.[32] Therefore, the ARGs transmitted from the phyllosphere may also accumulate in soil and contribute to the increase in soil ARG abundance. We observed similar trends of ARG abundances of the dominant ARG class(es) and the entire resistomes in both the phyllosphere and soil habitats, which indicate that there might be predictable biogeographic patterns of environmental ARGs in natural ecosystems. The biogeographic patterns of ARG abundance in the phyllosphere and soil were almost opposite, implying that the resistome profiles in the above-ground plant surface habitat and underground soil habitat might be differently shaped by biotic and abiotic factors.

The soil resistome varies more significantly across space than the phyllosphere resistome

The MEMs revealed that there were autocorrelation patterns of our sampling sites at a large spatial scale, indicating that geographic distance might play a role in driving the community structures for our samples. The distance-decay relationship is a fundamental ecological pattern to describe the relationship between community similarity and geographic distance.[33,34] In this study, we observed significant ($P < 0.001$) DDRs for ARGs in soil but not in the phyllosphere. The effect sizes of the DDRs for the microbial communities in the phyllosphere were substantially lower than those of the microbial communities in surrounding soils (Fig. 4) and reported in other natural soil ecosystems.[35] These results demonstrated that compared to those in soil, the phyllosphere microbial communities and resistomes vary less significantly across space which is further supported by the dbRDA results (Fig. S11). The distinct impacts of spatial distance on the phyllosphere and soil resistomes could be derived from the differences in microbial dispersal limitation.[36] The phyllosphere is an environment subjected to the fluctuations of the surrounding environment, for example, changes in wind and rainfall, which can facilitate the transmission of microbes in the phyllosphere from site to site.[22] The low dispersal limitation in the phyllosphere environment would lead to relatively similar microbial communities, and thus similar resistome profiles, among sites spatially far from each other.[37] Different from the phyllosphere, the soil is a relatively stable environment in which microorganisms are subject to slow-changing processes.[38,39] Therefore, soil microorganisms would experience high dispersal limitation which would result in more similar resistome profiles between sites closer to each other than those further apart.[40]

Distinct drivers of the biogeographic patterns of the phyllosphere and soil resistomes

Our results revealed that the ARG abundance in the phyllosphere was significantly correlated with the community compositions of bacterial, fungal and protistan communities but not with any of the investigated abiotic factors. While for soil, the ARG abundance was more apparently influenced by abiotic factors, including MAT, MAP, soil TC and TN, than by microbial community compositions. These results suggest that microbial interactions and abiotic climatic and edaphic factors might be the main drivers shaping the phyllosphere and soil resistomes, respectively. These contrasting responses could be potentially derived from the intrinsic differences of the two habitats. Compared to the soil resistome, the phyllosphere resistome and bacterial community were less heterogeneous across geographic locations (Fig. 4). Therefore, for the phyllosphere resistome the impacts of abiotic factors, which shift with geography, would be relatively weak and the roles of inter-kingdom interactions among microbial communities would become more important. The bacteria-fungal antagonism is a kind of very important inter-kingdom interaction that can lead to the production of considerable amounts of antibiotics by some bacterial and fungal cells which select against bacteria lacking ARGs.[8,11] Another inter-kingdom interaction that could greatly influence the expression of ARGs by bacterial cells is the predation of bacteria by protists, which could pose substantial biotic stress to the bacterial community.[41] The expression of some ARGs (for example, some efflux pump genes) can increase the general tolerance of bacteria to stresses other than the presence of antibiotics. Under protistan predation, bacterial cells would increase the expression of ARGs as a strategy to survive, which may partially explain the correlations between phyllosphere ARG abundance with the protistan community.[42] On the contrary, the soil is a stable habitat with relatively high spatial heterogeneity.[38,39] In soil habitat, the microbial interactions and gene expressions are underpinned by endemic abiotic factors.[39,43] A potential explanation for the observed significant correlations between MAT and MAP with soil ARG abundance could be that genotypic alternations of bacterial cells induced by environmental stresses (e.g. temperature extremes and water shortage) are similar to those induced by the action of antibiotics.[44] The availability of soil nutrients could also be closely related to the ARG abundance by influencing the types of microbial interactions.[45] The stress gradient hypothesis assumes that an increase in nutrient availability would enhance the frequency of negative microbial interactions which may induce antibiotic production.[45] Such a relationship between growth-limiting nutrient availability and the direction of microbial interactions could potentially explain the observed positive relationships between soil TC and TN with soil ARG abundance.

Nevertheless, it should be noted that there are some potential caveats in the interpretation of our results. The plant host species were not considered in the present study, but it has been identified as a potential influencing factor of phyllosphere

resistomes.[46,47] In addition, the presence of stochastic events and persistent microbial trait variations were not addressed, but those factors could play a role in shaping microbial community assembly[1] and thus resistome profiles. These limitations together with the potential sampling effects could explain why >60% of the variations in the ARG abundance remain unexplained for both the phyllosphere and the soils (Fig. 5). It is impractical to address all potential variables for a large-scale survey, and this is inconsistent with previous large-scale microbial studies which explained 10–50% of the variations in microbial patterns.[1,48–50] Despite these limitations, our results revealed that the biotic interactions among bacterial, fungal and protistan communities and abiotic factors, including MAT, MAP, soil TC and TN, differently drive the variations in the phyllosphere and soil resistome profiles.

CONCLUSION

In this study, we provided a systematic investigation into the biogeographic patterns of the phyllosphere and soil resistomes in natural ecosystems. We found contrasting biogeographic patterns of the phyllosphere and soil resistomes, which may derive from the distinct impacts of biotic and abiotic factors on the microbial communities in these two environmental habitats. The phyllosphere resistome, which was not sensitive to the changes in abiotic factors across space, was mainly impacted by the inter-kingdom interactions among bacterial, fungal and protistan communities. By contrast, MAT, MAP and soil nutrients were the main drivers shaping the soil resistome. Our results imply that the characteristics of microbial habitat are critical in underpinning the biogeographic patterns of resistomes in natural ecosystems. Therefore, it is necessary to consider the intrinsic differences in habitats when predicting the evolution and spread of environmental ARGs.

MATERIALS AND METHODS

Sampling campaign

Herbaceous plant and soil samples were collected during May 2019 from a total of 118 locations across eastern and northern Australia with minimal anthropogenic impacts (Fig. 1). MAT and MAP of the sampling sites ranged from 12.93–26.54 °C and 254–1901 mm, respectively. At each location, we established a 20 × 20 m plot in which three subplots (1 × 1 m) were established on the most predominant herbaceous vegetation type. The aerial parts of the herbaceous plants were collected using sterilized scissors to form a composite plant sample for each plot. Three independent soil samples were collected from each plot by mixing five soil cores (0–10 cm) into one composite sample. Our large-scale sampling collected a total of 103 herbaceous plant samples and 295 soil samples, which were transported to the laboratory on dry ice. The plant samples were immediately used for DNA extraction from the phyllosphere microbes. The soil samples were sieved through a 2 mm mesh and divided into two portions. One portion was air-dried for soil physicochemical characterization, and the other portion was stored at −20 °C before molecular analyses.

Soil physicochemical characterization and climatic data acquisition

Soil physicochemical properties including soil TC, TN and soil pH were determined using standardized protocols.[51] Briefly, soil TC and TN were determined using the Dumas combustion method on a LECO EP628 analyser (LECO Australia Pty, Ltd, Baulkham Hills, NSW, Australia). Soil pH was measured in 1:5 soil water suspension using an Orion Star A215 pH/Conductivity Benchtop Multiparameter Metre (Thermo Scientific Inc., Waltham, MA, USA). Detailed information on soil physicochemical properties is provided in Supplementary File 2. Estimates of MAT and MAP at 30 arc seconds (~1 km^2) were obtained from the WorldClim database (https://worldclim.org/).[52] MAT and MAP values of each sampling location are shown in Supplementary File 3.

Molecular analyses

Plant phyllosphere genomic DNA and soil genomic DNA were extracted using the DNeasy Power Soil kit (QIAGEN). Pty. Ltd, Chadstone Centre, VIC, Australia) *as per* the manufacture's instruction. The plant sample preparation for phyllosphere genomic DNA extraction was conducted according to a previous method.[23,53] Briefly, around 5 g leaf tissue was weighted into a conical flask (25 m mL) containing 100 mL of 0.01 M autoclaved phosphate-buffered saline (PBS). The mixture was sonicated for 7 min and shaken at 180 rpm at 30 °C for 1 h. The obtained solution was filtered with nylon gauze and then a 0.22 μM cellulose membrane. The cellulose membrane was cut into pieces and used for DNA extraction. ARG abundance was determined using an HT-qPCR technique on the Wafergen SmartChip Real-Time Platform (Fremont, CA, USA). The HT-qPCR array contains primers targeting 285 ARGs that confer resistance to all major classes of antibiotics commonly used in humans and animals and the 16 S rRNA gene. Detailed information on the primers is provided in Supplementary File 4. Amplification of ARGs was conducted in a 100 nL reaction system. The thermal cycle for the amplification was as follows: and initial enzyme activation at 95 °C for 10 min, followed by 40 cycles of 95 °C for 30 s and 60 °C for 30 s. The melting process was automatically generated by the Wafergen SmartChip software (V2.7.0). Only well data with a single melting peak and an amplification efficiency within 1.8–2.2 were retained. A cycle threshold (C_T) value of 31 was used as the detection limit. The relative copy numbers of ARGs were calculated according to the following equation: Relative gene copy number $= 10^{(31\text{-}Ct)/\ (10/3)}$.[54,55] The relative copy numbers of ARGs were transformed to absolute copy numbers by normalization with 16 S rRNA gene copy number quantified using a Bio-Rad CFX384 Real-Time PCR detection system (Bio-Rad, Hercules, USA). The 20 μl PCR reaction system for 16 S rRNA gene quantification contained 10 μl Sensimix SYBR NO-ROX reagent (Bioline, London, UK), 0.8 μl each primer (10 μM) and 2 μl DNA template. The amplicon condition was the same as that for the amplification of ARGs. It should be noted that because the surface areas of the plant cannot be accurately measured and the mass of the herbaceous plants is marginal compared to their surface area, we reported the ARG abundance in both the phyllosphere samples as ARG copies/gram plant tissue according to previous studies.[23,56] The ARG classes that are ubiquitously (detected in all samples) and abundant (accounted for >40% of total ARG abundance) were identified as dominant ARG classes in the phyllosphere and soil samples.

The 16 S rRNA gene, the ITS region, and the 18 S rRNA gene were amplified for the characterization of bacterial, fungal and protistan communities, respectively, on an Illumina Miseq EP300 platform at Shanghai Majorbio Bio-pharm Technology Co., Ltd. Primer sets used for the amplicon sequencings were 515FmodF and 806RmodR for 16 S rRNA gene,[57] ITS1F and ITS2R for ITS region[58] and TAReukFWD1F and TAReukREV3R for 18 S rRNA gene.[59] Raw sequencing reads were merged using FLASH[60] and quality filtered according to the following criteria: raw pair-end reads containing more than three ambiguous nucleotides, reads with an average quality score <20, short reads (< 100 nt) and the barcode was discarded. The generated high-quality sequences were analysed and processed using Quantitative Insight into Microbial Ecology (QIIME).[61] OTUs were picked at 97% similarity level using UCLUST.[62] Singleton OTUs and chimeric sequences, chloroplast and mitochondrial OTUs were discarded from the OTU table before downstream analysis. Taxonomic classification of OTUs was conducted using the SILVA database for the 16 S rRNA gene,[63] UNITE database 8.0 for the ITS region,[64] and Protists Ribosomal Reference (PR2) database for the 18 S rRNA gene PR2.[65]

Statistical analyses

All statistical analyses were conducted in the R platform (V3.6.3; http://www.r-project.org/) and visualised using the 'ggplot2' package.[66] Statistical results were considered significant at $P < 0.05$ level. P values for multiple comparisons were corrected using the Benjamini–Hochberg procedure. The differences in the numbers of the detected ARGs, the abundance of the detected ARGs, and microbial alpha-diversity indices between the phyllosphere and the soil samples were determined using Wilcoxon rank-sum test with the 'stats' package.[67] Log-transformed ARG abundances in all plant phyllosphere and soil samples were shown in heatmaps constructed with the 'pheatmap' package.[68] The relationships of resistomes (based on ARG abundance) and microbial communities (at the OTU level) in the phyllosphere and the soils were visualised by NMDS ordinations based on Bray–Curtis distance with the 'vegan' package.[69] The significant differences in the resistome compositions and microbial beta-diversities between the phyllosphere and the soils were determined using PERMANOVA analysis with ANOSIM function in the 'vegan' package.[69] The spatial distributions of the abundance of all detected ARGs and the ARGs belonging to the dominant

ARG classes in the phyllosphere and the soils were estimated using the kriging interpolation method with the 'automap' package.[70] Cross-validations of the predicted maps were based on the Pearson correlation between the prediction values and the observed values of the ARG abundances for the same site. MEMs for the sampling sites were constructed using the 'adespatial' package[71] based on the spatial weight matrix defined using the 'spdep' package.[72] Each MEM eigenvalue quantified a spatial autocorrelation at a given spatial scale. The eigenvalues of the MEMs are automatically sorted from large-scale to fine-scale. Moran's *I* for the spatial autocorrelation were calculated with 999 permutations using the 'adespatial' package.[71] MEMs with a positive eigenvalue and a significant Moran's*I*were considered to describe significant spatial autocorrelations.[73] DDRs for the resistomes and the microbial community compositions were calculated as the slopes of the OLS regression relationships between the community similarity (1-Bray–Curtis dissimilarity matrices) calculated with the 'vegan' package[69] and geographic distance calculated with the 'sp' package.[74] Spearman's correlations between the ARG abundances and NMDS1 values of bacterial, fungal and protistan communities as well as MAT, MAP, soil TC, TN and pH were explored with the 'stats' package.[67] dbRDA to explore the impacts of changes in spatial configurations and edaphic as well as climatic factors on the soil and phyllosphere resistomes were conducted with the 'vegan' package.[69]

Structure equation modelling

The SEMs[75] were conducted using IBM SPSS Amos (V25; Amos Development Corporation, Chicago, IL, USA) to evaluate the direct and indirect impacts of a variety of biotic and abiotic factors on variations in ARG abundance in the phyllosphere and the soils. A prior model was established based on hypothesized effects and relationships among the drivers of the ARG abundances (Fig. S12). NMDS1 values of the NMDS analysis were used for the representation of bacterial, fungal and protistan community structures in the SEMs. Bacterial abundance was estimated by the copy numbers of 16 S rRNA genes. The overall goodness of fit for the SEMs was determined by multiple criteria: chi-square test $P > 0.05$, goodness of fit index (GFI) > 0.90 and root mean square error of approximation (RMSEA) < 0.08.[76]

DATA AVAILABILITY

The raw sequence data reported have been deposited in the National Centre for Biotechnology Information (NCBI) Sequence Read Archive (SRA) under the accession number PRJNA659980 (soil and plant samples titled with S and G).

REFERENCES

1. Bay, S. K. et al. Soil bacterial communities exhibit strong biogeographic patterns at fine taxonomic resolution. *mSystems* **5**, 4 (2020).
2. Fierer, N., Strickland, M. S., Liptzin, D., Bradford, M. A. & Cleveland, C. C. Global patterns in belowground communities. *Ecol. Lett.* **12**, 1238–1249 (2009).
3. Leff, J. W. et al. Consistent responses of soil microbial communities to elevated nutrient inputs in grasslands across the globe. *Proc. Natl Acad. Sci. USA* **112**, 10967–10972 (2015).
4. Maestre, F. T. et al. Increasing aridity reduces soil microbial diversity and abundance in global drylands. *Proc. Natl Acad. Sci. USA* **112**, 15684–15689 (2015).
5. Rousk, J. et al. Soil bacterial and fungal communities across a pH gradient in an arable soil. *ISME J.* **4**, 1340–1351 (2010).
6. Zhou, J. et al. Temperature mediates continental-scale diversity of microbes in forest soils. *Nat. Commun.* **7**, 1–10 (2016).
7. Zhang, Y. J. et al. Salinity as a predominant factor modulating the distribution patterns of antibiotic resistance genes in ocean and river beach soils. *Sci. Total Environ.* **668**, 193–203 (2019).
8. Bahram, M. et al. Structure and function of the global topsoil microbiome. *Nature* **560**, 233–237 (2018).
9. Faust, K. & Raes, J. Microbial interactions: from networks to models. *Nat. Rev. Microbiol.* **10**, 538–550 (2012).
10. Oliverio, A. M. et al. The global-scale distributions of soil protists and their contributions to belowground systems. *Sci. Adv.* **6**, eeax8787. (2020).
11. Boer, W., Folman, L. B., Summerbell, R. C. & Boddy, L. Living in a fungal world: impact of fungi on soil bacterial niche development. *FEMS Microbiol. Rev.* **29**, 795–811 (2005).
12. Allen, H. K. et al. Call of the wild: antibiotic resistance genes in natural environments. *Nat. Rev. Microbiol.* **8**, 251–259 (2010).
13. D'Costa, V. M. et al. Antibiotic resistance is ancient. *Nature* **477**, 457–461 (2011).
14. Martínez, J. L. Antibiotics and antibiotic resistance genes in natural environments. *Science* **321**, 365–367 (2008).
15. Goh, E.-B. et al. Transcriptional modulation of bacterial gene expression by subinhibitory concentrations of antibiotics. *Proc. Natl Acad. Sci. USA* **99**, 17025–17030 (2002).
16. Piddock, L. J. Multidrug-resistance efflux pumps? Not just for resistance. *Nat. Rev. Microbiol.* **4**, 629–636 (2006).
17. Wright, G. D. The antibiotic resistome: the nexus of chemical and genetic diversity. *Nat. Rev. Microbiol.* **5**, 175–186 (2007).
18. Chen, Q.-L., Cui, H. L., Su, J. Q., Penuelas, J. & Zhu, Y. G. Antibiotic resistomes in plant microbiomes. *Trends Plant Sci.* **24**, 530–541 (2019).
19. Forsberg, K. J. et al. Bacterial phylogeny structures soil resistomes across habitats. *Nature* **509**, 612–616 (2014).
20. Zhu, Y. G. et al. Soil biota, antimicrobial resistance and planetary health. *Environ. Int.* **131**, 105059 (2019).
21. Bai, Y. et al. Functional overlap of the Arabidopsis leaf and root microbiota. *Nature* **528**, 364–369 (2015).
22. Vorholt, J. A. Microbial life in the phyllosphere. *Nat. Rev. Microbiol.* **10**, 828–840 (2012).
23. Chen, Q. L. et al. Application of struvite alters the antibiotic resistome in soil, rhizosphere, and phyllosphere. *Environ. Sci. Technol.* **51**, 8149–8157 (2017).
24. Leveau, J. H. & Lindow, S. E. Appetite of an epiphyte: quantitative monitoring of bacterial sugar consumption in the phyllosphere. *Proc. Natl Acad. Sci. USA* **98**, 3446–3453 (2001).
25. Vacher, C. et al. the phyllosphere: microbial jungle at the plant–climate interface. *Annu. Rev. Ecol. Evol. Syst.* **47**, 1–24 (2016).
26. Yan, Z. Z., Chen, Q. L., Zhang, Y. J., He, J. Z. & Hu, H. W. Industrial development as a key factor explaining variances in soil and grass phyllosphere microbiomes in urban green spaces. *Environ. Pollut.* **261**, 114201 (2020).
27. Delmotte, N. et al. Community proteogenomics reveals insights into the physiology of phyllosphere bacteria. *Proc. Natl Acad. Sci. USA* **106**, 16428–16433 (2009).
28. Horton, M. W. et al. Genome-wide association study of Arabidopsis thaliana leaf microbial community. *Nat. Commun.* **5**, 1–7 (2014).
29. Bardgett, R. D. & van der Putten, W. H. Belowground biodiversity and ecosystem functioning. *Nature* **515**, 505–511 (2014).
30. Delgado-Baquerizo, M. et al. A global atlas of the dominant bacteria found in soil. *Science* **359**, 320–325 (2018).
31. Dray, S., Legendre, P. & Peres-Neto, P. R. Spatial modelling: a comprehensive framework for principal coordinate analysis of neighbour matrices (PCNM). *Ecol. Model* **196**, 483–493 (2006).
32. Zhang, Y. J. et al. Transfer of antibiotic resistance from manure-amended soils to vegetable microbiomes. *Environ. Int.* **130**, 104932 (2019).
33. Morlon, H. et al. A general framework for the distance-decay of similarity in ecological communities. *Ecol .Lett.* **11**, 904–917 (2008).
34. Srivastava, D. S., Cadotte, M. W., MacDonald, A. A. M., Marushia, R. G. & Mirotchnick, N. Phylogenetic diversity and the functioning of ecosystems. *Ecol Lett.* **15**, 637–648 (2012).
35. Wang, X. B. et al. Habitat-specific patterns and drivers of bacterial β-diversity in China's drylands. *ISME J.* **1**, 1345–1358 (2017).
36. Jiao, S., Xu, Y., Zhang, J. & Lu, Y. Environmental filtering drives distinct continental atlases of soil archaea between dryland and wetland agricultural ecosystems. *Microbiome.* **7**, 1–13 (2019).
37. Nemergut, D. R. et al. Patterns and processes of microbial community assembly. *Microbiol. Mol. Biol. Rev.* **77**, 342–356 (2013).
38. Delgado-Baquerizo, M. et al. Changes in belowground biodiversity during ecosystem development. *Proc. Natl Acad. Sci. USA* **116**, 6891–6896 (2019).
39. Fierer, N. Embracing the unknown: disentangling the complexities of the soil microbiome. *Nat. Rev. Microbiol.* **15**, 579–590 (2017).
40. Bell, T. Experimental tests of the bacterial distance-decay relationship. *ISME J.* **4**, 1357–1365 (2010).
41. Gao, Z., Karlsson, I., Geisen, S., Kowalchuk, G. & Jousset, A. Protists: puppet masters of the rhizosphere microbiome. *Trends Plant Sci.* **24**, 165–176 (2019).
42. Bengtsson-Palme, J., Kristiansson, E. & Larsson, D. G. J. Environmental factors influencing the development and spread of antibiotic resistance. *FEMS Microbiol. Rev.* **42**, fux053 (2018).
43. Tedersoo, L. et al. Global diversity and geography of soil fungi. *Science* **346**, 6213 (2014).
44. McMahon, M. A. S., Xu, J., Moore, J. E., Blair, I. S. & McDowell, D. A. Environmental stress and antibiotic resistance in food-related pathogens. *Appl Environ. Microbiol.* **73**, 211–217 (2007).
45. Hammarlund, S. P. & Harcombe, W. R. Refining the stress gradient hypothesis in a microbial community. *Proc. Natl Acad. Sci. USA* **116**, 15760–15762 (2019).
46. Chen, Q.-L. et al. Host identity determines plant associated resistomes. *Environ. Poll.* **258**, 113709 (2020).
47. Lajoie, G., Maglione, R. & Kembel, S. W. Adaptive matching between phyllosphere bacteria and their tree hosts in a neotropical forest. *Microbiome.* **8**, 1–10 (2020).

48. Chen, W. et al. Stochastic processes shape microeukaryotic community assembly in a subtropical river across wet and dry seasons. *Microbiome.* **7**, 1–16 (2019).
49. Jiao, S., Yang, Y., Xu, Y., Zhang, J. & Lu, Y. Balance between community assembly processes mediates species coexistence in agricultural soil microbiomes across eastern China. *ISME J.* **14**, 202–216 (2020).
50. Ramette, A. & Tiedje, J. M. Multiscale responses of microbial life to spatial distance and environmental heterogeneity in a patchy ecosystem. *Proc. Natl Acad. Sci. USA* **104**, 2761–2766 (2007).
51. Rayment G. E., Lyons D. J. Soil chemical methods: Australasia. Vol. 3. CSIRO Publishing; 2011.
52. Fick, S. E. & Hijmans, R. J. WorldClim 2: new 1-km spatial resolution climate surfaces for global land areas. *Int. J. Climatol.* **37**, 4302–4315 (2017).
53. Yan, Z. Z., Chen, Q. L., Zhang, Y. J., He, J. Z. & Hu, H. W. Antibiotic resistance in urban green spaces mirrors the pattern of industrial distribution. *Environ. Int.* **132**, 105106 (2019).
54. Klappenbach, J. A., Saxman, P. R., Cole, J. R. & Schmidt, T. M. rrndb: the ribosomal RNA operon copy number database. *Nucleic Acids Res.* **29**, 181–184 (2001).
55. Stalder, T. et al. Quantitative and qualitative impact of hospital effluent on dissemination of the integron pool. *ISME J.* **8**, 768–777 (2014).
56. Chen, Q. L. et al. Effect of biochar amendment on the alleviation of antibiotic resistance in soil and phyllosphere of Brassica chinensis L. *Soil Biol. Biochem.* **119**, 74–82 (2018).
57. Walters, W. et al. Improved bacterial 16S rRNA gene (V4 and V4-5) and fungal internal transcribed spacer marker gene primers for microbial community surveys. *mSystems* **1**, e00009–e00015 (2016).
58. Adams, R. I., Miletto, M., Taylor, J. W. & Bruns, T. D. Dispersal in microbes: fungi in indoor air are dominated by outdoor air and show dispersal limitation at short distances. *ISME J.* **7**, 1262–1273 (2013).
59. Stoeck, T. et al. Multiple marker parallel tag environmental DNA sequencing reveals a highly complex eukaryotic community in marine anoxic water. *Mol Ecol.* **19**, 21–31 (2010).
60. Magoč, T. & Salzberg, S. L. FLASH: fast length adjustment of short reads to improve genome assemblies. *Bioinformatics* **27**, 2957–2963 (2011).
61. Caporaso, J. G. et al. QIIME allows analysis of high-throughput community sequencing data. *Nat. Methods* **7**, 335–336 (2010).
62. Edgar, R. C. Search and clustering orders of magnitude faster than BLAST. *Bioinformatics.* **26**, 2460–2461 (2010).
63. Quast, C. et al. The SILVA ribosomal RNA gene database project: improved data processing and web-based tools. *Nucleic Acids Res.* **41**, D590–D596 (2012).
64. Nilsson, R. H. et al. The UNITE database for molecular identification of fungi: handling dark taxa and parallel taxonomic classifications. *Nucleic Acids Res.* **47**, D259–D264 (2019).
65. Guillou, L. et al. The protist ribosomal reference database (PR2): a catalog of unicellular eukaryote small sub-unit rRNA sequences with curated taxonomy. *Nucleic Acids Res.* **41**, D597–D604 (2012).
66. Wickham, H. *ggplot2: Elegant Graphics for Data Analysis* (Springer, Berlin, 2016)..
67. Field, A., Miles, J. & Field, Z. *Discovering-Statistics-Using-R.* (Sage publications, California, 2012).
68. Kolde, R. Pheatmap: pretty heatmaps. *R Package.* **61**, 617 (2012).
69. Oksanen, J. et al. Package 'vegan'. *Commun. Ecol. Package* **2**, 1–295 (2013).
70. Hiemstra, P. H., Pebesma, E. J., Twenhöfel, C. J. & Heuvelink, G. B. Real-time automatic interpolation of ambient gamma dose rates from the Dutch radioactivity monitoring network. *Comput. Geosci.* **35**, 1711–1721 (2009).
71. Dray, S. et al. Package 'adespatial'. *R Package* **2018**, 3–8 (2018).
72. Bivand, R. & Wong, D. W. S. Comparing implementations of global and local indicators of spatial association. *TEST* **27**, 716–748 (2018).
73. Widenfalk, L. A., Malmström, A., Berg, M. P. & Bengtsson, J. Small-scale collembola community composition in a pine forest soil–overdispersion in functional traits indicates the importance of species interactions. *Soil Biol. Biochem.* **103**, 52–62 (2016). 2016.
74. Pebesma, E. & Bivand, R. Classes and methods for spatial data in R. *R-news.* **5**, 9–13 (2005).
75. Pugesek B. H., Tomer A., von Eye A. *Structural Equation Modeling: Applications in Ecological and Evolutionary Biology*. Cambridge: Cambridge University Press, 2003.
76. Schermelleh-Engel, K., Moosbrugger, H. & Müller, H. Evaluating the fit of structural equation models: Tests of significance and descriptive goodness-of-fit measures. *MPR Online* **8**, 23–74 (2003).

ACKNOWLEDGEMENTS

We thank the Melbourne Trace Analysis for Chemical, Earth and Environmental Sciences (TrACEES) Platform—Soil Node for the help with soil physicochemical characterization. We thank Qing Xie, School of Agriculture and Food, Faculty of Veterinary and Agricultural Sciences, The University of Melbourne, for the assistance with sample processing. This work was financially supported by the Australia Research Council (DP170103628, DE210100271).

AUTHOR CONTRIBUTIONS

Q.-L.C and H.-W.H. conceived and designed the research. Z.-Z.Y performed the experiments and drafted the manuscript. Z-Z.Y. and Q.-L.C analysed the data. C.-Y.L. contributed to sample collection and preparation. Q.-L.C, H.-W.H., J.-Z.H., Y.-G.Z. and B.-A.T.N. amended the manuscript. All authors read and accepted the final manuscript.

CONFLICT OF INTERESTS

The authors declare no competing interests.

ADDITIONAL INFORMATION

Supplementary information The online version contains supplementary material available at https://doi.org/10.1038/s43705-021-00012-4.

Correspondence and requests for materials should be addressed to Q.-L.C. or H.-W.H.

Reprints and permission information is available at http://www.nature.com/reprints

Publisher's note Springer Nature remains neutral with regard to jurisdictional claims in published maps and institutional affiliations.

Open Access This article is licensed under a Creative Commons Attribution 4.0 International License, which permits use, sharing, adaptation, distribution and reproduction in any medium or format, as long as you give appropriate credit to the original author(s) and the source, provide a link to the Creative Commons license, and indicate if changes were made. The images or other third party material in this article are included in the article's Creative Commons license, unless indicated otherwise in a credit line to the material. If material is not included in the article's Creative Commons license and your intended use is not permitted by statutory regulation or exceeds the permitted use, you will need to obtain permission directly from the copyright holder. To view a copy of this license, visit http://creativecommons.org/licenses/by/4.0/.

Supplementary information for Biotic and abiotic factors distinctly drive contrasting biogeographic patterns between phyllosphere and soil resistomes in natural ecosystems

Zhen-Zhen Yan [1], Qing-Lin Chen [1*], Chao-Yu Li [1], Bao-Anh Thi Nguyen [1], Yong-Guan Zhu [2], Ji-Zheng He [1], Hang-Wei Hu [1*]

[1] School of Agriculture and Food, Faculty of Veterinary and Agricultural Sciences, The University of Melbourne, VIC, 3010, Australia.

[2] Key Laboratory of Urban Environment and Health, Institute of Urban Environment, Chinese Academy of Sciences, 1799 Jimei Road, Xiamen, 361021, China

*Corresponding authors:

qinglin.chen@unimelb.edu.au (Q-L, Chen);

hang-we.hu@unimelb.edu.au (H-W, Hu).

Summary of contents

Supplementary file 1: Table S1; Table S2; Fig. S1 – S12, .docx file.

Supplementary file 2: list of soil properties, .xlsx file.

Supplementary file 3: list of climatic factors, .xlsx file.

Supplementary file 4: Information of primers used for the HT-qPCR quantification of ARGs, xlsx file.

Table S1 Moran's *I* for each axis of the Moran's eigenvector maps.

Test	Obs	Std.Obs	Alter	*P*-value
MEM1	1.016073	12.47069	greater	0.001
MEM2	1.007145	12.12525	greater	0.001
MEM3	1.001725	12.35922	greater	0.001
MEM4	0.994288	11.64666	greater	0.001
MEM5	0.985704	12.24134	greater	0.001
MEM6	0.983526	12.00557	greater	0.001
MEM7	0.961351	11.57866	greater	0.001
MEM8	0.948027	11.35398	greater	0.001
MEM9	0.936125	11.57989	greater	0.001
MEM10	0.92354	11.62942	greater	0.001
MEM11	0.920674	11.35698	greater	0.001
MEM12	0.911244	11.17902	greater	0.001
MEM13	0.89356	11.11894	greater	0.001
MEM14	0.876649	10.92835	greater	0.001
MEM15	0.869353	10.75226	greater	0.001
MEM16	0.861344	10.34135	greater	0.001
MEM17	0.836387	10.1415	greater	0.001
MEM18	0.826728	10.04655	greater	0.001
MEM19	0.820696	10.29073	greater	0.001
MEM20	0.79205	10.22037	greater	0.001
MEM21	0.772148	9.266583	greater	0.001
MEM22	0.764483	9.356284	greater	0.001
MEM23	0.731543	8.816545	greater	0.001
MEM24	0.71979	9.046406	greater	0.001
MEM25	0.7119	8.715064	greater	0.001
MEM26	0.689276	8.318112	greater	0.001
MEM27	0.672944	8.221434	greater	0.001
MEM28	0.645027	7.753772	greater	0.001
MEM29	0.605278	7.337623	greater	0.001
MEM30	0.603011	7.550533	greater	0.001
MEM31	0.577786	6.950992	greater	0.001
MEM32	0.562784	6.580494	greater	0.001
MEM33	0.552549	6.853402	greater	0.001
MEM34	0.499921	6.037462	greater	0.001
MEM35	0.478008	5.671883	greater	0.001
MEM36	0.435202	5.394886	greater	0.001
MEM37	0.421335	5.396996	greater	0.001
MEM38	0.413466	5.156617	greater	0.001
MEM39	0.386612	4.84586	greater	0.001
MEM40	0.36228	4.292384	greater	0.001
MEM41	0.328751	4.188434	greater	0.001
MEM42	0.297244	3.709412	greater	0.001

MEM43	0.281599	3.620684	greater	0.001
MEM44	0.263598	3.338538	greater	0.001
MEM45	0.243117	3.190355	greater	0.004
MEM46	0.211396	2.638925	greater	0.007
MEM47	0.186026	2.423659	greater	0.011
MEM48	0.169185	2.135982	greater	0.019
MEM49	0.151682	2.040945	greater	0.023
MEM50	0.117974	1.478805	greater	0.07
MEM51	0.108437	1.353437	greater	0.089
MEM52	0.102945	1.346525	greater	0.097
MEM53	0.061933	0.838264	greater	0.195
MEM54	0.019531	0.362509	greater	0.364
MEM55	0.000863	0.095527	greater	0.45
MEM56	-0.00283	0.128715	greater	0.439
MEM57	-0.02751	-0.20758	greater	0.572
MEM58	-0.06538	-0.70861	greater	0.759
MEM59	-0.07417	-0.74619	greater	0.766
MEM60	-0.10442	-1.24919	greater	0.899
MEM61	-0.10959	-1.25883	greater	0.893
MEM62	-0.12547	-1.38193	greater	0.919
MEM63	-0.15402	-1.72185	greater	0.956
MEM64	-0.16513	-1.87923	greater	0.966
MEM65	-0.1682	-1.88269	greater	0.971
MEM66	-0.19329	-2.27855	greater	0.987
MEM67	-0.22187	-2.78938	greater	0.996
MEM68	-0.23928	-2.71931	greater	0.998
MEM69	-0.25959	-2.89872	greater	1
MEM70	-0.29787	-3.43362	greater	1
MEM71	-0.29973	-3.52491	greater	1
MEM72	-0.31648	-3.75259	greater	1
MEM73	-0.32737	-3.86406	greater	1
MEM74	-0.36885	-4.48233	greater	1
MEM75	-0.37414	-4.45334	greater	1
MEM76	-0.40751	-4.8033	greater	1
MEM77	-0.40969	-4.98806	greater	1
MEM78	-0.43541	-5.07918	greater	1
MEM79	-0.44637	-5.27993	greater	1
MEM80	-0.45432	-5.43351	greater	1
MEM81	-0.47969	-5.65986	greater	1
MEM82	-0.48449	-5.54774	greater	1
MEM83	-0.50829	-5.92709	greater	1
MEM84	-0.51697	-6.1493	greater	1
MEM85	-0.5271	-6.22317	greater	1
MEM86	-0.53228	-6.49504	greater	1

MEM87	-0.56731	-6.57326	greater	1
MEM88	-0.57993	-7.11243	greater	1
MEM89	-0.5975	-6.87851	greater	1
MEM90	-0.60511	-7.47256	greater	1
MEM91	-0.62705	-7.31809	greater	1
MEM92	-0.63905	-7.26116	greater	1
MEM93	-0.64354	-7.68563	greater	1
MEM94	-0.64679	-7.77409	greater	1
MEM95	-0.67512	-8.18407	greater	1
MEM96	-0.6845	-8.31769	greater	1
MEM97	-0.70478	-8.7834	greater	1
MEM98	-0.71278	-8.79411	greater	1
MEM99	-0.75825	-9.08226	greater	1
MEM100	-0.79135	-9.86217	greater	1
MEM101	-0.79719	-10.3268	greater	1
MEM102	-0.80591	-10.0173	greater	1
MEM103	-0.81159	-10.241	greater	1
MEM104	-0.82422	-10.1243	greater	1
MEM105	-0.83742	-11.0436	greater	1
MEM106	-0.85271	-10.4442	greater	1
MEM107	-0.86892	-10.682	greater	1
MEM108	-0.8893	-10.9817	greater	1
MEM109	-0.89454	-11.9991	greater	1
MEM110	-0.90352	-10.8562	greater	1
MEM111	-0.90595	-10.9311	greater	1
MEM112	-0.93121	-12.2321	greater	1
MEM113	-0.94705	-12.2964	greater	1
MEM114	-0.94784	-11.6459	greater	1
MEM115	-0.9599	-12.2328	greater	1
MEM116	-0.99776	-12.4405	greater	1
MEM117	-1.01043	-13.0083	greater	1

Table S2 Spearman's correlation between the abundances and selected biotic and abiotic factors. Significant correlations ($P < 0.05$) are indicated as bold fonts.

		Bacterial NMDS1	**Fungal NMDS1**	**Protistan NMDS1**	**MAT (°C)**	**MAP (mm)**	**TC (%)**	**TN (%)**	**pH**
Phyllosphere	**Beta-lactamase resistance**	**0.613**	**-0.331**	**0.281**	-0.030	-0.157	-0.117	-0.039	0.092
		***P* < 0.001**	***P* < *0.001***	***P* = 0.004**	*P* = 0.768	*P* = 0.115	*P* = 0.242	*P* = 0.694	*P* = 0.358
	Multidrug resistance	**0.505**	**-0.230**	0.174	-0.129	-0.053	-0.048	0.002	0.004
		***P* < 0.001**	***P* = 0.019**	*P* = 0.081	*P* = 0.197	*P* = 0.597	*P* = 0.632	*P* = 0.983	*P* = 0.971
Soil	**Multidrug resistance**	**0.121**	0.093	0.007	**0.201**	0.101	**0.205**	**0.221**	0.053
		***P* = 0.049**	*P* = 0.129	*P* = 0.907	***P* = 0.001**	*P* = 0.099	***P* < 0.001**	***P* < 0.001**	*P* = 0.387

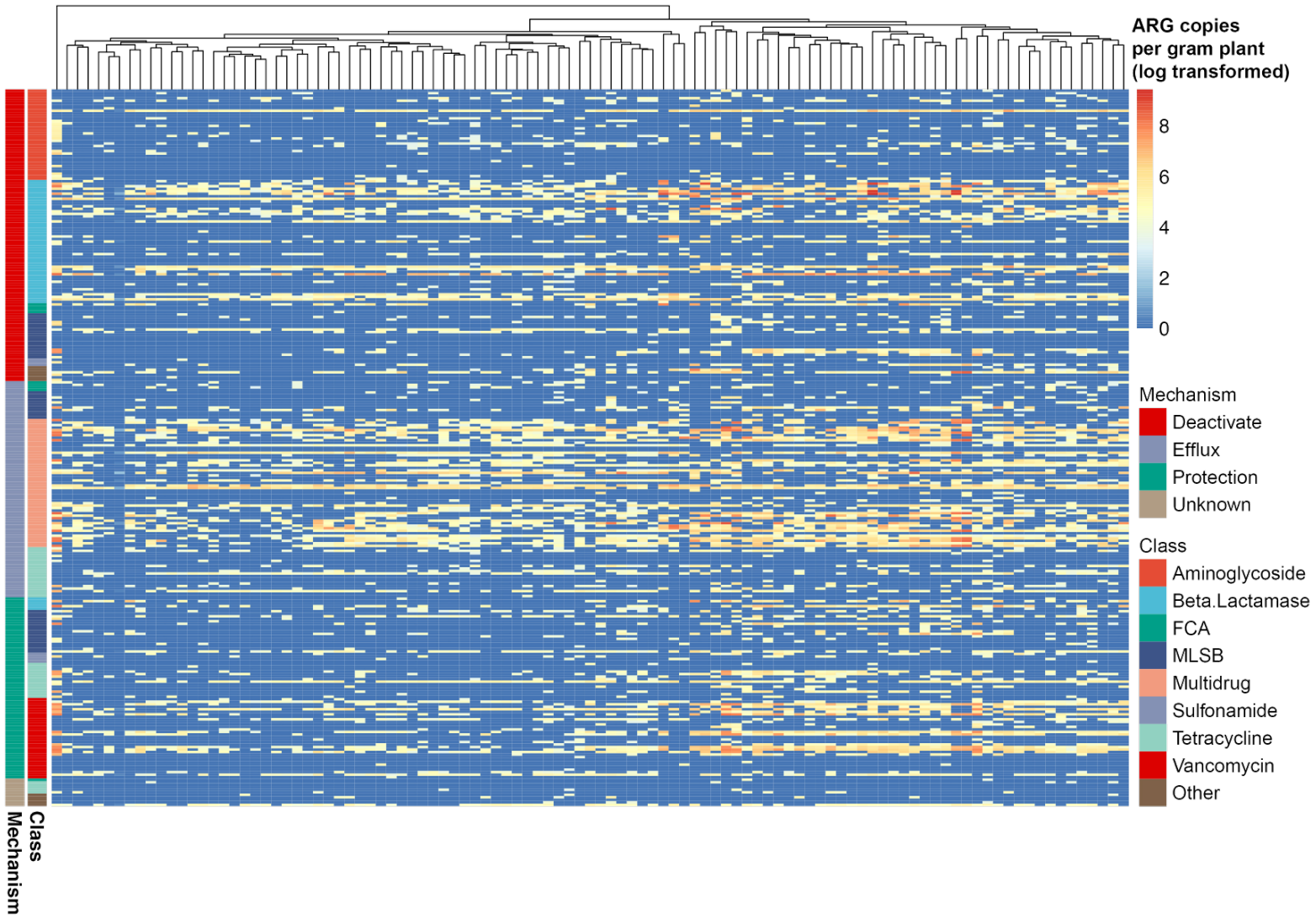

Fig. S1 Heatmap showing the abundance of the ARGs detected in the phyllosphere samples.

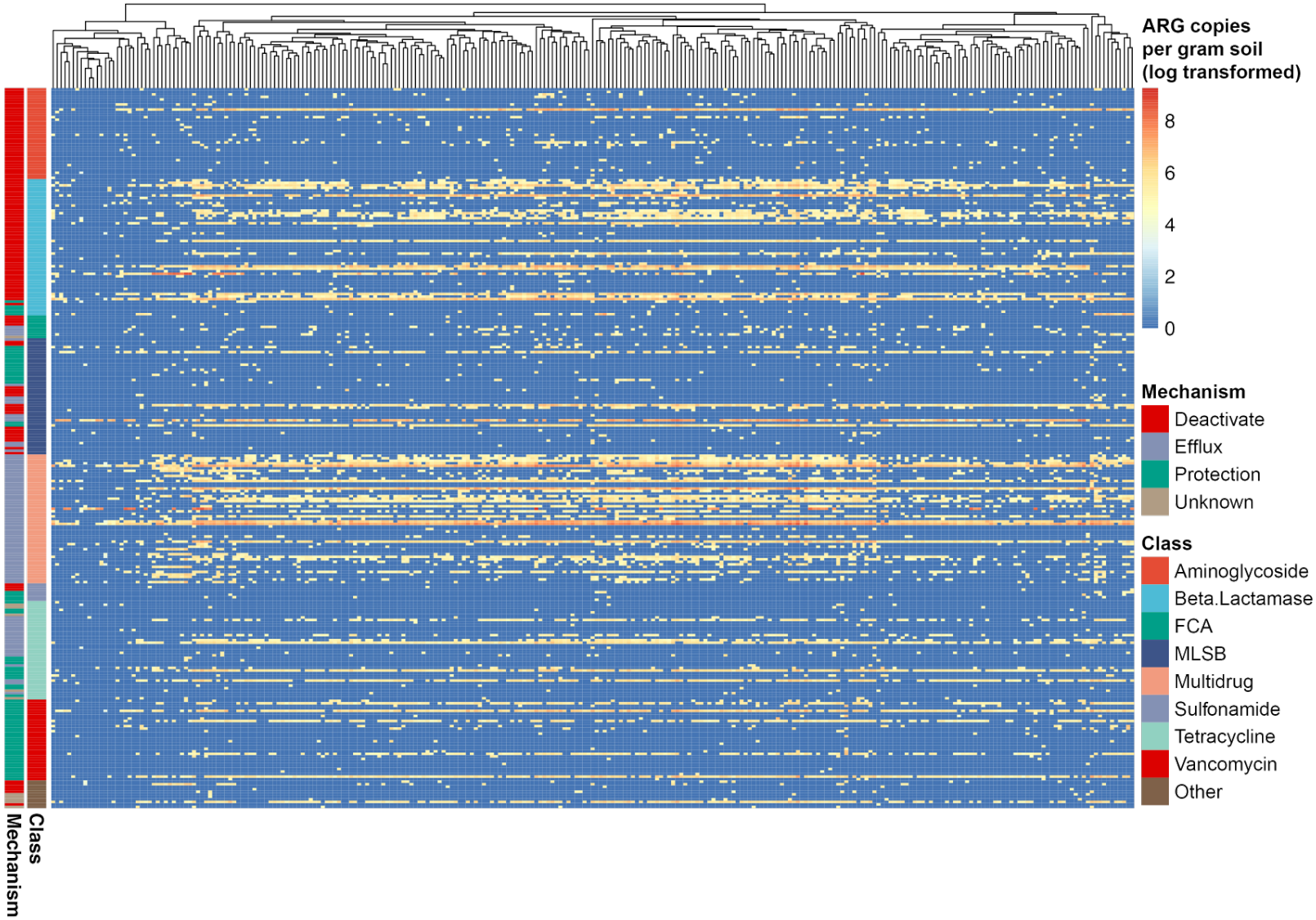

Fig. S2 Heatmap showing the abundance of the ARGs detected in the soil samples.

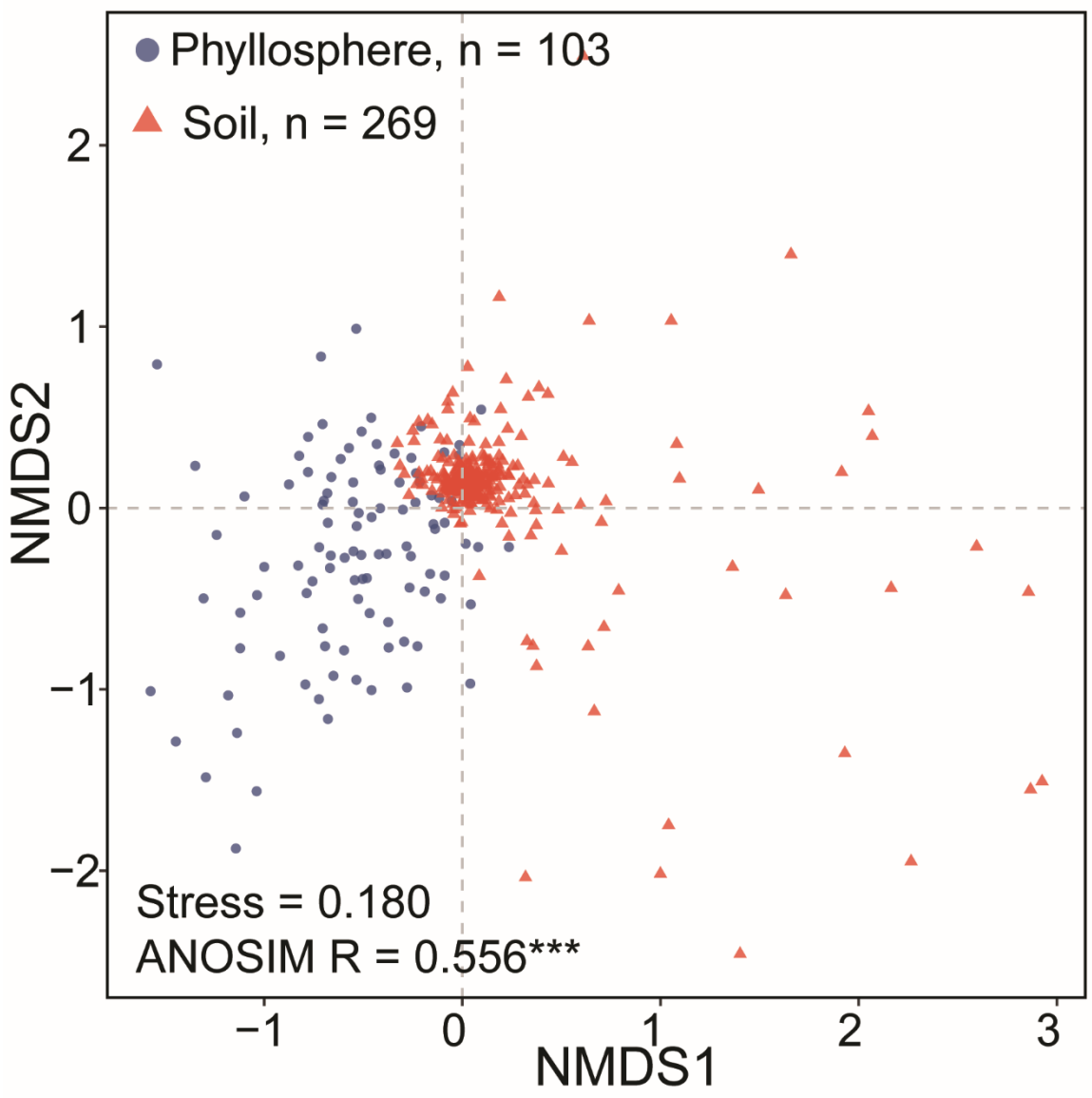

Fig. S3 Nonmetric multidimensional scaling ordinations showing the ARG profiles in phyllosphere and soils based on the Bray-Curtis distance and ARG abundances (copies per gram sample).

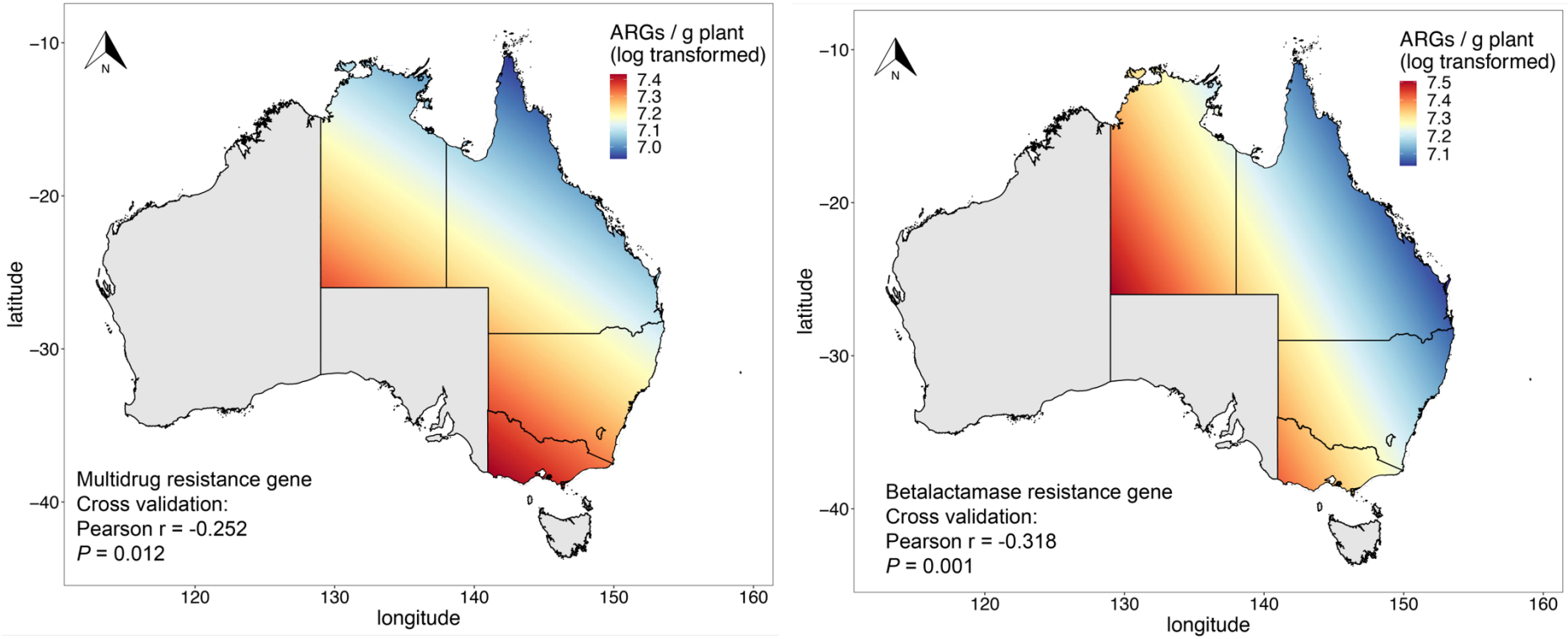

Fig. S4 Large-scale atlas of the abundances of the dominant ARG classes in phyllosphere across eastern and northern Australia.

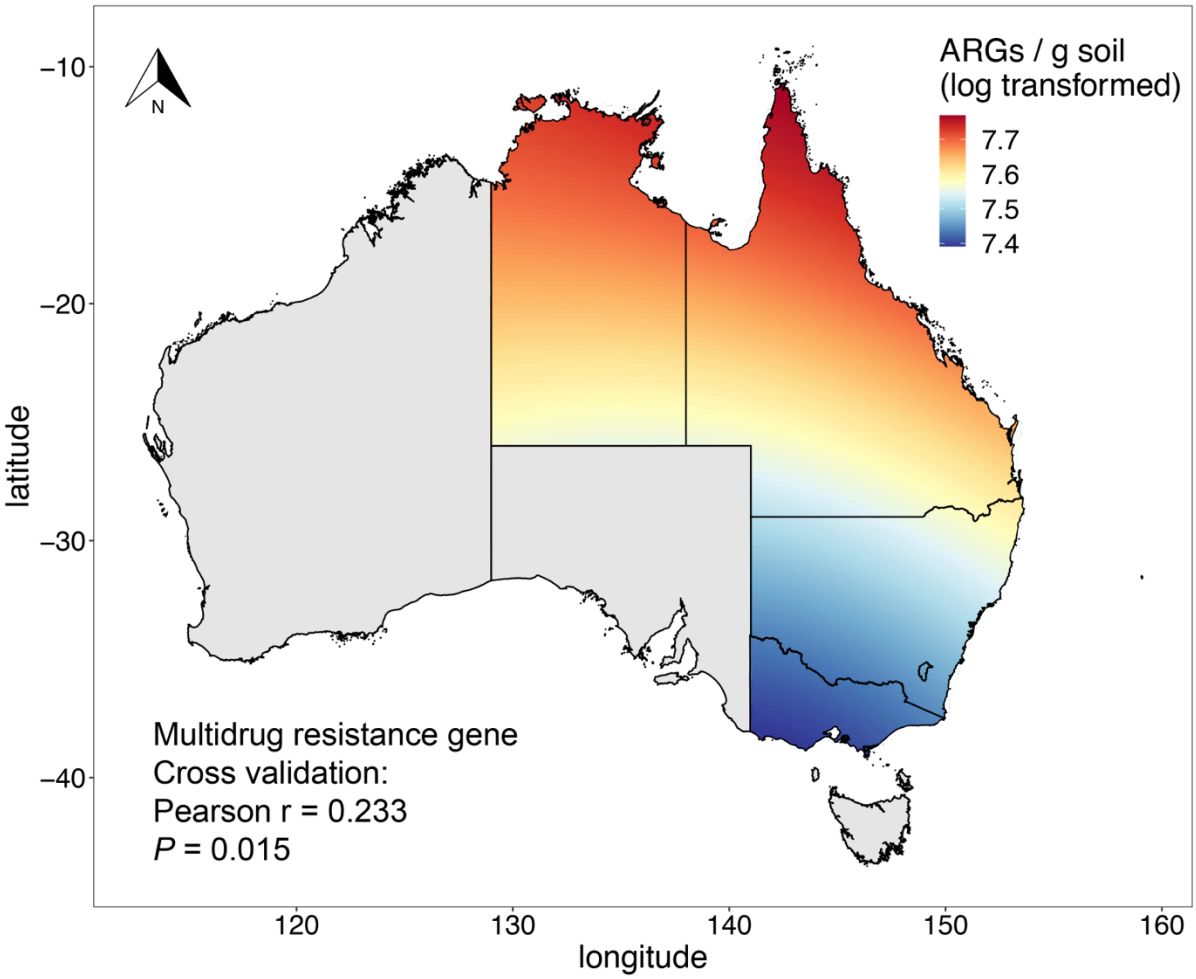

Fig. S5 Large-scale atlas of the abundance of the dominant ARG class in soils across eastern and northern Australia.

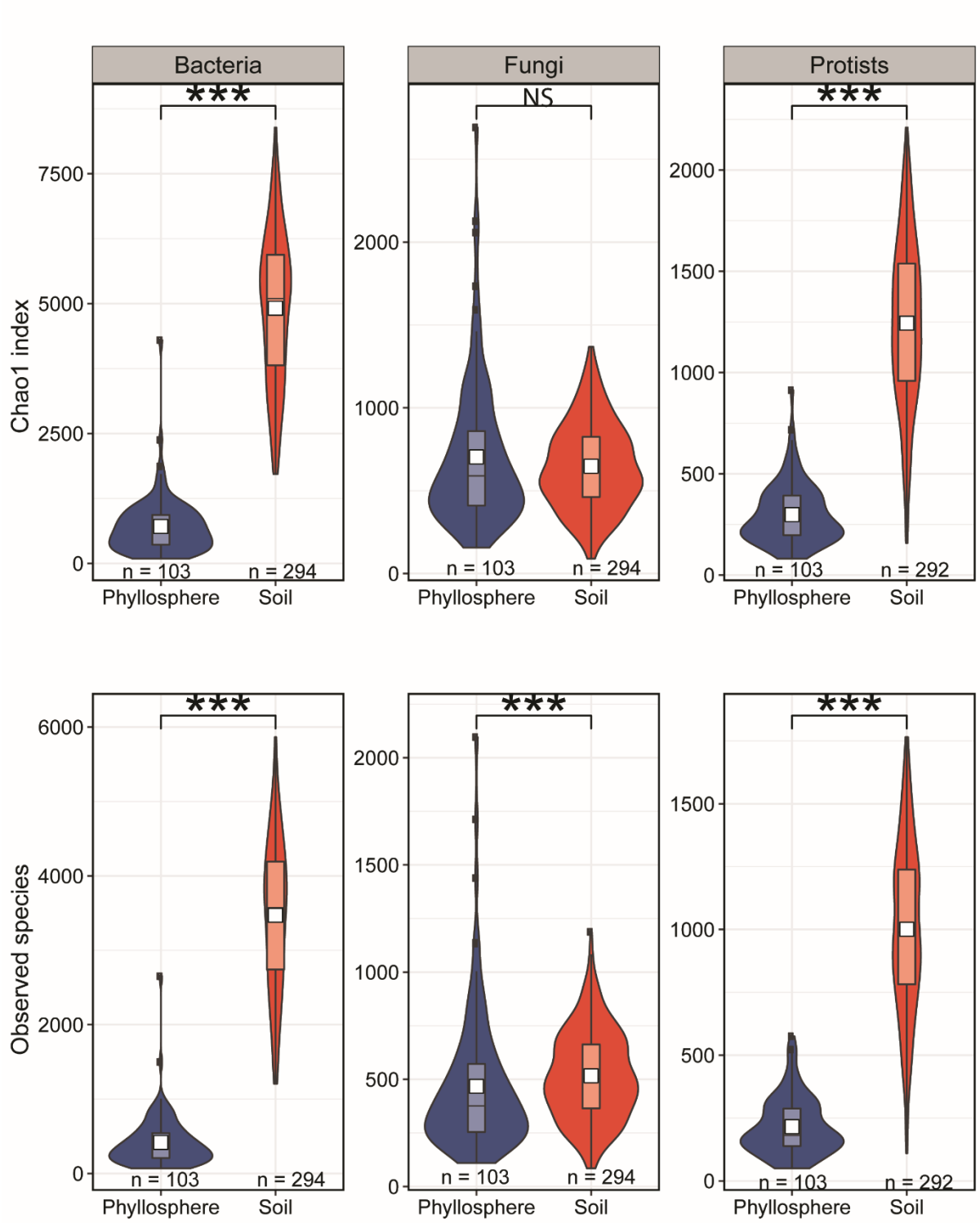

Fig. S6 Violin plots and boxplots showing the alpha-diversity index of bacterial, fungal, and protistan communities in the phyllosphere and soils as revealed by the numbers of observed species. *** indicates Wilcoxon rank0sum test $P < 0.001$. White squares inside the box plots indicate the mean values.

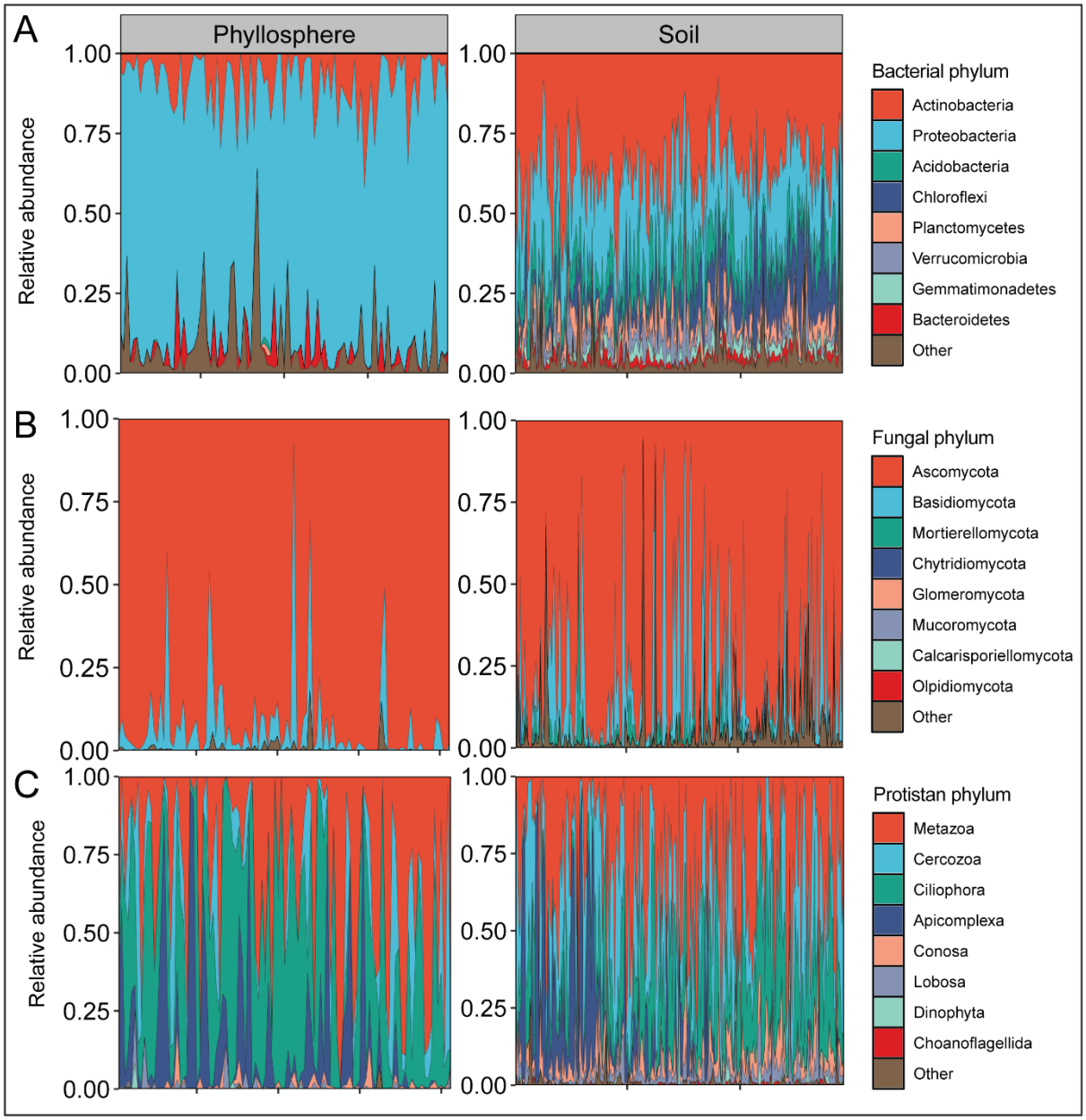

Fig. S7 Area charts showing taxonomic compositions of the bacterial (A), fungal (B), and protistan (C) communities at the phylum level. Samples were ordered by ascending in the latitude of the sampling locations.

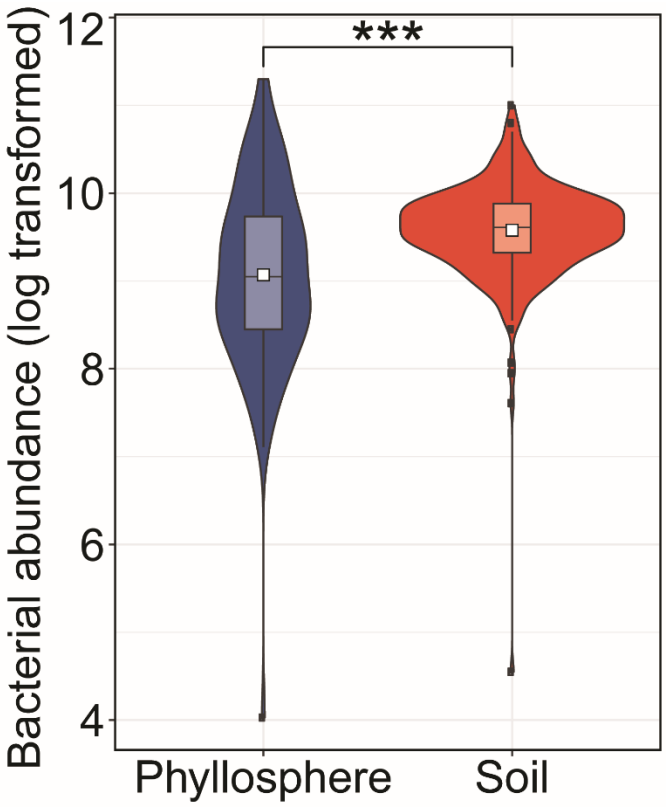

Fig. S8 Violin plots and boxplots showing bacterial abundances in the phyllosphere and soils as revealed by copy numbers of 16S rRNA gene. *** indicates Wilcoxon rank0sum test $P < 0.001$. White squares inside the box plots indicate the mean values

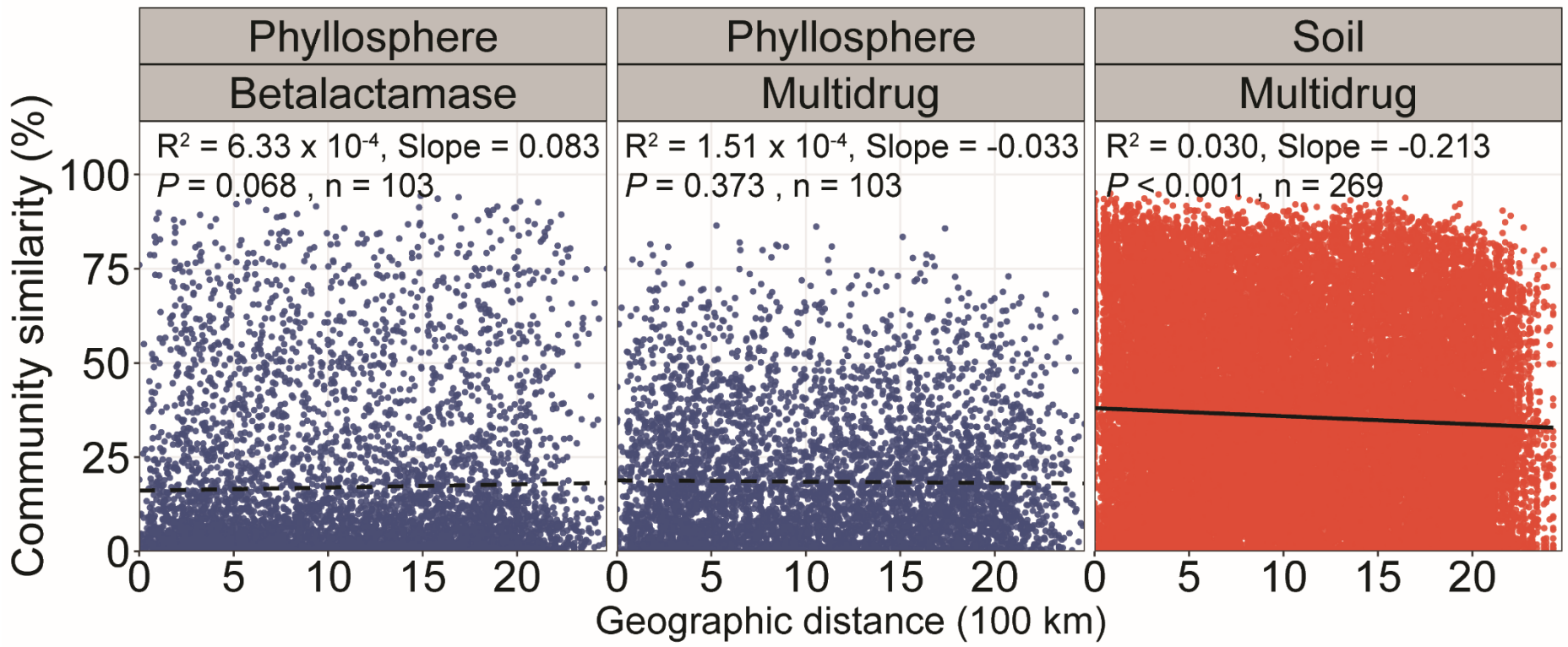

Fig. S9 Distance-decay relationships for the dominant ARG class(es) in phyllosphere and soils. *** indicates ordinary least square regression $P < 0.001$. Significant correlation ($P < 0.05$) and not significant correlations ($P > 0.05$) are shown in solid line and dashed lines, respectively.

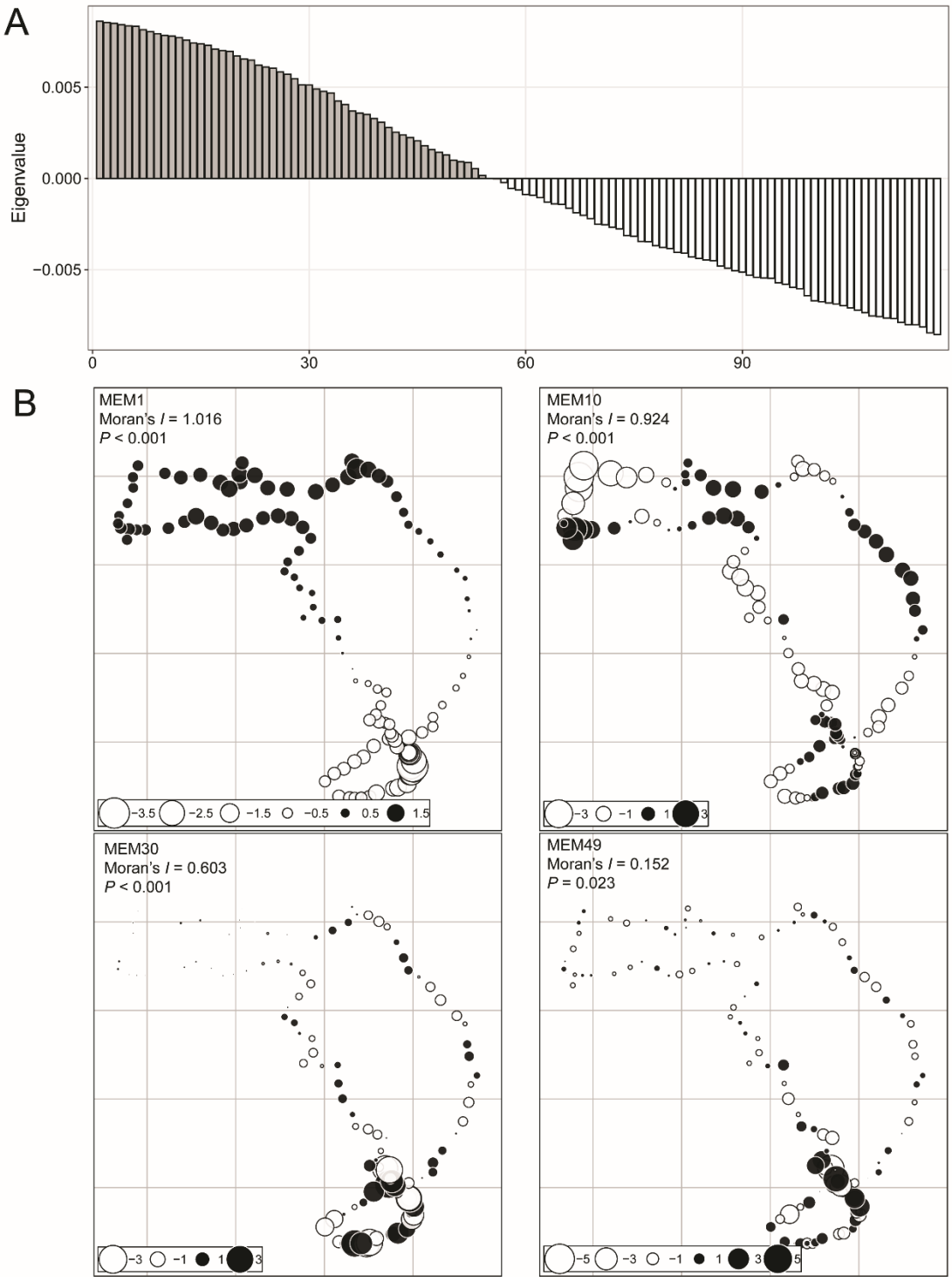

Fig. S10 (A) Eigenvalues of the spatial weighting matrix of the Moran's eigenvector maps (MEMs). (B) Examples of MEMs describing spatial patterns. MEM1 and MEM10 describe large scale spatial autocorrelation. MEM30 and MEM49 represent specific patterns in corners of the sampling area at the inter-mediate scale.

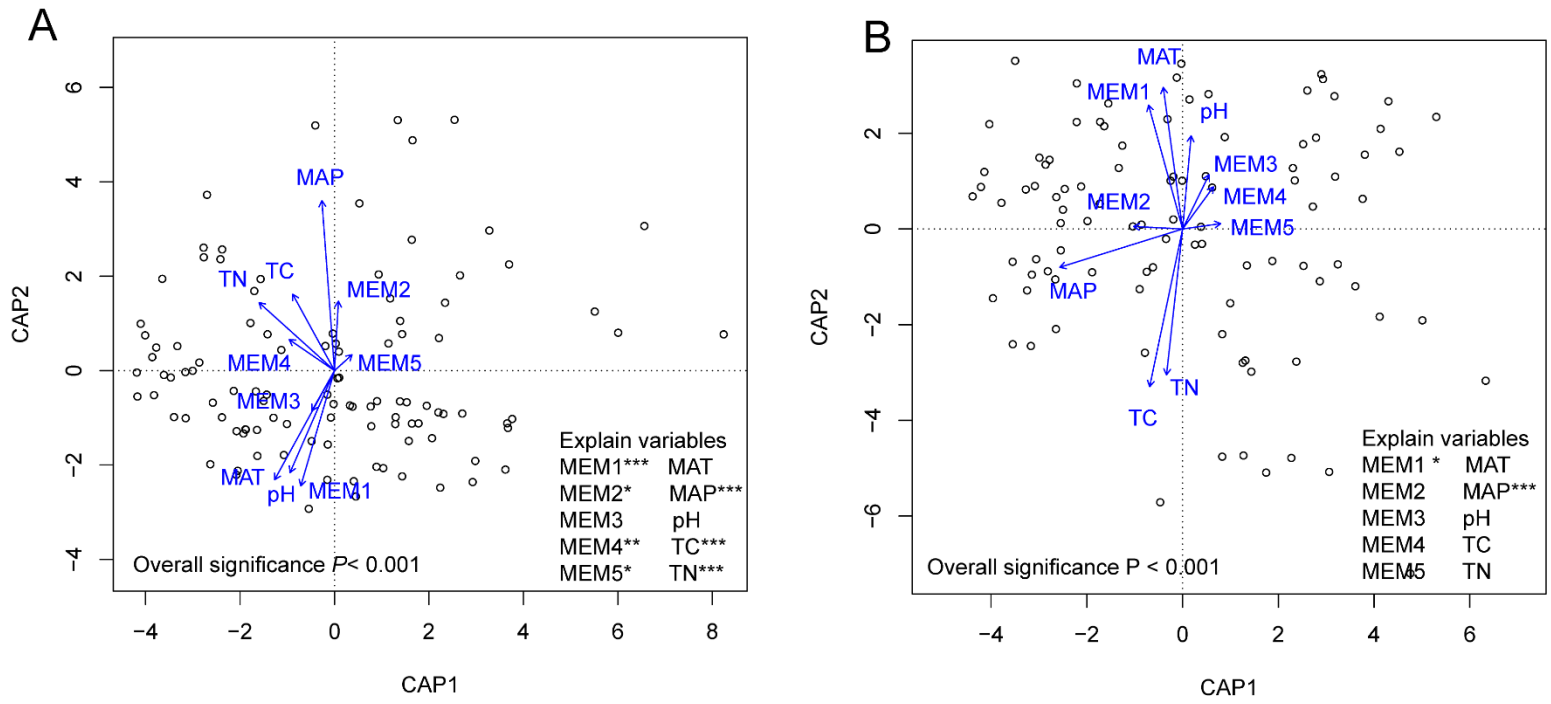

Fig. S11 Distance-based redundancy analysis results showing the impacts of changes in spatial patterns, edaphic and climatic factors in the variances in soil (A) and phyllosphere (B) resistome profiles. * $P < 0.05$, ** $P < 0.01$, *** $P < 0.001$. MEM1 -5: Top five largest eigenvalues of the spatial weighting matrix of the Moran's eigenvector maps. MAT: mean annual temperature (°C). MAP: mean annual precipitation (mm). TC: Soil total carbon (%). TN: soil total nitrogen (%).

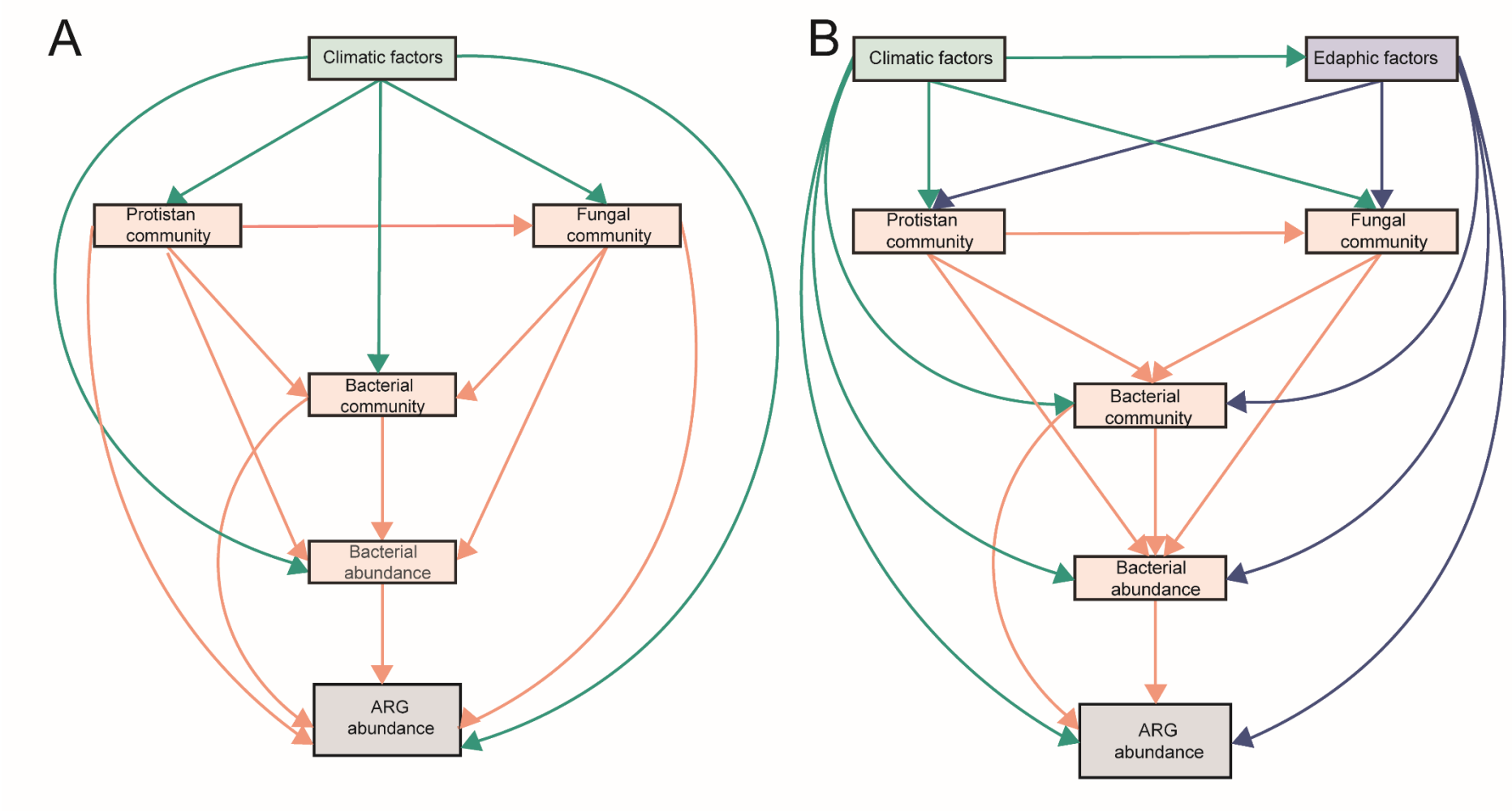

Fig. S12 *A priori* models for the structure equation models of variation in ARG abundances in phyllosphere (A) and soils (B) based on the hypothesized causal relationships between multiple factors and ARG abundances.

Chapter 5: Characterizations of the impacts of changes in habitat properties on antibiotic resistome profile

This chapter is based on a published article entitled:

Termite mound formation reduces the abundance and diversity of soil resistomes.

Environmental Microbiology, 23: 7761-7670. https://doi.org/10.1111/1462-2920.15631

environmental microbiology

Environmental Microbiology (2021) **23**(12), 7661–7670 doi:10.1111/1462-2920.15631

Special Issue Article

Termite mound formation reduces the abundance and diversity of soil resistomes

Zhen-Zhen Yan,[1] Qing-Lin Chen,[1*] Chao-Yu Li,[1] Bao-Anh Thi Nguyen,[1] Yong-Guan Zhu,[2] Ji-Zheng He[1] and Hang-Wei Hu[1]

[1]*School of Agriculture and Food, Faculty of Veterinary and Agricultural Sciences, The University of Melbourne, Melbourne, Victoria, 3010, Australia.*

[2]*Key Laboratory of Urban Environment and Health, Institute of Urban Environment, Chinese Academy of Sciences, 1799 Jimei Road, Xiamen, 361021, China.*

Summary

Termites are pivotal ecosystem engineers in tropical and subtropical habitats, where they construct massive nests ('mounds') that substantially modify soil properties and promote nutrient cycling. Yet, little is known about the roles of termite nesting activity in regulating the spread of antimicrobial resistance (AMR), one of the major Global Health challenges. Here, we conducted a large-scale (> 1500 km) investigation in northern Australia and found distinct resistome profiles in termite mounds and bulk soils. By profiling a wide spectrum of ARGs, we found that the abundance and diversity of antibiotic resistance genes (ARGs) were significantly lower in termite mounds than in bulk soils ($P < 0.001$). The proportion of efflux pump ARGs was significantly lower in termite mound resistome than in bulk soil resistome ($P < 0.001$). The differences in resistome profiles between termite mounds and bulk soils may result from the changes in microbial interactions owing to the substantial increase in pH and nutrient availability induced by termite nesting activities. These findings advance our understanding of the profile of ARGs in termite mounds, which is a crucial step to evaluate the roles of soil faunal activity in regulating soil resistome under global environmental change.

Received 21 February, 2021; revised 24 May, 2021; accepted 6 June, 2021. *For correspondence. E-mail qinglin.chen@unimelb.edu.au; Tel. (61) 478273195.

© 2021 Society for Applied Microbiology and John Wiley & Sons Ltd.

Introduction

Antimicrobial resistance (AMR) has been recognized as a major health issue of global concerns in the 21st century (Pruden *et al*., 2006; WHO, 2019). Currently, the annual death toll related to AMR has exceeded 700,000 globally. If no action is taken, the number of AMR-related death is projected to increase to 10 million per year by 2050 (WHO, 2019). The uncontrolled AMR could also, directly and indirectly, impact food production and trading, and the AMR-related economic damage is comparable to the catastrophic global financial crisis during 2008–2009 (WHO, 2019). Therefore, the influence of AMR on human, animal, and plant health and welfare, as well as its ecological and economic consequences, has reinforced the need for a concerted effort to track and control its emergence and dissemination. Recently, the 'One Health' concept that focuses on the role of geographically interconnected environments in the dissemination of ARGs has been developed to fight against AMR (Hernando-Amado *et al*., 2019).

As an intrinsic phenomenon of the soil microbiome, antibiotic resistance genes (ARGs) have existed in the environment for an extended time (Martínez, 2008; Hu *et al*., 2018). In natural environments, ARGs are critical to several metabolic processes that are essential for the survival of bacteria (Allen *et al*., 2010; D'Costa *et al*., 2011; Martínez, 2008). Currently, the factors driving the soil resistome, the collection of all ARGs in both pathogenic and non-pathogenic bacteria in a community (Wright, 2007), in various ecosystems have been explored in a large number of studies. Abiotic factors, including soil pH, soil nutrient availability, and soil salinity, are demonstrated to be crucial in shaping the soil resistome profile (Li *et al*., 2020; Sun *et al*., 2020; Xiao *et al*., 2016; Zhang *et al*., 2019). A recent study proposed that the relative abundance of ARGs in global topsoil could be a robust indicator for the intensity of interkingdom microbial antagonisms (Bahram *et al*., 2018). Despite the longstanding interest in soil resistome, the impacts of soil fauna, a critical component of soil food webs, on the dissemination and evolution of ARGs, as

well as the contribution of the environmental factors to those impacts, remain largely unresolved.

Termites are soil-dwelling macrofauna that is among the most abundant organisms on Earth, and they are widely distributed in tropical and subtropical regions (Marynowska *et al*., 2020). Termites have close relationships with soil microbes (i.e., bacteria, archaea, fungi, and/or protists) which enable them to digest cellulose and thus become the major ecosystem engineers that decompose dead woods and leaf litter (Jouquet *et al*., 2011; Ashton *et al*., 2019). Some termite colonies construct unique nest structures ('mounds') with soil materials, which change soil physical and chemical compositions through activities such as decomposition of soil organic matter and bioturbation. Therefore, termite mound environments are usually substantially different from surrounding bulk soils (Bonachela *et al*., 2015; Nishimura *et al*., 2020; Chen *et al*., 2021a). As 'islands of fertility', termite mounds harbour a broad range of microbial communities that play essential roles in regulating multiple ecosystem functions related to the ongoing global changes (Bonachela *et al*., 2015; Ashton *et al*., 2019; Chiri *et al*., 2020). It is estimated that termites produce ~1% to 3% of global greenhouse gas methane (CH_4), half of which was filtered in termite mounds before emission to the atmosphere (Nauer *et al*., 2018). This 'hidden biofilter' process is mediated by methanotrophic bacteria dwelling in termite mound walls, for which an internal intricate network of tunnels can facilitate CH_4 transport (Nauer *et al*., 2018). A recent study demonstrated that the microbial community assemblies in termite mounds were driven more by deterministic selection rather than stochastic forces, suggesting that soil properties and mean annual temperature were the major selection forces for termite mound dwelling microbes (Chen *et al*., 2021b). By comparison, the AMR related to termite mounds remains largely unknown, and a detailed comparative study of the resistome profiles in termite mounds and bulk soils would be imperative to bridge the knowledge gaps of the impacts regarding soil faunal activities on soil resistome.

In this study, we investigated the occurrence and abundance of 285 ARGs in 134 termite mounds collected from an over 1500 km transect in northern Australia using high throughput quantitative PCR (HT-qPCR) array. To our best knowledge, this study represents the first attempt to assess the resistome profile in termite mounds across a large spatial scale. Compare with local or regional scale studies, large-scale studies can better reveal the spatial patterns of resistome profile, and provide more insights into the underlying mechanisms of the development and spread of environmental AMR. We aimed to (i) explore how the nesting activity of termites influences the soil resistome profiles in natural terrestrial ecosystems and (ii) to identify the main determinants shaping the resistome profiles in termite mounds and bulk soils. We hypothesized that termite nesting activities would increase soil nutrient availability and alter soil pH, which would lead to alternations in resistance mechanisms of ARGs and shifts in ARG abundance.

Results

Physiochemical properties of termite mounds and bulk soils

Termite mounds formation led to significant alternations in soil physicochemical properties. Termite mound pH, which ranged from 5.29 to 7.86 (with an average of 6.66) was significantly higher (Wilcoxon rank-sum test $P < 0.001$) than the pH of bulk soils, which ranged from 4.93 to 7.36 (with an average of 6.22; Fig. 1). In addition, dissolved organic carbon (DOC) of termite mounds, which ranged from 139.02 to 2821.5 mg kg^{-1} (with an average of 572.78 mg kg^{-1}) was significantly higher than that of bulk soils (Wilcoxon rank-sum test $P < 0.001$), which ranged from 43.57 to 166.3 mg kg^{-1} (with an average of 87.48 mg kg^{-1}; Fig. 1). Dissolved organic nitrogen (DON) of termite mounds ranging from 5.26 to 310.50 mg kg^{-1} (with an average of 83.41 mg kg^{-1}), was also significantly higher than that of bulk soils (Wilcoxon rank-sum test $P < 0.001$) ranging from 1.64 to 39.21 mg kg^{-1} (with an average of 14.13 mg kg^{-1}; Fig. 1).

Microbial properties of termite mounds and bulk soils

Termite mounds were characterized by significantly higher bacterial and fungal abundances but significantly lower ratios of bacterial to fungal abundances in comparison to bulk soils (Wilcoxon rank-sum test $P < 0.001$; Fig. 1). Bacterial abundances ranged from 2.78×10^8 to 3.51×10^{10} copies/g (with an average of 5.61×10^9 copies/g) and 1.18×10^8 to 9.56×10^9 copies/g (with an average of 3.13×10^9 copies/g) for termite mounds and bulk soils, respectively (Fig. S2). Fungal abundances ranged from 2.87×10^5 to 2.66×10^{10} (with an average of 1.24×10^9 copies/g) and 1.37×10^6 to 1.00×10^9 copies/g (with an average of 9.41×10^7 copies/g) for termite mounds and bulk soils, respectively (Fig. S3).

Resistome profiles of termite mounds and bulk soils

The HT-qPCR results revealed that termite mounds harboured significantly less abundant and diverse ARGs than bulk soils (Wilcoxon rank-sum test, $P < 0.001$, Fig. 2). The absolute abundance of ARGs (copies/g

© 2021 Society for Applied Microbiology and John Wiley & Sons Ltd., *Environmental Microbiology*

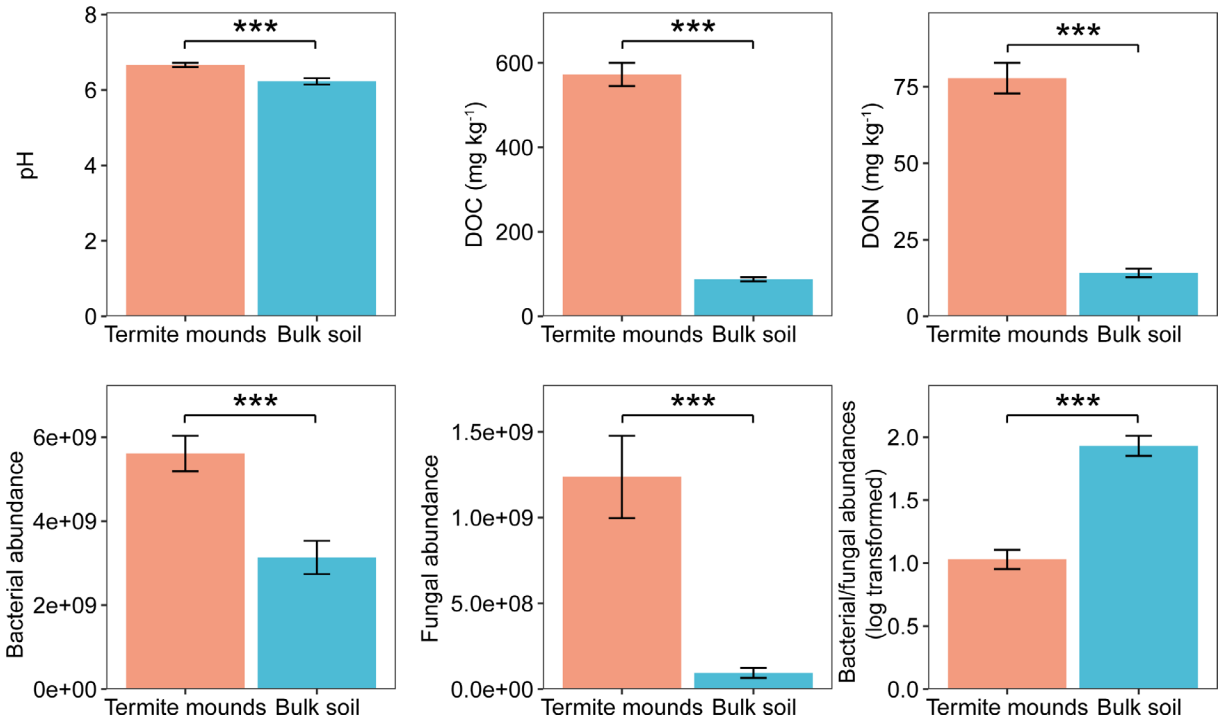

Fig 1. Comparison of the microbial and physicochemical properties between termite mounds and soil samples. *** indicates Wilcoxon rank-sum test $P < 0.001$. DOC: dissolved organic carbon. DON: dissolved organic nitrogen. [Color figure can be viewed at wileyonlinelibrary.com]

sample) in termite mounds and bulk soils ranged from 3.17×10^7 to 3.00×10^9 (with an average of 1.14×10^8) and 2.59×10^7 to 6.97×10^8 (with an average value of 1.43×10^8), respectively (Fig. S4). To minimize the variations in background bacterial abundances, the ARG absolute abundances were normalized to 16S rRNA gene copies as ARG copies per 16S rRNA gene. The relative abundance of ARGs detected in termite mound and bulk soil samples ranged from 1.20×10^{-3} to 1.72×10^{-1} (with an average of 2.28×10^{-2}) and 7.03×10^{-3} to 3.02×10^{-1} (with a median value of 7.28×10^{-2}), respectively (Fig. S5).

We further assessed the overall profiles of the resistomes in the termite mound and bulk soil samples and found there was a clear separation of ARGs depending on the sample type (Adonis test $P < 0.001$; Fig. 2B). In addition, the resistome compositions based on the antibiotic resistance mechanisms were distinct between termite mounds and bulk soils. Particularly, the proportion of efflux pump genes was significantly lower in termite mound resistome than in bulk soil resistome (Wilcoxon rank-sum test $P < 0.001$). The efflux pump genes accounted for 68.51% vs. 43.98% of the abundance of total ARGs detected in the bulk soil samples and termite mound samples, respectively (Fig. 2C). The ARGs shared between the termite mound and bulk soil samples and those detected exclusively in each type of sample were visualized using bipartite network analysis (Fig. 2D). A total of 190 ARGs were shared between termite mounds and bulk soils, 67 ARGs were detected only in termite mounds, and 14 ARGs were detected only in bulk soils.

Relationships between environmental factors and ARG abundances

To gain further insights into the potential drivers shaping the termite mound and bulk soil resistome profiles, we analysed the relationships between ARG abundances and selected environmental factors. The results showed that pH was one of the most important determinants of ARG abundances in both termite mounds and bulk soils. Spearman's rank correlation, as well as first and second-order polynomial regression models, revealed that pH was significantly negatively correlated with ARG abundances for both types of samples ($P < 0.001$; Fig. 3). Nutrient availability, as represented by DOC and DON, oppositely influenced the ARG abundances in termite mounds and bulk soils (Fig. 3). According to the correlation and regression analyses, the ARG abundance in termite mounds was positively correlated with DOC and DON. In contrast, the ARG abundance in bulk soils was negatively correlated with DOC and DON.

© 2021 Society for Applied Microbiology and John Wiley & Sons Ltd., *Environmental Microbiology*

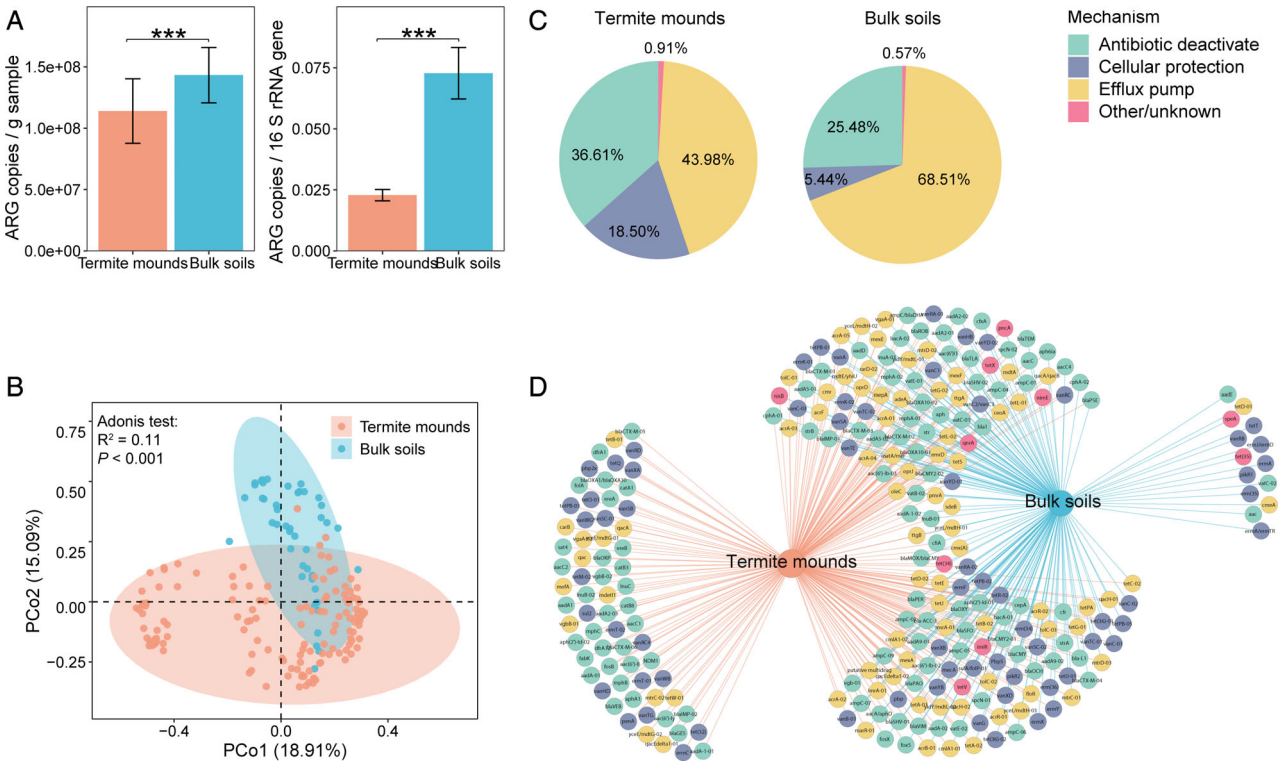

Fig 2. Profiles of the resistomes in termite mounds and soil samples.
A. Relative abundance and Shannon index of antibiotic resistance genes (ARGs) in termite mounds and bulk soils. Error bars represented as mean ± standard deviation. *** indicates Wilcoxon rank-sum test $P < 0.001$.
B. Principal coordinate analysis (PCoA) based on the Bray-Curtis distance showing the overall distribution patterns in the termite mounds and soil.
C. Classification of the ARGs detected based on the mechanisms of the resistance.
D. Bipartite network analysis revealing the shared and unique ARGs in termite mounds and soil. [Color figure can be viewed at wileyonlinelibrary.com]

Discussion

By using the large-scaled investigation, our study improved the understanding of the profiles of ARGs in widely distributed termite mounds. Consistent with our hypothesis, the results showed that compared with bulk soils, termite mounds harboured a lower level of ARG abundance and diversity, which may potentially result from the increases in pH and nutrient availability during the nesting processes (Fig. 4). In the following discussion, we will focus on the potential impacts of pH and nutrient availability on termite mounds ARGs.

Impact of pH on the profiles of ARGs in termite mounds

The quantitative results revealed that termite mound formation led to significant reductions in soil ARG abundance and diversity (Fig. 2). It is interesting to note that the relative abundance of ARGs in our bulk soil samples was comparable to those in urban soils as reported previously (Yan *et al*., 2019). The relatively high levels of ARGs in the bulk soil samples indicate that soils in natural habitats with no or limited anthropogenic impact do not necessarily contain lower levels of AMR than soils in habitats with continuously intensive anthropogenic impacts. These findings indicated that as an intrinsic component of soil microbiota, ARGs could be abundant in the environment, independent from selection pressures imposed by human activities such as overuse of antibiotics and waste discharge (Surette and Wright, 2017). The significantly lower ARG abundances in termite mounds than in bulk soils is likely related to the significant increases in pH values due to the termite nesting activities (Fig. 1), as pH value was significantly and negatively correlated with ARG abundances (Fig. 3). Such strong correlations between ARG abundances and pH could be a consequence of the close relationships between pH and soil bacteria, the potential hosts of ARGs. According to previous studies, most soil bacterial taxa exhibit a narrow pH optimum (Rousk *et al*., 2010; Xiao *et al*., 2016). Minor deviation from the optima pH (i.e., ∼1 pH unit) could greatly decrease the bacterial growth and substantially result in the bacterial community being rapidly outcompeted by the fungal

© 2021 Society for Applied Microbiology and John Wiley & Sons Ltd., *Environmental Microbiology*

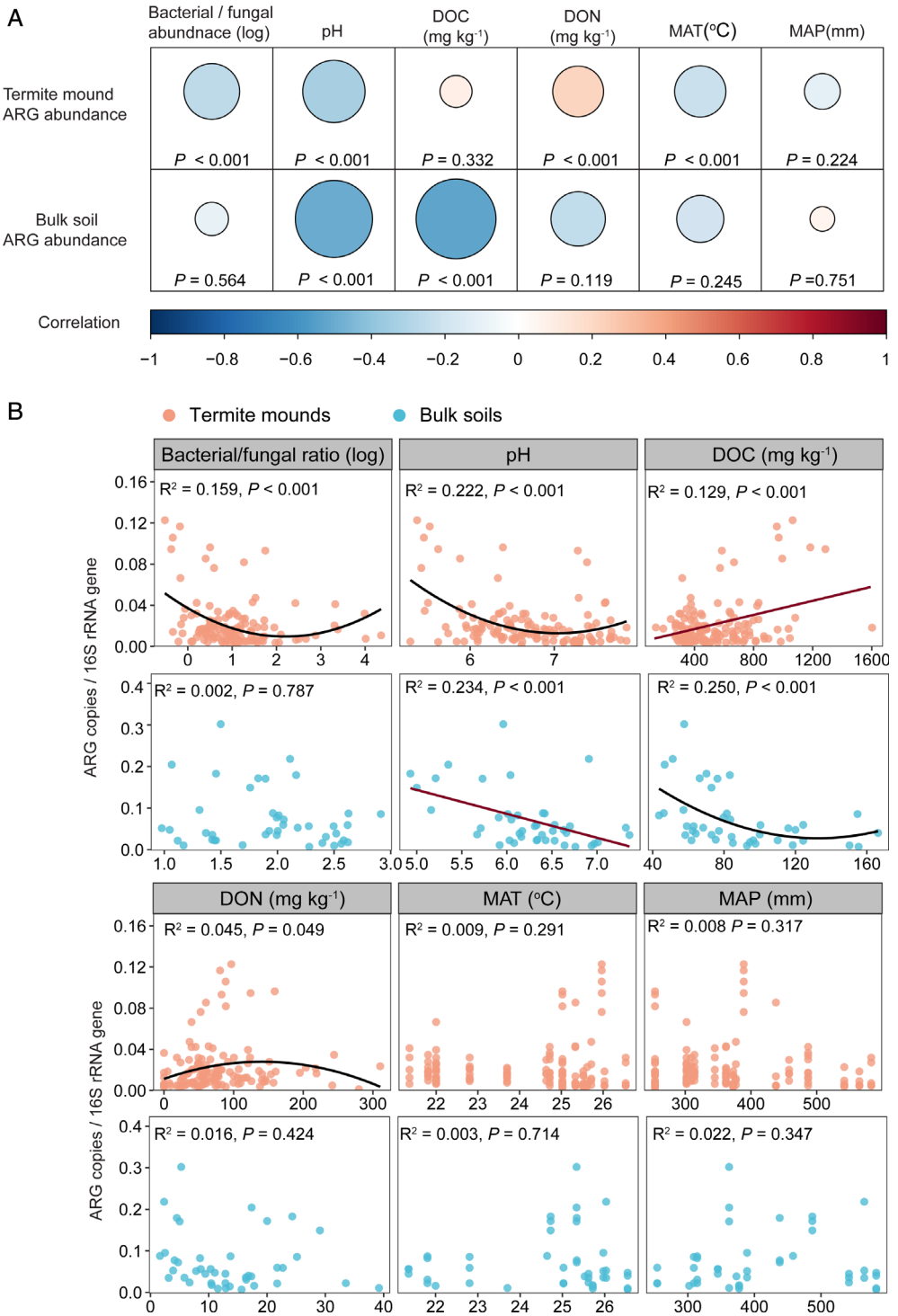

Fig 3. Main determinants of the relative abundance of antibiotic resistance genes (ARGs) in termite mounds and soil.
A. Spearman's correlation matrix.
B. Significant ($P < 0.05$) and the best fit (determined based on the corrected Akaike Information Criterion) polynomial fits of ARG relative abundance of selected determinants. Red and black lines represent first- and second-order polynomial fits, respectively.
DOC: dissolved organic carbon; DON: dissolved organic nitrogen; MAT: mean annual temperature; MAP: mean annual precipitation. [Color figure can be viewed at wileyonlinelibrary.com]

© 2021 Society for Applied Microbiology and John Wiley & Sons Ltd., *Environmental Microbiology*

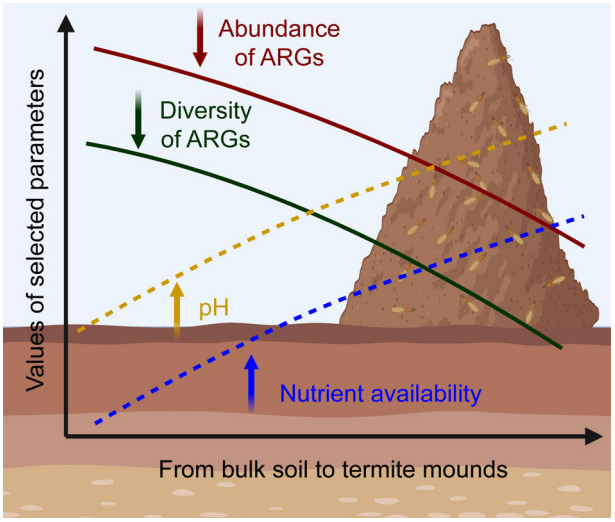

Fig 4. Schematic summary of the impact of termite mound formation on soil antibiotic resistance genes (ARGs). Termite nesting activity led to increases in soil pH and nutrient availability, which could alter the inter-kingdom interaction between bacteria and fungi and shift the soil resistome. The figure was created in BioRender.com. [Color figure can be viewed at wileyonlinelibrary.com]

community whose growth is far less sensitive to pH change (Rousk *et al*., 2010). The impacts of pH change on the competitive interactions between bacterial and fungal communities could also be revealed by the observation that the bacterial to fungal abundance ratio was significantly lower in termite mounds than in bulk soils (Fig. 1).

In addition, termite mound formation led to substantial alternations in the resistance mechanisms and classifications of ARGs. The clear separation in the termite mound and bulk soil resistomes (Fig. 2B) might be associated with the differences in resistome compositions, particularly the significantly lower proportion of efflux pump genes in termite mounds than in bulk soils (Fig. 2C). Efflux pumps are evolutionarily ancient and the most common antibiotic resistance mechanism in pristine ecosystems, such as the Tibetan plateau, deep ocean, and undomesticated old bog ecosystems (Chen *et al*., 2013; Chen *et al*., 2016; Obermeier *et al*., 2020). The multiprotein pumps encoded by the efflux pump genes typically confer resistance to several unrelated substances including solvents, heavy metals, and endogenous compounds produced by the bacterial hosts (Martinez *et al*., 2009). Their physiological roles also involve regulating intracellular pH, transporting quorum sensing molecules of cell-to-cell communications, and enhancing bacterial pathogenicity (Martinez *et al*., 2009). Resistance to antibiotics commonly used in clinical and agricultural sectors mediated by efflux pump genes is considered to be a by-product of the physiological functions of these genes that allow bacteria to survive in their ecological niches (Piddock, 2006). Consequently, the much higher proportion of efflux pump genes in the bulk soil resistome than in the termite mound resistome indicates that ARGs in the two habitats may evolve due to different reasons. Compared to termite mounds, bulk soils are nutrition poor and less suitable for the growth of an abundant bacterial community. Therefore, ARGs, especially the efflux pump ARGs, in bulk soils are likely evolved as a strategy of the bacteria to survive. The possible differences in evolutionary mechanisms between ARGs in termite mounds and bulk soils are further supported by the results of shared and unique ARGs in these two habitats. The finding that 67 ARGs were detected exclusively in termite mounds (Fig. 2D) suggests that there might be a termite mound endogenous resistome which is not originated from bulk soils.

Impacts of nutrient availability on the profiles of ARGs in termite mounds

Previous studies have shown that the evolution of resistomes in natural ecosystems without anthropogenic selection pressures is mainly driven by the inter-kingdom interactions among microbial communities within their environmental habitats (Bahram *et al*., 2018; Obermeier *et al*., 2020). Negative interactions among microbes, particularly the antagonism between bacterial and fungal communities, are commonly associated with an elevated level of ARGs, as many bacterial and fungal cells can produce antibiotics as weapons when competing with each other. These antibiotics can select against bacterial cells not encoding ARGs (Bahram *et al*., 2018). We assume that the distinct resistome profiles in termite mounds and bulk soils might result from the shifts in the forms of bacterial-fungal interactions which are consequences of the substantial increases in nutrient availability in termite mounds in comparison to bulk soils (Fig. 1). The stress gradient hypothesis (SGH) provides a framework to predict whether the interactions among microbes from different kingdoms are positive or negative in an environment (Hammarlund and Harcombe, 2019; Piccardi *et al*., 2019). The SGH states that nutrient availability is one of the most important factors that govern the direction of microbial interactions. In a benign environment with abundantly available nutrients, negative interactions among microbes should be more common. In contrast, in a stressful environment where resources essential for microbial growth are lacking, the interactions among microbes would switch to facilitation (Hammarlund and Harcombe, 2019; Piccardi *et al*., 2019). Due to the foraging activities of termites that involves the accumulation of plant litter and invertebrates in their mounds and the ability of termites in facilitating

© 2021 Society for Applied Microbiology and John Wiley & Sons Ltd., *Environmental Microbiology*

soil nutrient cycling (Bonachela *et al*., 2015), termite mounds are unique nutrient hotspots with significantly more abundant DOC and DON than bulk soils (Fig. 1). Therefore, it is likely that the ARGs in termite mounds are mainly evolved due to the selection pressures associated with the antagonism between bacterial and fungal communities. However, ARGs in bulk soils are mostly evolved as a strategy for the bacterial to survive in the stressful habitat. Our hypothesis is supported by the observation that DOC and DON oppositely impacted the ARG abundances in termite mounds and bulk soils and is further strengthened by the results that the abundance of ARGs in termite mounds but not in bulk soils was significantly correlated with the ratio of bacterial to fungal abundances (Fig. 3). However, to verify this hypothesis, more targeted analyses with additional data from different geographic locations and evolution experiments will be required.

Conclusions

Taken together, these findings improve our understanding of the resistome in termite mounds and provide evidence that the lower level of ARG abundance and diversity in termite mounds than in bulk soils could potentially result from the increases in pH and nutrient availability during the nesting processes. Given that termite mounds constitute an important soil compartment (up to $\sim$ 10%) especially in the savanna ecosystem, termite nesting activity might potentially mitigate the soil antibiotic resistance. Our results highlight the necessity to consider the roles of soil faunal activities in regulating AMR in terrestrial ecosystems, which would facilitate the development of strategies in fighting against AMR dissemination in natural ecosystems under the changing environment.

Experimental procedures

Termite mounds and soil sample processing

Termite mound and bulk soil samples were collected in May 2019 from 16 locations in northern Australia (133.36°E to 140.36°E, 22.98°S to 19.25°S; Fig. S1). Geographic coordinates of the sampling locations were recorded using a hand-held GPS device (eTrex Venture, Garmin, Olathe, KS, USA). Mean annual temperature (MAT) of the sampling region ranged from 21.36 to 26.54°C. Mean annual precipitation (MAP) ranged from 254 to 583 mm. At each location, we established a 50 $\times$ 50 m plot and collected eight to ten samples of termite mound samples. Three bulk soil samples were collected by mixing five cores (0–10 cm) for each sampling plot. In total, 134 termite mounds and 44 bulk soil samples were collected. All samples were sieved through a 2 mm mesh and divided into two portions. One portion was frozen at −80°C for molecular analyses and the other portion was stored at 4°C for soil physiochemical analyses.

Molecular analyses

Total genomic DNA was extracted from the termite mound and bulk soil samples using a DNeasy PowerSoil Kit (QIAGEN Pty, Ltd., Hilden, Germany) *as per* the manufacturer's instruction. The bacterial 16S rRNA gene and fungal ITS region were quantified on a CFX96 Touch™ PCR Detection System (Bio-Rad, Hercules, USA). Primers set 515FmodF (GTGYCAGCMGCCGCGGTAA) and 806RmodR (GGACTACNVGGGTWTCTAAT) were used for the amplicon of the bacterial 16S rRNA gene (Walters *et al*., 2016). Primer set ITS1F (TCCGTAGG TGAACCTGCGG) and ITS2R (TCCGTAGGTGAACCT GCGG) was used for the amplicon of the fungal ITS region (White *et al*., 1990). The bacterial and fungal quantification was conducted in a 20 μl reaction system which contained 10 μl Sensimix SYBR NO-ROX reagent (Bioline, London, UK), 0.8 μl each primer (10 μM), and 2 μl DNA template. Amplicon conditions for the 16S rRNA gene and ITS region were as follows: an initial enzyme activation at 95°C for 10 min, followed 40 cycles of 95°C for 20 s, 53°C for 30 s and 72°C for 45 s and a final 72°C for 10 min.

The abundances of ARGs were measured using HT-qPCR on the Wafergen SmartChip Real-time PCR system (Wafergen, Inc., CA, USA) as previously described (Hu *et al*., 2016). The HT-qPCR array contained 285 primers targeting ARGs conferring resistance to all major classes of antibiotics (Table S1). Amplification of ARGs was conducted in a 100 nl reaction system. The amplicon condition was as follows: an initial enzyme activation at 95°C for 10 min, followed by 40 cycles of 95°C for 30 s and 60°C for 30 s. The melting curve was generated by the Wafergen SmartChip qPCR software (V2.7.0) automatically. Only data with a single melting peak and an amplification efficiency between 1.8 to 2.2 were retained. A cycle threshold (C_T) of 31 was used as the detection limit. The relative copy numbers of ARGs were calculated according to the following equation: Relative gene copy number $= 10^{(31\text{-}Ct)/(10/3)}$ (Stalder *et al*., 2014).

Characterization of abiotic determinants of ARGs

Climatic attributes including MAT and MAP of each sampling site were obtained from the WolrdClim database version 2 (https://www.worldclim.org/) based on the spatial geographical coordinates (Fick and Hijmans, 2017). The obtained climatic data were processed with the 'sp' and 'raster' packages in R (V 3.6.2) (R Core

© 2021 Society for Applied Microbiology and John Wiley & Sons Ltd., *Environmental Microbiology*

Team, 2020; Pebesma and Bivand, 2005, Hijmans *et al*., 2012) and are shown in Table S2. Soil physicochemical properties including soil pH, DOC and DON were characterized using standard methods (Rayment and Lyons, 2011). Briefly, soil pH was measured in a 1:2.5 mass: volume of soil and water suspension using a pH meter (Thermo Scientific Inc. Waltham MA, USA). DOC and DON were extracted with MilliQ water and measured with a TOC analyser (Shimadzu, Kyoto, Japan). Detailed information about the physicochemical properties of each termite mound and bulk soil samples is provided in Table S3.

Statistical analyses

All statistical analyses were performed in the R platform (V 3.6.2) (R Core Team, 2020). Shannon diversity index of the detected ARGs in the termite mound and bulk soil samples was calculated with the 'vegan' package (Oksanen *et al*., 2013). The differences in soil microbial properties and physicochemical properties, as well as ARG abundance and diversity were determined using the Wilcoxon rank-sum test with the 'stat' package (Field *et al*., 2012). The overall profiles of resistome in the termite mound and bulk soil samples were determined using a Bray–Curtis dissimilarity matrix and illustrated in a principal coordinate analysis (PCoA) plot with the 'ggplot2' package (Wickham, 2016). The significance in the difference of termite mound and bulk soil resistomes was determined with the Adonis test with the 'vegan' package (Oksanen *et al*., 2013). The shared and unique ARGs in termite mounds and bulk soils were visualized using the bipartite network constructed with the Gephi software (V 0.9.2). Spearman's rank correlation coefficients between the maim factors and ARG abundances were calculated and visualized with the 'corrplot' package (Wei *et al*., 2017). The relationships between the ARG abundances and selected environmental factors were further explored with the first order and second-order polynomial regression models. The goodness of fits of the models was estimated based on the corrected Akaike information criterion (AICc) (Burnham *et al*., 2011) and the better fit models were selected and presented.

Acknowledgements

We thank the Melbourne Trace Analysis for Chemical, Earth, and Environmental Sciences (TrACEES) Platform – Soil Node for the help with soil physicochemical characterization. We thank Qing Xie, School of Agriculture and Food, Faculty of Veterinary and Agricultural Sciences, The University of Melbourne, for the assistance with sample processing. This research was funded by the Australian Research Council (DP17103628; DP210100332; DE210100271).

References

Allen, H.K., Donato, J., Wang, H.H., Cloud-Hansen, K.A., Davies, J., and Handelsman, J. (2010) Call of the wild: antibiotic resistance genes in natural environments. *Nat Rev Microbiol* **8**: 251–259.

Ashton, L.A., Griffiths, H.M., Parr, C.L., Evans, T.A., D'Idham, R.K., Hasan, F., *et al*. (2019) Termites mitigate the effects of drought in tropical rainforest. *Science* **363**: 174–177.

Bahram, M., Hildebrand, F., Forslund, S.K., Anderson, J.L., Soudzilovskaia, N.A., Bodegom, P.M., *et al*. (2018) Structure and function of the global topsoil microbiome. *Nature* **560**: 233–237.

Bonachela, J.A., Pringle, R.M., Sheffer, E., Coverdale, T.C., Guyton, J.A., Caylor, K.K., *et al*. (2015) Termite mounds can increase the robustness of dryland ecosystems to climatic change. *Science* **347**: 5.

Burnham, K.P., Anderson, D.R., and Huyvaert, K.P. (2011) AIC model selection and multimodel inference in behavioral ecology: some background, observations, and comparisons. *Behav Ecol Sociobiol* **65**: 23–35.

Chen, B., Yang, Y., Liang, X., Yu, K., Zhang, T., and Li, X. (2013) Metagenomic profiles of antibiotic resistance genes (ARGs) between human impacted estuary and deep ocean sediments. *Environ Sci Technol* **47**: 12753–12760.

Chen, B., Yuan, K., Chen, X., Yang, Y., Zhang, T., Wang, Y., *et al*. (2016) Metagenomic analysis revealing antibiotic resistance genes (ARGs) and their genetic compartments in the Tibetan environment. *Environ Sci Technol* **50**: 6670–6679.

Chen, Q.L., Hu, H.W., Yan, Z.Z., Li, C.Y., Nguyen, B.A.T., Sun, A.Q., *et al*. (2021b) Deterministic selection dominates microbial community assembly in termite mounds. *Soil Biol Biochem* **152**: 108073.

Chen, Q.L., HU, H.W., Yan, Z.Z., Li, C.Y., Nguyen, B.T.A., Sun, A.Q., *et al*. (2021a) Termite mounds reduce soil microbial diversity by filtering rare microbial taxa. *Environ Microbiol* **23**: 2659–2668.

Chiri, E., Greening, C., Lappan, R., Waite, D.W., Jirapanjawat, T., Dong, X., *et al*. (2020) Termite mounds contain soil-derived methanotroph communities kinetically adapted to elevated methane concentrations. *ISME J* **14**: 2715–2731.

D'Costa, V.M., King, C.E., Kalan, L., Morar, M., Sung, W.W., Schwarz, C., *et al*. (2011) Antibiotic resistance is ancient. *Nature* **477**: 457–461.

Fick, S.E., and Hijmans, R.J. (2017) WorldClim 2: new 1-km spatial resolution climate surfaces for global land areas. *Int J Climatol* **37**: 4302–4315.

Field, A., Miles, J., and Field, Z. (2012) *Discovering-Statistics-Using-R*. California, USA: Sage Publications.

Hammarlund, S.P., and Harcombe, W.R. (2019) Refining the stress gradient hypothesis in a microbial community. *Proc Natl Acad Sci U S A* **116**: 15760–15762.

Hernando-Amado, S., Coque, T.M., Baquero, F., and Martinez, J.L. (2019) Defining and combating antibiotic resistance from One Health and Global Health perspectives. *Nat Microbiol* **4**: 1432–1442.

Hijmans, R.J., Van Etten, J., Cheng, J., Matttiuzzi, M., Sumner, M., Greenberg, J.A., *et al*. (2015) raster:

© 2021 Society for Applied Microbiology and John Wiley & Sons Ltd., *Environmental Microbiology*

geographic data analysis and modeling. *R package*, p. 734. http://CRAN.R-project.org/package=raster.

Hu, H.W., Wang, J.T., Li, J., Li, J.J., Ma, Y.B., Chen, D., & He, J.Z. (2016). Field-based evidence for copper contamination induced changes of antibiotic resistance in agricultural soils. *Environ. Microbiol.*, **18**(11), 3896–3909.

Hu, H.W., Wang, J.T., Singh, B.K., Liu, Y.R., Chen, Y.L., Zhang, Y.J., and He, J.Z. (2018) Diversity of herbaceous plants and bacterial communities regulates soil resistome across forest biomes. *Environ Microbiol* **20**: 2186–3220.

Jouquet, P., Traoré, S., Choosai, C., Hartmann, C., and Bignell, D. (2011) Influence of termites on ecosystem functioning. Ecosystem services provided by termites. *Eur J Soil Biol* **47**: 215–222.

Li, B., Chen, Z., Zhang, F., Liu, Y., and Yan, T. (2020) Abundance, diversity and mobility potential of antibiotic resistance genes in pristine Tibetan plateau soil as revealed by soil metagenomics. *FEMS Microbiol Ecol* **96**:fiaa172.

Martínez, J.L. (2008) Antibiotics and antibiotic resistance genes in natural environments. *Science* **321**: 365–367.

Martinez, J.L., Sanchez, M.B., Martinez-Solano, L., Hernandez, A., Garmendia, L., Fajardo, A., and Alvarez-Ortega, C. (2009) Functional role of bacterial multidrug efflux pumps in microbial natural ecosystems. *FEMS Microbiol Rev* **33**: 430–449.

Marynowska, M., Goux, X., Sillam-Dusses, D., Rouland-Lefevre, C., Halder, R., Wilmes, P., *et al*. (2020) Compositional and functional characterisation of biomass-degrading microbial communities in guts of plant fibre- and soil-feeding higher termites. *Microbiome* **8**: 1–18.

Nauer, P.A., Hutley, L.B., and Arndt, S.K. (2018) Termite mounds mitigate half of termite methane emissions. *Proc Natl Acad Sci U S A* **115**: 13306–13311.

Nishimura, Y., Otagiri, M., Yuki, M., Shimizu, M., Inoue, J.I., Moriya, S., and Ohkuma, M. (2020) Division of functional roles for termite gut protists revealed by single-cell transcriptomes. *ISME J* **14**: 2449–2460.

Obermeier, M.M., Wicaksono, W.A., Taffner, J., Bergna, A., Poehlein, A., Cernava, T., *et al*. (2020) Plant resistome profiling in evolutionary old bog vegetation provides new clues to understand emergence of multi-resistance. *ISME J* **11**: 1–17.

Oksanen, J., Blanchet, F.G., Kindt, R., Legendre, P., Minchin, P. R., O'Hara, R., *et al*. (2013) *R package version2.4-4*, pp. 1–295. http://CRAN.R-project.org/package=vegan.

Pebesma, E., and Bivand, R. (2005) Classes and methods for spatial data in R. *R-news* **5**: 9–13.

Piccardi, P., Vessman, B., and Mitri, S. (2019) Toxicity drives facilitation between 4 bacterial species. *Proc Natl Acad Sci U S A* **116**: 15979–15984.

Piddock, L.J. (2006) Multidrug-resistance efflux pumps? not just for resistance. *Nat Rev Microbiol* **4**: 629–636.

Pruden, A., Pei, R., Storteboom, H., and Carlson, K.H. (2006) Antibiotic resistance genes as emerging contaminants: studies in northern Colorado. *Environ Sci Technol* **40**: 7445–7450.

R Core Team. (2020) *R: A language and environment for statistical computing*. Vienna, Austria: R Foundation for Statistical Computing. http://www.R-project.org/.

Rayment, G.E., and Lyons, D.J. (2011) *Soil Chemical Methods: Australasia*. Clayton, Australia: CSIRO Publishing.

Rousk, J., Baath, E., Brookes, P.C., Lauber, C.L., Lozupone, C., Caporaso, J.G., *et al*. (2010) Soil bacterial and fungal communities across a pH gradient in an arable soil. *ISME J* **4**: 1340–1351.

Stalder, T., Barraud, O., Jove, T., Casellas, M., Gaschet, M., Dagot, C., and Ploy, M.C. (2014) Quantitative and qualitative impact of hospital effluent on dissemination of the integron pool. *ISME J* **8**: 768–777.

Sun, S., Lu, C., Liu, J., Williams, M.A., Yang, Z., Gao, Y., and Hu, X. (2020) Antibiotic resistance gene abundance and bacterial community structure in soils altered by ammonium and nitrate concentrations. *Soil Biol Biochem* **149**: 407965.

Surette, M.D., and Wright, G.D. (2017) Lessons from environmental antibiotic resistome. *Annu Rev Microbiol* **71**: 309–329.

Walters, W., Hyde, E.R., Berg-Lyons, D., Ackermann, G., Humphrey, G., Parada, A., *et al*. (2016) Improved bacterial 16S rRNA gene (V4 and V4-5) and fungal internal transcribed spacer marker gene primers for microbial community surveys. *Msystems* **1**: e00009–e00015.

Wei, T., Simko, V., Levy, M., Xie, Y., Jin, Y., and Zemla, J. (2017) Package 'corrplot'. *Statistician* **56**: 316–324.

White, T.J., Bruns, T., Lee, S., and Taylor, J. (1990) Amplification and direct sequencing of fungal ribosomal RNA genes for phylogenetics. In *PCR Protocols: A Guide to Methods and Applications*, Vol. **18**, pp. 315–322. Massachusetts, USA: Academic Press Inc.

Wickham, H. (2016) *ggplot2: elegant graphics for data analysis*: New York, USA: Springer-Verlag. http://ggplot2.tidyverse.org.

World Health Organization (WHO). (2019) *New Report Calls for Urgent Action to Avert Antimicrobial Resistance Crisis*. Geneva, Switzerland: World Health Organization. https://www.who.int/news/item/29-04-2019-new-report-calls-for-urgent-action-to-avert-antimicrobial-resistance-crisis.

Wright, G.D. (2007) The antibiotic resistome: the nexus of chemical and genetic diversity. *Nat Rev Microbiol* **5**: 175–186.

Xiao, K.Q., Li, B., Ma, L., Bao, P., Zhou, X., Zhang, T., and Zhu, Y.G. (2016) Metagenomic profiles of antibiotic resistance genes in paddy soils from South China. *FEMS Microbiol Ecol* **92**: fiw023.

Yan, Z.Z., Chen, Q.L., Zhang, Y.J., He, J.Z., and Hu, H.W. (2019) Antibiotic resistance in urban green spaces mirrors the pattern of industrial distribution. *Environ Int* **132**: 105106.

Zhang, Y.J., Hu, H.W., Yan, H., Wang, J.T., Lam, S.K., Chen, Q.L., *et al*. (2019) Salinity as a predominant factor modulating the distribution patterns of antibiotic resistance genes in ocean and river beach soils. *Sci Total Environ* **668**: 193–203.

Supporting Information

Additional Supporting Information may be found in the online version of this article at the publisher's web-site:

Fig. S1. Locations of the sampling sites and photos of termite mounds.

Fig. S2. Bacterial abundances in each termite mound and bulk soil samples.

© 2021 Society for Applied Microbiology and John Wiley & Sons Ltd., *Environmental Microbiology*

Fig. S3. Fungal abundances in each termite mound and bulk soil samples.

Fig. S4. Absolute abundances of ARGs in each termite mound and bulk soil samples.

Fig. S5. Relative abundances of ARGs in each termite mound and bulk soil samples.

Table S1. List of primers for the targeted antibiotic resistance genes in this study and their classification by target drug and mechanism of resistance.

Table S2. Climatic factors used in this study.

Table S3. Physiochemical properties of termite mounds and bulk soil samples.

© 2021 Society for Applied Microbiology and John Wiley & Sons Ltd., *Environmental Microbiology*

Supplementary material for Termite Mound Formation Reduces Soil Antibiotic Resistance Gene Abundance and Diversity

Zhen-Zhen Yan[1], Qing-Lin Chen[1]*, Chao-Yu Li[1], Bao-Anh Thi Nguyen[1], Yong-Guan Zhu[2], Ji-Zheng He[1], Hang-Wei Hu[1]

1 School of Agriculture and Food, Faculty of Veterinary and Agricultural Sciences, The University of Melbourne, VIC 3010, Australia.

2 Key Laboratory of Urban Environment and Health, Institute of Urban Environment, Chinese Academy of Sciences, 1799 Jimei Road, Xiamen, 361021, China.

* For correspondence:

Qing-Lin Chen, Email: qinglin.chen@unimelb.edu.au

Contents

Fig. S1. Locations of the sampling sites and photos of termite mounds.

Fig. S2. Bacterial abundances in each termite mound and bulk soil samples.

Fig. S3. Fungal abundances in each termite mound and bulk soil samples.

Fig. S4. Absolute abundances of ARGs in each termite mound and bulk soil samples.

Fig. S5. Relative abundances of ARGs in each termite mound and bulk soil samples.

Table S1 List of primers for the targeted antibiotic resistance genes in this study and their classification by target drug and mechanism of resistance.

Table S2 Climatic factors used in this study.

Table S3 Physiochemical properties of termite mounds and bulk soil samples.

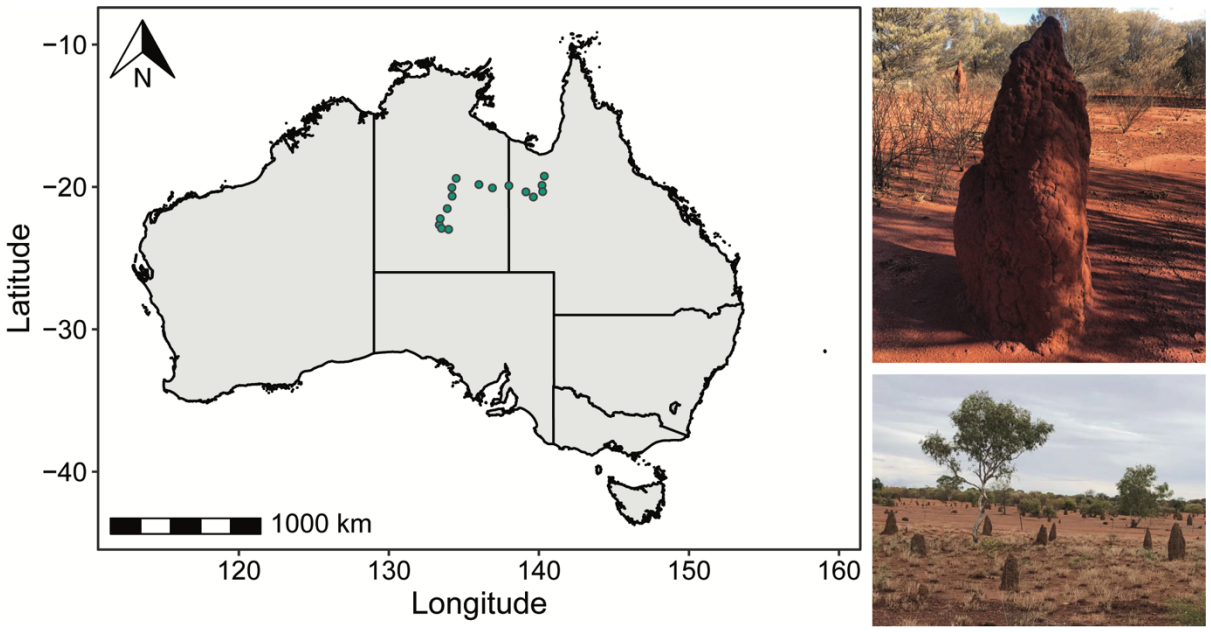

Fig. S1. Locations of the sampling sites and photos of termite mounds.

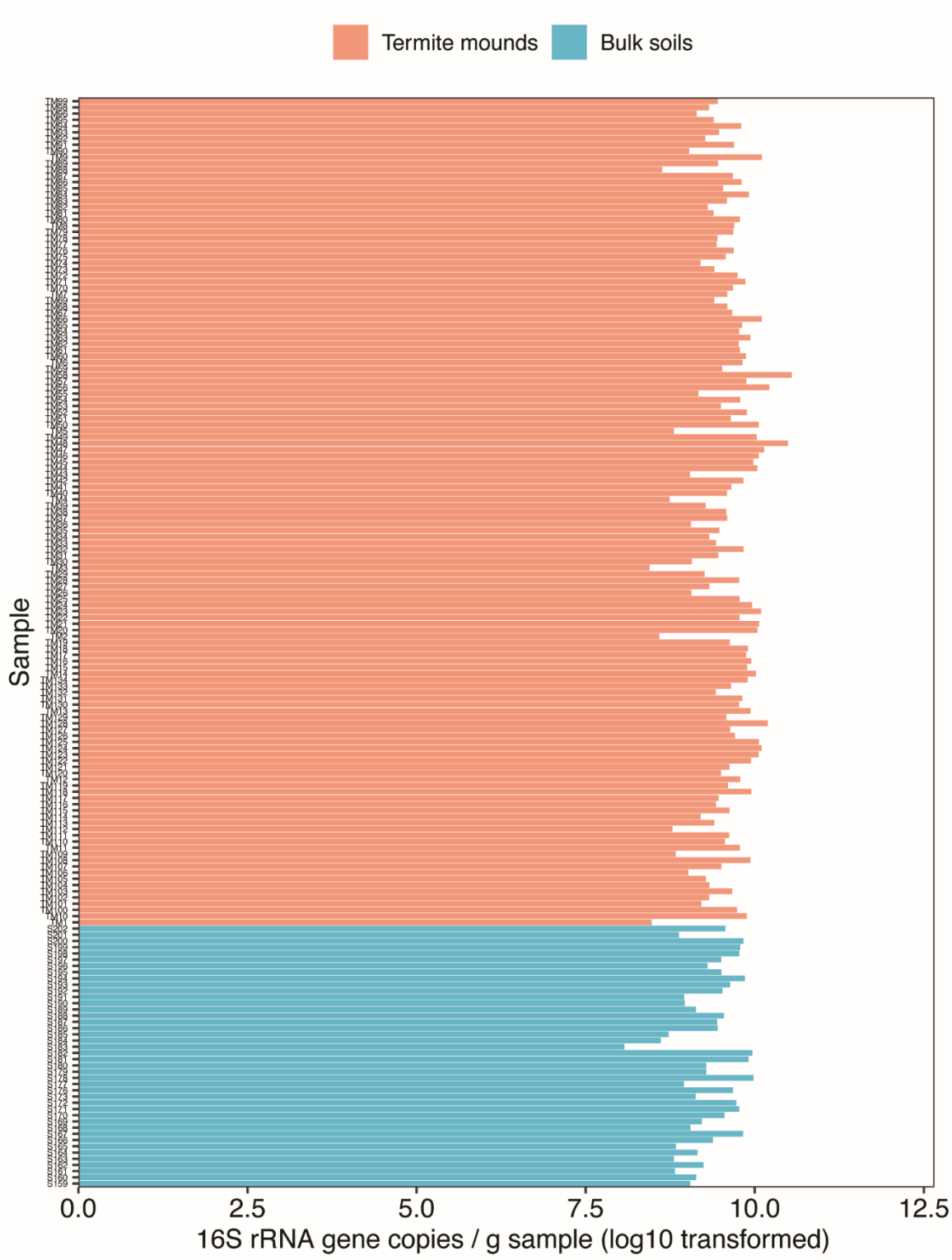

Fig. S2. Bacterial abundances in each termite mound and bulk soil samples.

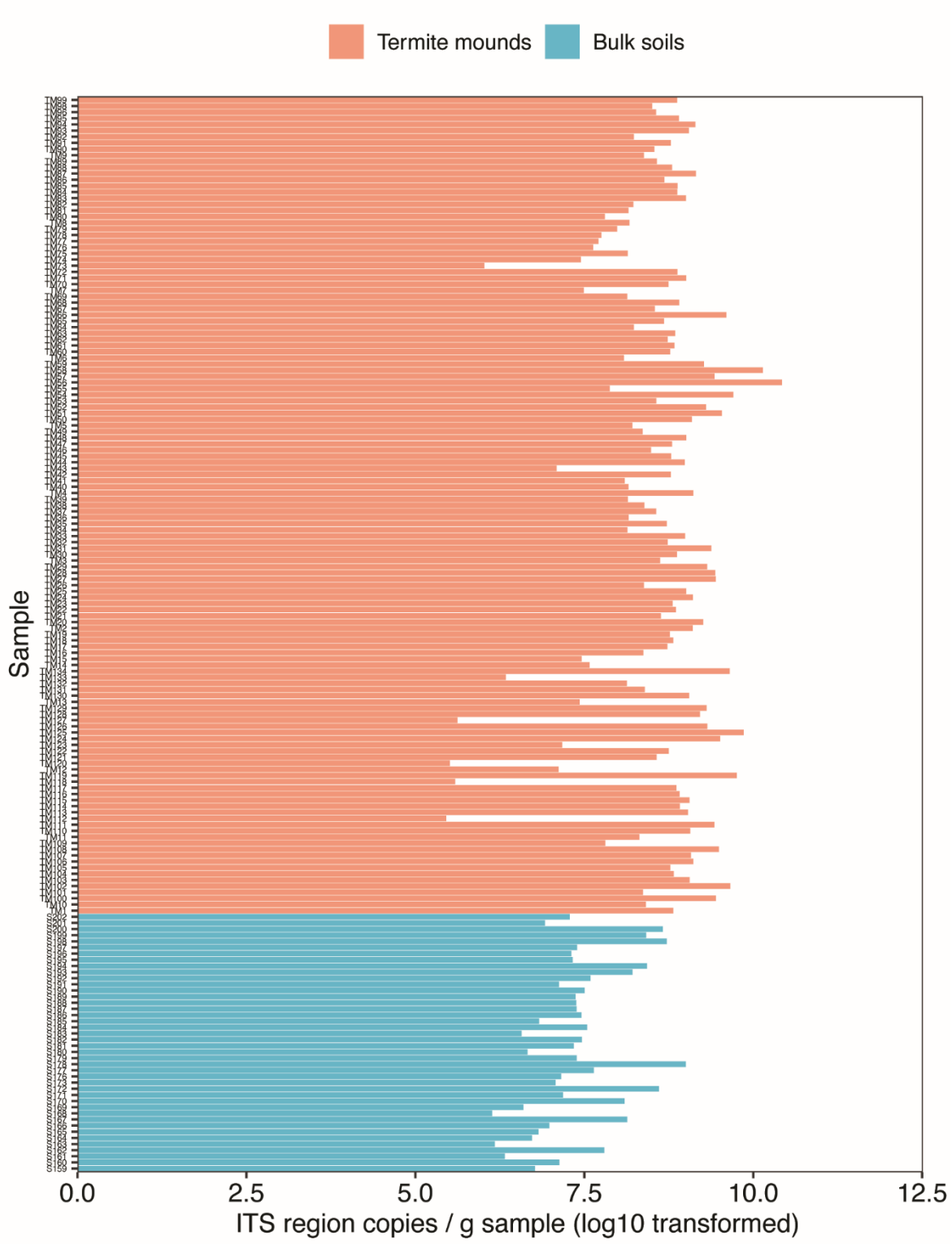

Fig. S3. Fungal abundances in each termite mound and bulk soil samples.

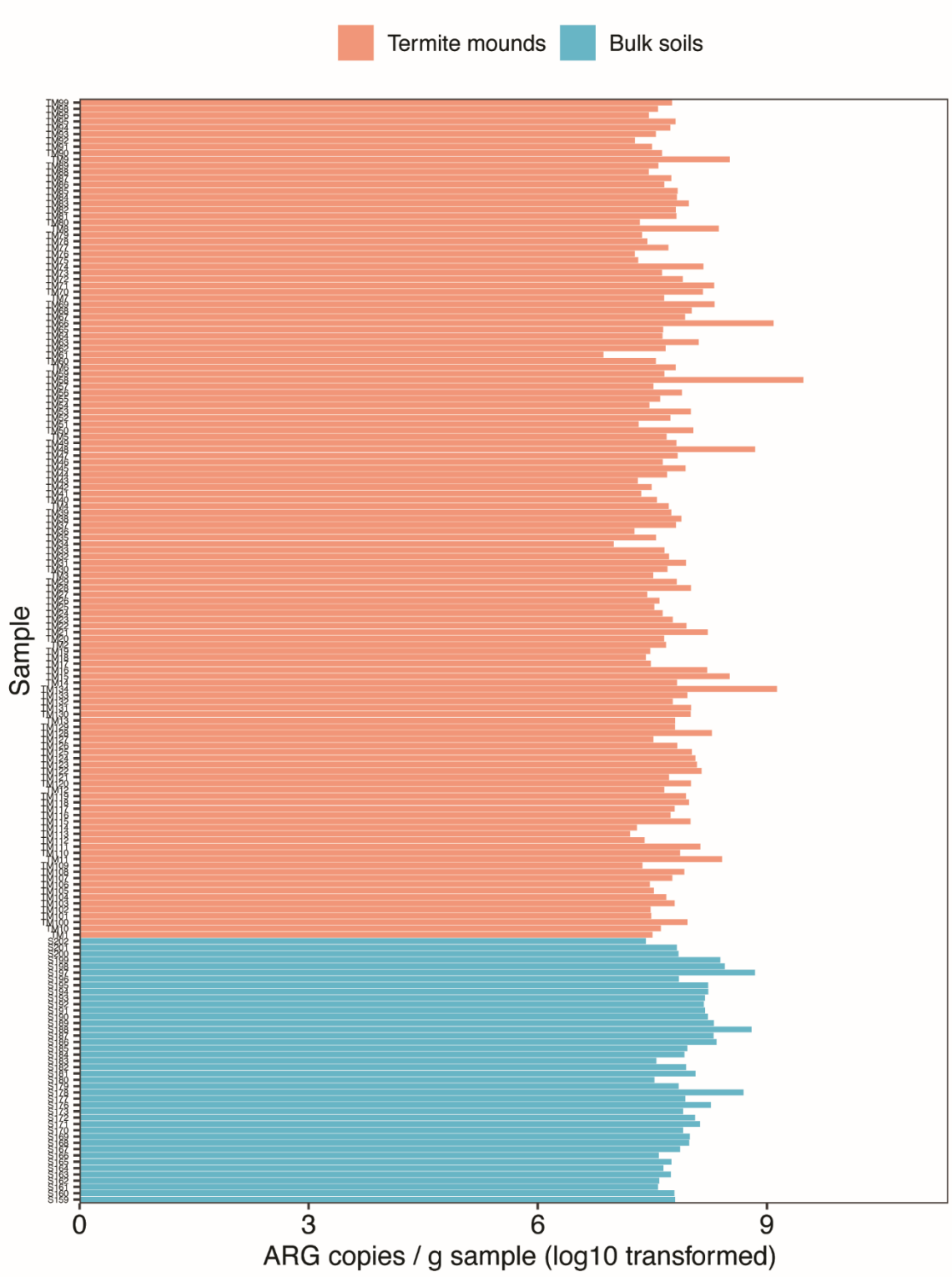

Fig. S4. Absolute abundances of ARGs in each termite mound and bulk soil samples.

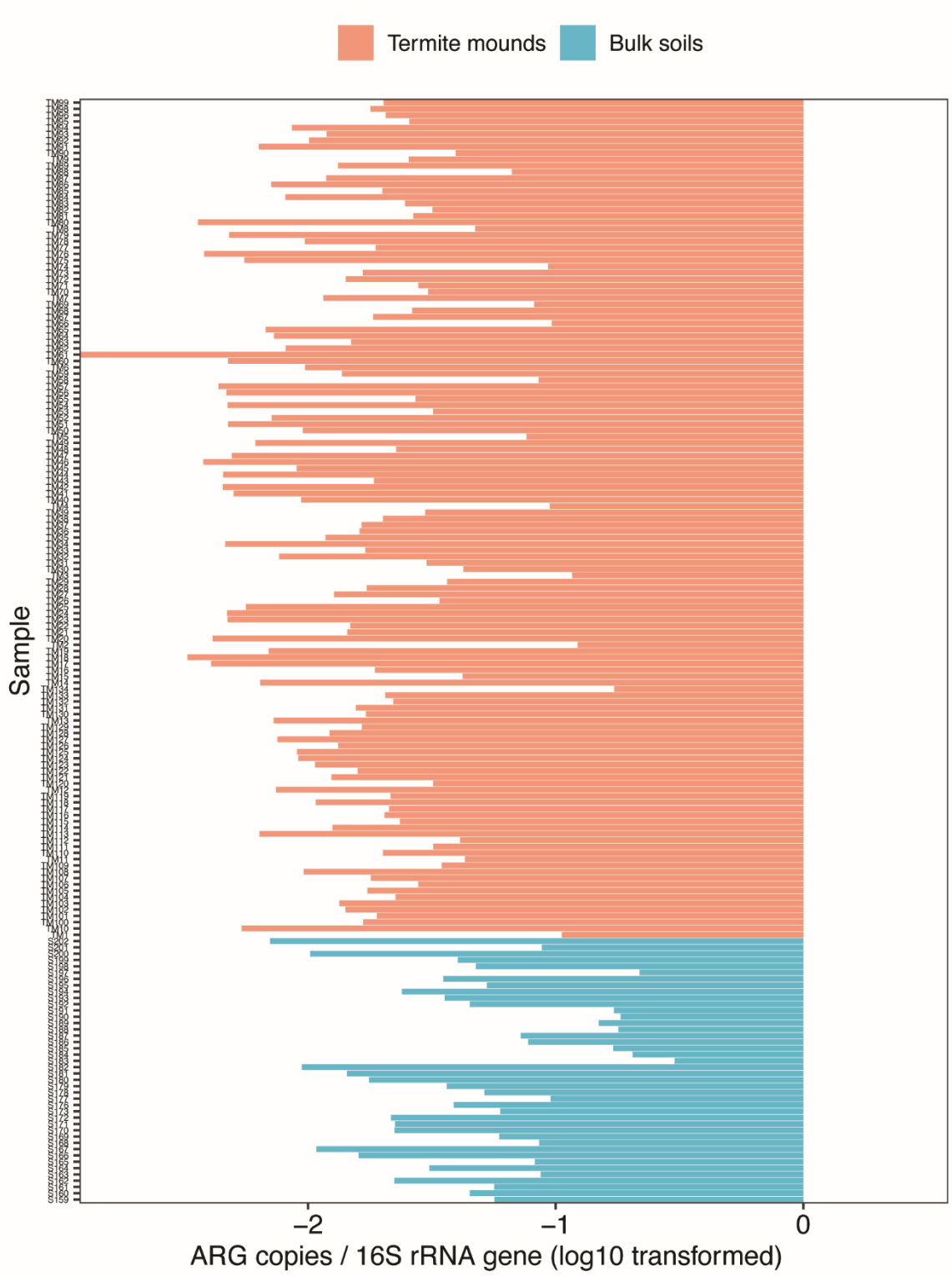

Fig. S5. Relative abundances of ARGs in each termite mound and bulk soil samples.

Table S1 List of primers for the targeted antibiotic resistance genes in this study and their classification by target drug and mechanism of resistance. FCA: fluoroquinolone, quinolone, florfenicol, chloramphenicol, and amphenicol resistance genes. MLSB: Macrolide-Lincosamide-Streptogramin B resistance. IS: Insertion sequence.

Gene Name	Forward Primer	Reverse Primer	Gene Classification	Resistance Mechanism
16S rRNA	GGGTTGCGCTCGTTGC	ATGGYTGTCGTCAGCTCGTG	16S rRNA	NA
catB3	GCACTCGATGCCTTCCAAAA	AGAGCCGATCCAAACGTCAT	FCA	deactivate
catB8	CACTCGACGCCTTCCAAAG	CCGAGCCTATCCAGACATCATT	FCA	deactivate
cfr	GCAAAATTCAGAGCAAGTTACGAA	AAAATGACTCCCAACCTGCTTTAT	FCA	deactivate
floR	ATTGTCTTCACGGTGTCCGTTA	CCGCGATGTCGTCGAACT	FCA	efflux
cmlA1-01	TAGGAAGCATCGGAACGTTGAT	CAGACCGAGCACGACTGTTG	FCA	efflux
cmlA1-02	AGGAAGCATCGGAACGTTGA	ACAGACCGAGCACGACTGTTG	FCA	efflux
cmx(A)	GCGATCGCCATCCTCTGT	TCGACACGGAGCCTTGGT	FCA	efflux
catA1	GGGTGAGTTTCACCAGTTTTGATT	CACCTTGTCGCCTTGCGTATA	FCA	deactivate
qnrA	AGGATTTCTCACGCCAGGATT	CCGCTTTCAATGAAACTGCAA	FCA	unknown
aac	CCCTGCGTTGTGGCTATGT	TTGGCCACGCCAATCC	Aminoglycoside	deactivate
aacC1	GGTCGTGAGTTCGGAGACGTA	GCAAGTTCCCGAGGTAATCG	Aminoglycoside	deactivate
aacC2	ACGGCATTCTCGATTGCTTT	CCGAGCTTCACGTAAGCATTT	Aminoglycoside	deactivate
aacC4	CGGCGTGGGACACGAT	AGGGAACCTTTGCCATCAACT	Aminoglycoside	deactivate
aac(6')I1	GACCGGATTAAGGCCGATG	CTTGCCTTGATATTCAGTTTTTATAACCA	Aminoglycoside	deactivate
aacA/aphD	AGAGCCTTGGGAAGATGAAGTTT	TTGATCCATACCATAGACTATCTCATCA	Aminoglycoside	deactivate
aac(6')-Iy	GCTTTGCGGATGCCTCAAT	GGAGAACAAAAATACCTTCAAGGAAA	Aminoglycoside	deactivate
aac(6')-II	CGACCCGACTCCGAACAA	GCACGAATCCTGCCTTCTCA	Aminoglycoside	deactivate
aacC	CGTCACTTATTCGATGCCCTTAC	GTCGGGCGCGGCATA	Aminoglycoside	deactivate
aac(6')-Ib-01	GTTTGAGAGGCAAGGTACCGTAA	GAATGCCTGGCGTGTTTGA	Aminoglycoside	deactivate
aac(6')-Ib-02	CGTCGCCGAGCAACTTG	CGGTACCTTGCCTCTCAAACC	Aminoglycoside	deactivate
aadA5-01	ATCACGATCTTGCGATTTTGCT	CTGCGGATGGGCCTAGAAG	Aminoglycoside	deactivate
aadA5-02	GTTCTTGCTCTTGCTCGCATT	GATGCTCGGCAGGCAAAC	Aminoglycoside	deactivate

aac(6')-Ib-03	AGAAGCACGCCCGACACTT	GCTCTCCATTCAGCATTGCA	Aminoglycoside	deactivate
aadA1	AGCTAAGCGCGAACTGCAAT	TGGCTCGAAGATACCTGCAA	Aminoglycoside	deactivate
aadA2-01	ACGGCTCCGCAGTGGAT	GGCCACAGTAACCAACAAATCA	Aminoglycoside	deactivate
aadA-01	GTTGTGCACGACGACATCATT	GGCTCGAAGATACCTGCAAGAA	Aminoglycoside	deactivate
aadA2-02	CTTGTCGTGCATGACGACATC	TCGAAGATACCCGCAAGAATG	Aminoglycoside	deactivate
aadD	CCGACAACATTTCTACCATCCTT	ACCGAAGCGCTCGTCGTATA	Aminoglycoside	deactivate
aadA2-03	CAATGACATTCTTGCGGGTATC	GACCTACCAAGGCAACGCTATG	Aminoglycoside	deactivate
aadA9-01	CGCGGCAAGCCTATCTTG	CAAATCAGCGACCGCAGACT	Aminoglycoside	deactivate
aadA-02	CGAGATTCTCCGCGCTGTA	GCTGCCATTCTCCAAATTGC	Aminoglycoside	deactivate
aadA9-02	GGATGCACGCTTGGATGAA	CCTCTAGCGGCCGGAGTATT	Aminoglycoside	deactivate
aadE	TACCTTATTGCCCTTGGAAGAGTTA	GGAACTATGTCCCTTTTAATTCTACAATCT	Aminoglycoside	deactivate
spcN-01	AAAAGTTCGATGAAACACGCCTAT	TCCAGTGGTAGTCCCCGAATC	Aminoglycoside	deactivate
spcN-02	CAGAATCTTCCTGAAAAGTTTGATGAA	CGCAGACACGCCGAATC	Aminoglycoside	deactivate
aadA-1-01	AAAAGCCCGAAGAGGAACTTG	CATCTTTCACAAAGATGTTGCTGTCT	Aminoglycoside	deactivate
aph6ia	CCCATCCCATGTGTAAGGAAA	GCCACCGCTTCTGCTGTAC	Aminoglycoside	deactivate
aph(2')-Id-02	TGAGCAGTATCATAAGTTGAGTGAAAAG	GACAGAACAATCAATCTCTATGGAATG	Aminoglycoside	deactivate
aph(2')-Id-01	TAAGGATATACCGACAGTTTTGGAAA	TTTAATCCCTCTTCATACCAATCCATA	Aminoglycoside	deactivate
aph	TTTCAGCAAGTGGATCATGTTAAAAT	CCAAGCTGTTTCCACTGTTTTTC	Aminoglycoside	deactivate
aphA1	TGAACAAGTCTGGAAAGAAATGCA	CCTATTAATTTCCCCTCGTCAAAAA	Aminoglycoside	deactivate
aadA-1-02	CGGAATTGAAAAAACTGATCGAA	ATACCGGCTGTCCGTCATTT	Aminoglycoside	deactivate
str	AATGAGTTTTGGAGTGTCTCAACGTA	AATCAAAACCCCTATTAAAGCCAAT	Aminoglycoside	deactivate
strA	CCGGTGGCATTTGAGAAAAAG	GTGGCTCAACCTGCGAAAAG	Aminoglycoside	deactivate
strB	GCTCGGTCGTGAGAACAATCT	CAATTTCGGTCGCCTGGTAGT	Aminoglycoside	deactivate
ampC-01	TGGCGTATCGGGTCAATGT	CTCCACGGGCCAGTTGAG	Beta Lactamase	deactivate
ampC-02	GCAGCACGCCCCGTAA	TGTACCCATGATGCGCGTACT	Beta Lactamase	deactivate
ampC-04	TCCGGTGACGCGACAGA	CAGCACGCCGGTGAAAGT	Beta Lactamase	deactivate
ampC-05	CTGTTCGAGCTGGGTTCTATAAGTAAA	CAGTATCTGGTCACCGGATCGT	Beta Lactamase	deactivate
ampC-06	CCGCTCAAGCTGGACCATAC	CCATATCCTGCACGTTGGTTT	Beta Lactamase	deactivate
ampC-07	CCGCCCAGAGCAAGGACTA	GCTCGACTTCACGCCGTAAG	Beta Lactamase	deactivate
ampC-09	CAGCCGCTGATGAAAAAATATG	CAGCGAGCCCACTTCGA	Beta Lactamase	deactivate

ampC/blaDHA	TGGCCGCAGCAGAAAGA	CCGTTTTATGCACCCAGGAA	Beta Lactamase	deactivate
bla1	GCAAGTTGAAGCGAAAGAAAAGA	TACCAGTATCAATCGCATATACACCTAA	Beta Lactamase	deactivate
bla-ACC-1	CACACAGCTGATGGCTTATCTAAAA	AATAAACGCGATGGGTTCCA	Beta Lactamase	deactivate
blaCMY	CCGCGGCGAAATTAAGC	GCCACTGTTTGCCTGTCAGTT	Beta Lactamase	deactivate
blaCMY2-01	AAAGCCTCAT GGGTGCATAAA	ATAGCTTTTGTTTGCCAGCATCA	Beta Lactamase	deactivate
blaCMY2-02	GCGAGCAGCCTGAAGCA	CGGATGGGCTTGTCCTCTT	Beta Lactamase	deactivate
blaCTX-M-01	GGAGGCGTGACGGCTTTT	TTCAGTGCGATCCAGACGAA	Beta Lactamase	deactivate
blaCTX-M-02	GCCGCGGTGCTGAAGA	ATCGGATTATAGTTAACCAGGTCAGATTT	Beta Lactamase	deactivate
blaCTX-M-03	CGATACCACCACGCCGTTA	GCATTGCCCAACGTCAGATT	Beta Lactamase	deactivate
blaCTX-M-04	CTTGGCGTTGCGCTGAT	CGTTCATCGGCACGGTAGA	Beta Lactamase	deactivate
blaCTX-M-05	GCGATAACGTGGCGATGAAT	GTCGAGACGGAACGTTTCGT	Beta Lactamase	deactivate
blaCTX-M-06	CACAGTTGGTGACGTGGCTTAA	CTCCGCTGCCGGTTTTATC	Beta Lactamase	deactivate
blaGES	GCAATGTGCTCAACGTTCAAG	GTGCCTGAGTCAATTCTTTCAAAG	Beta Lactamase	deactivate
blaIMP-01	AACACGGTTTGGTGGTTCTTGTA	GCGCTCCACAAACCAATTG	Beta Lactamase	deactivate
blaIMP-02	AAGGCAGCATTTCCTCTCATTTT	GGATAGATCGAGAATTAAGCCACTCT	Beta Lactamase	deactivate
bla-L1	CACCGGGTTACCAGCTGAAG	GCGAAGCTGCGCTTGTAGTC	Beta Lactamase	deactivate
blaMOX/blaCMY	CTATGTCAATGTGCCGAAGCA	GGCTTGTCCTCTTTCGAATAGC	Beta Lactamase	deactivate
blaOCH	GGCGACTTGCGCCGTAT	TTTTCTGCTCGGCCATGAG	Beta Lactamase	deactivate
blaOKP	GCCGCCATCACCATGAG	GGTGACGTTGTCACCGATCTG	Beta Lactamase	deactivate
blaOXA1/blaOXA30	CGGATGGTTTGAAGGGTTTATTAT	TCTTGGCTTTTATGCTTGATGTTAA	Beta Lactamase	deactivate
blaOXA10-01	CGCAATTATCGGCCTAGAAACT	TTGGCTTTCCGTCCCATTT	Beta Lactamase	deactivate
blaOXA10-02	CGCAATTATCGGCCTAGAAACT	TTGGCTTTCCGTCCCATTT	Beta Lactamase	deactivate
blaOXY	CGTTCAGGCGGCAGGTT	GCCGCGATATAAGATTTGAGAATT	Beta Lactamase	deactivate
blaPAO	CGCCGTACAACCGGTGAT	GAAGTAATGCGGTTCTCCTTTCA	Beta Lactamase	deactivate
blaPER	TGCTGGTTGCTGTTTTTGTGA	CCTGCGCAATGATAGCTTCAT	Beta Lactamase	deactivate
blaPSE	TTGTGACCTATTCCCCTGTAATAGAA	TGCGAAGCACGCATCATC	Beta Lactamase	deactivate
blaROB	GCAAAGGCATGACGATTGC	CGCGCTGTTGTCGCTAAA	Beta Lactamase	deactivate
blaSFO	CCGCCGCCATCCAGTA	GGGCCGCCAAGATGCT	Beta Lactamase	deactivate
blaSHV-01	TCCCATGATGAGCACCTTTAAA	TTCGTCACCGGCATCCA	Beta Lactamase	deactivate
blaSHV-02	CTTTCCCATGATGAGCACCTTT	TCCTGCTGGCGATAGTGGAT	Beta Lactamase	deactivate

blaTEM	AGCATCTTACGGATGGCATGA	TCCTCCGATCGTTGTCAGAAGT	Beta Lactamase	deactivate
blaTLA	ACACTTTGCCATTGCTGTTTATGT	TGCAAATTTCGGCAATAATCTTT	Beta Lactamase	deactivate
blaVEB	CCCGATGCAAAGCGTTATG	GAAAGATTCCCTTTATCTATCTCAGACAA	Beta Lactamase	deactivate
blaVIM	GCACTTCTCGCGGAGATTG	CGACGGTGATGCGTACGTT	Beta Lactamase	deactivate
blaZ	GGAGATAAAGTAACAAATCCAGTTAGATATGA	TGCTTAATTTTCCATTTGCGATAAG	Beta Lactamase	deactivate
cepA	AGTTGCGCAGAACAGTCCTCTT	TCGTATCTTGCCCGTCGATAAT	Beta Lactamase	deactivate
cfiA	GCAGCGTTGCTGGACACA	GTTCGGGATAAACGTGGTGACT	Beta Lactamase	deactivate
cfxA	TCATTCCTCGTTCAAGTTTTCAGA	TGCAGCACCAAGAGGAGATGT	Beta Lactamase	deactivate
cphA-01	GCGAGCTGCACAAGCTGAT	CGGCCCAGTCGCTCTTC	Beta Lactamase	deactivate
cphA-02	GTGCTGATGGCGAGTTTCTG	GGTGTGGTAGTTGGTGTTGATCAC	Beta Lactamase	deactivate
fox5	GGTTTGCCGCTGCAGTTC	GCGGCCAGGTGACCAA	Beta Lactamase	deactivate
mecA	GGTTACGGACAAGGTGAAATACTGAT	TGTCTTTTAATAAGTGAGGTGCGTTAATA	Beta Lactamase	protection
NDM1	ATTAGCCGCTGCATTGAT	CATGTCGAGATAGGAAGTG	Beta Lactamase	deactivate
pbp	CCGGTGCCATTGGTTTAGA	AAAATAGCCGCCCCAAGATT	Beta Lactamase	protection
pbp2x	TTTCATAAGTATCTGGACATGGAAGAA	CCAAAGGAAACTTGCTTGAGATTAG	Beta Lactamase	protection
Pbp5	GGCGAACTTCTAATTAATCCTATCCA	CGCCGATGACATTCTTCTTATCTT	Beta Lactamase	protection
penA	AGACGGTAACGTATAACTTTTTGAAAGA	GCGTGTAGCCGGCAATG	Beta Lactamase	protection
carB	GGAGTGAGGCTGACCGTAGAAG	ATCGGCGAAACGCACAAA	MLSB	efflux
ereA	CCTGTGGTACGGAGAATTCATGT	ACCGCATTCGCTTTGCTT	MLSB	deactivate
ereB	GCTTTATTTCAGGAGGCGGAAT	TTTTAAATGCCACAGCACAGAATC	MLSB	deactivate
erm(34)	GCGCGTTGACGACGATTT	TGGTCATACTCGACGGCTAGAAC	MLSB	protection
erm(35)	TTGAAAACGATGTTGCATTAAGTCA	TCTATAATCACAACTAACCACTTGAACGT	MLSB	protection
erm(36)	GGCGGACCGACTTGCAT	TCTGCGTTGACGACGGTTAC	MLSB	protection
ermA	TTGAGAAGGGATTTGCGAAAAG	ATATCCATCTCCACCATTAATAGTAAACC	MLSB	protection
ermA/ermTR	ACATTTTACCAAGGAACTTGTGGAA	GTGGCATGACATAAACCTTCATCA	MLSB	protection
ermB	TAAAGGGCATTTAACGACGAAACT	TTTATACCTCTGTTTGTTAGGGAATTGAA	MLSB	protection
ermC	TTTGAAATCGGCTCAGGAAAA	ATGGTCTATTTCAATGGCAGTTACG	MLSB	protection
ermF	CAGCTTTGGTTGAACATTTACGAA	AAATTCCTAAAATCACAACCGACAA	MLSB	protection
ermJ/ermD	GGACTCGGCAATGGTCAGAA	CCCCGAAACGCAATATAATGTT	MLSB	protection
ermK-01	GTTTGATATTGGCATTGTCAGAGAAA	ACCATTGCCGAGTCCACTTT	MLSB	protection

ermK-02	GAGCCGCAAGCCCCTTT	GTGTTTCATTTGACGCGGAGTAA	MLSB	protection
ermT-01	GTTCACTAGCACTATTTTTAATGACAGAAGT	GAAGGGTGTCTTTTTAATACAATTAACGA	MLSB	protection
ermT-02	GTAAAATCCCTAGAGAATACTTTCATCCA	TGAGTGATATTTTTGAAGGGTGTCTT	MLSB	protection
ermX	GCTCAGTGGTCCCCATGGT	ATCCCCCCGTCAACGTTT	MLSB	protection
ermY	TTGTCTTTGAAAGTGAAGCAACAGT	TAACGCTAGAGAACGATTTGTATTGAG	MLSB	protection
lmrA-01	TCGACGTGACCGTAGTGAACA	CGTGACTACCCAGGTGAGTTGA	MLSB	efflux
lnuA-01	TGACGCTCAACACACTCAAAAA	TTCATGCTTAAGTTCCATACGTGAA	MLSB	deactivate
lnuB-01	TGAACATAATCCCCTCGTTTAAAGAT	TAATTGCCCTGTTTCATCGTAAATAA	MLSB	deactivate
lnuB-02	AAAGGAGAAGGTGACCAATACTCTGA	GGAGCTACGTCAAACAACCAGTT	MLSB	deactivate
lnuC	TGGTCAATATAACAGATGTAAACCAGATTT	CACCCCAGCCACCATCAA	MLSB	deactivate
matA/mel	TAGTAGGCAAGCTCGGTGTTGA	CCTGTGCTATTTTAAGCCTTGTTTCT	MLSB	efflux
mdtA	CCTAACGGGCGTGACTTCA	TTCACCTGTTTCAAGGGTCAAA	MLSB	efflux
mefA	CCGTAGCATTGGAACAGCTTTT	AAACGGAGTATAAGAGTGCTGCAA	MLSB	efflux
mphA-01	CTGACGCGCTCCGTGTT	GGTGGTGCATGGCGATCT	MLSB	deactivate
mphA-02	TGATGACCCTGCCATCGA	TTCGCGAGCCCCTCTTC	MLSB	deactivate
mphB	CGCAGCGCTTGATCTTGTAG	TTACTGCATCCATACGCTGCTT	MLSB	deactivate
mphC	CGTTTGAAGTACCGAATTGGAAA	GCTGCGGGTTTGCCTGTA	MLSB	deactivate
msrA-01	CTGCTAACACAAGTACGATTCCAAAT	TCAAGTAAAGTTGTCTTACCTACACCATT	MLSB	efflux
msrC-01	TCAGACCGGATCGGTTGTC	CCTATTTTTTGGAGTCTTCTCTCTAATGTT	MLSB	efflux
oleC	CCCGGAGTCGATGTTCGA	GCCGAAGACGTACACGAACAG	MLSB	efflux
pikR1	TCGACATGCGTGACGAGATT	CCGCGAATTAGGCCAGAA	MLSB	protection
pikR2	TCGTGGGCCAGGTGAAGA	TTCCCCTTGCCGGTGAA	MLSB	protection
vatB-01	GGAAAAAGCAACTCCATCTCTTGA	TCCTGGCATAACAGTAACATTCTGA	MLSB	deactivate
vatB-02	TTGGGAAAAAGCAACTCCATCT	CAATCCACACATCATTTCCAACA	MLSB	deactivate
vatC-01	CGGAAATTGGGAACGATGTT	GCAATAATAGCCCCGTTTCCTA	MLSB	deactivate
vatC-02	CGATGTTTGGATTGGACGAGAT	GCTGCAATAATAGCCCCGTTT	MLSB	deactivate
vatE-01	GGTGCCATTATCGGAGCAAAT	TTGGATTGCCACCGACAAT	MLSB	deactivate
vatE-02	GACCGTCCTACCAGGCGTAA	TTGGATTGCCACCGACAATT	MLSB	deactivate
vgaA-01	CGAGTATTGTGGAAAGCAGCTAGTT	CCCGTACCGTTAGAGCCGATA	MLSB	efflux
vgaA-02	GACGGGTATTGTGGAAAGCAA	TTTCCTGTACCATTAGATCCGATAATT	MLSB	efflux

vgb-01	AGGGAGGGTATCCATGCAGAT	ACCAAATGCGCCCGTTT	MLSB	deactivate
vgbB-01	CAGCCGGATTCTGGTCCTT	TACGATCTCCATTCAATTGGGTAAA	MLSB	efflux
vgbB-02	ATACGAGCTGCCTAATAAAGGATCTT	TGTGAACCACAGGGCATTATCA	MLSB	deactivate
sul2	TCATCTGCCAAACTCGTCGTTA	GTCAAAGAACGCCGCAATGT	Sulfonamide	protection
sul1	CAGCGCTATGCGCTCAAG	ATCCCGCTGCGCTGAGT	Sulfonamide	protection
sulA/folP-01	CAGGCTCGTAAATTGATAGCAGAAG	CTTTCCTTGCGAATCGCTTT	Sulfonamide	protection
sulA/folP-03	CACGGCTTCGGCTCATGT	TGCCATCCTGTGACTAGCTACGT	Sulfonamide	protection
dfrA1	GGAATGGCCCTGATATTCCA	AGTCTTGCGTCCAACCAACAG	Sulfonamide	deactivate
dfrA12	CCTCTACCGAACCGTCACACA	GCGACAGCGTTGAAACAACTAC	Sulfonamide	deactivate
folA	CGAGCAGTTCCTGCCAAAG	CCCAGTCATCCGGTTCATAATC	Sulfonamide	deactivate
tet(32)	CCATTACTTCGGACAACGGTAGA	CAATCTCTGTGAGGGCATTTAACA	Tetracycline	protection
tet(34)	CTTAGCGCAAACAGCAATCAGT	CGGTGATACAGCGCGTAAACT	Tetracycline	unknown
tet(35)	ACCCCATGACGTACCTGTAGAGA	CAACCCACACTGGCTACCAGTT	Tetracycline	unknown
tet(36)-01	AGAATACTCAGCAGAGGTCAGTTCCT	TGGTAGGTCGATAACCCGAAAAT	Tetracycline	protection
tet(36)-02	TGCAGGAAAGACCTCCATTACAG	CTTTGTCCACACTTCCACGTACTATG	Tetracycline	protection
tet(37)	GAGAACGTTGAAAAGGTGGTGAA	AACCAAGCCTGGATCAGTCTCA	Tetracycline	unknown
tetA-01	GCTGTTTGTTCTGCCGGAAA	GGTTAAGTTCCTTGAACGCAAACT	Tetracycline	efflux
tetA-02	CTCACCAGCCTGACCTCGAT	CACGTTGTTATAGAAGCCGCATAG	Tetracycline	efflux
tetB-01	AGTGCGCTTTGGATGCTGTA	AGCCCCAGTAGCTCCTGTGA	Tetracycline	efflux
tetB-02	GCCCAGTGCTGTTGTTGTCAT	TGAAAGCAAACGGCCTAAATACA	Tetracycline	efflux
tetC-01	CATATCGCAATACATGCGAAAAA	AAAGCCGCGGTAAATAGCAA	Tetracycline	efflux
tetC-02	ACTGGTAAGGTAAACGCCATTGTC	ATGCATAAACCAGCCATTGAGTAAG	Tetracycline	efflux
tetD-01	TGCCGCGTTTGATTACACA	CACCAGTGATCCCGGAGATAA	Tetracycline	efflux
tetD-02	TGTCATCGCGCTGGTGATT	CATCCGCTTCCGGGAGAT	Tetracycline	efflux
tetE	TTGGCGCTGTATGCAATGAT	CGACGACCTATGCGATCTGA	Tetracycline	efflux
tetG-01	TCAACCATTGCCGATTCGA	TGGCCCGGCAATCATG	Tetracycline	efflux
tetG-02	CATCAGCGCCGGTCTTATG	CCCCATGTAGCCGAACCA	Tetracycline	efflux
tetH	TTTGGGTCATCTTACCAGCATTAA	TTGCGCATTATCATCGACAGA	Tetracycline	efflux
tetJ	GGGTGCCGCATTAGATTACCT	TCGTCCAATGTAGAGCATCCATA	Tetracycline	efflux
tetK	CAGCAGTCATTGGAAAATTATCTGATTATA	CCTTGTACTAACCTACCAAAAATCAAAATA	Tetracycline	efflux

tetL-01	AGCCCGATTTATTCAAGGAATTG	CAAATGCTTTCCCCCTGTTCT	Tetracycline	efflux
tetL-02	ATGGTTGTAGTTGCGCGCTATAT	ATCGCTGGACCGACTCCTT	Tetracycline	efflux
tetM-01	CATCATAGACACGCCAGGACATAT	CGCCATCTTTTGCAGAAATCA	Tetracycline	protection
tetM-02	TAATATTGGAGTTTTAGCTCATGTTGATG	CCTCTCTGACGTTCTAAAAGCGTATTAT	Tetracycline	protection
tetO-01	ATGTGGATACTACAACGCATGAGATT	TGCCTCCACATGATATTTTTCCT	Tetracycline	protection
tetPA	AGTTGCAGATGTGTATAGTCGTAAACTATCTATT	TGCTACAAGTACGAAAACAAAACTAGAA	Tetracycline	efflux
tetPB-01	ACACCTGGACACGCTGATTTT	ACCGTCTAGAACGCGGAATG	Tetracycline	protection
tetPB-02	TGATACACCTGGACACGCTGAT	CGTCCAAAACGCGGAATG	Tetracycline	protection
tetPB-03	TGGGCGACAGTAGGCTTAGAA	TGACCCTACTGAAACATTAGAAATATACCT	Tetracycline	protection
tetPB-05	CTGAAGTGGAGCGATCATTCC	CCCTCAACGGCAGAAATAACTAA	Tetracycline	protection
tetQ	CGCCTCAGAAGTAAGTTCATACACTAAG	TCGTTCATGCGGATATTATCAGAAT	Tetracycline	protection
tetR-02	CGCGATAGACGCCTTCGA	TCCTGACAACGAGCCTCCTT	Tetracycline	efflux
tetR-03	CGCGATGGAGCAAAAGTACAT	AGTGAAAAACCTTGTTGGCATAAAA	Tetracycline	efflux
tetS	TTAAGGACAAACTTTCTGACGACATC	TGTCTCCCATTGTTCTGGTTCA	Tetracycline	protection
tetT	CCATATAGAGGTTCCACCAAATCC	TGACCCTATTGGTAGTGGTTCTATTG	Tetracycline	protection
tetU-01	GTGGCAAAGCAACGGATTG	TGCGGGCTTGCAAAACTATC	Tetracycline	unknown
tetV	GCGGGAACGACGATGTATATC	CCGCTATCTCACGACCATGAT	Tetracycline	efflux
tetW-01	ATGAACATTCCCACCGTTATCTTT	ATATCGGCGGAGAGCTTATCC	Tetracycline	protection
tetX	AAATTTGTTACCGACACGGAAGTT	CATAGCTGAAAAAATCCAGGACAGTT	Tetracycline	unknown
vanA	AAAAGGCTCTGAAAACGCAGTTAT	CGGCCGTTATCTTGTAAAAACAT	Vancomycin	protection
vanB-01	TTGTCGGCGAAGTGGATCA	AGCCTTTTTCCGGCTCGTT	Vancomycin	protection
vanC-01	ACAGGGATTGGCTATGAACCAT	TGACTGGCGATGATTTGACTATG	Vancomycin	protection
vanC-02	CCTGCCACAATCGATCGTT	CGGCTTCATTCGGCTTGATA	Vancomycin	protection
vanC-03	AAATCAATACTATGCCGGGCTTT	CCGACCGCTGCCATCA	Vancomycin	protection
vanC1	AGGCGATAGCGGGTATTGAA	CAATCGTCAATTGCTCATTTCC	Vancomycin	protection
vanC2/vanC3	TTTGACTGTCGGTGCTTGTGA	TCAATCGTTTCAGGCAATGG	Vancomycin	protection
vanG	ATTTGAATTGGCAGGTATACAGGTTA	TGATTTGTCTTTGTCCATACATAATGC	Vancomycin	protection
vanHB	GAGGTTTCCGAGGCGACAA	CTCTCGGCGGCAGTCGTAT	Vancomycin	protection
vanHD	GTGGCCGATTATACCGTCATG	CGCAGGTCATTCAGGCAAT	Vancomycin	protection
vanRA-01	CCCTTACTCCCACCGAGTTTT	TTCGTCGCCCCATATCTCAT	Vancomycin	protection

vanRA-02	CCACTCCGGCCTTGTCATT	GCTAACCACATTCCCCTTGTTTT	Vancomycin	protection
vanRB	GCCCTGTCGGATGACGAA	TTACATAGTCGTCTGCCTCTGCAT	Vancomycin	protection
vanRC	TGCGGGAAAAACTGAACGA	CCCCCCATACGGTTTTGATTA	Vancomycin	protection
vanRC4	AGTGCTTTGGCTTATCTCGAAAA	TCCGGCAGCATCACATCTAA	Vancomycin	protection
vanRD	TTATAATGGCAAGGATGCACTAAAGT	CGTCTACATCCGGAAGCATGA	Vancomycin	protection
vanSA	CGCGTCATGCTTTCAAAATTC	TCCGCAGAAAGCTCAATTTGTT	Vancomycin	protection
vanSB	GCGCGGCAAATGACAAC	TTTGCCATTTTATTCGCACTGT	Vancomycin	protection
vanSC-01	ATCAACTGCGGGAGAAAAGTCT	TCCGCTGTTCCGCTTCTT	Vancomycin	protection
vanSC-02	GCCATCAGCGAGTCTGATGA	CAGCTGGGATCGTTTTTCCTT	Vancomycin	protection
vanTC-01	CACACGCATTTTTTCCCATCTAG	CAGCCAACAGATCATCAAAACAA	Vancomycin	protection
vanTC-02	ACAGTTGCCGCTGGTGAAG	CGTGGCTGGTCGATCAAAA	Vancomycin	protection
vanTE	GTGGTGCCAAGGAAGTTGCT	CGTAGCCACCGCAAAAAAAT	Vancomycin	protection
vanTG	CGTGTAGCCGTTCCGTTCTT	CGGCATTACAGGTATATCTGGAAA	Vancomycin	protection
vanWB	CGGACAAAGATACCCCCTATAAAG	AAATAGTAAATTGCTCATCTGGCACAT	Vancomycin	protection
vanWG	ACATTTTCATTTTGGCAGCTTGTAC	CCGCCATAAGAGCCTACAATCT	Vancomycin	protection
vanXA	CGCTAAATATGCCACTTGGGATA	TCAAAAGCGATTCAGCCAACT	Vancomycin	protection
vanXB	AGGCACAAAATCGAAGATGCTT	GGGTATGGCTCATCAATCAACTT	Vancomycin	protection
vanXD	TAAACCGTGTTATGGGAACGAA	GCGATAGCCGTCCCATAAGA	Vancomycin	protection
vanYB	GGCTAAAGCGGAAGCAGAAA	GATATCCACAGCAAGACCAAGCT	Vancomycin	protection
vanYD-01	AAGGCGATACCCTGACTGTCA	ATTGCCGGACGGAAGCA	Vancomycin	protection
vanYD-02	CAAACGGAAGAGAGGTCACTTACA	CGGACGGTAATAGGGACTGTTC	Vancomycin	protection
acrA-01	CAACGATCGGACGGGTTTC	TGGCGATGCCACCGTACT	Multidrug	efflux
acrA-02	GGTCTATCACCCTACGCGCTATC	GCGCGCACGAACATACC	Multidrug	efflux
acrA-03	CAGACCCGCATCGCATATT	CGACAATTTCGCGCTCATG	Multidrug	efflux
acrA-04	TACTTTGCGCGCCATCTTC	CGTGCGCGAACGAACAT	Multidrug	efflux
acrB-01	AGTCGGTGTTCGCCGTTAACACC	CAAGGAAACGAACGCAATACC	Multidrug	efflux
acrR-01	GCGCTGGAGACACGACAAC	GCCTTGCTGCGAGAACAAA	Multidrug	efflux
acrR-02	GATGATACCCCCTGCTGTGAGA	ACCAAACAAGAAGCGCAAGAA	Multidrug	efflux
adeA	CAGTTCGAGCGCCTATTTCTG	CGCCCTGACCGACCAAT	Multidrug	efflux
acrA-05	CGTGCGCGAACGAACA	ACTTTGCGCGCCATCTTC	Multidrug	efflux
acrF	GCGGCCAGGCACAAAA	TACGCTCTTCCCACGGTTTC	Multidrug	efflux
ceoA	ATCAACACGGACCAGGACAA	GGAAAGTCCGCTCACGATG	Multidrug	efflux

	G	A		
cmeA	GCAGCAAAGAAGAAGCACCAA	AGCAGGGTAAGTAAAACTAAGTGGTAAATCT	Multidrug	efflux
cmr	CGGCATCGTCAGTGGAATT	CGGTTCCGAAAAAGATGGAA	Multidrug	efflux
emrD	CTCAGCAGTATGGTGGTAAGCATT	ACCAGGCGCCGAAGAAC	Multidrug	efflux
marR-01	GCGGCGTACTGGTGAAGCTA	TGCCCTGGTCGTTGATGA	Multidrug	efflux
mdetl1	ATACAGCAGTGGATATTGGTTTAATTGT	TGCATAAGGTGAATGTTCCATGA	Multidrug	efflux
mdtE/yhiU	CGTCGGCGCACTCGTT	TCCAGACGTTGTACGGTAACCA	Multidrug	efflux
mepA	ATCGGTCGCTCTTCGTTCAC	ATAAATAGGATCGAGCTGCTGGAT	Multidrug	efflux
mexA	AGGACAACGCTATGCAACGAA	CCGGAAAGGGCCGAAAT	Multidrug	efflux
mexD	TTGCCACTGGCTTTCATGAG	CACTGCGGAGAACTGTCTGTAGA	Multidrug	efflux
mexE	GGTCAGCACCGACAAGGTCTAC	AGCTCGACGTACTTGAGGAACAC	Multidrug	efflux
mexF	CCGCGAGAAGGCCAAGA	TTGAGTTCGGCGGTGATGA	Multidrug	efflux
mtrC-01	GGACGGGAAGATGGTCCAA	CGTAGCGTTCCGGTTCGAT	Multidrug	efflux
mtrC-02	CGGAGTCCATCGACCATTTG	ATCGTCGGCAAGGAGAATCA	Multidrug	efflux
mtrD-02	GGTCGGCACGCTCTTGTC	TGAAGAATTTGCGCACCACTAC	Multidrug	efflux
mtrD-03	CCGCCAAGCCGATATAGACA	GGCCGGGTTGCCAAA	Multidrug	efflux
oprD	ATGAAGTGGAGCGCCATTG	GGCCACGGCGAACTGA	Multidrug	efflux
oprJ	ACGAGAGTGGCGTCGACAA	AAGGCGATCTCGTTGAGGAA	Multidrug	efflux
pmrA	TTTGCAGGTTTTGTTCCTAATGC	GCAGAGCCTGATTTCTCCTTTG	Multidrug	efflux
putative multidrug	AATTTTGCCGATTATTGCTGAAA	GATTGTCATCATTCGTTTATCACCAA	Multidrug	efflux
qac	CAATAATAACCGAAATAATAGGGACAAGTT	AATAAGTGTTCCTAGTGTTGGCCATAG	Multidrug	efflux
qacA	TGGCAATAGGAGCTATGGTGTTT	AAGGTAACACTATTTTCGGTCCAAATC	Multidrug	efflux
qacA/qacB	TTTAGGCAGCCTCGCTTCA	CCGAATCCAAATAAAACCCAATAA	Multidrug	efflux
qacEdelta1-01	TCGCAACATCCGCATTAAAA	ATGGATTTCAGAACCAGAGAAAGAAA	Multidrug	efflux
qacEdelta1-02	CCCCTTCCGCCGTTGT	CGACCAGACTGCATAAGCAACA	Multidrug	efflux
qacH-01	GTGGCAGCTATCGCTTGGAT	CCAACGAACGCCCACAA	Multidrug	efflux
qacH-02	CATCGTGCTTGTGGCAGCTA	TGAACGCCCAGAAGTCTAGTTTT	Multidrug	efflux
rarD-02	TGACGCATCGCGTGATCT	AAATTTTCTGTGGCGTCTGAATC	Multidrug	efflux
sdeB	CACTACCGCTTCCGCACTTAA	TGAAAAAACGGGAAAAGTCCAT	Multidrug	efflux
tolC-01	GGCCGAGAACCTGATGCA	AGACTTACGCAATTCCGGGTTA	Multidrug	efflux
tolC-02	CAGGCAGAGAACCTGATGCA	CGCAATTCCGGGTTGCT	Multidrug	efflux
tolC-03	GCCAGGCAGAGAACCTGATG	CGCAATTCCGGGTTGCT	Multidrug	efflux
ttgA	ACGCCAATGCCAAACGATT	GTCACGGCGCAGCTTGA	Multidrug	efflux
ttgB	TCGCCCTGGATGTACACCTT	ACCATTGCCGACATCAACA	Multidrug	efflux

		AC		
yceE/mdtG-01	TGGCACAAAATATCTGGCAGTT	TTGTGTGGCGATAAGAGCATTAG	Multidrug	efflux
yceE/mdtG-02	TTATCTGTTTTCTGCTCACCTTCTTTT	GCGTGGTGACAAACAGGCTTA	Multidrug	efflux
yceL/mdtH-01	TCGGGATGGTGGGCAAT	CGATAACCGAGCCGATGTAGA	Multidrug	efflux
yceL/mdtH-02	CGCGTGAAACCTTAAGTGCTT	AGACGGCTAAACCCCATATAGCT	Multidrug	efflux
yceL/mdtH-03	CTGCCGTTAAATGGATGTATGC	ACTCCAGCGGGCGATAGG	Multidrug	efflux
yidY/mdtL-01	GCAGTTGCATATCGCCTTCTC	CTTCCCGGCAAACAGCAT	Multidrug	efflux
yidY/mdtL-02	TGCTGATCGGGATTCTGATTG	CAGGCGCGACGAACATAAT	Multidrug	efflux
fabK	TTTCAGCTCAGCACTTTGGTCAT	AAGGCATCTTTTTCAGCCAGTTC	other	deactivate
imiR	CCGGACTAGAGCTTCATGTAAGC	CCCACGCGGTACTCTTGTAAA	other	unknown
nisB	GGGAGAGTTGCCGATGTTGTA	AGCCACTCGTTAAAGGGCAAT	other	unknown
speA	GCAAGAGGTATTTGCTCAACAAGA	CAGGGTCACCCTCATAAAGAAAA	other	unknown
bacA-01	CGGCTTCGTGACCTCGTT	ACAATGCGATACCAGGCAAAT	other/bacitracin	deactivate
bacA-02	TTCCACGACACGATTAAGTCATTG	CGGCTCTTTCGGCTTCAG	other/bacitracin	deactivate
fosB	TCACTGTAACTAATGAAGCATTAGACCAT	CCATCTGGATCTGTAAAGTAAAGAGATC	other/fosfomycin	deactivate
fosX	GATTAAGCCATATCACTTTAATTGTGAAAG	TCTCCTTCCATAATGCAAATCCA	other/fosfomycin	deactivate
nimE	TGCGCCAAGATAGGGCATA	GTCGTGAATTCGGCAGGTTTA	other/nitroimidazole	unknown
pncA	GCAATCGAGGCGGTGTTC	TTGCCGCAGCCAATTCA	other/Pyrazinamide	unknown
sat4	GAATGGGCAAAGCATAAAAACTTG	CCGATTTTGAAACCACAATTATGATA	other/streptothricin	deactivate

Table S2 Climatic factors used in this study. MAT: mean annual temperature. MAP: mean annual precipitation.

Termite mound sample	Bulk soil sample	Longitude	Latitude	MAT(°C)	MAP (mm)
TM1	S177	134.4845	-19.4009	25.9666671	389
TM2	S178	134.4845	-19.4009	25.9666671	389
TM3	S179	134.4845	-19.4009	25.9666671	389
TM4	S177	134.4845	-19.4009	25.9666671	389
TM5	S178	134.4845	-19.4009	25.9666671	389
TM6	S180	136	-19.8333	25.7166663	377
TM7	S181	136	-19.8333	25.7166663	377
TM8	S182	136	-19.8333	25.7166663	377
TM9	S180	136	-19.8333	25.7166663	377
TM10	S181	136	-19.8333	25.7166663	377
TM11	S183	136.9	-20.07	25.3333333	362
TM12	S184	136.9	-20.07	25.3333333	362
TM13	S185	136.9	-20.07	25.3333333	362
TM14	S183	136.9	-20.07	25.3333333	362
TM15	S184	136.9	-20.07	25.3333333	362
TM16	S174	134.2	-20.05	25.5250001	373
TM17	S175	134.2	-20.05	25.5250001	373
TM18	S176	134.2	-20.05	25.5250001	373
TM19	S174	134.2	-20.05	25.5250001	373
TM20	S175	134.2	-20.05	25.5250001	373
TM21	S176	134.2	-20.05	25.5250001	373
TM22	S174	134.2	-20.05	25.5250001	373
TM23	S175	134.2	-20.05	25.5250001	373
TM24	S176	134.2	-20.05	25.5250001	373
TM25	S174	134.2	-20.05	25.5250001	373
TM26	S189	139.1333	-20.35	24.7208334	487
TM27	S190	139.1333	-20.35	24.7208334	487
TM28	S191	139.1333	-20.35	24.7208334	487
TM29	S189	139.1333	-20.35	24.7208334	487
TM30	S190	139.1333	-20.35	24.7208334	487
TM31	S191	139.1333	-20.35	24.7208334	487
TM32	S189	139.1333	-20.35	24.7208334	487
TM33	S190	139.1333	-20.35	24.7208334	487
TM34	S191	139.1333	-20.35	24.7208334	487
TM35	S190	139.1333	-20.35	24.7208334	487
TM36	S201	139.630737	-20.707308	24.6374998	458
TM37	S201	139.630737	-20.707308	24.6374998	458
TM38	S201	139.630737	-20.707308	24.6374998	458
TM39	S201	139.630737	-20.707308	24.6374998	458
TM40	S201	139.630737	-20.707308	24.6374998	458

TM41	S195	140.2082	-19.8903	26.0333333	565
TM42	S196	140.2082	-19.8903	26.0333333	565
TM43	S197	140.2082	-19.8903	26.0333333	565
TM44	S195	140.2082	-19.8903	26.0333333	565
TM45	S196	140.2082	-19.8903	26.0333333	565
TM46	S192	140.25	-20.33	25.6166666	542
TM47	S193	140.25	-20.33	25.6166666	542
TM48	S194	140.25	-20.33	25.6166666	542
TM49	S192	140.25	-20.33	25.6166666	542
TM50	S193	140.25	-20.33	25.6166666	542
TM51	S202	140.358582	-19.246329	26.5416667	583
TM52	S198	140.358582	-19.246329	26.5416667	583
TM53	S199	140.358582	-19.246329	26.5416667	583
TM54	S200	140.358582	-19.246329	26.5416667	583
TM55	S200	140.358582	-19.246329	26.5416667	583
TM56	S186	138	-19.9167	25.3374999	438
TM57	S187	138	-19.9167	25.3374999	438
TM58	S188	138	-19.9167	25.3374999	438
TM59	S186	138	-19.9167	25.3374999	438
TM60	S187	138	-19.9167	25.3374999	438
TM61	S171	134.2167	-20.65	25.0249998	254
TM62	S172	134.2167	-20.65	25.0249998	254
TM63	S173	134.2167	-20.65	25.0249998	254
TM64	S171	134.2167	-20.65	25.0249998	254
TM65	S172	134.2167	-20.65	25.0249998	254
TM66	S173	134.2167	-20.65	25.0249998	254
TM67	S171	134.2167	-20.65	25.0249998	254
TM68	S172	134.2167	-20.65	25.0249998	254
TM69	S173	134.2167	-20.65	25.0249998	254
TM70	S171	134.2167	-20.65	25.0249998	254
TM71	S172	134.2167	-20.65	25.0249998	254
TM72	S173	134.2167	-20.65	25.0249998	254
TM73	S171	134.2167	-20.65	25.0249998	254
TM74	S172	134.2167	-20.65	25.0249998	254
TM75	S173	134.2167	-20.65	25.0249998	254
TM76	S171	134.2167	-20.65	25.0249998	254
TM77	S172	134.2167	-20.65	25.0249998	254
TM78	S173	134.2167	-20.65	25.0249998	254
TM79	S172	134.2167	-20.65	25.0249998	254
TM80	S173	134.2167	-20.65	25.0249998	254
TM81	S166	133.360291	-22.665977	21.9999998	302
TM82	S166	133.360291	-22.665977	21.9999998	302
TM83	S166	133.360291	-22.665977	21.9999998	302

TM84	S166	133.360291	-22.665977	21.9999998	302
TM85	S166	133.360291	-22.665977	21.9999998	302
TM86	S166	133.360291	-22.665977	21.9999998	302
TM87	S166	133.360291	-22.665977	21.9999998	302
TM88	S166	133.360291	-22.665977	21.9999998	302
TM89	S166	133.360291	-22.665977	21.9999998	302
TM90	S166	133.360291	-22.665977	21.9999998	302
TM91	S166	133.360291	-22.665977	21.9999998	302
TM92	S166	133.360291	-22.665977	21.9999998	302
TM93	S166	133.360291	-22.665977	21.9999998	302
TM94	S166	133.360291	-22.665977	21.9999998	302
TM95	S166	133.360291	-22.665977	21.9999998	302
TM96	S166	133.360291	-22.665977	21.9999998	302
TM97	S166	133.360291	-22.665977	21.9999998	302
TM98	S166	133.360291	-22.665977	21.9999998	302
TM99	S166	133.360291	-22.665977	21.9999998	302
TM100	S165	133.508606	-22.910333	21.8083335	314
TM101	S162	133.508606	-22.910333	21.8083335	314
TM102	S163	133.508606	-22.910333	21.8083335	314
TM103	S164	133.508606	-22.910333	21.8083335	314
TM104	S165	133.508606	-22.910333	21.8083335	314
TM105	S162	133.508606	-22.910333	21.8083335	314
TM106	S163	133.508606	-22.910333	21.8083335	314
TM107	S164	133.508606	-22.910333	21.8083335	314
TM108	S163	133.508606	-22.910333	21.8083335	314
TM109	S164	133.508606	-22.910333	21.8083335	314
TM110	S159	133.98	-22.98	21.3624999	345
TM111	S160	133.98	-22.98	21.3624999	345
TM112	S161	133.98	-22.98	21.3624999	345
TM113	S160	133.98	-22.98	21.3624999	345
TM114	S161	133.98	-22.98	21.3624999	345
TM115	S168	133.42	-22.23	22.8041666	309
TM116	S169	133.42	-22.23	22.8041666	309
TM117	S170	133.42	-22.23	22.8041666	309
TM118	S168	133.42	-22.23	22.8041666	309
TM119	S169	133.42	-22.23	22.8041666	309
TM120	S170	133.42	-22.23	22.8041666	309
TM121	S168	133.42	-22.23	22.8041666	309
TM122	S169	133.42	-22.23	22.8041666	309
TM123	S170	133.42	-22.23	22.8041666	309
TM124	S170	133.42	-22.23	22.8041666	309
TM125	S167	133.890381	-21.524627	23.6999999	362
TM126	S167	133.890381	-21.524627	23.6999999	362

TM127	S167	133.890381	-21.524627	23.6999999	362
TM128	S167	133.890381	-21.524627	23.6999999	362
TM129	S167	133.890381	-21.524627	23.6999999	362
TM130	S167	133.890381	-21.524627	23.6999999	362
TM131	S167	133.890381	-21.524627	23.6999999	362
TM132	S167	133.890381	-21.524627	23.6999999	362
TM133	S167	133.890381	-21.524627	23.6999999	362
TM134	S167	133.890381	-21.524627	23.6999999	362

Table S3 Physiochemical properties of termite mounds and bulk soil samples.

Sample ID	pH	DOC (mg kg^{-1})	DON (mg kg^{-1})	Sample type
Sample	5.45	970.2	88.5075	Termite mounds
TM2	5.37	1064.25	96.6	Termite mounds
TM3	5.52	957.3	80.505	Termite mounds
TM4	5.62	1285.95	124.335	Termite mounds
TM5	5.42	573.3	52.59	Termite mounds
TM6	7.67	270.05	24	Termite mounds
TM7	7.54	275.4	25.885	Termite mounds
TM8	7.29	374.3	36.75	Termite mounds
TM9	7.67	799.65	48.54	Termite mounds
TM10	7.86	411.05	31.46	Termite mounds
TM11	7.61	703.65	64.02	Termite mounds
TM12	7.66	361.4	40.19	Termite mounds
TM13	7.67	462.75	36.705	Termite mounds
TM14	7.79	284.15	0	Termite mounds
TM15	7.6	557.7	39.495	Termite mounds
TM16	7.45	479	61.1	Termite mounds
TM17	7.3	374.15	0	Termite mounds
TM18	7.3	473.1	0	Termite mounds
TM19	7.44	550.2	58.065	Termite mounds
TM20	7.26	510.45	48.795	Termite mounds
TM21	7.68	771.3	99.915	Termite mounds
TM22	7.18	655.65	77.835	Termite mounds
TM23	7.46	322.7	0	Termite mounds
TM24	7.23	293.8	0	Termite mounds
TM25	7.24	454.8	0	Termite mounds
TM26	6.39	637.2	85.215	Termite mounds
TM27	5.74	436.45	0	Termite mounds
TM28	6.12	481.45	0	Termite mounds
TM29	5.87	347.3	0	Termite mounds
TM30	5.5	834.3	45.39	Termite mounds
TM31	5.91	452.25	66.525	Termite mounds
TM32	6.53	900.6	99.51	Termite mounds
TM33	6.14	348.4	69.1	Termite mounds
TM34	6.62	457.2	74.04	Termite mounds
TM35	6.79	739.35	110.535	Termite mounds
TM36	6.9	358.8	33.585	Termite mounds
TM37	6.94	375.45	33.345	Termite mounds
TM38	7.05	458.55	55.44	Termite mounds
TM39	6.89	361.05	36.03	Termite mounds
TM40	7.32	430.05	47.325	Termite mounds
TM41	7.28	692.7	77.07	Termite mounds

TM42	7.11	511.2	53.07	Termite mounds
TM43	7.86	139.02	5.259	Termite mounds
TM44	7.55	354.15	21.03	Termite mounds
TM45	7.71	335.25	29.19	Termite mounds
TM46	7.11	557.7	137.775	Termite mounds
TM47	7.45	402.15	43.71	Termite mounds
TM48	7.5	564.75	76.05	Termite mounds
TM49	7.25	474.3	57.12	Termite mounds
TM50	7.42	411	58.125	Termite mounds
TM51	5.93	814.35	28.68	Termite mounds
TM52	6.09	317.7	7.7955	Termite mounds
TM53	6.63	298.05	18.495	Termite mounds
TM54	5.84	657	18.165	Termite mounds
TM55	6.53	331.35	23.685	Termite mounds
TM56	5.29	983.55	24.825	Termite mounds
TM57	5.62	731.1	25.125	Termite mounds
TM58	5.88	994.05	60.21	Termite mounds
TM59	6.28	451.05	28.395	Termite mounds
TM60	6.09	387.15	9.342	Termite mounds
TM61	6.61	2821.5	279.9	Termite mounds
TM62	6.8	333	41.205	Termite mounds
TM63	6.76	537.3	73.635	Termite mounds
TM64	6.79	373.35	42.765	Termite mounds
TM65	7.15	556.5	60.285	Termite mounds
TM66	6.39	1183.95	159	Termite mounds
TM67	6.78	1602	160.35	Termite mounds
TM68	6.61	832.95	120.645	Termite mounds
TM69	7.39	667.65	88.83	Termite mounds
TM70	7.4	399.9	54.165	Termite mounds
TM71	6.99	1081.65	151.2	Termite mounds
TM72	6.79	439.65	52.005	Termite mounds
TM73	7.1	481.8	60.87	Termite mounds
TM74	7.28	585.75	82.695	Termite mounds
TM75	6.99	814.35	83.055	Termite mounds
TM76	6.9	613.35	88.71	Termite mounds
TM77	6.44	272.85	60.315	Termite mounds
TM78	6.37	296.1	72.3	Termite mounds
TM79	7.3	479.4	241.65	Termite mounds
TM80	7.23	332.25	49.455	Termite mounds
TM81	6.28	239.55	49.38	Termite mounds
TM82	6.66	307.5	49.485	Termite mounds
TM83	6.69	399.9	60.57	Termite mounds
TM84	6.89	1045.5	143.055	Termite mounds

TM85	7.4	314.7	82.695	Termite mounds
TM86	6.53	685.2	109.845	Termite mounds
TM87	6.7	381.9	55.725	Termite mounds
TM88	6.33	317.25	39.525	Termite mounds
TM89	6.96	552.9	78.36	Termite mounds
TM90	6.47	824.25	120.585	Termite mounds
TM91	6.52	739.05	106.56	Termite mounds
TM92	6.04	870.15	140.64	Termite mounds
TM93	6.3	540.45	66.24	Termite mounds
TM94	6.55	530.4	66.81	Termite mounds
TM95	6.44	377.7	50.73	Termite mounds
TM96	5.95	696.6	107.295	Termite mounds
TM97	5.88	962.7	121.38	Termite mounds
TM98	6.46	380.4	56.1	Termite mounds
TM99	6.46	300.9	39.855	Termite mounds
TM100	6.04	483.9	74.625	Termite mounds
TM101	5.71	423.6	136.515	Termite mounds
TM102	6.32	323.7	54.735	Termite mounds
TM103	6.11	342	57.285	Termite mounds
TM104	6.16	276.15	54.3	Termite mounds
TM105	6.07	189.3	35.28	Termite mounds
TM106	6.04	668.85	91.845	Termite mounds
TM107	5.96	610.65	94.44	Termite mounds
TM108	6.37	574.8	72.285	Termite mounds
TM109	5.46	391.95	244.2	Termite mounds
TM110	6.24	474.6	81.45	Termite mounds
TM111	6.35	644.7	123.525	Termite mounds
TM112	6.02	376.8	69.78	Termite mounds
TM113	6.38	338.1	77.505	Termite mounds
TM114	6.08	560.1	105.54	Termite mounds
TM115	6.14	635.1	310.5	Termite mounds
TM116	6.48	303.45	42.18	Termite mounds
TM117	6.48	271.2	46.89	Termite mounds
TM118	6.62	370.8	72.69	Termite mounds
TM119	6.72	764.4	217.8	Termite mounds
TM120	6.34	444.15	100.365	Termite mounds
TM121	6.61	606.6	119.145	Termite mounds
TM122	7	734.25	140.97	Termite mounds
TM123	6.76	774.15	144.885	Termite mounds
TM124	6.54	670.2	146.565	Termite mounds
TM125	6.4	661.35	125.505	Termite mounds
TM126	6.67	361.95	75.24	Termite mounds
TM127	6.5	872.85	157.2	Termite mounds

TM128	7.01	662.1	116.235	Termite mounds
TM129	6.33	962.55	219	Termite mounds
TM130	6.88	1036.5	195.15	Termite mounds
TM131	6.52	687.75	153.45	Termite mounds
TM132	6.47	742.95	203.7	Termite mounds
TM133	6.69	425.4	77.7	Termite mounds
TM134	6.52	650.55	124.92	Termite mounds
S159	6.7	59.15	10.33	Soil
S160	6.51	62.45	9.42	Soil
S161	6.31	62.95	8.625	Soil
S162	6.33	61.75	10.43	Soil
S163	6.42	81.55	13.735	Soil
S164	6.16	84.25	16.425	Soil
S165	6.12	43.565	8.51	Soil
S166	6.08	84.95	17.79	Soil
S167	5.92	118.5	39.205	Soil
S168	6.01	154.8	25.135	Soil
S169	6.33	100.4	22.71	Soil
S170	6.03	110.05	33.515	Soil
S171	6.43	96.35	12.86	Soil
S172	6.53	124.35	21.74	Soil
S173	6.53	124.35	21.74	Soil
S174	6.12	68.8	24.65	Soil
S175	6.16	110.8	38.175	Soil
S176	6.14	64.15	17.31	Soil
S177	5.16	57.25	2.5005	Soil
S178	5.71	116	7.83	Soil
S179	5.67	100	16.375	Soil
S180	7.01	94.45	10.51	Soil
S181	6.97	97.6	13.605	Soil
S182	6.94	92.85	11.565	Soil
S183	5.96	57.65	5.28	Soil
S184	5.35	46.72	17.355	Soil
S185	5.73	76.3	5.01	Soil
S186	5.91	79.7	4.132	Soil
S187	6.05	83.55	4.742	Soil
S188	6.04	83.25	4.5295	Soil
S189	5	72.95	29.07	Soil
S190	4.93	70.15	24.33	Soil
S191	5.21	66.35	20.015	Soil
S192	6.17	77.15	12.86	Soil
S193	6.39	73	5.83	Soil
S194	6.34	75.35	6.71	Soil

S195	7.32	68.3	3.893	Soil
S196	7.36	58.3	3.127	Soil
S197	6.91	51.25	2.3455	Soil
S198	6.63	120	11.04	Soil
S199	6.66	166.3	16.8	Soil
S200	6.64	150.3	12.91	Soil
S201	6.4	46.21	1.64	Soil
S202	6.76	155.4	15.63	Soil

Chapter 6: General discussion and conclusions

6.1 Key findings and general discussion

Industrial development was an important factor in influencing ARG abundance in urban green spaces

The first study of the project was an investigation of the resistomes in plant phyllosphere and soil in urban green spaces (Chapter 2). Since previous studies reported that the intensity of anthropogenic impacts was positively correlated with soil ARG abundance in urban ecosystems (Li et al., 2018). Initially, we hypotheses for the soil samples collected from urban green spaces a pattern of increase in ARG abundance with an increase in population density of the area would be observed. Because soil is recognized as the primary source of ARGs in plant phyllosphere (Bai et al., 2015). We also hypothesized that the resistome profiles in plant phyllosphere and soil would follow the same pattern and the ARG abundance in plant phyllosphere would also be positively associated with human population density in the area. However, statistical analyses results indicated that there was no correlation between population density with the ARG abundance in either soil or plant phyllosphere. These results were against our initial hypothesis. Therefore, to figure out the factors shaping ARG profiles in urban green spaces, we collected additional anthropogenic data and analysed the correlations between various anthropogenic factors including average household income, number of businesses, number of industries, and ARG abundance. The results indicated that industrial development, as represented by the number of industries in the region was the most important factor in shaping resistome profiles in both soil and plant phyllosphere in urban green spaces. A potential explanation for such observation could be that industrial wastes normally contain a high level of metals which can act as a selection factor for ARGs, as metal-resistance genes and ARGs commonly share high genetic similarities (Fiorentino et al., 2019, Pärnänen et al.,

2019). Another unexpected result was the resistome profiles in soil and plant phyllosphere was distinct from each other with a core resistome was identified for plant phyllosphere but not for soil. This result indicated that the mechanisms for ARG expression might be different for bacterial communities in plant phyllosphere and soil which may be related to the different properties of these two environmental habitats.

Industrial development significantly impacted bacterial communities in urban ecosystems

Since the results of the first study (Chapter 2) and previous research consistently showed that the community assemblies of bacteria (the potential hosts of ARGs) play important roles in influencing environment resistome profiles (Forsberg et al., 2014, Jia et al., 2015, Zhu et al., 2017). Therefore, we hypothesized that the influences of industrial development on resistome profiles might be derived from its impact on bacteria community assemblies. In addition, we also hypothesized that the influences of industrial development would be different for soil and plant phyllosphere bacterial communities. To test these hypotheses, we used high-throughput sequencing to characterize the bacterial communities in soil and plant phyllosphere samples from 40 urban green spaces that are the same as those in Chapter 2. To better observe the impacts of urbanization on bacterial community assemblies we collected soil and plant samples from 3 national parks which are under minimal anthropogenic impacts. Our hypotheses were supported by the results of this study. Firstly, we observed that the bacterial community assemblies (as revealed by principal coordinated analysis results) in soil and plant phyllosphere were distinct from each other. In addition, urbanization and associated anthropogenic activities might differently impact soil and plant phyllosphere bacterial communities with bacterial diversity in soil but not in plant phyllosphere. Lastly, the results of correlation analyses and variation partitioning provided evidence that industrial development

played important role in shaping bacterial community assemblies in urban green spaces with the impact more profound for soil bacterial community than for plant phyllosphere bacterial community.

Habitat properties are important determinants of environmental resistome profiles

The investigation of urban ecosystems (Chapter 2 and 3) indicated that habitat properties may be a fundamental factor in determining bacterial community assemblies and thus ARG expression. We carried out a comparative study of soil and plant phyllosphere resistome profiles in natural ecosystems across a large spatial scale (Chapter 4). The main aim of this study was to gain a better understanding of the roles of habitat properties in influencing environmental resistome. We found that similar to those in urban ecosystems the plant phyllosphere and soil resistomes were very different from each other in natural ecosystems. The resistomes in plant phyllosphere and soil exhibited almost opposite biogeographic patterns, with the phyllosphere harbouring more diverse but less abundant ARGs than the soil. Plant phyllosphere and soil are different environmental habitats that are characterized by being highly dynamic and highly stable, respectively (Cordovez et al., 2019, Klánová et al., 2008, Manz et al., 2001, Reid et al., 2000). These observations provided important support for the importance of habitat properties in determining environmental resistome profiles.

To better understand how changes in habitat properties impact environmental resistomes, we investigated the impacts of termite mound formation on soil resistome profile (Chapter 5). We found that termite mound formation led to a significant reduction in both the abundance and diversity of soil ARGs. In addition, the resistome profile in termite mounds was found to be different from that in surrounding bulk soil with the proportion of efflux pump ARGs significantly lower in termite mound resistome than in bulk soil resistome. Correlation analyses indicated that the different resistome profiles between termite mound and bulk soil

might result from the significant increase in soil pH due to termite mound formation. It has been reported that in natural ecosystems, ARG abundance is closely related to the pressures from competition between bacteria and fungi. Most soil bacterial taxa are very sensitive to pH change and have a narrow pH optimum (Rousk et al., 2010, Xiao et al., 2016). However, the growth of soil fungi was found to be not sensitive to changes in pH (Rousk et al., 2010). Therefore, the increase in pH in termite mounds than in bulk soils may alter the competitive relationships between co-occurring bacterial and fungal communities and thus the ARG abundance.

6.2 Conclusions

This thesis provided a systematic investigation of environmental resistomes in plant phyllosphere and soil in urban and natural ecosystems. The investigation of the resistomes in urban ecosystems demonstrated that soil urban green spaces are overlooked hotspots of ARGs which may associate with potential public health risks. In addition, we found that in urban ecosystems the differences in resistome profiles in plan phyllosphere and soil may result from the differences in the community assemblies of bacteria in these two distinct habitats. Most importantly, we provided evidence that industrial development was the most important anthropogenic factor in influencing both resistome profiles and bacterial community assemblies in urban green spaces.

The large-scale investigation of the resistomes in plant phyllosphere and soil in natural ecosystems demonstrated that ARG abundance in soil and plant phyllosphere exhibited almost opposite biogeographic patterns which were found to be caused by the different influences of biotic and abiotic factors. These findings highlighted the importance of considering habitat property when studying environmental resistomes.

Lastly, the comparative study of termite mound resistome and soil resistome in natural ecosystems provided support for the important roles of soil faunal activities in

influencing environmental resistome profiles. We found that termite formation has led to significant reductions in the abundance and diversity of ARGs. This finding may provide valuable information for the mitigation of the dissemination of environmental ARGs by utilizing soil fauna.

6.3 Implications of the study

Understanding the determinants of resistome profiles in urban and natural ecosystems is essential to mitigating the problem of the dissemination of environmental ARGs. This thesis provided evidence that urban green spaces, which are not traditionally recognized as hot spots of antibiotic use are important reservoirs of a large number of clinically important ARGs. This study elucidated that industrial development was a critical factor associated with increased ARG abundance and bacterial biodiversity in urban green spaces. These findings take the next step towards identifying how urbanization impacts the microbial properties of urban environments. These findings would provide novel information for future urban planning and infrastructure design to achieve better management of public health risks associated with exposure to environmental ARGs. Under the current global trend of rapid urbanization, this information will be of great value. This study also explored the biogeographic patterns of ARGs in a variety of natural ecosystems including plant phyllosphere, soil, and termite mounds. The results of the investigations provided solid evidence for the significant roles of habitat properties in determining resistome profiles in natural ecosystems. In addition, the results of the study provided evidence for the ecological hypothesis that biotic and abiotic environmental stresses could trigger genotypic responses of bacteria that are similar to those induced by antibiotic selection pressure and thus further confirmed the natural origin of environmental ARGs in ecosystems.

6.4 Limitations of the study

It should be noted that there are some limitations of the current study. Firstly, in this study, the profiling of resistomes in both urban (Chapter 2) and natural (Chapter 4 and 5) ecosystems was based on the technique of high through-put qPCR (HT-qPCR). Although HT-qPCR is a state-of-the-art technology for the monitoring of environmental ARGs, it is associated with some drawbacks including high primer dependency, PCR bias, and relatively lower ARG subtype identification capacity compared with metagenomic approach (Liu et al., 2019). In addition, in the current study, the plant species in urban green spaces and natural ecosystems were not identified. However, plant species has been reported to play a pivotal role in influencing phyllosphere microbial community assemblies and ARG expression (Chen et al., 2019b, Lajoie et al., 2020).

6.5 Suggestions for future study

In this study, we illustrated the main factors influencing the distribution patterns of resistomes in urban and natural ecosystems. These results were mainly relying on DNA-based methods and correlation-based analyses. However, correlations between two variables can be spurious and thus not indicate any causal relationships between the two variables (El-Gohary and McNames, 2007). In addition, it has been reported that DNA-based methods, especially qPCR, may lead to an underestimation of the abundance and transmission of ARGs (Liu et al., 2019, Blau et al., 2018). Therefore, cultivation-based studies which elucidated the mechanisms of ARGs in different types of environmental samples will be highly needed in the future.

Environmental ARGs are dangerous to humans only if they can be acquired by human pathogens. Although most environmental bacteria carrying ARGs are non-pathogenic (Zhang et al., 2011), there are chances that ARGs can be transmitted from non-pathogenic bacteria to human pathogens by HGT via MGEs (Monteil et al., 2020, Bottery et al., 2019). Therefore,

future studies to elucidate the mechanisms of ARG transmissions through HGT and the factors that could facilitate the transmission of ARGs in urban and natural ecosystems are highly recommended. In addition, future research attention should also be paid to the occurrence of ARGs in human pathogens colonized in environmental samples which could potentially infect humans through direct and indirect contact, for example, *Shigella*, *Salmonella*, and *Campylobacter jejuni* (Gerba, 2009).

Lastly, although this study has provided valuable information on the plant resistome, researches focusing on plant-related resistomes are still far less compared with resistomes in other environmental habitats like soil and water. Since plant microbiome represents one of the most common and important pathways through which humans are exposed to environmental microbiome, plant resistome should be investigated more thoroughly in future studies (Chen et al., 2019a).

References

Bai, Y., Muller, D.B., Srinivas, G., Garrido-Oter, R., Potthoff, E., Rott, M., Dombrowski, N., Munch, P.C., spaepen, S., Remus-Emsermann, M., Huttel, B., Mchardy, A.C., Vorholt, J.A., and Schulze-Lefert, P. (2015) Functional overlap of the Arabidopsis leaf and root microbiota. *Nature*, 528:364-369.

Blau, K., Bettermann, A., Jechalke, S., Fornefeld, E., Vanrobaeys, Y., Stalder, T., Top, E.M., and Smalla, K. (2018) The transferable resistome of produce. *MBio.*, 9:e01300-18.

Bottery, M.J., Wood, A.J., and Brockhurst, M.A. (2019) Temporal dynamics of bacteria-plasmid coevolution under antibiotic selection. *ISME J.*, 13:559-562.

Chen, Q.L., Cui, H.L., Su, J.Q., Penulas, J., and Zhu, Y.G. (2019)a Antibiotic Resistomes in Plant Microbiomes. *Trends Plant Sci*., 24:530-541.

Chen, Q.L., Hu, H.W., Zhu, D., Ding, J., Yan, Z.Z., He, J.Z., and Zhu, Y.G. (2019)b. Host identity determines plant associated resistomes. *Environ. Pollut*., 258:113709.

Cordovez, V., Dini-Andreote, F., Carrion, V.J., and Raaijmakers, J.M. (2019) Ecology and Evolution of Plant Microbiomes. *Annu Rev Microbiol*., 73:69-88.

El-Gohary, M., and Mcnames, J. (2007) Establishing causality with whitened cross-correlation analysis. *IEEE Trans. Biomed. Eng.*, 54:2214-2222.

Fiorentino, A., Di Cesare, A., Eckert, E.M., Rizzo, L., Fontaneto, D., Yang, Y., and Corno, G. (2019) Impact of industrial wastewater on the dynamics of antibiotic resistance genes in a full-scale urban wastewater treatment plant. *Sci. Total. Environ.*, 646:1204-1210.

Forsberg, K.J., Patel, S., Gibson, M.K., Lauber, C.L., Knight, R., FIerer, N., and Dantas, G. (2014) Bacterial phylogeny structures soil resistomes across habitats. *Nature*, 509:612-616.

Gerba, C.P. (2009) Environmentally transmitted pathogens. Environ. Microbiol., 445-484. Academic Press

Jia, S., Shi, P., Hu, Q., Li, B., Zhang, T., and Zhang, X.X. (2015) Bacterial community shift drives antibiotic resistance promotion during drinking water chlorination. *Environ. Sci. Technol.*, 49:12271-12279.

Klánová, J., Matykiewiczová, N., Máčka, Z., Prošek, P., Láska, K., and Klán, P. (2008) Persistent organic pollutants in soils and sediments from James Ross Island, Antarctica. *Environ. Pollut.*, 152:416-423.

Lajoie, G., Maglione, R., and Kembel, S.W. (2020) Adaptive matching between phyllosphere bacteria and their tree hosts in a neotropical forest. *Microbiome*, 8:70.

Li, G., Sun, G.X., Ren, Y., Luo, X.S., and Zhu, Y.G. (2018) Urban soil and human health: a review. *Eur. J. Soil Sci.*, 69:196-215.

Liu, X., Xiao, P., Guo, Y., Liu, L., and Yang, J. (2019) The impacts of different high-throughput profiling approaches on the understanding of bacterial antibiotic resistance genes in a freshwater reservoir. *Sci. Total. Environ.*, 693:133585.

Manz, M., Wenzel, K.D., Dietze, U., and Schüürmann, G. (2001) Persistent organic pollutants in agricultural soils of central Germany. *Sci. Total Environ.*, 277:187-198.

Monteil, C.L., Grouzdev, D.S., Perrière, G., Alonso, B., Rouy, Z., Cruveiller, S., Ginet, N., Pignol, D., and Lefevre, C.T. (2020) Repeated horizontal gene transfers triggered parallel evolution of magnetotaxis in two evolutionary divergent lineages of magnetotactic bacteria. *ISME J.*, 14:1783-1794.

Pärnänen, K.M.M., Narciso-Da-Rocha, C., Kneis, D., Berendonk, T.U., Cacace, D., Do, T. T., Elpers, C., Fatta-Kassinos, D., Henriques, I., Jaeger, T., Karkman, A., Martinez, J.L., Michael, S.G., Michael-Kordatou, I., O'Sullivan, K., Rodriguez-Mozaz, S., Schwartz, T., Sheng, H., Sørum, H., Stedtfeld, R.D., Tiedje, J.M., Giustina, S.V.D.,

Walsh, F., Vaz-Moreira, I., Virta, M., and Manaia, C.M. (2019) Antibiotic resistance in European wastewater treatment plants mirrors the pattern of clinical antibiotic resistance prevalence. *Sci. Adv.*, 5:eaau9124.

Reid, B.J., Jones, K.C., and Semple, K.T. (2000) Bioavailability of persistent organic pollutants in soils and sediments—a perspective on mechanisms, consequences and assessment. *Environ. Pollut.*, 108:103-112.

Zhang, L., KInkelaar, D., Huang, Y., Li, Y., Li, X., and Wang, H.H. (2011) Acquired antibiotic resistance: are we born with it? *Appl. Environ. Microbiol.*, 77:7134-7141.

Zhu, B., Chen, Q., Chen, S., and Zhu, Y.G. (2017) Does organically produced lettuce harbor higher abundance of antibiotic resistance genes than conventionally produced? *Environ. Int.*, 98:152-159.